
# Novel Supramolecular Gold(I)-Cavitand Catalysts and Approach to the Total Synthesis of Monomarginine

**Gala Ogalla Estévez**

UNIVERSITAT ROVIRA i VIRGILI

ICIQ Institut Català d'Investigació Química

# Novel Supramolecular Gold(I)-Cavitand Catalysts and Approach to the Total Synthesis of Monomarginine

---

**Gala Ogalla Estévez**

**DOCTORAL THESIS**
**2024**

UNIVERSITAT ROVIRA I VIRGILI
Novel Supramolecular Gold(I)-Cavitand Catalysts and Approach to the Total Synthesis of Monomarginine
Gala Ogalla Estévez

UNIVERSITAT ROVIRA I VIRGILI
Novel Supramolecular Gold(I)-Cavitand Catalysts and Approach to the Total Synthesis of Monomarginine
Gala Ogalla Estévez

Gala Ogalla Estévez

# Novel Supramolecular Gold(I)-Cavitand Catalysts and Approach to the Total Synthesis of Monomarginine

DOCTORAL THESIS

Supervised by Prof. Antonio M. Echavarren

Institute of Chemical Research of Catalonia (ICIQ)



Tarragona 2024

UNIVERSITAT ROVIRA I VIRGILI
Novel Supramolecular Gold(I)-Cavitand Catalysts and Approach to the Total Synthesis of Monomarginine
Gala Ogalla Estévez

I STATE that the present study, entitled "*Novel Supramolecular Gold(I)-Cavitand Catalysts and Approach to the Total Synthesis of Monomarginine*", presented by Gala Ogalla Estévez for the award of the degree of Doctor, has been carried out under my supervision at the Institut Català d'Investigació Química (ICIQ).

Tarragona, November 6th, 2024

Doctoral Thesis Supervisor

Prof. Antonio M. Echavarren Pablos

UNIVERSITAT ROVIRA I VIRGILI
Novel Supramolecular Gold(I)-Cavitand Catalysts and Approach to the Total Synthesis of Monomarginine
Gala Ogalla Estévez

*A mis padres y mi hermana*

UNIVERSITAT ROVIRA I VIRGILI
Novel Supramolecular Gold(I)-Cavitand Catalysts and Approach to the Total Synthesis of Monomarginine
Gala Ogalla Estévez

*"A veces hay que saltar y construir tus alas en el camino"*
Ray Bradbury

UNIVERSITAT ROVIRA I VIRGILI
Novel Supramolecular Gold(I)-Cavitand Catalysts and Approach to the Total Synthesis of Monomarginine
Gala Ogalla Estévez

**Acknowledgments**

En primer lugar, me gustaría agradecer a mi director de Tesis, Prof. Antonio M. Echavarren por darme la oportunidad de desarrollar esta tesis doctoral. Formar parte del grupo durante estos 5 años ha sido una experiencia que me llevo para toda la vida. Gracias por creer y confiar en mí desde un principio. En segundo lugar, agradecer a la Dra. Imma Escofet y a Sònia Gavaldà por el apoyo conínuo e incondicional en esta etapa. Sin vosotras nada de esto habría sido posible, sois el alma del grupo, gracias por tanto.

I would like to expres my sincere gratitude to Prof. Igor Larrossa for giving me the opportunity to join his group in the University of Manchester, throughout the summer of 2023. Thank you for letting me feel like a member of the group and for the chemistry discussions. Also, special thanks to Dr. Gillian McArthur, who guided me during the whole process and to Dr. Cassandre Bories, Dr. Nacho Perez and Dr. Pablo Domingo, you made my time there so special.

Muchas gracias a todas las unidades de soporte técnico que me han ayudado desde el ICIQ: Nuclear Magnetic Ressonance, X-Ray Diffraction, High Resolution Mass Spectrometry, HTE, CHROMTAE and CRTU.

I would like to thank all the past and present members of the group. Specially, the people with whom I had the opportunity to collaborate with: Dr. Inmaculada Martín, Dr. Eduardo García, Àlex Martí, Dr. Federica Cester, Dr. M. Paul Beller and Gabriele Giovanardi.

A continuación, agradecir a mi familia tarragonina que se ha formado a lo largo de estos años. Dra. Inma Martín, mi apoyo desde el primer día, me enseñaste a crecer como química desde un principio, cuando aún nadie sabía que esto se iba a convertir en una amistad tan especial. Eres un pilar fundamental en mi vida y espero compartir contigo todo lo que nos aceche. Dra. Tania Medina, mi eterna compañera, sin ti nada de esta etapa habría sido igual. Consigues que lo imposible me parezca fácil en cuestión de minutos, sacándome siempre una carcajada, gracias por tanto! A la Dra. Anna Sadurní, per ser-hi sempre, incondicionalment. Des de que vam forjar la nostre amistat, he sentit un vincle especial i únic. Amb tu em sento compresa fins i tot en els moments menys comprensibles, gràcies. A Laura, por tu aire jerezano con esa dulzura que me acaricia siempre que lo necesito y por saber que puedo contar contigo siempre… gracias, amiga! A la Dra. Alba Helena Pérez, por tu cariño y acogida desde el principio, haciendo que nuestra amistad creciera sin ni siquiera darnos cuenta, gracias de corazón. A la Dra. Ana Arroyo, que siempre nos echamos unas risas y un baile que otro para alegrar el cuerpo. Y a la Dra. Elena Borrego, que te has unido al team *Golden girls* del que una vez se entra ya no se sale, welcome!

Gracias a los vecinos del 2.2: Dr. Andrea Cataffo, eres ese rayito de luz que asoma por el pasillo cuando se oye algo al otro lado, siempre logrando sacarme una sonrisa. Gracias por iluminar tanto y por todo lo compartido. Dra. Isabel Arranz, gracias por andar por ahí regalando sonrisas, valen más que todo el oro del laboratorio! Dr. Eduardo García, per la teva energia i les nostres estones, team *marge* 4ever! Dr. M. Paul Beller, thanks for sharing all your knowledge and time with me, it was great to have you in my final year pushing the clouds away whenever I needed it. Arnau, gràcies per compartir tota la teva cultura catalana amb una servidora de la terra, reconec que em queda molt per aprendre!

Y por último, el querido (y desterrado) 2.11… Àlex, company de batalles des del començament, t'hi sento sempre present, avançant en la mateixa dirección passet a passet junts, gràcies per acompanyar-m'hi. Pablo, otro compañero de viaje con el que comparto cada etapa y fase de esta montaña rusa, las subidas y las bajadas. Gracias por compartir tus puntos de vista con tu innata naturalidad, no cambies nunca! Y al Dr. Nicolás Fincias, por formar parte de esto y por todas tus ricas y dulces tartas!

A todos los Echavarrinos que os habéis ido despidiendo a mitad de mi camino pero que habéis ganado un espacio en este puzle de emociones durante este tiempo: a la Dra. Helena Armengol y a la Dra. Margherita Zanini, que al principio de mi tiempo en el grupo me transmitisteis tanto cariño, os he tenido presente en todo el camino: gracias, chicas. Al Dr. Leonardo Nannini, gracias por nuestro tiempo, esta aventura no habría sido la misma sin ti en ella. Al Dr. Marc Montesinos i al Dr. Víctor García, gràcies per totes les estones compartides.

A los que hicieron de Macnhester un hogar durante mi estancia: Dra. Cristina García, Dr. Ciro Romano, Dr. Ángel Mudarra y Dr. Giaccomo Crisenza. Gracias por acogerme y compartir tanto conmigo durante aquellos meses, ese verano no habría sido lo mismo sin vosotros.

Y a todos los *Echavarren outsiders* con los que he tenido el placer de compartir momentos especiales: Dra. Alba Martínez (mi descubrimiento conquense más maravilloso), Eric (que sin darnos cuenta nos hemos acompañado más de lo que creemos, sobretodo los últimos meses en la sala de tesis…), Dra. Aliénor Jeandin (gracias por transmitir tanto, tan solo siendo como eres). Y a las parejas que han acabado siendo parte de esta familia: Dr. David Nieto, Miki, Dani y David.

A mis químichicas, Marina e Irene: nuestra amistad empezó siendo rutinaria, haciendo piña para estudiar y apoyándonos durante la carrera. Lo que se pudo quedar en una amistad pasajera, se ha hecho inmensa y hoy no me imagino mi vida sin vosotras. Os quiero bonitas.

Als meus amics de sempre. Les meves nenes. Ia, Laia i Anna: gràcies per mantenir la nostre amistat intacte i saber que tot i les meves anades i vingudes, sempre torno a casa. Miki, gràcies per fer que la nostre amistat sigui com és, i que dins del nostre caos (que mai és poc) sempre ens tornem a trobar i està tot igual, tant de bo així sempre. I a tota la colla Igualadina, gràcies per fer-me sentir que seguim sent els adolescents que èrem!

Por último agradecer a mi familia, las personas más importantes de mi vida, que me han acompañado siempre sin dudar ni en un solo momento de mi. Mamá, gracias por tu paciencia conmigo, por conocerme mejor que nadie y saber siempre lo que me hace falta. Papá, tu apoyo incondicional me hace sentir segura. Siempre sabes como conducir mis emociones, realzando las alegrías y encogiendo las penas. Vinyet, mi otra mitad. Eres la luz que sé que siempre va a alumbrar mi vida, pase lo que pase. Te quiero pequeñaja. A mis abuelos, eternos luchadores, gracias por todo el cariño, apoyo y amor que me hacéis sentir cada día. Y por supuesto, a Carbó, por enseñarme otro tipo de amor que me faltaba por descubrir. Todos vosotros sois mi motor, siempre. Os quiero.

This work was carried out with the support of the Ministerio de Ciencia e Innovación (projects MICIU/AEI/10.13039/501100011033/FEDER, UE and PID2022-136623NB-I00), the European Research Council Funded by the European Union (835080-Foldmetcat), the AGAUR (2021 SGR 001256), the CERCA Program/Generalitat de Catalunya and the ICIQ foundation for financial support.

UNIVERSITAT ROVIRA I VIRGILI
Novel Supramolecular Gold(I)-Cavitand Catalysts and Approach to the Total Synthesis of Monomarginine
Gala Ogalla Estévez

At the time of writing this thesis, the research summarized herein has been published in the following article:

***"Enantioselective Alkoxycyclization of 1,6-Enynes with Gold(I)-Cavitands: Total Synthesis of Mafaicheenamine C"***
Martín-Torres, I.; Ogalla, G.; Yang, J.-M.; Rinaldi, A.; Echavarren, A. M. *Angew. Chem. Int. Ed.* **2021**, *60*, 9339–9344.

***"Hydrogen-Bonded Matched Ion Pair Gold(I) Catalysis"***

Martí, À.; Ogalla, G.; Echavarren A. M. *ACS Catal.* **2023**, *13*, 10217–10223.

UNIVERSITAT ROVIRA I VIRGILI
Novel Supramolecular Gold(I)-Cavitand Catalysts and Approach to the Total Synthesis of Monomarginine
Gala Ogalla Estévez

# Table of Contents

# Prologue

This PhD dissertation manuscript is divided into four main parts, including a general introduction, two research chapters and an appendix section describing the experimental results, and the general conclusions. These sections are preceeded by a list of abbreviations and acronyms, the abstract and general objectives. Each research chapter contains five sections that includes an introduction on the research topic, the objectives, the results and discussion, the conclusions and outlook, and the experimental section. The numbering of compounds, figures, schemes, tables, and references is organized by chapters. In case of collaborative projects, the researchers involved are indicated in each chapter or section.

**General Introduction**, provides an overview of the principles of homogeneous gold(I) catalysis and the cycloisomerization of 1,*n*-enynes and summarizes the main approaches to enantioselective gold(I) catalysis.

**Chapter I**, '*Design and Synthesis of Novel Supramolecular Gold(I) Complexes for the Cycloisomerization of Enynes*', describes our efforts to expand the family of supramolecular gold(I)-cavitand complexes. For clarity, the results in this section have been subdivided into three sections corresponding to the different approaches, that include a specific introduction to each topic and the experimental section is located at the end of the main research chapter.

Part of the results obtained were published in: Martí, À.; Ogalla, G.; Echavarren A. M. Hydrogen-Bonded Matched Ion Pair Gold(I) Catalysis *ACS Catal.* **2023**, *13*, 10217–10223.

**Chapter II**, '*Towards the Total Synthesis of Monomarginine*', presents the structure elucidation and our attempts to synthesize monomarginine, a natural product from the *monocarpia marginalis* family.

**Appendix**, '*Truxenes Gold(I) Complexes*', introduces the preliminar studies on the synthesis of a novel truxenes gold(I) complex family.

**General Conclusions** are provided for the research topics.

UNIVERSITAT ROVIRA I VIRGILI
Novel Supramolecular Gold(I)-Cavitand Catalysts and Approach to the Total Synthesis of Monomarginine
Gala Ogalla Estévez

## List of Abbreviations and Acronyms

In this manuscript, the abbreviations and acronyms most commonly used in organic and organometallic chemistry have been used following the recommendations of "*Guidelines of Authors*" of the *Journal of Organic Chemistry*.

Additional abbreviations and acronyms used in this manuscript are listed below:

| | |
|---|---|
| APCI | atmospheric pressure chemical ionization |
| $BAr_4^{F-}$ | tetrakis[3,5-bis(trifluoromethyl)phenylborate] |
| CAN | ceric ammonium nitrate |
| COSY | correlated spectroscopy |
| CPME | cyclopentyl methyl ether |
| 1,2-DCE | 1,2-dichloroethane |
| DEPT | distortionless enhancement by polarization transfer. |
| DMFDMA | *N*,*N*-dimethylformamide dimethyl acetal |
| DIPA | diisopropylamine |
| DIPEA | di-*iso*-propyl ethyl amine |
| DMAP | 4-dimethylaminopyridine |
| *dr* | diastereomeric ratio |
| *ee* | enantiomeric excess |
| *er* | enantiomeric ratio |
| ESI | electrospray ionization |
| GC-MS | gas chromatography-mass spectrometry |
| GOESY | gradient-enhanced nuclear overhauser effect spectroscopy |
| HATU | hexafluorophosphate azabenzotriazole tetramethyl uranium |
| HMBC | heteronuclear multiple bond correlation |
| HMTE | hexamethylenetetramine |
| HRMS | high resolution mass spectrometry |
| HSQC | heteronuclear single quantum coherence spectroscopy |
| IPr | 1,3-bis(2,4,6-trimethylphenyl)imidazole-2-ylidene |
| JohnPhos | (2-biphenyl)di-*tert*-butylphosphine |
| n.d. | not detected |
| NMR | nuclear magnetic resonance |
| n.r. | no reaction |
| $NTf_2^-$ | bis(trifluoromethyl)imidate |
| L | ligand |
| M | metal |
| MALDI | matrix assisted laser desorption ionization |
| MW | microwave irradiation |
| Nu | nucleophile |
| $OTf^-$ | trifluoromethanesulfonate |
| PG | protecting group |
| THF | tetrahydrofuran |
| TLC | thin layer chromatography |

UNIVERSITAT ROVIRA I VIRGILI
Novel Supramolecular Gold(I)-Cavitand Catalysts and Approach to the Total Synthesis of Monomarginine
Gala Ogalla Estévez

## Abstract

Over the last two decades, gold(I)-catalyzed transformations have shown great potential for building molecular complexity. Our research group has played a key role in this area by synthesizing gold(I) complexes, applying them in the creation of novel synthetic methodologies, and exploring their underlying mechanisms. This Doctoral Thesis is centered on expanding the understanding of asymmetric gold(I) catalysis, developing new gold(I) catalysts, and pursuing innovative synthetic strategies towards natural products.

Previous approaches for the design of different ligands for gold(I) complexes have been a widely studied topic in our group. This work is centered on bulky cavitand ligands that offer a cavity pocket to shape the reaction outcomes as well as direct the selectivities in different reactions. Inspired by the success of the first gold(I)-cavitand family previously developed, the synthesis and applications of a novel family of gold(I)-cavitand complexes has been explored. Different modifications in their structure have been proposed and carried out to new applications.

Other area of study is centered in the structure elucidation and total synthesis of monomarginine, a natural product from *monocarpia marginalis*. The structure of this natural product has been reassigned and efforts towards its preparation have been undertaken. This work summarizes several synthetic strategies followed towards the total synthesis of this molecule.

UNIVERSITAT ROVIRA I VIRGILI
Novel Supramolecular Gold(I)-Cavitand Catalysts and Approach to the Total Synthesis of Monomarginine
Gala Ogalla Estévez

## General Objectives

The objectives of this Doctoral Thesis are the development of new gold(I) complexes and studying their catalytic reactivity. In particular, the aims were focused on:

- The design and synthesis of a new generation of gold(I)-cavitand complexes in the context of asymmetric transformations by:
    - Introducting a chiral moiety in the cavitand's ligand core, which would be responsible for the enantioinduction in gold(I)-catalyzed reactions.
    - Using an achiral gold(I)-complex as part of a dual-component system with a chiral silver salt for enantioselective cyclizations.
- In another context, structure elucidations and attempts for the the total synthesis of monomarginine will be covered.

Each chapter of this PhD manuscript provides a more detailed description of the specific objectives.

UNIVERSITAT ROVIRA I VIRGILI
Novel Supramolecular Gold(I)-Cavitand Catalysts and Approach to the Total Synthesis of Monomarginine
Gala Ogalla Estévez

# *General Introduction*

UNIVERSITAT ROVIRA I VIRGILI
Novel Supramolecular Gold(I)-Cavitand Catalysts and Approach to the Total Synthesis of Monomarginine
Gala Ogalla Estévez

## Homogeneous Gold(I) Catalysis

### Origin of Gold Chemistry

Gold is a precious metal whose symbol, Au, comes from Latin *aurum*.[1] The element presents, in its metallic form, unique properties like ductility and malleability. As a result of its aesthetic qualities, it has long been considered as a valuable possession. The earliest uses in decorative items and jewelry dates to 4600-4200 (Before Common Era) in the necropolis of Varna (now in Bulgaria), and later by the Egyptians (*ca.* 3000 BCE) that utilize electrum, a gold and silver alloy, and the Sumer civilization in Mesopotamia (*ca.* 2500 BCE) (Figure 1). Ever since, every human culture has associated gold to beauty, power, and success.

**Figure 1**. Neolithic Gold Bead.

Nonetheless, despite its remarkable properties, gold is scientifically known for its low reactivity and inertness.[2] Moreover, gold's potential in catalysis was long overlooked and it wasn't until the 1970s that its catalytic abilities in heterogeneous reactions were first recognized during hydrogenation studies performed on a $SiO_2$-supported gold surface.[3] The field of homogeneous gold catalysis began to take shape in 1986, with the first gold(I)-catalyzed aldol reaction (Scheme 1, top).[4] Then, in 1998, Teles reported the gold(I)-catalyzed

1 de Vaan, M. Etymological Dictionary of Latin and the Other Italic Languages, *Brill: Leiden*, **2008**.

2 Stephen, A.; Hashmi, K. Homogeneous Catalysis by Gold, *Gold Bull.* **2004**, *37*, 51–65.

3 Bond, G. C.; Sermon, P. A.; Webb, G.; Buchanan, D. A.; Wells, P. B. Hydrogenation over Supported Gold Catalysts, *J. Chem. Soc. Chem. Commun.* **1973**, *13*, 444b–4445.

4 Ito, Y.; Sawamura, M.; Hayashi, T. Catalytic Asymmetric Aldol Reaction: Reaction of Aldehydes with Isocyanoacetate Catalyzed by a Chiral Ferrocenylphosphine-Gold(1) Complex, *J. Am. Chem. Soc.* **1986**, *108*, 6405–6406.

addition of alcohols to alkynes to form acetals (Scheme 1, bottom),[5] which was shortly followed by Tanaka's studies in a similar system for alkyne hydration[6a] or hydroamination.[6b]

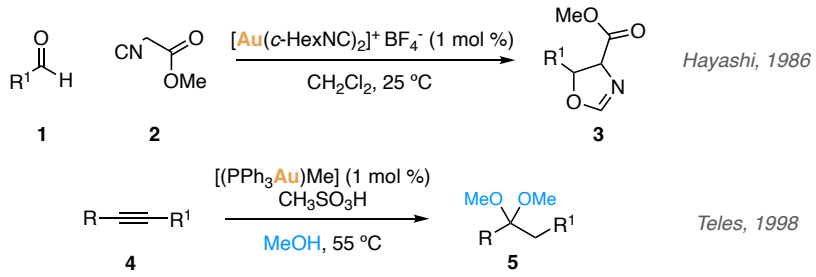


**Scheme 1**. First homogeneous gold(I)-catalyzed reactions.

Alternatively, to the uses of gold(I), gold(III) salts were developed for the synthesis of phenols by reaction between alkynes and furans.[7] Later on, the uses of gold(I) complexes have become an important field of study in organic chemistry for the formation of carbon–carbon and carbon–heteroatom bonds.[8]

**Generalities of Gold(I) Catalysis**

The exceptional ability of gold(I) complexes to selectively activate π-bonds has been attributed to its relativistic effects,[9] which are related to the acceleration of electrons that orbit around a heavy nucleus. As the atomic number increases, electrons closer to the nucleus experience a greater acceleration, establishing a proportional relationship between the relativistic effects and the atomic number. Thus, the mass of the electrons also increases, leading to the contraction of the *s* and *p* orbitals while simultaneously causes the *d* and *f* orbitals to expand,

---

5 Teles, J. H.; Brode, S.; Chabanas, M. Cationic Gold(I) Complexes: Highly Efficient Catalysts for the Addition of Alcohols to Alkynes, *Angew. Chem. Int. Ed.* **1998**, *37*, 1415–1418.

6 (a) Mizushima, E.; Sato, K.; Hayashi, T.; Tanaka, M. Highly Efficient $Au^{I}$-Catalyzed Hydration of Alkynes, *Angew. Chem. Int. Ed.* **2002**, *41*, 4563–4565. (b) Mizushima, E.; Hayashi, T.; Tanaka, M. Au(I)-Catalyzed Highly Efficient Intermolecular Hydroamination of Alkynes, *Org. Lett.* **2003**, *5*, 3349–3352.

7 Hashmi, A. S. K.; Frost, T. M.; Bats, J. W. Highly Selective Gold-Catalyzed Arene Synthesis, *J. Am. Chem. Soc.* **2000**, *122*, 11553–11554.

8 (a) Fürstner, A. Gold and Platinum Catalysis—a Convenient Tool for Generating Molecular Complexity, *Chem. Soc. Rev.* **2009**, *38*, 3208–3221. (b) Obradors, C.; Echavarren, A. M. Gold-Catalyzed Rearrangements and Beyond, *Acc. Chem. Res.* **2014**, *47*, 902–912. (c) Dorel, R.; Echavarren, A. M. Gold(I)-Catalyzed Activation of Alkynes for the Construction of Molecular Complexity, *Chem. Rev.* **2015**, *115*, 9028–9072.

9 (a) Pyykkö, P. Relativity, Gold, Closed-Shell Interactions, and $CsAu{\cdot}NH_3$, *Angew. Chem. Int. Ed.* **2002**, *41*, 3573–3578. (b) Schwarz, H. Relativistic Effects in Gas-Phase Ion Chemistry: An Experimentalist's View, *Angew. Chem. Int. Ed.* **2003**, *42*, 4442–4454. (c) Gorin, D. J.; Toste, F. D. Relativistic Effects in Homogeneous Gold Catalysis, *Nature* **2007**, *446*, 395–403.

resulting in a weaker attraction of their electrons to the nucleus. This contraction/expansion effect is particularly pronounced in heavy metals with filled 4*f* and 5*d* orbitals, reaching a maximum in gold. Consequently, the contraction of the 6*s* orbital leads to a significant expansion of the 5*d* orbital, minimizing the electron–electron repulsion. This arrangement facilitates the interaction between gold's filled 5*d* orbital and the filled π orbitals of unsaturated bonds, drawing electron density towards gold and activating these π-bonds for nucleophilic attack due to their enhanced electrophilicity (Figure 2).

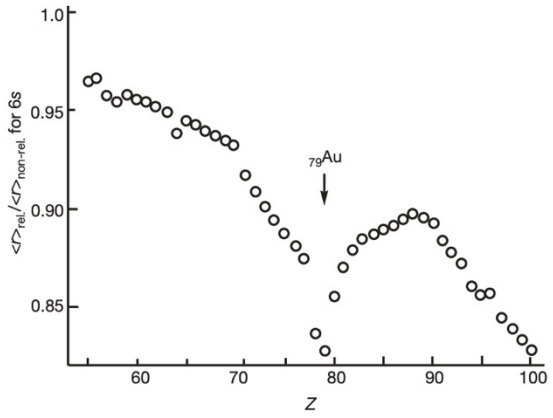


**Figure 2**. Relativistic contraction of the 6s orbital.[10]

Another important impact of this effect is the thermodynamic stability of gold towards oxidation. As mentioned, the 6*s* orbital of gold is contracted and energetically stabilized which results in a high electron affinity and therefore, a distinct tendency to adopt negatively polarized valence states.[11] This explains the high electronegativity of gold, its Lewis acidic character and the occurrence of aurophilic interactions[12] (tendency to form Au–Au interactions). Moreover, due to this contraction, the *s*/*p* or *s*/*d* hybridizations explain the structural preference of gold(I) to adopt a linear coordination geometry.[13] These linear gold(I) complexes do not easily undergo oxidative addition or *β*-hydride elimination.[14] However, recent discoveries have demonstrated that by rational ligand design, and using appropriate

10 Graph taken from reference 9b.

11 Jansen, M. The Chemistry of Gold as an Anion, *Chem. Soc. Rev.* **2008**, *37*, 1826–1835.

12 Scherbaum, F.; Grohmann, A.; Huber, B.; Krüger, C.; Schmidbaur, H. "Aurophilicity" as a Consequence of Relativistic Effects: The Hexakis(Triphenylphosphaneaurio)Methane Dication $[(Ph_3PAu)_6C]^{2+}$, *Angew. Chem. Int. Ed. Engl.* **1988**, 27, 1544–1546.

13 Gimeno, M. C.; Laguna, A. Three- and Four-Coordinate Gold(I) Complexes, *Chem. Rev.* **1997**, *97*, 511–522.

14 Livendahl, M.; Goehry, C.; Maseras, F.; Echavarren, A. M. Rationale for the Sluggish Oxidative Addition of Aryl Halides to Au(I), *Chem. Commun.* **2014**, *50*, 1533–1536.

substrates, gold(I) complexes can promote oxidative addition.[15] Instead, the *β*-hydride elimination process has only been observed from square planar gold(III) complexes.[16]

**Gold(I) Complexes: General Considerations**

A further consequence of relativistic effects involves the Au–L coordination, which results in a contracted and strong bond, having a big impact in the complex behaviors. For this reason, tuning the steric and the electronic properties of the ligands has become a trending topic for lately studies to modulate such effect.[17]

In general, complexes bearing highly *N*-heterocyclic carbenes (NHC) (more σ-donating) are less electrophilic, acting more as a carbene-like intermediates. On the other hand, phosphite-type ligands (less σ-donating) give rise to highly electrophilic catalysts, acting more as carbocation-like species. In between, Buchwald-type ligands display an intermediate electrophilicity and have shown that can activate alkynes in intra- and intermolecular transformations successfully (Figure 3).[18]

15 (a) Joost, M.; Zeineddine, A.; Estévez, L.; Mallet−Ladeira, S.; Miqueu, K.; Amgoune, A.; Bourissou, D. Facile Oxidative Addition of Aryl Iodides to Gold(I) by Ligand Design: Bending Turns on Reactivity, *J. Am. Chem. Soc.* **2014**, *136*, 14654–14657. (b) Cambeiro, X. C.; Ahlsten, N.; Larrosa, I. Au-Catalyzed Cross-Coupling of Arenes *via* Double C–H Activation, *J. Am. Chem. Soc.* **2015**, *137*, 15636–15639. (c) Zeineddine, A.; Estévez, L.; Mallet-Ladeira, S.; Miqueu, K.; Amgoune, A.; Bourissou, D. Rational Development of Catalytic Au(I)/Au(III) Arylation Involving Mild Oxidative Addition of Aryl Halides, *Nat. Commun.* **2017**, *8*, 565.

16 (a) Castiñeira Reis, M.; López, C. S.; Kraka, E.; Cremer, D.; Faza, O. N. Rational Design in Catalysis: A Mechanistic Study of *β*-Hydride Eliminations in Gold(I) and Gold(III) Complexes Based on Features of the Reaction Valley, *Inorg. Chem.* **2016**, *55*, 8636–8645. (b) Rekhroukh, F.; Estevez, L.; Mallet-Ladeira, S.; Miqueu, K.; Amgoune, A.; Bourissou, D. *β*-Hydride Elimination at Low-Coordinate Gold(III) Centers, *J. Am. Chem. Soc.* **2016**, *138*, 11920–11929. (c) Kumar, R.; Krieger, J.-P.; Gómez-Bengoa, E.; Fox, T.; Linden, A.; Nevado, C. The First Gold(III) Formate: Evidence for *β*-Hydride Elimination, *Angew. Chem. Int. Ed.* **2017**, *56*, 12862–12865.

17 Gorin, D. J.; Sherry, B. D.; Toste, F. D. Ligand Effects in Homogeneous Au Catalysis, *Chem. Rev.* **2008**, *108*, 3351–3378.

18 Zuccarello, G.; Zanini, M.; Echavarren, A. M. Buchwald-Type Ligands on Gold(I) Catalysis, *Isr. J. Chem.* **2020**, *60*, 360–372.

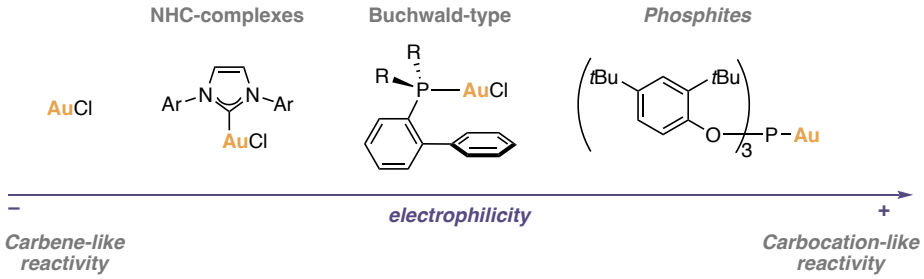


**Figure 3**. Electrophilicity increased by ancillary ligand modification for cationic gold(I) complexes.

Neutral gold(I) chloride complexes [LAuCl] are usually prepared by the direct treatment of the ligand with commercially available (dimethylsulfide)gold(I) chloride ($AuCl{\cdot}SMe_2$) (Scheme 2). However, such [LAuCl] complexes are still catalytically inactive, also known as precatalysts. To activate them, a chloride abstraction process is required, consisting in the coordination of the gold(I) center to a labile ligand that can be replaced through an associative mechanism by the substrate of the reaction.[19] For this, one commonly used method relies on the "*in situ*" activation, using a halide scavenger agent, usually silver,[20] to abstract the chloride, forming AgCl as byproduct and allowing the substrate to coordinate to the gold(I) center (Scheme 2, path a). However, this method can promote side reactions or the formation of less reactive chloride-bridged digold(I) species.[21] Another approach is the formation of the air-stable cationic species in which, upon the chloride abstraction step with silver, gold(I) is coordinated to a neutral labile ligand, such as acetonitrile or other nitrile, which can subsequently be substituted by a suitable substrate (Scheme 2, path b). In both cases, the use of a counterion is required for the cationic forms of the catalysts $X^-$ (such as $SbF_6^-$, $BF_4^-$, or $PF_6^-$).

19 (a) Nieto-Oberhuber, C.; López, S.; Muñoz, M. P.; Cárdenas, D. J.; Buñuel, E.; Nevado, C.; Echavarren, A. M. Divergent Mechanisms for the Skeletal Rearrangement and [2+2] Cycloaddition of Enynes Catalyzed by Gold, *Angew. Chem. Int. Ed.* **2005**, *44*, 6146–6148. (b) Rocchigiani, L.; Fernandez-Cestau, J.; Agonigi, G.; Chambrier, I.; Budzelaar, P. H. M.; Bochmann, M. Gold(III) Alkyne Complexes: Bonding and Reaction Pathways, *Angew. Chem. Int. Ed.* **2017**, *56*, 13861–13865.

20 Weber, S. G.; Rominger, F.; Straub, B. F. Isolated Silver Intermediate of Gold Precatalyst Activation, *Eur. J. Inorg. Chem.* **2012**, 2863–2867.

21 (a) Wang, D.; Cai, R.; Sharma, S.; Jirak, J.; Thummanapelli, S. K.; Akhmedov, N. G.; Zhang, H.; Liu, X.; Petersen, J. L.; Shi, X. "Silver Effect" in Gold(I) Catalysis: An Overlooked Important Factor, *J. Am. Chem. Soc.* **2012**, *134*, 9012–9019. (b) Homs, A.; Escofet, I.; Echavarren, A. M. On the Silver Effect and the Formation of Chloride-Bridged Digold Complexes, *Org. Lett.* **2013**, *15*, 5782–5785.

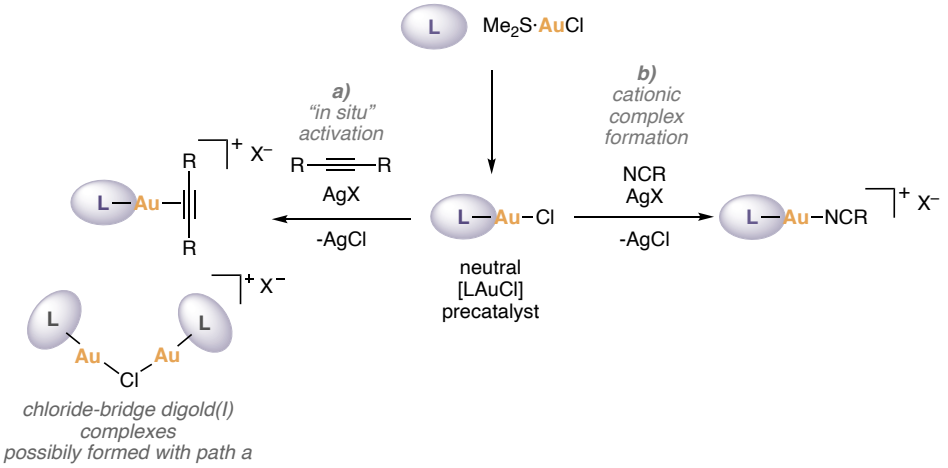


**Scheme 2**.Strategies for the activation of gold(I) chloride precatalysts.

### Cycloisomerization of 1,*n*-Enynes

According to the Dewer-Chatt-Duncanson model,[22] the activation of alkynes by gold(I) is a result of a combination of a σ- and a π-interaction: the donation of density from the alkyne to an empty *d*-orbital of the metal by a σ-interaction and a back-bonding π-interaction between the *d*-orbital of the metal and the empty antibonding π* orbital of the alkyne (Figure 4).[23] Overall, the gold(I)-alkyne bond is most commonly polarized leaving an electron-rich gold(I) center and an electron-deficient and weakened C–C multiple bond.

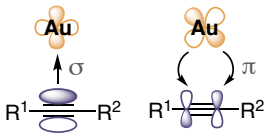


**Figure 4**. The Dewer-Chatt-Duncanson model for the interaction of an alkyne with a gold(I) center.

Studies that combined DFT-based calculations together with experimental work proved that in homogenous gold(I) catalysts, alkenes rather than alkynes are preferentially coordinated to gold, but electro- and nucleophilic attacks are thermodynamically more favored for alkynes, which is the origin of the known alkynophilicity of gold(I). Moreover, enyne cyclizations in

22 Chatt, J.; Duncanson, L. A. Olefin Co-Ordination Compounds. Part III. Infra-Red Spectra and Structure: Attempted Preparation of Acetylene Complexes, *J. Chem. Soc. Resumed* **1953**, 2939–2947.

23 Halliday, C. J. V.; Lynam, J. M. Gold–Alkynyls in Catalysis: Alkyne Activation, Gold Cumulenes and Nuclearity, *Dalton Trans.* **2016**, *45*, 12611–12626.

homogeneous systems are mainly driven by the exceptionally low LUMO (lowest unoccupied molecular orbital) of the coordinated triple bond.[24]

Due to its mentioned alkynophilic character, gold(I) complexes can selectively activate alkynes in complex molecular settings. As a result, the increased electrophilicity of these substrates makes them more susceptible to nucleophilic addition. In general, the nucleophilic Markovnikov attack to $\eta^2$-[AuL]$^+$-activated alkynes forms *trans*-alkenyl gold complexes as intermediates (Scheme 3).[9c] Many nucleophiles are used in inter- and intramolecular manners, being alkenes the most studied in the group.[8c,25]

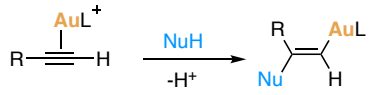


**Scheme 3**. Nucleophilic attack to $\eta^2$-[AuL]$^+$-activated alkynes.

Moreover, gold(I) induces a variety of skeletal rearrangements of 1,*n*-enynes, which, depending on their substitution pattern, give rise to diverse cyclic products through complex mechanisms (Scheme 4). In the case of 1,6-enynes, gold(I) initially coordinates to the alkyne forming ($\eta^2$-alkyne)-gold(I) complex **I** that acts as an electrophile on the alkyne reacting intramolecularly with the alkene as a nucleophile to generate cyclopropyl gold(I) carbene intermediates **II** and **III** by 5-*exo*-dig or 6-*endo*-dig cyclization, respectively.[19a] Cyclopropyl gold(I) carbenes **II** can evolve to form 1,3-dienes **IV** by a single-cleavage skeletal rearrangement since only the alkene moiety at the substrate (carbons in red) suffers C–C bond cleavage. On the other hand, intermediates **II** can also undergo a so-called double-cleavage rearrangement by opening the cyclopropyl ring. This involves the formal insertion of the terminal alkene carbon (carbons in red, bound to $R^2$) into the alkyne carbons of the original 1,6-enynes (carbons in green), producing new gold(I) carbenes **V**, which then undergo α-proton elimination to form product **VI**. The configuration of such exocyclic alkenes can be *E* or *Z*, but the *Z* configuration is more common, especially when $R^2$ is a proton.

24 García-Mota, M.; Cabello, N.; Maseras, F.; Echavarren, A. M.; Pérez-Ramírez, J.; López, N. ChemPhysChem. **2008**, *9*, 1624–1629.

25 (a) de Orbe, M. E.; Amenós, L.; Kirillova, M. S.; Wang, Y.; López-Carrillo, V.; Maseras, F.; Echavarren, A. M. Cyclobutene vs 1,3-Diene Formation in the Gold-Catalyzed Reaction of Alkynes with Alkenes: The Complete Mechanistic Picture, *J. Am. Chem. Soc.* **2017**, *139*, 10302–10311. (b) García-Morales, C.; Ranieri, B.; Escofet, I.; López-Suarez, L.; Obradors, C.; Konovalov, A. I.; Echavarren, A. M. Enantioselective Synthesis of Cyclobutenes by Intermolecular [2+2] Cycloaddition with Non-$C_2$ Symmetric Digold Catalysts, *J. Am. Chem. Soc.* **2017**, *139*, 13628–13631.

On the other hand, intermediates **III**, resulting from an initial 6-*endo*-dig cyclization of intermediate **I**, also undergo α-proton elimination leading to the formation of bicyclo[4.1.0]hept-2-ene derivatives **VII**. Alternatively, intermediated **III** can suffer ring expansion forming ($\eta^2$-cyclobutene)gold(I) complexes **VIII** leading to product **IX** after a double-bond isomerization.[26] A more detailed mechanism of this transformation (intermediated **VIII** to **IX**) was reported by Widenhoefer and co-workers in 2013,[26a] suggesting how the involvement of a Brønsted acid, generated in situ from the gold(I) catalyst counterion, can influence the reaction outcome.[26a,b] Interestingly, intermediates **VIII** can also open up to form ($\eta^2$-alkyne)gold(I) complexes **X**, which generate 1,3-dienes **IV** by a pathway different from that of the 5-*exo*-dig cyclization.

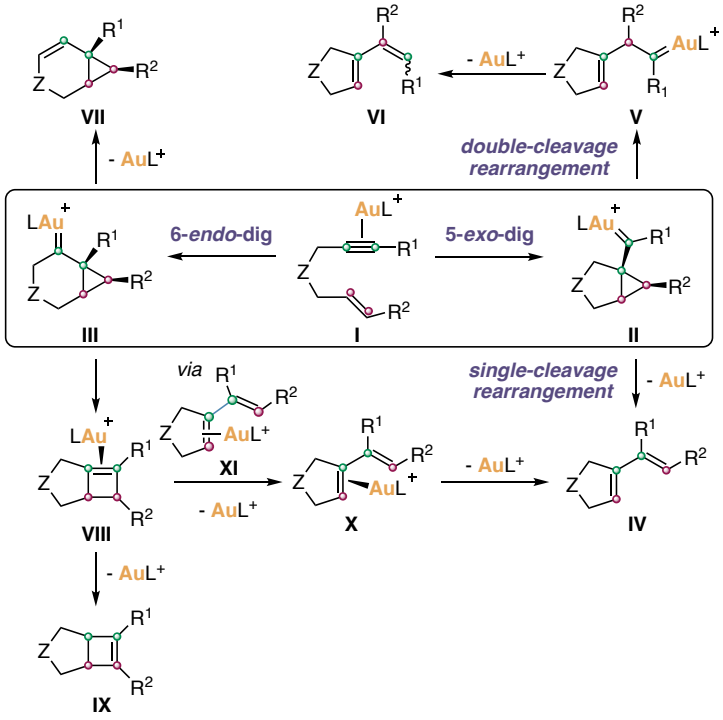


**Scheme 4**. General pathways for the cycloisomerization of 1,6-enynes catalyzed by gold(I).

26 (a) Brooner, R. E. M.; Brown, T. J.; Widenhoefer, R. A. Direct Observation of a Cationic Gold(I)–Bicyclo[3.2.0]Hept-1(7)-Ene Complex Generated in the Cycloisomerization of a 7-Phenyl-1,6-Enyne, *Angew. Chem. Int. Ed.* **2013**, *52*, 6259–6261. (b) Nieto-Oberhuber, C.; Pérez-Galán, P.; Herrero-Gómez, E.; Lauterbach, T.; Rodríguez, C.; López, S.; Bour, C.; Rosellón, A.; Cárdenas, D. J.; Echavarren, A. M. Gold(I)-Catalyzed Intramolecular [4+2] Cycloadditions of Arylalkynes or 1,3-Enynes with Alkenes: Scope and Mechanism, *J. Am. Chem. Soc.* **2008**, *130*, 269–279. (c) Kim, N.; Brooner, R. E. M.; Widenhoefer, R. A. Unexpected Skeletal Rearrangement in the Gold(I)/Silver(I)-Catalyzed Conversion of 7-Aryl-1,6-enynes to Bicyclo[3.2.0]hept-6-enes *via* Hidden Brønsted Acid Catalysis, *Organometallics* **2017**, *36*, 673–678.

Besides the many different rearrangements of 1,6-enynes, the addition of external nucleophiles further expands the possibilities in the reaction outcome. For instance, carbon- and heteronucleophiles have been employed in intra- and intermolecular gold(I)-catalyzed transformations.[27] One of the most studied reactions in this regard is the alkoxycyclization reaction, where the addition of alcohols as nucleophiles takes place under mild conditions in gold(I) catalysis.[28] The analogous general scheme for this transformation is shown in Scheme 5. After the formation of ($\eta^2$-alkyne)-gold(I) complex **I**, cyclopropyl metal carbenes **II** or **III** formed by the *exo*- or *endo*-dig cyclization, could react with water or alcohols to give hydroxy- or alkoxycyclyzation products **XII** and/or **XIII**[29] from **II**, and **XIV** from **III**.[30]

27 For some examples see: (a) Kitamura, T. Transition-Metal-Catalyzed Hydroarylation Reactions of Alkynes Through Direct Functionalization of C–H Bonds: A Convenient Tool for Organic Synthesis, *Eur. J. Org. Chem.* **2009**, *2009*, 1111–1125. (b) Amijs, C. H. M.; López-Carrillo, V.; Raducan, M.; Pérez-Galán, P.; Ferrer, C.; Echavarren, A. M. Gold(I)-Catalyzed Intermolecular Addition of Carbon Nucleophiles to 1,5- and 1,6-Enynes, *J. Org. Chem.* **2008**, *73*, 7721–7730. (c) Qian, J.; Liu, Y.; Cui, J.; Xu, Z. Gold(I)-Catalyzed Synthesis of 1,5-Benzodiazepines Directly from *o*-Phenylenediamines and Alkynes, *J. Org. Chem.* **2012**, *77*, 4484–4490.

28 (a) Teles, J. H.; Brode, S.; Chabanas, M. Cationic Gold(I) Complexes: Highly Efficient Catalysts for the Addition of Alcohols to Alkynes, *Angew. Chem. Int. Ed.* **1998**, *37*, 1415–1418. (b) Nieto-Oberhuber, C.; Muñoz, M. P.; López, S.; Jeménez-Núñez, E.; Nevado, C.; Herrero-Gómez, E.; Raducan, M.; Echavarren, A. M. Gold(I)-Catalyzed Cyclizations of 1,6-Enynes: Alkoxycyclizations and *exo*/*endo* Skeletal Rearrangements, *Chem. Eur. J.* **2008**, *14*, 5096–5096.

29 (a) Méndez, M.; Muñoz, M. P.; Nevado, C.; Cárdenas, D. J.; Echavarren, A. M. Cyclizations of Enynes Catalyzed by $PtCl_2$ or Other Transition Metal Chlorides: Divergent Reaction Pathways, *J. Am. Chem. Soc.* **2001**, *123*, 10511–10520. (b) Muñoz, M. P.; Méndez, M.; Nevado, C.; Cárdenas, D. J.; Echavarren, A. M. Hydroxy- and Alkoxycyclizations of Enynes Catalyzed by Platinum(II) Chloride, *Synthesis* **2003**, No. 18, 2898–2902. (c) Muñoz, M. P.; Adrio, J.; Carretero, J. C.; Echavarren, A. M. Ligand Effects in Gold- and Platinum-Catalyzed Cyclization of Enynes: Chiral Gold Complexes for Enantioselective Alkoxycyclization, *Organometallics* **2005**, *24*, 1293–1300. (d) Echavarren, A. M.; Nevado, C. Non-Stabilized Transition Metal Carbenes as Intermediates in Intramolecular Reactions of Alkynes with Alkenes, *Chem. Soc. Rev.* **2004**, *33*, 431.

30 Nevado, C.; Cárdenas, D. J.; Echavarren, A. M. Reaction of Enol Ethers with Alkynes Catalyzed by Transition Metals: 5-*exo*-*dig* versus 6-*endo*-*dig* Cyclizations *via* Cyclopropyl Platinum or Gold Carbene Complexes, *Chem. Eur. J.* **2003**, *9*, 2627–2635.

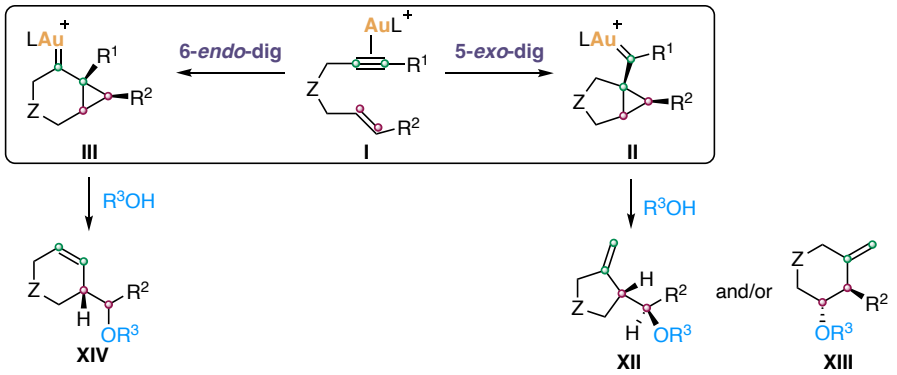


**Scheme 5**. Mechanisms for the *endo*- and *exo*-alkoxycyclization of enynes.

Larger 1,*n*-enynes (n ≥ 7) react intramolecularly by a formal [2+2] cycloaddition to afford cyclobutene-fused bicyclic compounds.[31] For example, 1,15-enyne **6** undergoes a gold(I)-catalyzed macrocyclization leading to a 15-membered ring macrocycle **7**, incorporating a cyclobutene moiety (Scheme 6).[32]

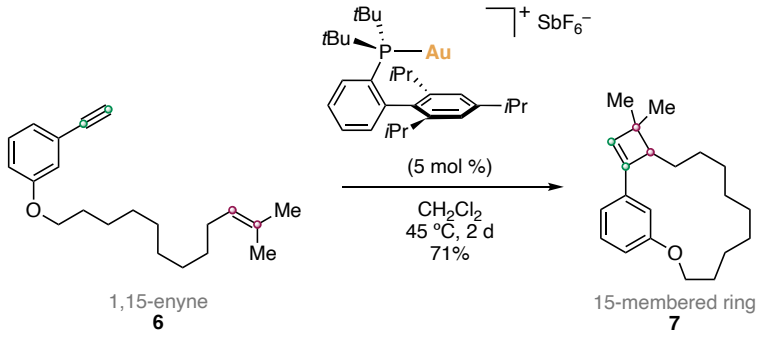


**Scheme 6**. Selected example of a gold(I)-catalyzed cyclization of 1,*n*-enyne (n ≥ 7).

Finally, the intermolecular gold(I)-catalyzed reaction of terminal alkynes with alkenes as nucleophiles has also been studied.[33] However, these transformations are more challenging

31 (a) Odabachian, Y.; Gagosz, F. Cyclobutenes as Isolable Intermediates in the Gold(I)-Catalysed Cycloisomerisation of 1,8-Enynes, *Adv. Synth. Catal.* **2009**, *351*, 379–386. (b) Inagaki, F.; Matsumoto, C.; Okada, Y.; Maruyama, N.; Mukai, C. Air-Stable Cationic Gold(I) Catalyst Featuring a *Z*-Type Ligand: Promoting Enyne Cyclizations, *Angew. Chem. Int. Ed.* **2015**, *54*, 818–822. (c) Iwai, T.; Ueno, M.; Okochi, H.; Sawamura, M. Synthesis of Cyclobutene-Fused Eight-Membered Carbocycles through Gold-Catalyzed Intramolecular Enyne [2+2] Cycloaddition, *Adv. Synth. Catal.* **2018**, *360*, 670–675.

32 (a) Obradors, C.; Leboeuf, D.; Aydin, J.; Echavarren, A. M. Gold(I)-Catalyzed Macrocyclization of 1,*n*-Enynes, *Org. Lett.* **2013**, *15*, 1576–1579.

33 Muratore, M. E.; Homs, A.; Obradors, C.; Echavarren, A. M. Meeting the Challenge of Intermolecular Gold(I)-Catalyzed Cycloadditions of Alkynes and Allenes, *Chem. Asian J.* **2014**, *9*, 3066–3082. (b) García-Morales, C.; Echavarren, A. M. *Synlett* **2018**, *29*, 2225–2237.

since there are present two unsaturated substrates that compete for coordination to gold(I)[34] and, at the same time, gold(I) can promote polymerization of the alkenes.[35] Nonetheless, in the last years different examples of these type of reactions have been studied.[36]

**Asymmetric Gold(I) Catalysis**

The development of enantioselective gold(I) catalysis has been widely studied over the last years, but it has advanced in a rather slow pace.[37] Overall, it is considered a challenge due to a combination of several facts being the most highlighted one the linear dicoordination geometry adopted by gold(I), the chiral ligand and the substrate. This generates an outer-sphere situation for the enantio-determining step which locates the chiral environment, present on the ligand, far away from the reactive site (Scheme 7).

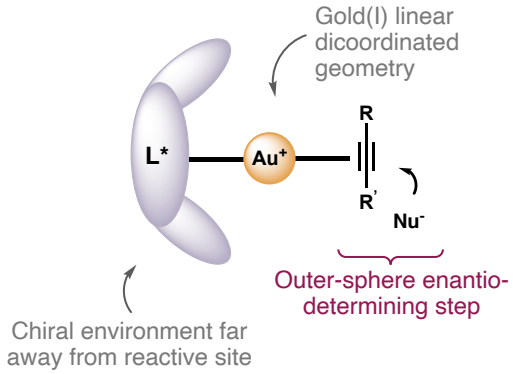


**Scheme 7**. Main limitations of enantioselective gold(I) catalysis.

34 (a) Brown, T. J.; Dickens, M. G.; Widenhoefer, R. A. Syntheses, X-Ray Crystal Structures, and Solution Behavior of Monomeric, Cationic, Two-Coordinate Gold(I) π-Alkene Complexes, *J. Am. Chem. Soc.* **2009**, *131*, 6350–6351. (b) Brooner, R. E. M.; Widenhoefer, R. A. Cationic, Two-Coordinate Gold π Complexes, *Angew. Chem. Int. Ed.* **2013**, *52*, 11714–11724.

35 Urbano, J.; Hormigo, A. J.; Frémont, P. de; Nolan, S. P.; Díaz-Requejo, M. M.; Pérez, P. J. Gold-Promoted Styrene Polymerization, *Chem. Commun.* **2008**, *6*, 759–761.

36 For some examples see: (a) Hashmi, A. S. K.; Blanco, M. C.; Kurpejović, E.; Frey, W.; Bats, J. W. Gold Catalysis: First Applications of Cationic Binuclear Gold(I) Complexes and the First Intermolecular Reaction of an Alkyne with a Furan, *Adv. Synth. Catal.* **2006**, *348*, 709–713. (b) Suárez-Rodríguez, T.; Suárez-Sobrino, Á. L.; Ballesteros, A. Gold(I)-Catalyzed Intermolecular Formal [4+2] Cycloaddition of *o*-Aryl Ynol Ethers and Enol Ethers: Synthesis of Chromene Derivatives, *Chem. Eur. J.* **2021**, *27*, 13079–13084. (c) Elena de Orbe, M.; Echavarren, A. M. Broadening the Scope of the Gold-Catalyzed [2+2] Cycloaddition Reaction: Synthesis of Vinylcyclobutenes and Further Transformations, *Eur. J. Org. Chem.* **2018**, *2018*, 2740–2752.

37 Widenhoefer, R. A. Recent Developments in Enantioselective Gold(I) Catalysis, *Chem. Eur. J.* **2008**, *14*, 5382–5391.

One of the most common strategies to overcome this challenge is based on the design of new ligands to modulate the position of the chiral environment.[38] One example is the use of bimetallic gold(I) complexes bearing atropoisomeric bidentate phosphines (Figure 5a).[39] It was shown that in these cases, the second gold atom plays a crucial role in the enantiodiscrimination. Another strategy recently explored is the use of chiral counteranions which stay close in proximity to the reaction site (Figure 5b).[40] Alternatively, monogold(I) complexes based on phosphoramidites have also demonstrated to perform enantioselective catalytic reactions (Figure 5c).[41] These complexes proved their ability to catalyse enantioselectively reactions such as the [2+2] or the [4+2] cycloaddition of allenes.[41a,b] Finally, the use of bulky ligands has been another strategy which has been pointing out in recent asymmetric studies (Figure 5d).[42]

---

38 One example of a latest review on the topic: Zuccarello, G.; Escofet, I.; Caniparoli, U.; Echavarren, A. M. New-Generation Ligand Design for the Gold-Catalyzed Asymmetric Activation of Alkynes, *ChemPlusChem* **2021**, *86*, 1283–1296.

39 (a) Wang, Y.-M.; Kuzniewski, C. N.; Rauniyar, V.; Hoong, C.; Toste, F. D. Chiral (Acyclic Diaminocarbene)Gold(I)-Catalyzed Dynamic Kinetic Asymmetric Transformation of Propargyl Esters, *J. Am. Chem. Soc.* **2011**, *133*, 12972–12975. (b) Niemeyer, Z. L.; Pindi, S.; Khrakovsky, D. A.; Kuzniewski, C. N.; Hong, C. M.; Joyce, L. A.; Sigman, M. S.; Toste, F. D. Parameterization of Acyclic Diaminocarbene Ligands Applied to a Gold(I)-Catalyzed Enantioselective Tandem Rearrangement/Cyclization, *J. Am. Chem. Soc.* **2017**, *139*, 12943–12946.

40 Inamdar, S. M.; Konala, A.; Patil, N. T. When Gold Meets Chiral Brønsted Acid Catalysts: Extending the Boundaries of Enantioselective Gold Catalysis, *Chem. Commun.* **2014**, *50*, 15124–15135.

41 (a) Luzung, M. R.; Mauleón, P.; Toste, F. D. Gold(I)-Catalyzed [2 + 2]-Cycloaddition of Allenenes, *J. Am. Chem. Soc.* **2007**, *129*, 12402–12403. (b) Nieto-Oberhuber, C.; Pérez-Galán, P.; Herrero-Gómez, E.; Lauterbach, T.; Rodríguez, C.; López, S.; Bour, C.; Rosellón, A.; Cárdenas, D. J.; Echavarren, A. M. Gold(I)-Catalyzed Intramolecular [4+2] Cycloadditions of Arylalkynes or 1,3-Enynes with Alkenes: Scope and Mechanism, *J. Am. Chem. Soc.* **2008**, *130*, 269–279. (c) Teller, H.; Corbet, M.; Mantilli, L.; Gopakumar, G.; Goddard, R.; Thiel, W.; Fürstner, A. One-Point Binding Ligands for Asymmetric Gold Catalysis: Phosphoramidites with a TADDOL-Related but Acyclic Backbone, *J. Am. Chem. Soc.* **2012**, *134*, 15331–15342.

42 (a) Guitet, M.; Zhang, P.; Marcelo, F.; Tugny, C.; Jiménez-Barbero, J.; Buriez, O.; Amatore, C.; Mouriès-Mansuy, V.; Goddard, J.; Fensterbank, L.; Zhang, Y.; Roland, S.; Ménand, M.; Sollogoub, M. NHC-Capped Cyclodextrins (ICyDs): Insulated Metal Complexes, Commutable Multicoordination Sphere, and Cavity-Dependent Catalysis, *Angew. Chem. Int. Ed.* **2013**, *52*, 7213–7218. (b) Zhang, P.; Meijide Suárez, J.; Driant, T.; Derat, E.; Zhang, Y.; Ménand, M.; Roland, S.; Sollogoub, M. Cyclodextrin Cavity-Induced Mechanistic Switch in Copper-Catalyzed Hydroboration, *Angew. Chem. Int. Ed.* **2017**, *56*, 10821–10825. (c) Kaya, Z.; Andna, L.; Matt, D.; Bentouhami, E.; Djukic, J.-P.; Armspach, D. Benzimidazolium- and Benzimidazolilydene-Capped Cyclodextrins: New Perspectives in Anion Encapsulation and Gold-Catalyzed Cycloisomerization of 1,6-Enynes, *Chem. Eur. J.* **2018**, *24*, 17921–17926. (d) Kaya, Z.; Andna, L.; Matt, D.; Bentouhami, E.; Djukic, J.-P.; Armspach, D. A Comparative Study of Confining Ligands Derived from Methylated Cyclodextrins in Gold-Catalyzed Cycloisomerization of 1,6-Enynes, *Eur. J. Org. Chem.* **2019**, *2019*, 4528–4537. (e) Zhu, X.; Xu, G.;

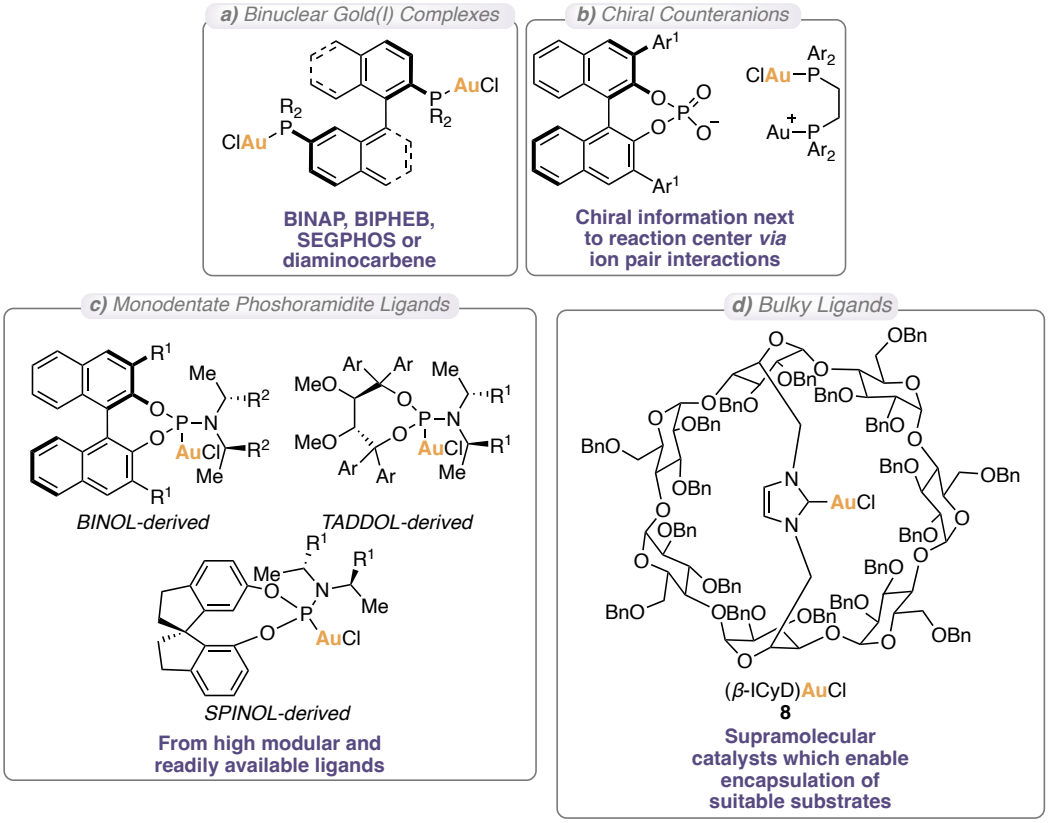


**Figure 5**. Last commonly used strategies in ligand design for asymmetric gold(I) catalysis.

For instance, using NHC-capped *β*-cyclodextrin gold(I) catalyst **8**, the Sollogoub group developed a family of cyclodextrin-NHC ligands in the cycloisomerization of enynes. In 2019, they reported the formation of the bicyclic compounds **10**, obtaining up to 80% *ee* if a phenyl group was present as R group in 1,6-enynes **9**, using complex **8** (Scheme 8, top).[42e] Most recently, they applied their methodology achieving excellent enantioselectivites in the hydroxy- and methoxycylization of 1,6-enynes **11** (Scheme 8, bottom).[43]

Chamoreau, L.-M.; Zhang, Y.; Mouriès-Mansuy, V.; Fensterbank, L.; Bistri-Aslanoff, O.; Roland, S.; Sollogoub, M. Permethylated NHC-Capped *α*- and *β*-Cyclodextrins (ICyDMe) Regioselective and Enantioselective Gold-Catalysis in Pure Water, *Chem. Eur. J.* **2020**, *26*, 15901–15909. (f) Meijide Suárez, J.; Bistri-Aslanoff, O.; Roland, S.; Sollogoub, M. Cavity-Controlled Coordination of Square Planar Metal Complexes and Substrate Selectivity by NHC-Capped Cyclodextrins (ICyDs), *ChemCatChem* **2022**, *14*, e202101411.

43 Tugny, C.; del Rio, N.; Koohgard, M.; Vanthuyne, N.; Lesage, D.; Bijouard, K.; Zhang, P.; Meijide Suárez, J.; Roland, S.; Derat, E.; Bistri-Aslanoff, O.; Sollogoub, M.; Fensterbank, L.; Mouriès-Mansuy, V. *β*-Cyclodextrin–NHC–Gold(I) Complex (*β*-ICyD)AuCl: A Chiral Nanoreactor for Enantioselective and Substrate-Selective Alkoxycyclization Reactions, *ACS Catal.* **2020**, *10*, 5964–5972.

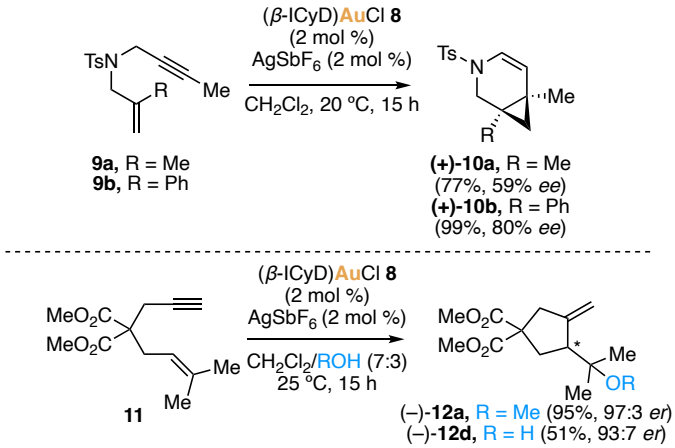


**Scheme 8**. Enantioselective reactions catalyzed by the bulky NHC-capped *β*-cyclodextrin gold(I) catalyst **8**.

The same year, our group reported the synthesis of new chiral gold(I) complexes based on JohnPhos-type ligands bearing a $C_2$-symmetric diaryl pyrrolidine at the *para*-position of the biphenyl core.[44] They were applied, for instance, in the enantioselective synthesis of compounds **15**, which led to the synthesis of the natural products carexanes O, I and P (Scheme 9a). Recently, our group has been working on expanding this family of JohnPhos-type ligands with pyrrolidinyl gold(I) complexes, incorporating variations in the ligand core.[45] One example is the atroposelective cyclization of **16** to form 2-arylindole **17** (Scheme 9b). Interestingly, it was observed that gold(I) complex (*R*,*R*)-**13b** led to the formation of the opposite enantiomer with good enantioselectivities. This allowed obtaining both series of products in an enantiodivergent manner using catalysts that have the same absolute configuration at the $C_2$-chiral pyrrolidine.

44 Zuccarello, G.; Mayans, J. G.; Escofet, I.; Scharnagel, D.; Kirillova, M. S.; Pérez-Jimeno, A. H.; Calleja, P.; Boothe, J. R.; Echavarren, A. M. Enantioselective Folding of Enynes by Gold(I) Catalysts with a Remote $C_2$-Chiral Element, *J. Am. Chem. Soc.* **2019**, *141*, 11858–11863.

45 Zuccarello, G.; Nanini, L.; Arroyo-Bondía, A.; Fincias, N.; Arranz, I.; Pérez-Jimeno, A. H.; Peeters, M.; Martín-Torres, I.; Sadurní, A.; García-Vázquez, V.; Wang, Y.; Kirillova, M. S.; Montesinos-Magraner, M.; Caniparoli, U.; Núñez, G. D.; Maseras, F.; Besora, M.; Escofet, I.; Echavarren, A. M. Enantioselective Catalysis with Pyrrolidinyl Gold(I) Complexes: DFT and NEST Analysis of the Chiral Binding Pocket, Enantioselective Catalysis with Pyrrolidinyl Gold(I) Complexes: DFT and NEST Analysis of the Chiral Binding Pocket. ChemRxiv March 28, **2023**.

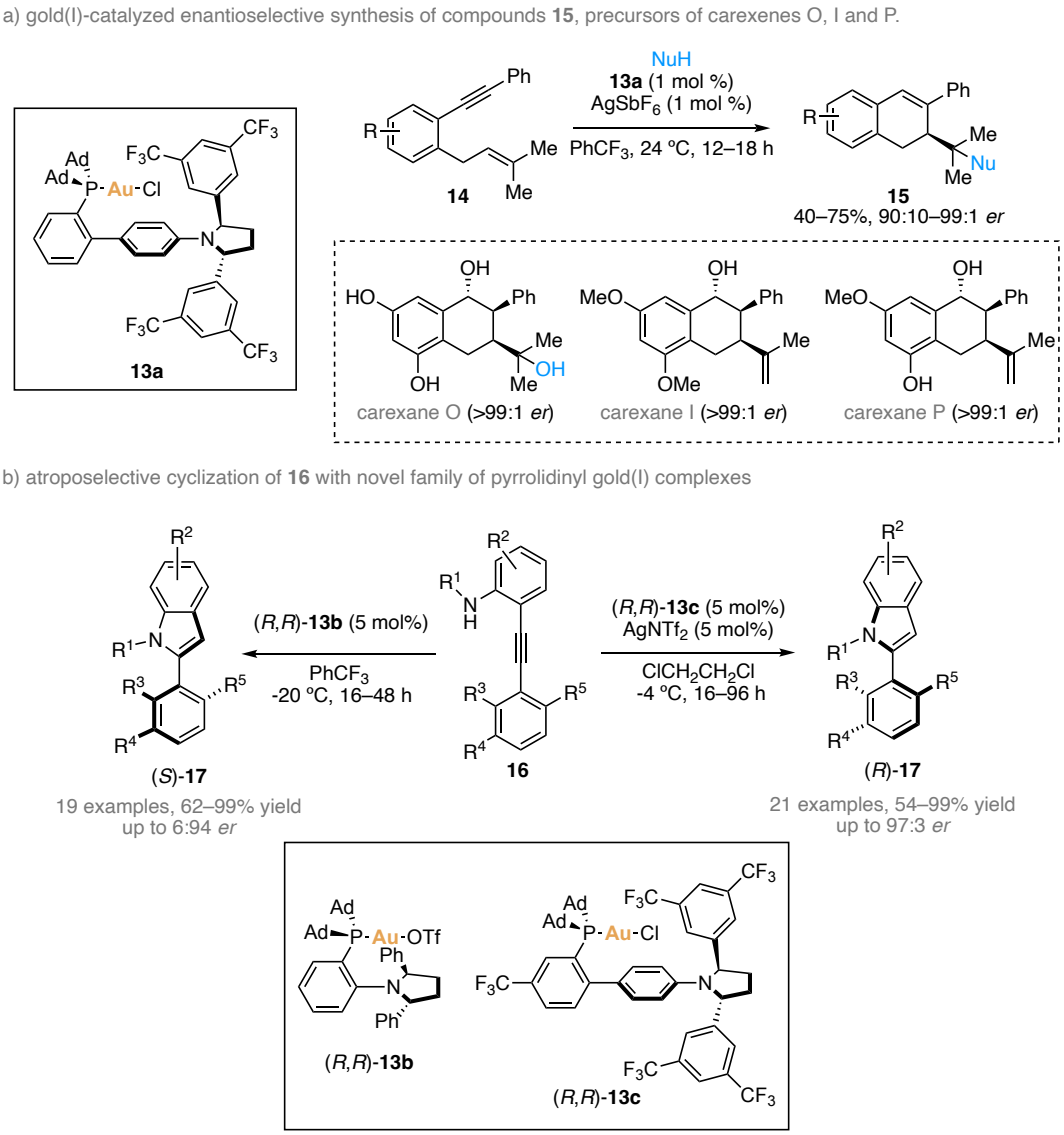


**Scheme 9**. Gold(I)-catalyzed enantioselective transformations using derived JohnPhos-type gold(I) complexes developed in our group.

Finally, the use of gold(III) catalysts in homogeneous catalysis remains undeveloped,[46] mainly, due to the high redox potential of gold(III), which facilitates reduction to gold(I) or formation of gold(0) species.[47] Moreover, the potential of chiral gold(III) catalysts lied in their square-

46 (a) H. Schmidbaur, A. Schier, Arabian J. Gold(III) Compounds for Homogeneous Catalysis *Sci. Eng.* **2012**, *37*, 1187–1225. (b) Rodriguez, J.; Bourissou, D. Well-Defined Chiral Gold(III) Complexes: New Opportunities in Asymmetric Catalysis, *Angew. Chem. Int. Ed.* **2018**, *57*, 386–388. (c) Rodriguez, J.; Szalóki, G.; Sosa Carrizo, E. D.; Saffon-Merceron, N.; Miqueu, K.; Bourissou, D. Gold(III) π-Allyl Complexes, *Angew. Chem. Int. Ed.* **2020**, *59*, 1511–1515.

47 (a) Hashmi, A. S. K.; Blanco, M. C.; Fischer, D.; Bats, J. W. Gold Catalysis: Evidence for the In-Situ Reduction of Gold(III) During the Cyclization of Allenyl Carbinols, *Eur. J. Org. Chem.* **2006**, *2006*, 1387–1389. (b) De Frémont, P.; Singh, R.; Stevens, E. D.; Petersen, J. L.; Nolan, S. P. Synthesis, Characterization and Reactivity of *N*-Heterocyclic Carbene Gold(III) Complexes, *Organometallics*

planar coordination geometry, that brings the chiral information closer to the reative center and therefore, which simplifies enantioinduction. Toste's group, for example, reported the use of catalyst **18** for the kinetic resolution of racemic 1,5 enynes **19**, affording chiral bicyclo[3.1.0]hexane **20** and enantioenriched 1,5-enyne **19** in the same transformation (Scheme 10).[48]

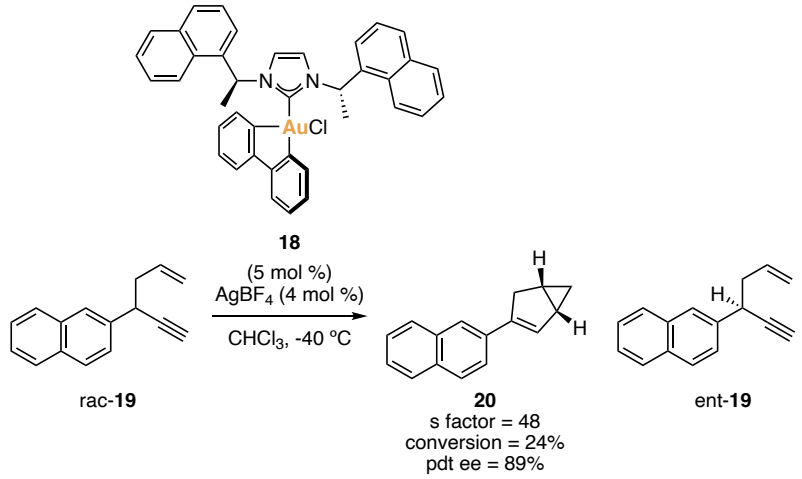


**Scheme 10**. Enantioselective gold(III)-catalyzed cyclization of 1,5 enyne **19**.

**2007**, *26*, 1376–1385. (c) Wolf, W. J.; Winston, M. S.; Toste, F. D. Exceptionally Fast Carbon–Carbon Bond Reductive Elimination from Gold(III), *Nat. Chem.* **2014**, *6*, 159–164.

48 Bohan, P. T.; Toste, F. D. Well-Defined Chiral Gold(III) Complex Catalyzed Direct Enantioconvergent Kinetic Resolution of 1,5-Enynes, *J. Am. Chem. Soc.* **2017**, *139*, 11016–11019.

# Chapter I*: Design and Synthesis of Novel Cavitand Gold(I) Complexes for the Cycloisomerization of Enynes*

**Introduction: Supramolecular Cavitands for Gold(I) Catalysis**

Supramolecular approaches in catalysis went through an important development during the last decades. Inspired by Nature's most efficient catalysts, enzymes, much effort has been devoted to modulating catalyst properties by placing active catalytic sides in molecular cages. Such enzyme mimics can be obtained by encapsulation of catalysts through covalent binding within cages or by supramolecular binding using complementary interactions with the capsule. As a result, the metal complex is isolated from the bulk phase leading to possible changes in reactivity in terms of selectivity as well as improved chemical recognition.[1]

In 2000, Rebek's group investigated the possibility of a synthetic receptor with an open, cleft-like structure. As a result, they designed a group of introverted functionalized resorcin[4]arene-based cavitands that generate a concave surface which would be used as a reactive site.[2] These compounds were used for chemical recognition of amines such as nicotine, by hydrogen bonding with introverted amide functionalities placed at the upper rim of the cavitands and directed towards the guest inside. Since then, the resorcin[4]arene cavity has become a widely utilized motif due to its capacity to stabilize intermediates and selectively bind guests of specific sizes[3] or which in turn can have an impact in the outcomes of chemical reactions.[4]

Additionally, Cram's pioneer work led to the definition of velcrands or velcraprexes as compounds whose molecules stick to one another leading to structures of starkly different shapes and behaviours.[5a] For instance, their initial studies on the conformational interconversion between *vase* and *kite* conformers on resorcin[4]arene-cavitand skeletons bearing four quinoxaline walls was rationalized by solvation-solvophobic effect (Scheme 1a).[5b] Taking advantage of this known equilibrium, Diederich and coworkers evaluated various H-bond acceptor groups, for their propensity to induce conformation

1 (a) Raynal, M.; Ballester, P.; Vidal-Ferran, A.; Leeuwen, P. W. N. M. van. Supramolecular Catalysis. Part 1: Non-Covalent Interactions as a Tool for Building and Modifying Homogeneous Catalysts, *Chem. Soc. Rev.* **2014**, *43*, 1660–1733. (b) Raynal, M.; Ballester, P.; Vidal-Ferran, A.; Leeuwen, P. W. N. M. van. Supramolecular Catalysis. Part 2: Artificial Enzyme Mimics, *Chem. Soc. Rev.* **2014**, *43*, 1734–1787.

2 Renslo, A. R.; Rebek, J., Jr. Molecular Recognition with Introverted Functionality, *Angew. Chem. Int. Ed.* **2000**, *39*, 3281–3283.

3 Iwasawa, T.; Hooley, R. J.; Rebek, J. Stabilization of Labile Carbonyl Addition Intermediates by a Synthetic Receptor, *Science* **2007**, *317*, 493–496.

4 Shenoy, S. R.; Pinacho Crisóstomo, F. R.; Iwasawa, T.; Rebek, J. Jr. Organocatalysis In a Synthetic Receptor with an Inwardly Directed Carboxylic Acid, *J. Am. Chem. Soc.* **2008**, *130*, 5658–5659.

5 (a) Moran, J. R.; Karbach, S.; Cram, D. J. Cavitands: Synthetic Molecular Vessels, *J. Am. Chem. Soc.* **1982**, *104*, 5826–5828. (b) Moran, J. R.; Ericson, J. L.; Dalcanale, E.; Bryant, J. A.; Knobler, C. B.; Cram, D. J. Vases and Kites as Cavitands, *J. Am. Chem. Soc.* **1991**, *113*, 5707–5714.

in resorcin[4]arene cavitands upon redox interconversion (Scheme 1b).[6a] The H-bond acceptors were placed on quinoxaline-type walls with the purpose of stabilizing the *vase* form only in the reduced hydroquinone state of the cavitand by forming H-bond with the hydroquinone OH groups.

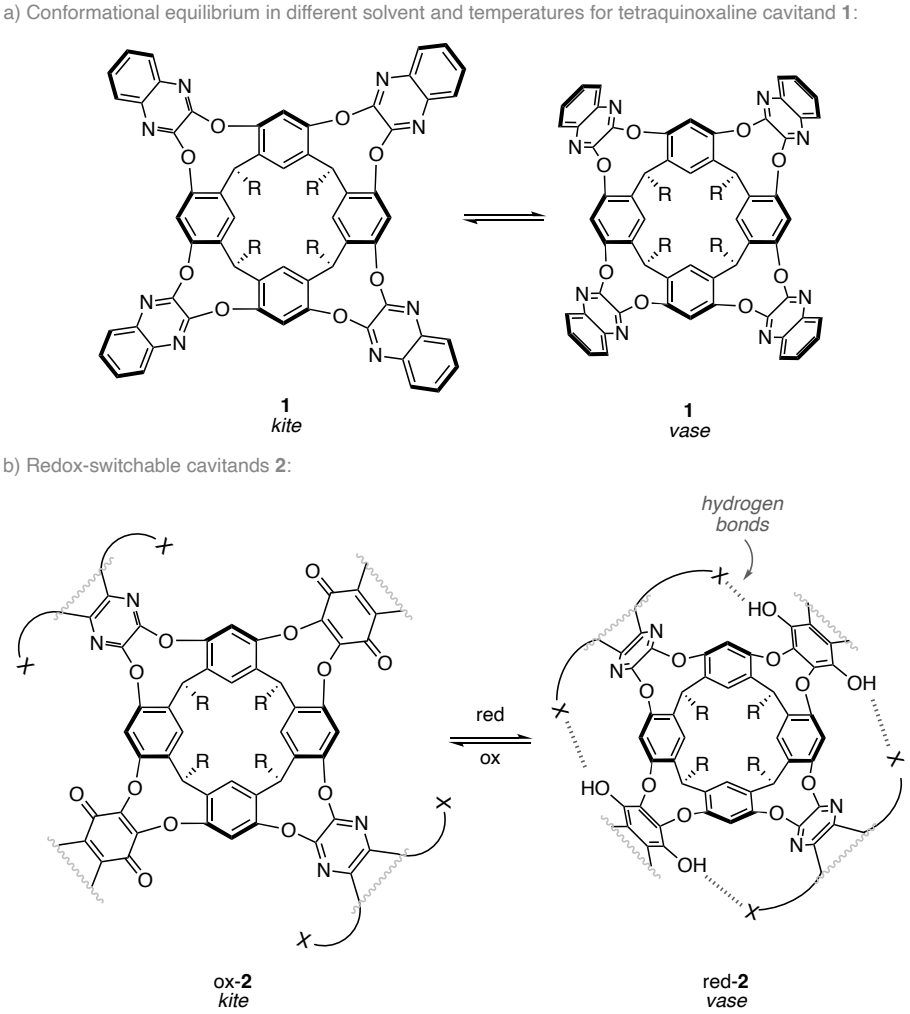


**Scheme 1**. Conformational equilibrium between *vase* and *kite* conformers of tetraquinoxaline cavitand **1** (a) and **2** (b). R = aliphatic chain. X = H-bond acceptor.

The design of semiquinone-based resorcin[4]arene cavitands expands the toolbox of switchable molecular grippers by introducing the first paramagnetic representatives.[6b] Later, the methodology was

6 (a) Pochorovski, I.; Milić, J.; Kolarski, D.; Gropp, C.; Schweizer, W. B.; Diederich, F. Evaluation of Hydrogen-Bond Acceptors for Redox-Switchable Resorcin[4]Arene Cavitands, *J. Am. Chem. Soc.* **2014**, *136*, 3852–3858. (b) Milić, J.; Zalibera, M.; Pochorovski, I.; Trapp, N.; Nomrowski, J.; Neshchadin, D.; Ruhlmann, L.; Boudon, C.; Wenger, O. S.; Savitsky, A.; Lubitz, W.; Gescheidt, G.; Diederich, F. Paramagnetic Molecular Grippers: The Elements of Six-State Redox Switches, *J. Phys. Chem. Lett.* **2016**, *7*, 2470–2477. (c) Milić, J.; Zalibera, M.; Talaat, D.; Nomrowski, J.; Trapp, N.; Ruhlmann, L.; Boudon, C.; Wenger, O. S.; Savitsky, A.; Lubitz, W.; Diederich, F. Photoredox-Switchable Resorcin[4]Arene Cavitands: Radical Control of Molecular Gripping Machinery *via* Hydrogen Bonding, *Chem. Eur. J.* **2018**, *24*, 1431–1440.

expanded towards the analysis of several H-bond donor groups that mimic natural amino acids residues in the reaction center.[6c]

Furthermore, it has long been recognized that catalysts possessing two or more metal centres in proximity can be uniquely effective in catalyzing certain types of reactions.[7] Molecular modelling studies indicate that the two metallic centers should be at an optimal 6–7 Å distance to interact both with the alkyne and the nearest alkene in transformations involving enyne-type substrates. These required M–M distances can be easily achieved with digold(I) complexes of resorcin[4]arene-phosphonite cavitand ligands, which have been proved to catalyze cross-dimerizations of terminal alkynes.[8]

In the field of homogeneous gold(I) catalysis, the encapsulation of gold(I) nucleolus centers within complexes that form a cage-like structure has been of great interest for studying its properties and abilities for folding substrates. In this context, Iwasawa's group reported a synthetic strategy towards the first resorcin[4]arene-based gold(I)-cavitand with phosphoramidite, phosphite or phosphonite moieties outside the cavities (Scheme 2, **3a**, **3b** and **3c**, respectively).[9] Such complexes show catalytic activity in the addition of water to terminal alkynes **4** (Scheme 2, top) and in the intramolecular cyclization of diketo-alkyne **6**, also known as Conia-ene reaction, giving a mixture of products **6a** and **7b** (Scheme 2, bottom). Even though different product ratios were observed with each complex, the best outcome in terms of selectivity and yield was obtained when using phosphoramidite complex **3a**.

7 Gavrilova, A. L.; Bosnich, B. Principles of Mononucleating and Binucleating Ligand Design, *Chem. Rev.* **2004**, *104*, 349–384.

8 Jans, A. C. H.; Caumes, X.; Reek, J. N. H. Gold Catalysis in (Supra)Molecular Cages to Control Reactivity and Selectivity, *ChemCatChem* **2019**, *11*, 287–297.

9 Schramm, M. P.; Kanaura, M.; Ito, K.; Ide, M.; Iwasawa, T. Introverted Phosphorus-Au Cavitands for Catalytic Use, *Eur. J. Org. Chem.* **2016**, 813–820.

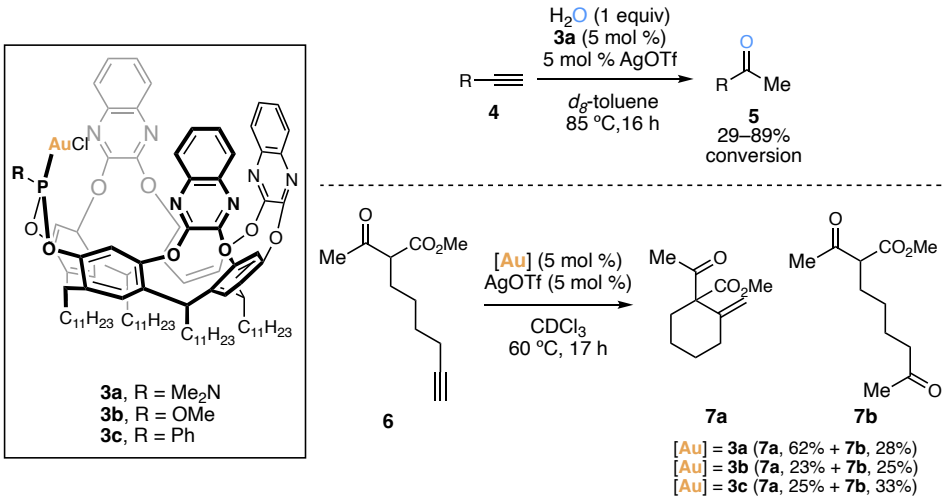


**Scheme 2**. First gold(I)-cavitand complexes and their applied catalytic reactions: hydration of terminal alkynes (top) and Conia-ene reaction (bottom).

Later, the same group published the synthesis of an analogous cavitand containing two gold(I) units, with both metal centres located inside the cavity (Scheme 3, **8a**).[10] In this case, **8a** efficiently catalyzes inter- and intramolecular dimerization of terminal alkynes to afford conjugated enynes, leaving behind any kind of homo-dimerizations (Scheme 3, top). Cross-dimerizations give rise to different products, including highly strained enyne **13** by intramolecular dimerization, which can be reduced in very good yields to afford the cyclic structure **14** (Scheme 3, center). Analogously, they prepared a functionalized gold(I)-cavitand with inwardly oriented gold(I) center and P=O **8b**, using it for the selective hydration of internal alkynes **15** because of the interaction between water and the P=O moiety (Scheme 3, bottom).

10 Endo, N.; Kanaura, M.; Schramm, M. P.; Iwasawa, T. An Introverted Bis-Au Cavitand and Its Catalytic Dimerization of Terminal Alkynes, *Eur. J. Org. Chem.* **2016**, *14*, 2514–2521.

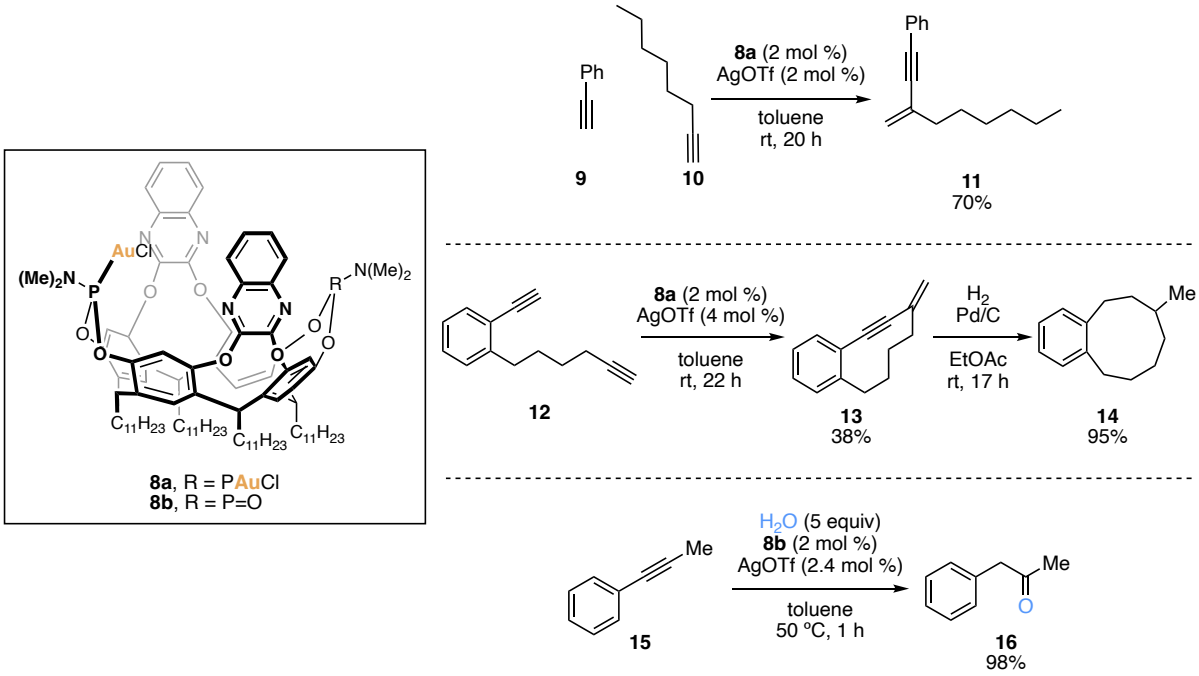


**Scheme 3**. Studied reactivity of binuclear gold(I)-cavitand **8a** and oxidized mononuclear gold(I)-cavitand **8b**.

Schramm's group also evaluated the activity of resorcin[4]arene gold(I)-cavitands, focusing on the relevance of the cavity size created, which can discriminate between different guests.[11] Another example is their studies in the cycloisomerization reaction of alkyne-arenes, comparing the activity of gold(I)-cavitand complex **8a** with an electronically similar gold(I)-phosphite complex **17** (Scheme 4).[11b] Their studies demonstrated that due to the cavity, there is a size-selection effect with shapes that are complementary for cavitand binding (Scheme 4).

11 (a) Ho, T. D.; Schramm, M. P. Au-Cavitand Catalyzed Alkyne-Acid Cyclizations, *Eur. J. Org. Chem.* **2019**, *33*, 5678–5684. (b) Rusali, L. E.; Schramm, M. P. Au-Cavitands: Size Governed Arene-Alkyne Cycloisomerization, *Tetrahedron Lett.* **2020**, *61*, 152333.

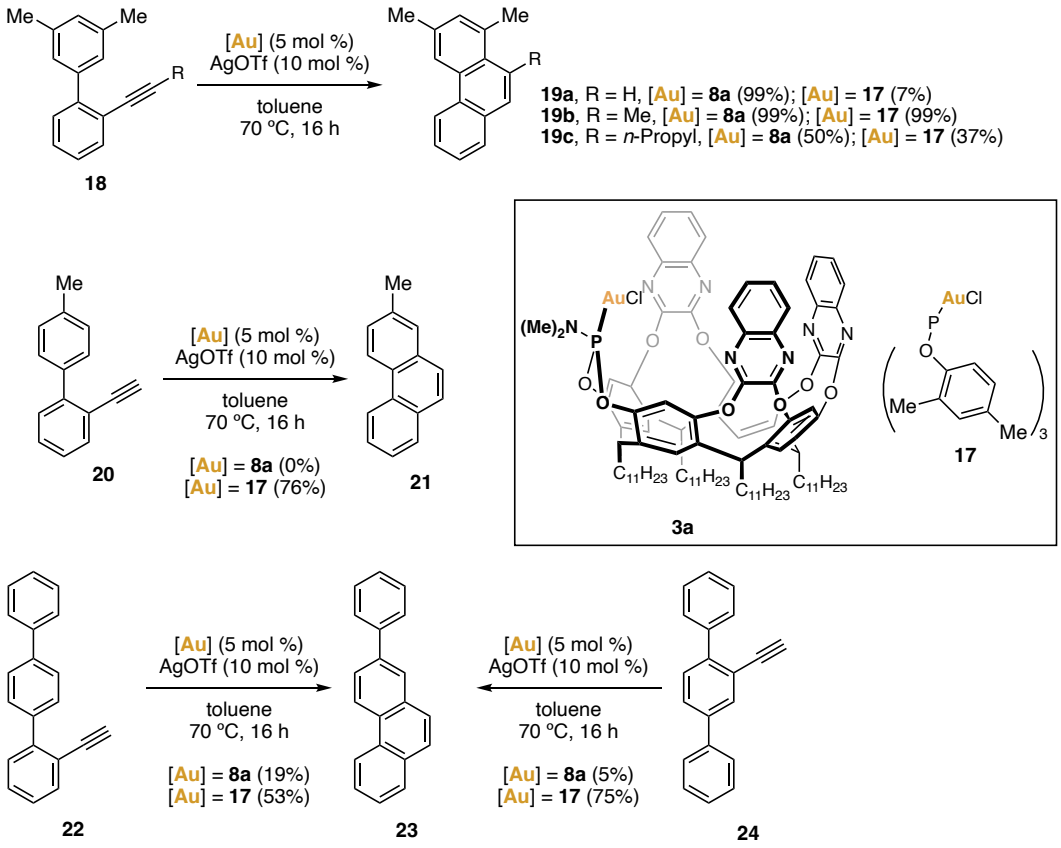


**Scheme 4**. Size-governed arene-alkyne cycloisomerization.

Moreover, the impact of different cavitand walls in gold(I)-cavitand complexes has also been explored in reactivity. For that, different alternatives to quinoxaline walls were synthesized giving rise to gold(I)-cavitands **25a**, **25b** and **25c** (Scheme 5).[12] The studies have shown that the quinoxaline walls play a crucial role by promoting interactions between the two alkyne substrates and stabilizing intermediates through the formation of a strong π-cloud. For example, the cross-dimerization of terminal alkynes produced a mixture of **11** and **25** with such gold(I)-cavitand complexes but adduct **11** was produced in higher yield with complex **25a** (Scheme 5, bottom).[12b]

12 (a) Kanaura, M.; Endo, N.; Schramm, M. P.; Iwasawa, T. Evaluation of the Reactivity of Metallocatalytic Cavities in the Dimerization of Terminal Alkynes, *Eur. J. Org. Chem.* **2016**, 4970–4975. (b) Natarajan, N.; Brenner, E.; Sémeril, D.; Matt, D.; Harrowfield, J. The Use of Resorcinarene Cavitands in Metal-Based Catalysis, *Eur. J. Org. Chem.* **2017**, 6100–6113.

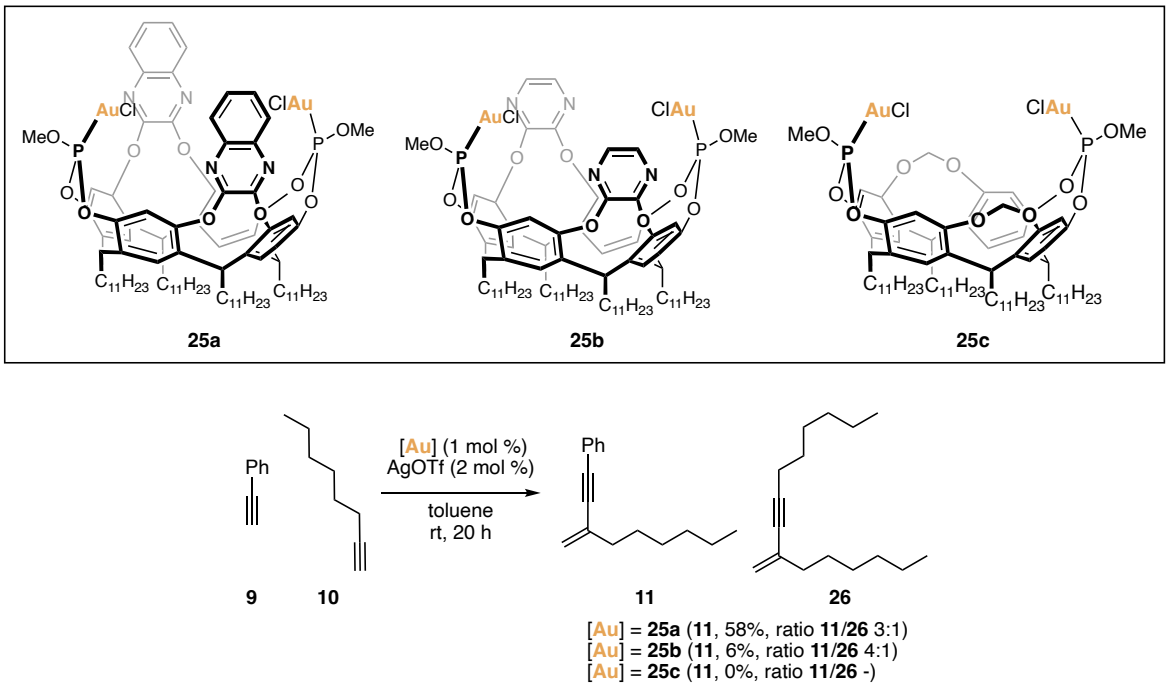


**Scheme 5**. Variations in the wall effect influencing the reactivity of gold(I)-cavitand systems.

Our group reported in 2021 the synthesis of a family of gold(I)-cavitand complexes bearing both quinoxaline and quinone walls in their core.[13] The family included achiral and chiral gold(I)-cavitand complexes, composed by mononuclear, binuclear, and cationic species (Scheme 6a). On one hand, new selectivity[14] was uncovered in the cyclization of dienynes with achiral gold(I)-cavitand complex **27** (Scheme 6b). On the other hand, chiral catalyst (*S*,*S*,*S*,*S*)-**28** allowed to develop an enantioselective alkoxycyclization of 1,6-enynes **31** in good to excellent yields and enantioselectivities (Scheme 6c). These studies demonstrated that the cavity of the gold(I) complexes forces the high observed regio- and stereoselectivities.

13 Martín-Torres, I.; Ogalla, G.; Yang, J.-M.; Rinaldi, A.; Echavarren, A. M. Enantioselective Alkoxycyclization of 1,6-Enynes with Gold(I)-Cavitands: Total Synthesis of Mafaicheenamine C, *Angew. Chem. Int. Ed.* **2021**, *60*, 9339–9344.

14 Nieto-Oberhuber, C.; Muñoz, M. P.; López, S.; Jiménez-Núñez, E.; Nevado, C.; Herrero-Gómez, E.; Raducan, M.; Echavarren, A. M. Gold(I)-Catalyzed Cyclizations of 1,6-Enynes: Alkoxycyclizations and *exo*/*endo* Skeletal Rearrangements, *Chem. Eur. J.* **2006**, *12*, 1677–1693.

a) Selected cationic gold(I)-cavitand complexes **27** and (*S*,*S*,*S*,*S*)-**28**

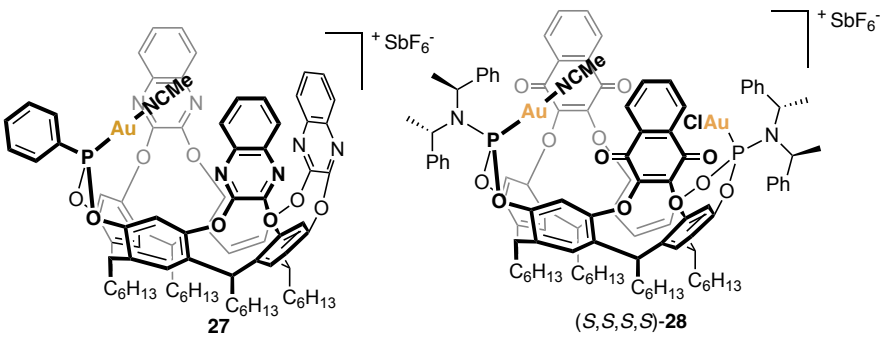


a) *Exo*/*endo* selectivity in the cyclization of *Z*-1,6-dienyne **29**

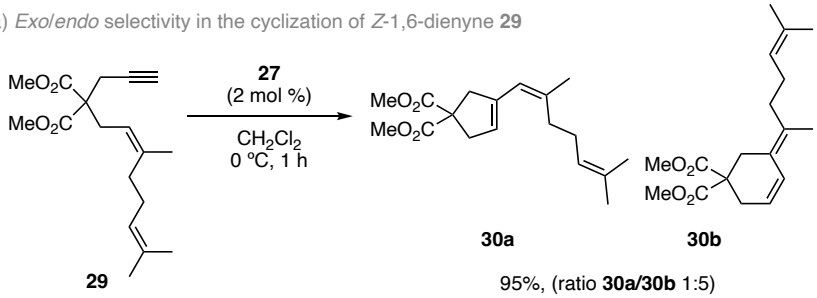


b) Enantioselective alkoxycyclization of 1,6-dienyne **31**

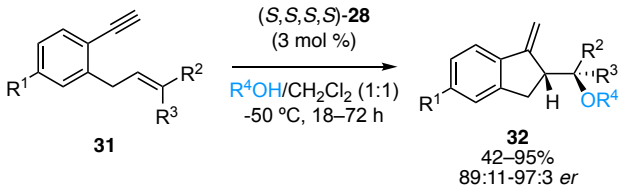


**Scheme 6**. Gold(I)-cavitand complexes (a) for the (b) selective *endo*-cyclization of dienyne **29** and (c) enantioselective alkoxycyclization of dienyne **31**.

## Objectives

Our objective was the design and synthesis of a new family of gold(I)-cavitand complexes based on the use of cavitands as ligands for new enantioselective transformations. Different approaches have been developed and will be discussed over the chapter.

First, our objective was the introduction of chirality in the ligand's skeleton that will be facing the gold(I) center inside the cavity by using (1) amino-acids or (2) phthalimide moieties.

Second, the use of chiral silver counteranions with achiral gold(I)-cavitands aiming to perform asymmetric H-bonded counterion directed catalysis.

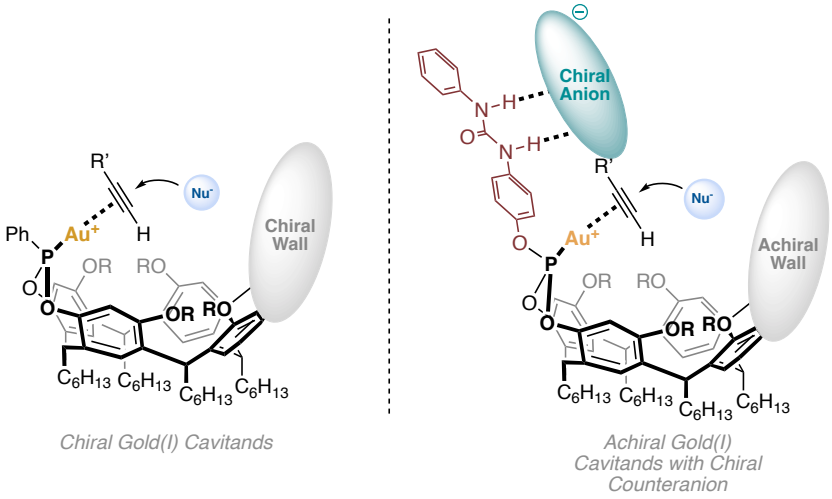


**Figure 1**. New gold(I)-cavitand complexes design strategies.

## Results and Discussion

### Synthesis of Common Ligand Core for the Novel Gold(I)-Cavitand Complexes

The synthesis of the cavitand-ligand precursors present in the gold(I)-cavitand complexes had already been developed[9,10] and so, the synthesis was performed by adapting this reported procedure. The route starts from the condensation of resorcinol and heptanal under acidic conditions to obtain resorcin[4]arene **34** (Scheme 7).

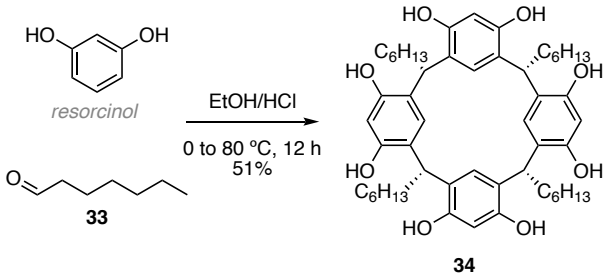


**Scheme 7**. Synthesis of resorcin[4]arene **34**.

Tetraquinoxaline and tetranaphthoquinone cavitands **1a** and **1b** are obtained by treating **34** with 2,3-dichloroquinoxaline **35a** or 2,3-dichloronaphthoquinone **35b** under basic conditions (Scheme 8).

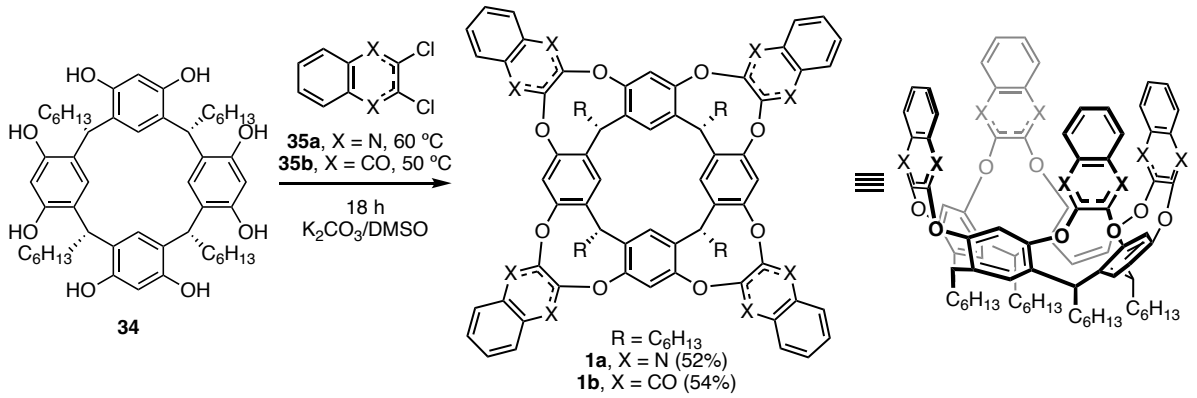


**Scheme 8**. Synthesis of tetraquinoxaline **1a** and tetranaphthoquinone **1b**.

Then, as previously reported by Tunstad,[15] an excision of one quinoxaline wall units is performed selectively to form **36**. Alternatively, two wall units can be excissioned by using 2.4 equiv of catechol to obtain the corresponding tetraphenols **37a** and **37b** (Scheme 9).

15 Castro, P. P.; Zhao, G.; Masangkay, G. A.; Hernandez, C.; Gutierrez-Tunstad, L. M. Quinoxaline Excision: A Novel Approach to Tri- and Diquinoxaline Cavitands, *Org. Lett.* **2004**, *6*, 333–336.

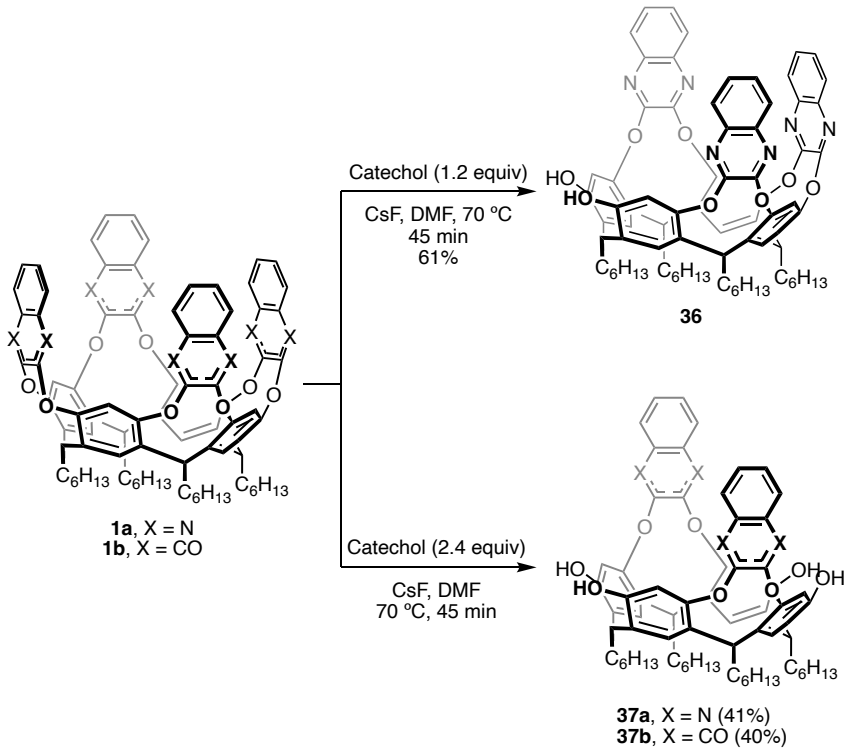


**Scheme 9.** Synthesis of cavitand-ligand precursors.

With these ligand precursors in hand, different routes have been designed to synthesize a new family of gold(I)-cavitand complexes. Their preparation and performance in catalysis will be covered through the different sections in this chapter.

## Attempted Synthesis of Chiral Amino Acid-Cavitand Gold(I) Complex

### Introduction

Amino acids are organic compounds which contain one or more amino groups (–$NH_2$), one or more carboxyl groups (–COOH) and a side chain (–R) in their structure. Two amino acids can form a dipeptide through a peptide bond by condensation reaction between the carboxylic group of one amino acid and the amino group of the other one, giving an amide upon release of water. If they further react, they become the building blocks of longer peptides, proteins, and components of other complex polymers (Scheme 10).[16]

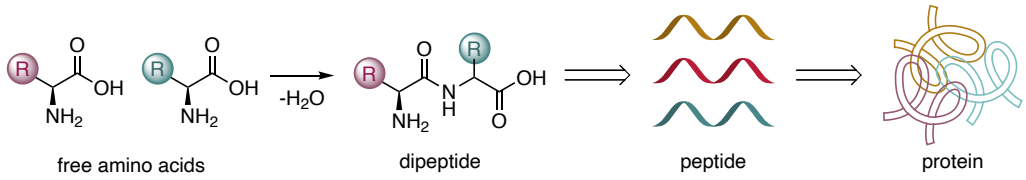


**Scheme 10**. General structure of amino acids and their assembly to give proteins.

Their absolute configuration at the *α*-carbon atom of the *α*-amino acids is designated by the prefix *D*/*L* or the *R*/*S* system. Interestingly, although more than 300 amino acids have been identified in nature, proteins of humans are made almost exclusively from 20 *L*-*α*-amino acids. On the other hand, *D*-amino acids are known to be more present in antibiotics or bacterial peptides.[17]

Amino acids are known to be involved in the enzymatic activity of several enzymes.[18] Recently, it has been proved their ability to catalyze reactions in the prebiotic world,[19] based on the hypothesis that the first catalyst was an RNA molecule.[20]

Additionally, several decades after the first use of an amino acid as a catalyst, amino acids and simple peptides have become an important subset in asymmetric catalysts.[21] They have provided a chiral

16 Moo-Young, M. Comprehensive Biotechnology, 2d ed.; *Science Direct*, **2011**.

17 Takei, Y.; Hironori, A.; Kazuyoshi, T.; Handbook of Hormones: Comparative Endocrinology for Basic and Clinical Research, *Brand New Hardcover*, **2015**.

18 Ribeiro, A. J. M.; Tyzack, J. D.; Borkakoti, N.; Holliday, G. L.; Thornton, J. M. A Global Analysis of Function and Conservation of Catalytic Residues in Enzymes, *J. Biol. Chem.* **2020**, *295*, 314–324.

19 Agazani, O.; Tulpin, A.; Reches, M. An Individual Amino Acid as a Possible Prebiotic Catalyst, *ChemSystemsChem* **2021**, *3*, e2100005.

20 (a) Ruiz-Mirazo, K.; Briones, C.; de la Escosura, A. Prebiotic Systems Chemistry: New Perspectives for the Origins of Life, *Chem. Rev.* **2014**, *114*, 285–366.

21 Jarvo, E. R.; Miller, S. J. Amino Acids and Peptides as Asymmetric Organocatalysts, *Tetrahedron* **2002**, *58*, 2481–2495.

environment for asymmetric catalyzed transformations such as in aldol reactions,[22] hydrocyanation[23] or epoxidation.[24]

Barbas III's group demonstrated that one of the most efficient amino acids for asymmetric transformations is *L*-proline.[25] For instance, the synthesis of the Wieland-Miescher ketone **40** was reported through an *L*-proline catalyzed asymmetric Robinson annulation reaction with 76% *ee* (Scheme 11).[25b]

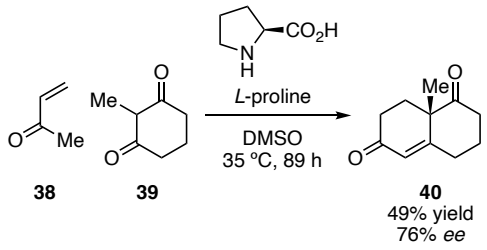


**Scheme 11**. *L*-Proline catalyzed asymmetric Robinson annulation reaction.

Furthermore, the use of peptide–metal complexes as asymmetric catalysts has also shown been developed.[26] For instance, the first catalytic enantioselective Diels–Alder reaction in water was developed by Engberts, who studied a catalytic system based on copper(II) using $\alpha$-amino acid ligands and observed higher enantioselectivities than in organic solvents (Scheme 12, left).[27] Another example

22 (a) Eder, U.; Sauer, G.; Wiechert, R. New Type of Asymmetric Cyclization to Optically Active Steroid CD Partial Structures, *Angew. Chem. Int. Ed. Engl.* **1971**, *10*, 496–497. (b) List, B. The Direct Catalytic Asymmetric Three-Component Mannich Reaction, *J. Am. Chem. Soc.* **2000**, *122*, 9336–9337. (c) List, B.; Pojarliev, P.; Biller, W. T.; Martin, H. J. The Proline-Catalyzed Direct Asymmetric Three-Component Mannich Reaction: Scope, Optimization, and Application to the Highly Enantioselective Synthesis of 1,2-Amino Alcohols, *J. Am. Chem. Soc*. **2002**, *124*, 827–833.

23 Iyer, M. S.; Gigstad, K. M.; Namdev, N. D.; Lipton, M. Asymmetric Catalysis of the Strecker Amino Acid Synthesis by a Cyclic Dipeptide, *Amino Acids* **1996**, *11*, 259–268.

24 Porter, M. J.; Skidmore, J. Asymmetric Epoxidation of Electron-Deficient Olefins, *Chem. Commun.* **2000**, *14*, 1215–1225.

25 (a) List, B.; Lerner, R. A.; Barbas, C. F. Proline-Catalyzed Direct Asymmetric Aldol Reactions, *J. Am. Chem. Soc*. **2000**, *122*, 2395–2396. (b) Bui, T.; Barbas, C. F. A Proline-Catalyzed Asymmetric Robinson Annulation Reaction, *Tetrahedron Lett.* **2000**, *41*, 6951–6954. (c) Sakthivel, K.; Notz, W.; Bui, T.; Barbas, C. F. Amino Acid Catalyzed Direct Asymmetric Aldol Reactions: A Bioorganic Approach to Catalytic Asymmetric Carbon−Carbon Bond-Forming Reactions, *J. Am. Chem. Soc.* **2001**, *123*, 5260–5267.

26 Paradowska, J.; Stodulski, M.; Mlynarski, J. Catalysts Based on Amino Acids for Asymmetric Reactions in Water, *Angew. Chem. Int. Ed.* **2009**, *48*, 4288–4297.

27 Otto, S.; Engberts, J. B. F. N. A Systematic Study of Ligand Effects on a Lewis-Acid-Catalyzed Diels−Alder Reaction in Water. Water-Enhanced Enantioselectivity, *J. Am. Chem. Soc*. **1999**, *121*, 6798–6806.

is a chiral Cr(II) complex for the reduction of prochiral ketones **43**,[28] where the enantioselectivities were highly dependent on the structure of the ligand and the composition of the metal-ligand complex (Scheme 12, right).

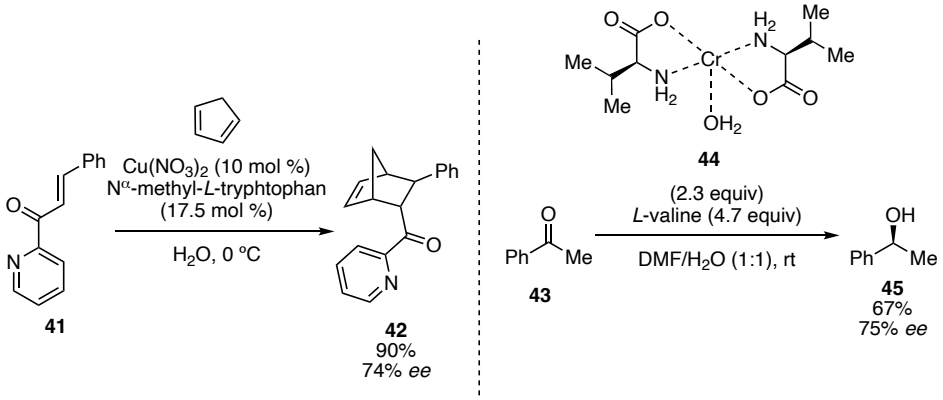


**Scheme 12**. Selected examples of amino acid-catalyzed asymmetric reactions.

Recently in our group, it was developed the synthesis of JohnPhos-type gold(I) complexes with one or more *α*-amino acid in their structure as chiral element.[29] Their catalytic activity was tested, for instance in the formal [4+2] cycloaddition of 1,6-arylenyne **47** (Scheme 13). Despite its catalytic activity in the reaction, enantioselectivities were poor, presumably due to its location far from the reaction site.

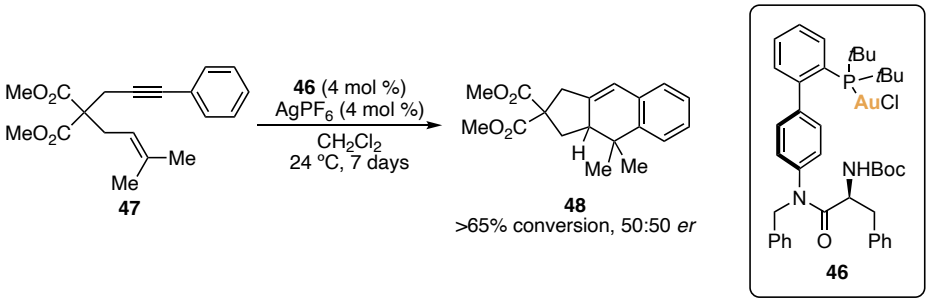


**Scheme 13**. Amino acid-Phos gold(I) complex **46** for the formal [4+2] cycloaddition of enyne **47**.

28 Micskei, K.; Hajdu, C.; Wessjohann, L. A.; Mercs, L.; Kiss-Szikszai, A.; Patonay, T. Enantioselective Reduction of Prochiral Ketones by Chromium(II) Amino Acid Complexes, *Tetrahedron Asymmetry* **2004**, *15*, 1735–1744.

29 Arroyo Bondía, A. Doctoral Thesis, Design of New Gold(I) Catalysts: Dissecting Electronic and Steric Effects, **2023**, URV-ICIQ.

**Synthetic Approaches Towards the Chiral Amino Acid-Cavitand Gold(I) Complex**

For the synthesis of gold(I)-cavitand complexes containing one amino acid in their structure, we planned to follow the retrosynthetic pathway outlined in Scheme 14. This involved using a cycloaddition reaction as the key step to form the core of the new chiral wall, followed by attachment to the resorcin[4]arene–based cavitand skeleton, and finally, the introduction of the gold(I) center.

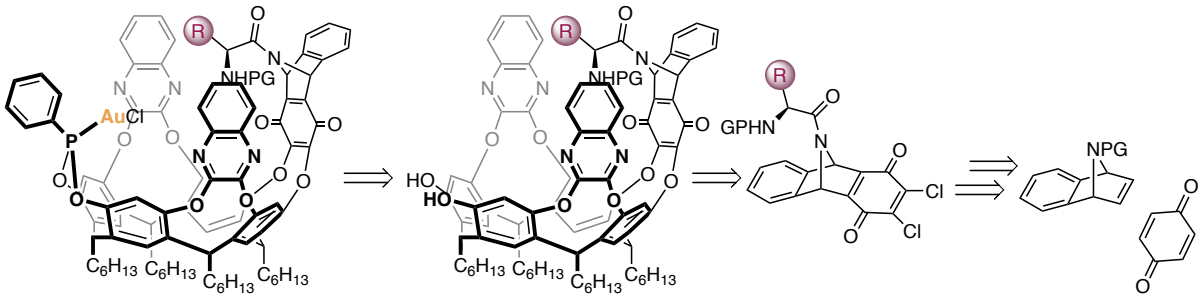


**Scheme 14**. Retrosynthetic analysis for the synthesis of the amino acid gold(I)-cavitand complexes. PG = protecting group.

The synthesis started with the preparation of **51a**, synthesized as a result from the Diels Alder reaction between benzine, generated from silyl-aryl triflate **49** and *N*-(2'-pyridylsulfonyl)pyrrole **50** in the presence of CsF. Then, following a well-studied cycloaddition reaction between 7-azabenzonorbornadiene and monocyclic dienophiles,[30] **51a** was obtained as the only product when reacting **51a** and *p*-benzoquinone (Scheme 15).

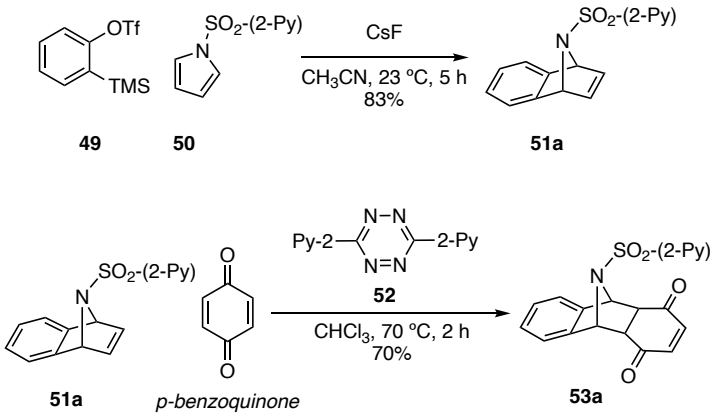


**Scheme 15**. Synthesis of cycloadduct **53a**.

30 Sasaki, T.; Manabe, T.; Nishida, S. Cycloaddition Reactions of 1,4-[(*tert*-butyloxycarbonyl)imino]-1,4-dihydronaphthalene, *J. Org. Chem.* **1980**, *45*, 476–479.

Next, relying on the reported procedures for the deprotection of arenesulfonamides by magnesium reduction under ultrasonic conditions,[31] we tried to perform the arenesulfonamide cleavage from *N*-azabycicle **53a**. However, this reaction failed. Alternatively, we tried to keep the protecting group and chlorinate the structure using $SOCl_2$ and pyridine, but **55a** was not obtained (Scheme 16).

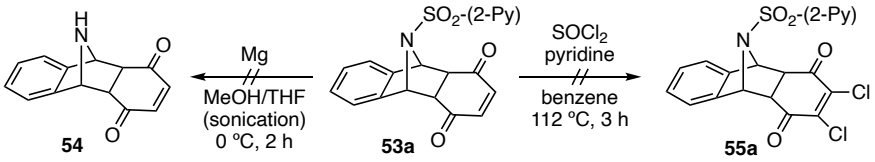


**Scheme 16**. Attempts for the functionalization of **53a**.

In another approach, we used a different *N*-protecting group. We followed a similar route with a revised strategy to obtain **51b**,[32] this time, featuring an *N*-Boc-protected amine. Then, the cycloaddition reaction was carried out with the already chlorinated *p*-benzoquinone **59b**, prepared in two steps from *para*-benzoquinone, leading to the formation of the tetracyclic compound **55b** (Scheme 17).

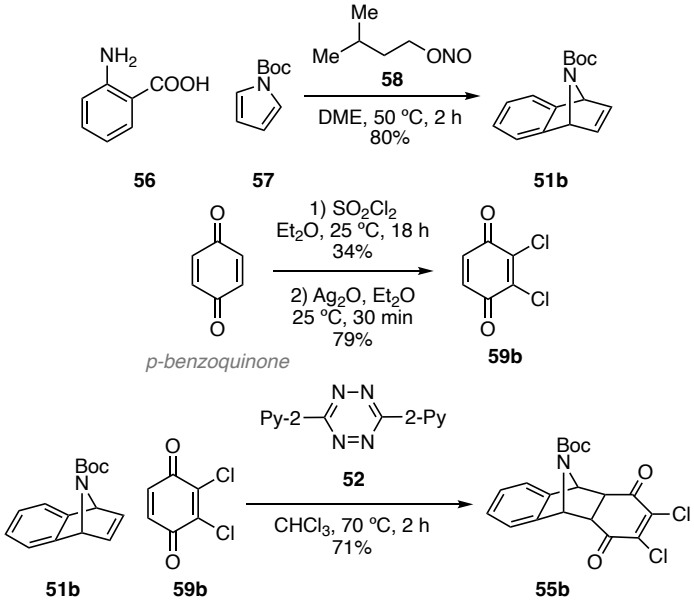


**Scheme 17**. Synthesis of cycloadduct **55b**.

31 (a) Nyasse, B.; Grehn, L.; Ragnarsson, U. Mild, Efficient Cleavage of Arenesulfonamides by Magnesium Reduction, *Chem. Commun.* **1997**, *11*, 1017–1018. (b) Pak, C. S.; Lim, D. S. Deprotection of 2-Pyridyl sylfonyl Group from Pyridine-2-sulfonamides by Magnesium in Methanol, *Synth. Commun.* **2001**, *31*, 2209–2214.

32 Arrayás, R. G.; Cabrera, S.; Carretero, J. C. Copper-Catalyzed Anti-Stereocontrolled Ring-Opening of Azabicyclic Alkenes with Grignard Reagents, *Org. Lett.* **2005**, *7*, 219–221.

Despite various attempts at amine deprotection, each trial resulted in decomposition without yielding free amine **60**. Likewise, our efforts to aromatize the quinone ring to **61b**, with the intention to further oxidize the ring later to form **62b**, were unsuccessful (Scheme 18).

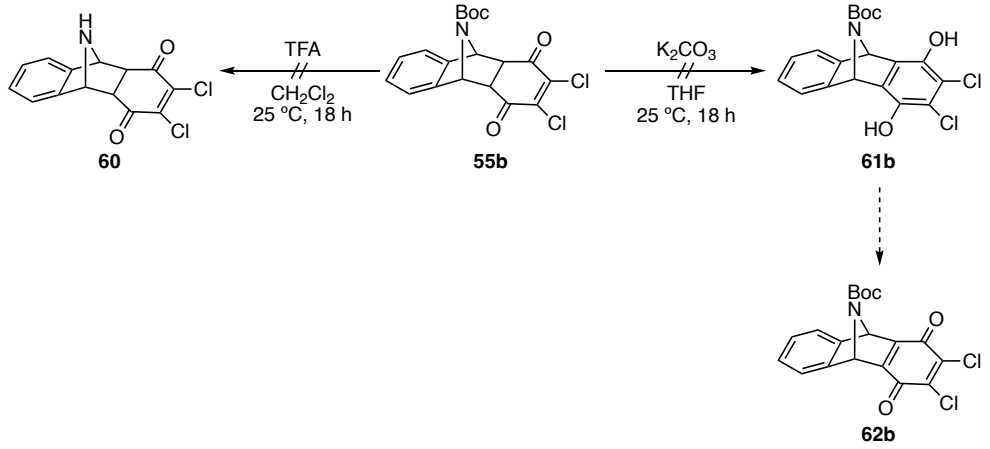


**Scheme 18**. Attempts for the functionalization of **55b**.

Our next strategy involved working directly with the amino acid on the skeleton to construct the desired amino acid-cavitand wall. Following the *N*-Boc deprotection of **51b**, we used *N*-protected amino acid *N*-Boc-L-valine to form an amide bond using HATU as coupling agent, obtaining **51c** in 93% yield over two steps (Scheme 19). The structure of this adduct **51c** was confirmed by X-ray diffraction (Figure 2). The cycloaddition reaction with chlorinated *p*-beznoquinone **59b** then, yielded **55c** in 70% yield.

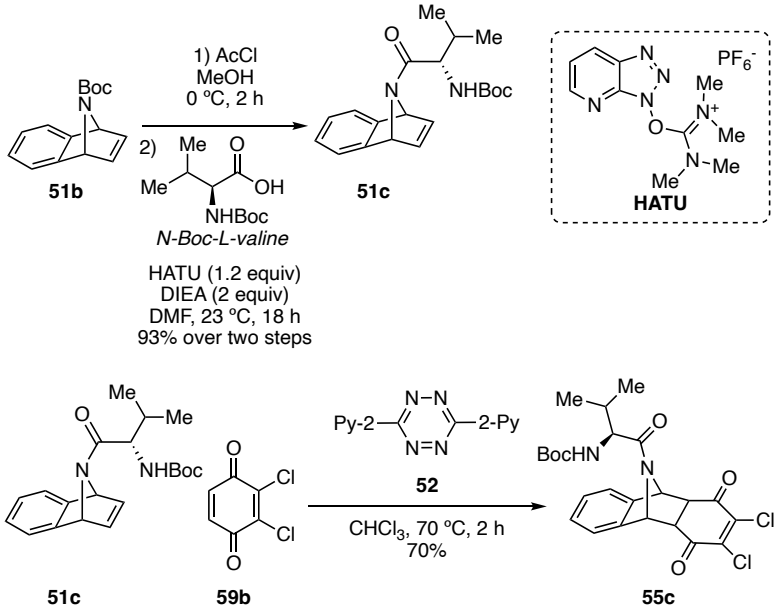


**Scheme 19**. Synthesis of amino acid cycloadduct **57c**.

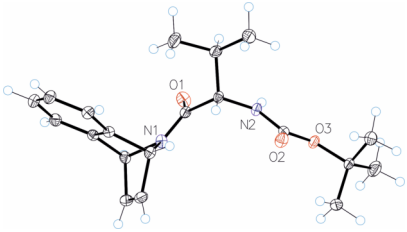


**Figure 2**. X-Ray structure of **51c**.

At this stage, the oxidation of the chlorinated ring, prior to its attachment to the resorcin[4]arene cavitand core, was still required. To achieve this, the first step involved aromatizing **55c** under basic conditions, resulting in the formation of diphenol **61c**, which was subsequently oxidized using 2,3-dichloro-5,6-dicyano-1,4-benzoquinone (DDQ), yielding its benzoquinone adduct **62c** in 61% yield (Scheme 20).

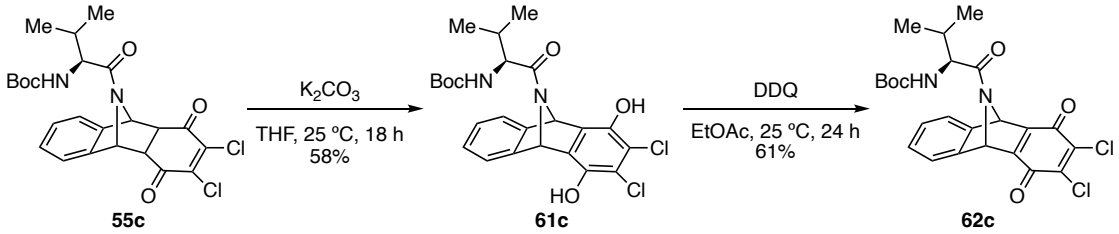


**Scheme 20**. Synthesis of amino acid-cavitand wall **62c**.

Then, we explored various conditions to attach the afforded amino acid-cavitand wall **62c** to the symmetric resorcin[4]arene cavitand core: tetraphenol bearing two quinoxaline **37a** or two naphthoquinone walls **37b** (Scheme 21). Unfortunately, all our attempts were unsuccessful, resulting in decomposition or the formation of inseparable mixtures of unknown compounds. These results underscored the challenges of optimizing the reaction conditions for this specific transformation.

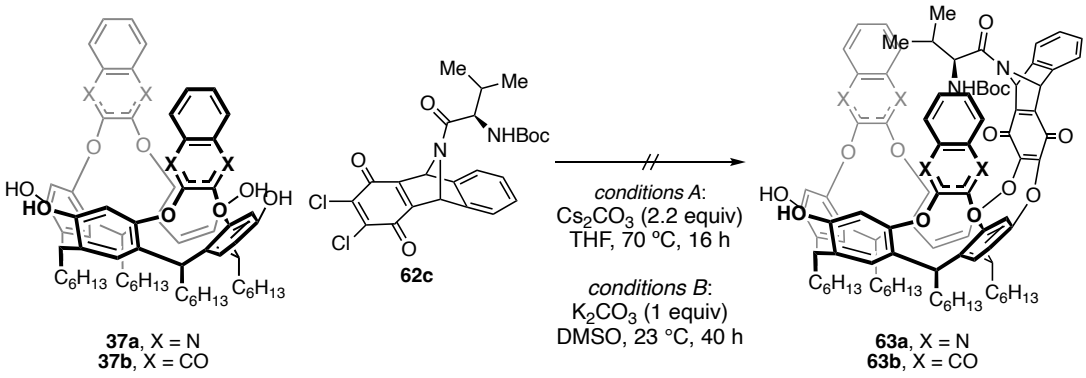


**Scheme 21**. Attempts for the introduction of the new amino acid-cavitand wall **62c** into the resorcin[4]arene cavitand core.

Due to the difficulties for introducing the amino acid wall into the cavitand, we decided to continue exploring the introduction of a chiral moiety on the cavitand core by other means.

## Gold(I)-Cavitand Complex Bearing a Phthalimide Chiral Wall[33]

### Introduction

The first introduction of phthalimide–type walls in cavitand cores was part of Cram's pioneering research in this field.[34] They used *N*-methylphtalamide as an example from a family of synthesized velcraplexes. It was reported the controlled conformational *vase-kite* interconversion of diquinoxaline-based cavitands bearing different types of walls were modified by protonation,[35a] or metal coordination.[35b]

Analogously, Rebek's group has been studying methodologies involving resorcin[4]arene based cavitands for generating 'container' complexes: molecular capsules that are hold together by hydrogen bonds and are capable of hosting guest molecules inside.[36] They developed a family of cylindrical molecular cavitand capsules that forms dimers in solution through hydrogen bonding at their edges. This is due to the presence of the phthalimide walls, which offer hydrogens of one molecule that interact with two carbonyl oxygens of another cavitand (Scheme 22).

33 Work done in collaboration with Dr. Martín Torres.

34 Cram, D. J.; Choi, H. J.; Bryant, J. A.; Knobler, C. B. Host-Guest Complexation. 62. Solvophobic and Entropic Driving Forces for Forming Velcraplexes, Which Are 4-Fold, Lock-Key Dimers in Organic Media, *J. Am. Chem. Soc*. **1992**, *114*, 7748–7765.

35 (a) Szafraniec, A.; Iwanek, W. Intramolecular Hydrogen Bond Driven Conformational Selectivity of Coumarin Derivatives of Resorcin[4]Arene, *Int. J. Mol. Sci.* **2020**, *21*, 6160. (b) García-López, V.; Zalibera, M.; Trapp, N.; Kuss-Petermann, M.; Wenger, O. S.; Diederich, F. Stimuli-Responsive Resorcin[4]Arene Cavitands: Toward Visible-Light-Activated Molecular Grippers, *Chem. Eur. J.* **2020**, *26*, 11451–11461.

36 (a) Heinz, T.; Rudkevich, D. M.; Rebek, J. Pairwise Selection of Guests in a Cylindrical Molecular Capsule of Nanometre Dimensions, *Nature* **1998**, *394*, 764–766. (b) Körner, S. K.; Tucci, F. C.; Rudkevich, D. M.; Heinz, T.; Rebek, Jr., J. A Self-Assembled Cylindrical Capsule: New Supramolecular Phenomena through Encapsulation, *Chem. Eur. J.* **2000**, *6*, 187–195. (c) Jiang, W.; Rebek, J. Guest-Induced, Selective Formation of Isomeric Capsules with Imperfect Walls, *J. Am. Chem. Soc.* **2012**, *134*, 17498–17501.

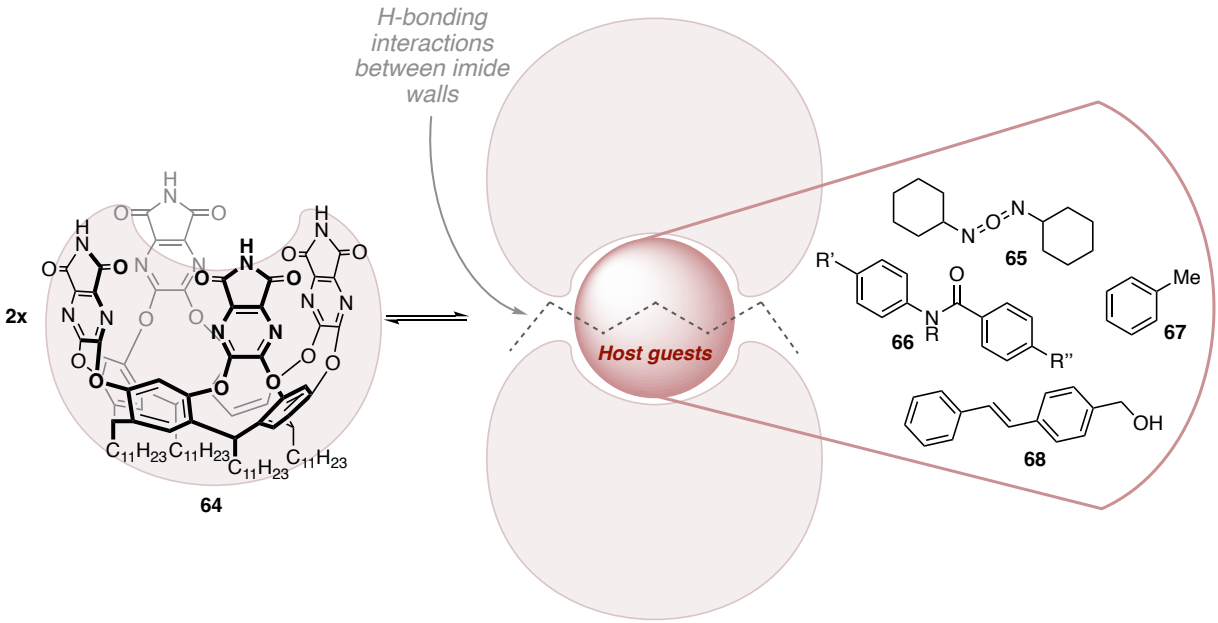


**Scheme 22**. Guest encapsulation in cavitand dimers bearing phthalimide walls.

Moreover, Diederich's group described in 2003 the synthesis of switchable resorcin[4]arene-derived cavitands bearing analogous walls based on phthalimide skeleton as part of their studies for mechanistic investigations of the switching dynamics as well as a continuation on the *vase*/*kite* conformations behaviours (Scheme 23).[37]

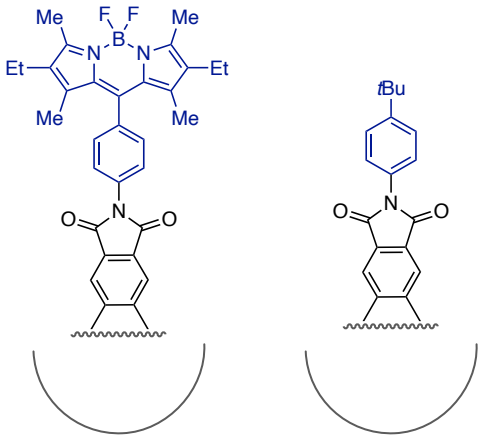


**Scheme 23**. Phthalimide-type walls included in Diederich's cavitands.

37 Azov, V. A.; Skinner, P. J.; Yamakoshi, Y.; Seiler, P.; Gramlich, V.; Diederich, F. Functionalized and Partially or Differentially Bridged Resorcin[4]Arene Cavitands: Synthesis and Solid-State Structures, *Helv. Chim. Acta* **2003**, *86*, 3648–3670.

**Synthesis of Chiral Gold(I)-Cavitand Complex (*R*)-80**

A three-step sequence was followed to synthesize the chiral phthalimide-based wall. The two first steps were based on studies that Knobler's group developed in 1992.[34] Starting from 2,3-dichloroquinoxaline **37a**, oxidation with $KMnO_4$ gave dicarboxylic acid **69**, which was transformed into the corresponding cyclic anhydride **70** by using $SOCl_2$ as the ring-closing reagent. The last step of the synthesis was inspired by the work reported by Diederich[37] using oxalyl chloride and pyridine as activating reagents and using the commercially available (*R*)-1-phenylethan-1-amine **71** for the formation of phthalimide wall (*R*)-**72** (Scheme 24).

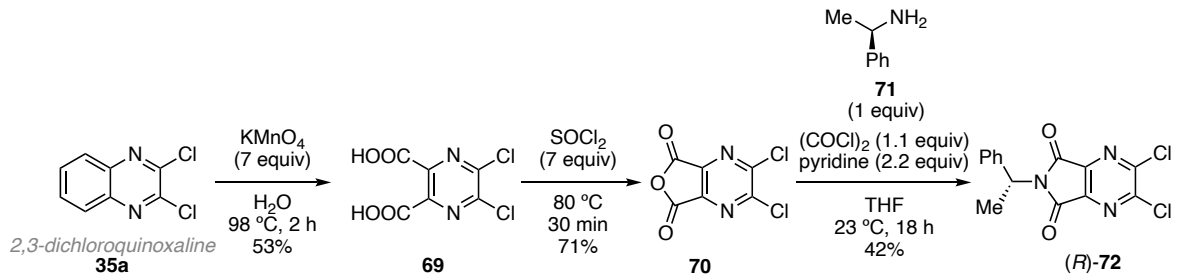


**Scheme 24**. Synthesis of (*R*)-**72**.

For the introduction of the new chiral wall moiety into the cavitand core, first we attempted to start from resorcin[4]arene **34**, using $K_2CO_3$ in DMSO at 60 °C as for the synthesis of tetraquinoxaline (*R*,*R*,*R*,*R*)-**73**. However, only complex mixtures were observed under this reaction conditions. This was presumably due to all the conformational isomers that could be formed depending on the attachment side of the chiral wall into the resorcin[4]arene core (Scheme 25).

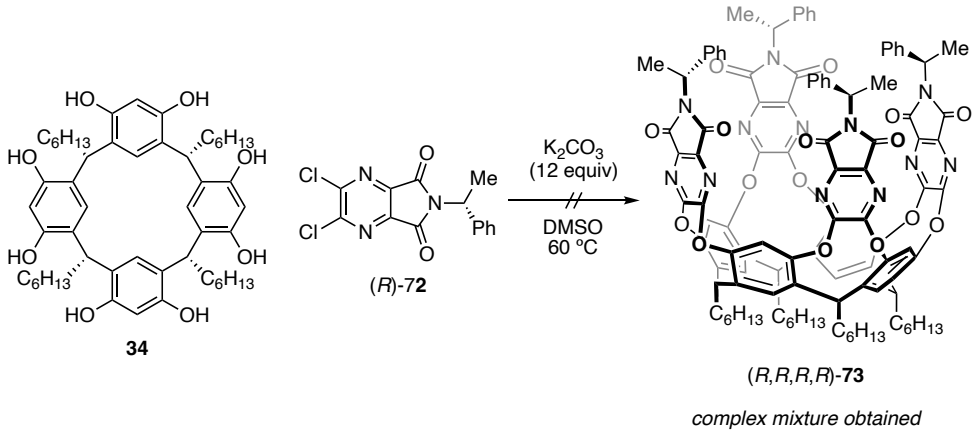


**Scheme 25**. Unsuccessful synthesis of cavitand (*R*,*R*,*R*,*R*)-**73**.

Alternatively, we decided to work from the symmetrical tetraphenol **37a** bearing two quinoxaline walls as starting material. First, we aimed to introduce selectively one chiral phthalimide wall into the cavitand core following the two different alternative conditions for the introduction of new walls to tetraphenols (Scheme 26). On one hand, *conditions A* produced the desired cavitand (*R*)-**74** in poor yield

(10%). Despite the low amount used of phthalimide wall (*R*)-**72** (0.8 equiv), the difunctionalized cavitand (*R*,*R*)-**75** was detected as side-product. On the other hand, with *conditions B*, the product was not detected and only a complex mixture was observed.

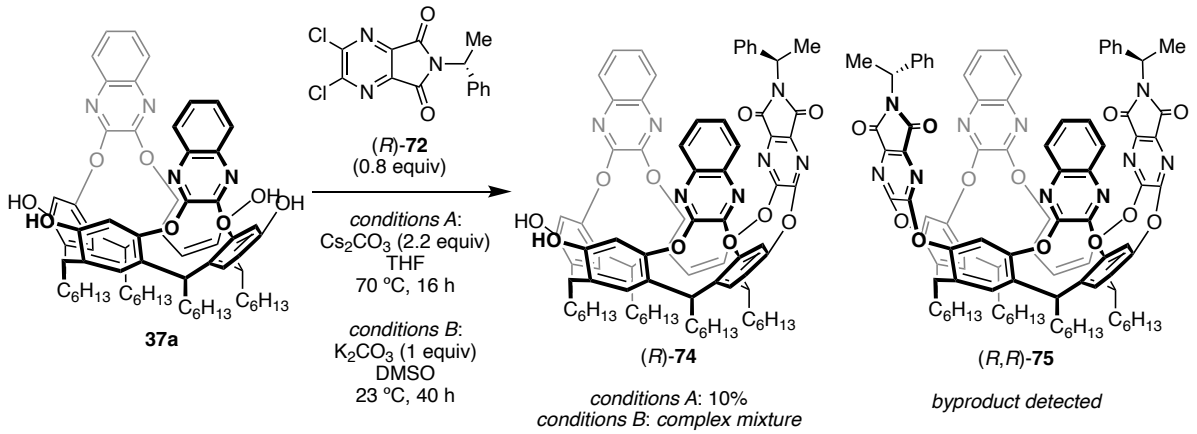


**Scheme 26**. Unsuccessful synthesis towards cavitand (*R*)-**74**.

Next, we decided to avoid the difunctionalization side reaction by protecting one side of the tetraphenol cavitand **37a**. Therefore, silyl protection was performed selectively on one side of the molecule to form cavitand **76**. Then, introduction of the phthalimide chiral wall using $Cs_2CO_3$ in THF at 70 °C for 18 hours, resulted in the desired protected cavitand (*R*)-**77** which after desilylation delivered the biphenol cavitand (*R*)-**78** (Scheme 27).

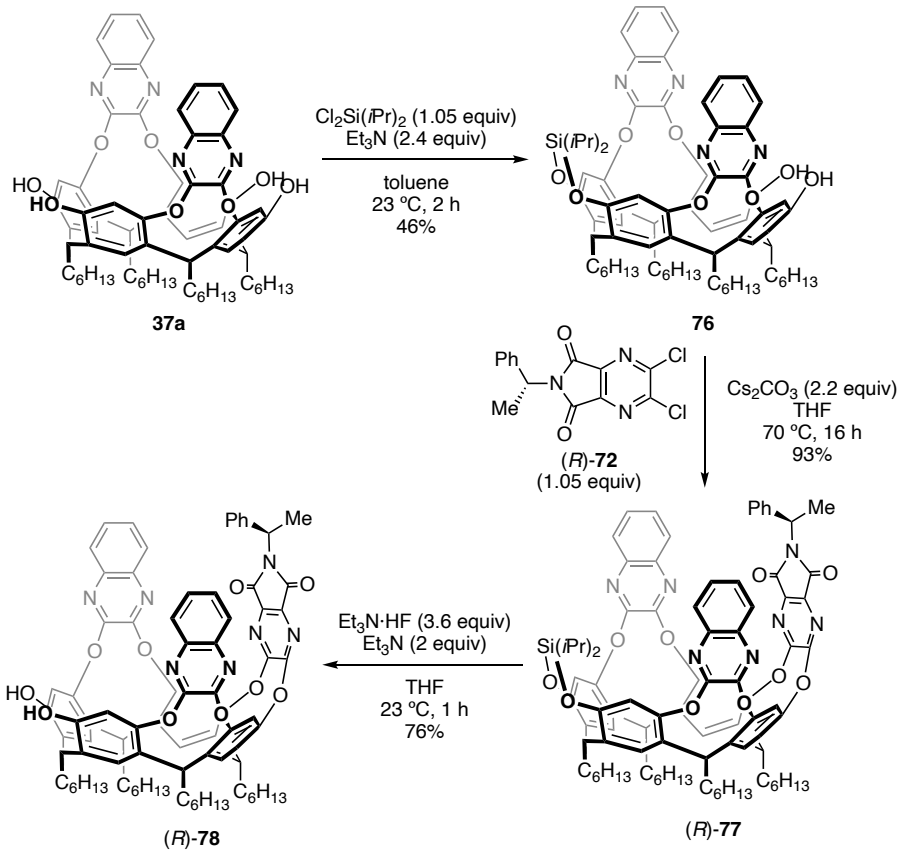


**Scheme 27**. Synthesis of biphenol cavitand (*R*)-**78**.

Finally, dichloro(phenyl)phosphane ($PhPCl_2$) reacted with diphenol chiral cavitand (*R*)-**78** to form phosphonite (*R*)-**79**, which was directly exposed to $AuCl{\cdot}SMe_2$ form the gold(I)-cavitand complex (*R*)-**80** (Scheme 28). The structure of the complex was confirmed by X-ray diffraction analysis, which showed the location of the gold(I) nucleus pointing inside the cavity. Also, the phenyl moiety of the phthalimide wall was found to be pointing inwards the cavity, whereas the methyl group remains pointing outwards (Figure 3).

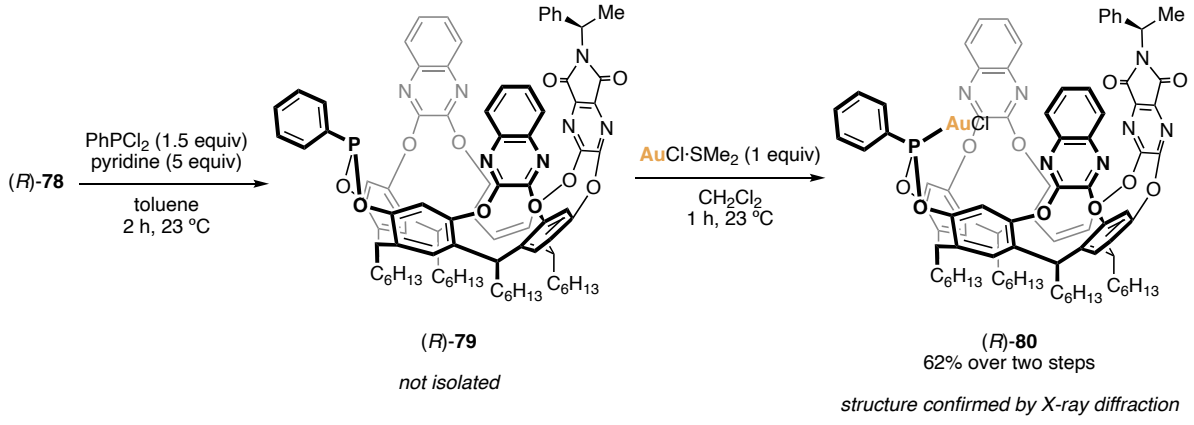


**Scheme 28**. Synthesis of gold(I)-cavitand complex (*R*)-**80**.

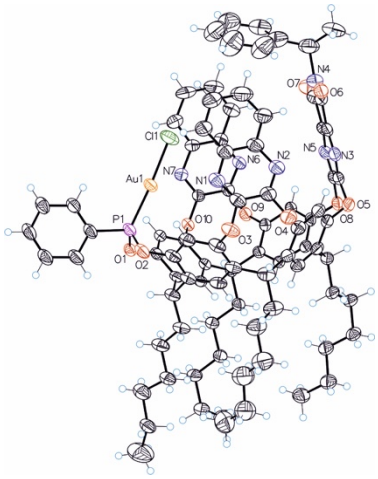


**Figure 3**. X-Ray structure of gold(I)-cavitand complex (*R*)-**80**.

**Enantioselective Tests**

The reactivity of the synthesized novel chiral cavitand gold(I) complex (*R*)-**80** was studied. For that, we tried first the alkoxycylization reaction of 1,6-dienyne **30a** using ethanol as nucleophile, which had been studied previously in our group using the first family of chiral gold(I)-cavitand complexes observing high *ee* values towards **31a** (Scheme 29a).[13] Complex (*R*)-**80** was active in the catalysis giving **31a** in 57%. However, very poor enantioselectivity was obtained.

Another reaction tested was the addition of indole to 1,6-enyne **81**.[38] Nonetheless, using complex (*R*)-**80** a similar outcome was observed: the reaction performed well towards the desired product in 57% yield but with very poor enantioselectivity (Scheme 29b).

38 Reaction further studied later using another catalytic system, see section 3 of this chapter.

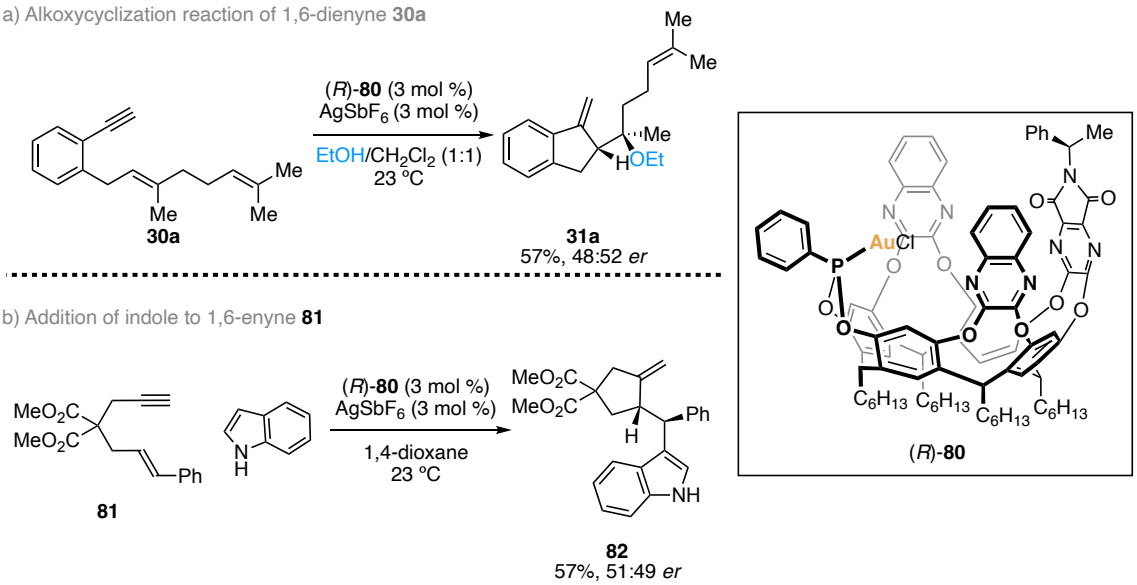


**Scheme 29**. Test of gold(I) complex (*R*)-**80** in a) the alkoxycyclization reaction of 1,6-dienyne **30a** and b) the addition of indole to 1,6-enyne **81**.

These results could be rationalized considering the X-ray structure of complex (*R*)-**80** where it is possible to see how the chiral information on the phthalimide wall in front of the gold(I) chloride moiety is probably too far away to induce enantioselectivity during the reaction (Figure 3).

## Gold(I)-Cavitand Complexes in Hydrogen-bonded Ion Pair Catalysis[39]

### Introduction

Asymmetric counteranion-directed catalysis (ACDC) involves inducing enantioselectivity in a reaction that proceeds through a cationic intermediate by ion pairing with a chiral, enantiomerically pure anion of the catalyst.[40]

After the introduction of the ACDC concept, Toste's research group developed a reversed-polarity phase-transfer catalysis (Scheme 30a).[41] As an example, they reported a ring opening reaction of tetrasubstituted *meso*-aziridinium ions with alcohol nucleophiles proceeding *via* a chiral ion pair with a binaphthol-phosphate anion (Scheme 30b). The transformation is initiated by silver-induced ring closure of *β*-chloroamines **81** using the silver salt of the chiral anion as *in situ* generated catalyst. Notably, no obvious hydrogen bonds or other directional interaction were shown to be stabilizing the ion pairs formed in this system, resulting as an example of ACDC *via* intermediates without strong stabilizing effects.

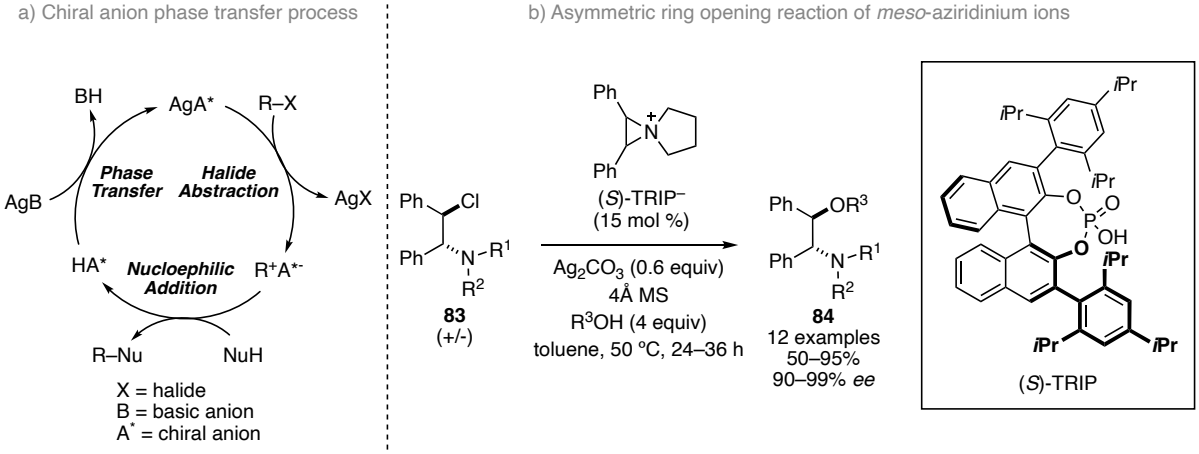


**Scheme 30**. Chiral anion phase transfer process as an ACDC example without strong stabilizing effects.

When applying ACDC to transition-metal catalysis, List's group studied the *α*-allylation of *α*-branched aldehydes using allyl amines through a Pd-catalyzed system that involves chiral counteranions and creates all-carbon quaternary stereogenic centers (Scheme 31, top).[42a] Later, they developed the

39 Work done in collaboration with Àlex Martí Zaragoza.

40 Mahlau, M.; List, B. Asymmetric Counteranion-Directed Catalysis: Concept, Definition, and Applications, *Angew. Chem. Int. Ed.* **2013**, *52*, 518–533.

41 Hamilton, G. L.; Kanai, T.; Toste, F. D. Chiral Anion-Mediated Asymmetric Ring Opening of Meso-Aziridinium and Episulfonium Ions, *J. Am. Chem. Soc.* **2008**, *130*, 14984–14986.

42 (a) Mukherjee, S.; List, B. Chiral Counteranions in Asymmetric Transition-Metal Catalysis: Highly Enantioselective Pd/Brønsted Acid-Catalyzed Direct *α*-Allylation of Aldehydes, *J. Am. Chem. Soc.* **2007**, *129*,

analogue reaction using allylic alcohols as allylating agents in a triple catalytic methodology by the incorporation of benzhydryl amine **89** to the system (Scheme 31, bottom).[42b]

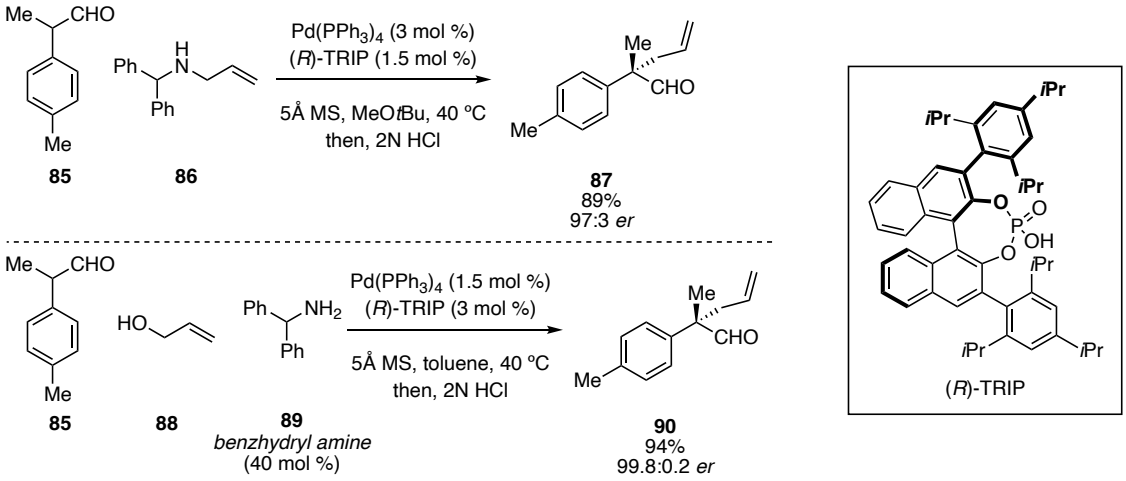


**Scheme 31**. Pd–TRIP-catalyzed $\alpha$-allylation of $\alpha$-branched aldehydes.

Analogously, Toste and co-workers performed studies on enantioselective gold(I) catalysis by using achiral ligands together with chiral anions, combining dinuclear gold(I) complexes with a chiral silver phosphate to perform the asymmetric cyclization of allenes (Scheme 32a).[43] In this case, the gold(I) complex is generated through ion exchange, which forms the Au(I)–TRIP salt bearing the phosphine ligand. Another example for Au(I)–ACDC is employed is the desymmetrization of diynes, described by Czekelius in 2012 (Scheme 32b).[44]

11336–11337. (b) Jiang, G.; List, B. Direct Asymmetric $\alpha$-Allylation of Aldehydes with Simple Allylic Alcohols Enabled by the Concerted Action of Three Different Catalysts, *Angew. Chem. Int. Ed.* **2011**, *50*, 9471–9474.

43 Hamilton, G. L.; Kang, E. J.; Mba, M.; Toste, F. D. A Powerful Chiral Counterion Strategy for Asymmetric Transition Metal Catalysis, *Science* **2007**, *317*, 496–499.

44 Mourad, A. K.; Leutzow, J.; Czekelius, C. Anion-Induced Enantioselective Cyclization of Diynamides to Pyrrolidines Catalyzed by Cationic Gold Complexes, *Angew. Chem. Int. Ed.* **2012**, *51*, 11149–11152.

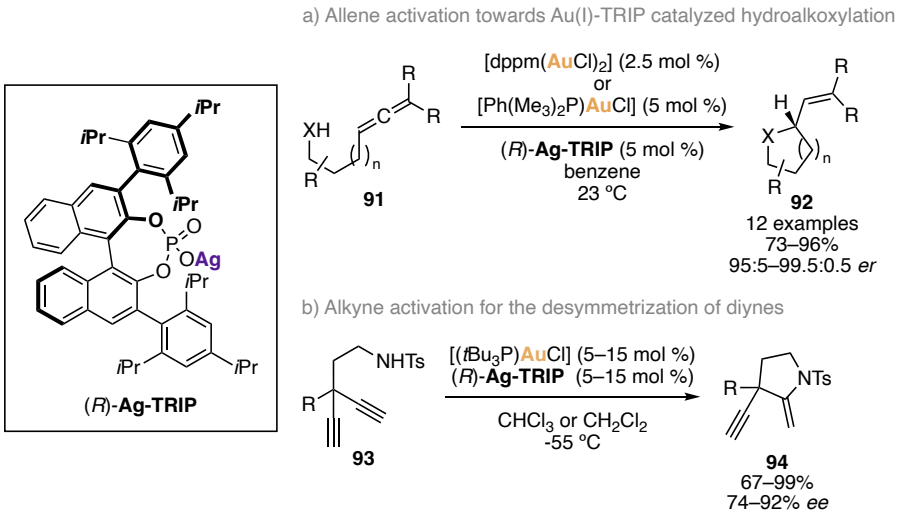


**Scheme 32**. Previous reports on achiral gold(I) complexes combined with chiral anions.

Inspired by the ACDC approach, in 2022 our group developed an alternative approach based on H-bonded counterion directed catalysis (HCDC).[45] A H-bond donor group (urea moiety) tethered on the phosphine ligand of a JohnPhos gold(I) chloride complex was combined with a BINOL-derived silver(I) phosphoramidate. This methodology involves, the activation of the gold(I) complex by chloride abstraction performed by the silver salt. At the same time, upon AgCl formation, the resulting anion would be placed close to the active site due to the H-bonding interactions. Upon substrate coordination, transmission of the stereochemical information takes place during the reaction. The application of this concept was demonstrated, for example, in the enantioselective 6-*endo*-dig cyclization of 1,6-enyne **95** (Scheme 33a). In this reaction, the stereocenter was formed by intramolecular attack of the alkene onto the gold(I)-activated triple bond. A related "tethered-counterion directed catalysis" (TCDC) concept was introduced by Marinetti, Guinchard and coworkers, wherein a chiral phosphoric acid is covalently bound to the scaffold of a phosphine Au(I) chloride complex.[46] In 2022, our group reported the use of

45 Franchino, A.; Martí, À.; Echavarren, A. M. H-Bonded Counterion-Directed Enantioselective Au(I) Catalysis, *J. Am. Chem. Soc.* **2022**, *144*, 3497–3509.

46 (a) Zhang, Z.; Smal, V.; Retailleau, P.; Voituriez, A.; Frison, G.; Marinetti, A.; Guinchard, X. Tethered Counterion-Directed Catalysis: Merging the Chiral Ion-Pairing and Bifunctional Ligand Strategies in Enantioselective Gold(I) Catalysis, *J. Am. Chem. Soc.* **2020**, *142*, 3797–3805. (b) Yu, Y.; Zhang, Z.; Voituriez, A.; Rabasso, N.; Frison, G.; Marinetti, A.; Guinchard, X. Enantioselective Au(I)-Catalyzed Dearomatization of 1-Naphthols with Allenamides through Tethered Counterion-Directed Catalysis, *Chem. Commun.* **2021**, *57*, 10779–10782. (c) Zhang, Z.; Sabat, N.; Frison, G.; Marinetti, A.; Guinchard, X. Enantioselective Au(I)-Catalyzed Multicomponent Annulations via Tethered Counterion-Directed Catalysis, *ACS Catal.* **2022**, *12*, 4046–4053.

a phosphinosquaramide gold(I) chloride complex **96** in combination with the chiral silver salt (*R*)-**Ag G** for the addition to 2-alkynyl enones **98** (Scheme 33b).[47]

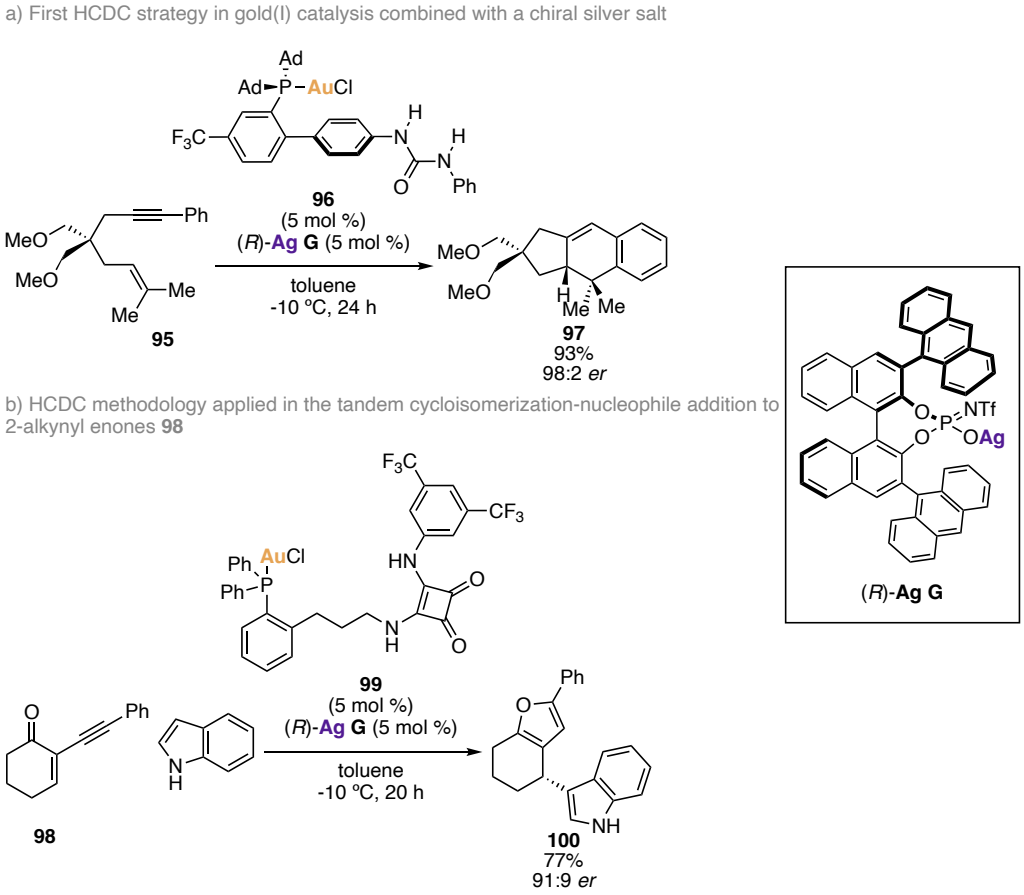


**Scheme 33**. First reports on the HCDC concept in gold(I) asymmetric catalysis.

47 Martí, À.; Montesinos-Magraner, M.; Echavarren, A. M.; Franchino, A. H-Bonded Counterion-Directed Catalysis: Enantioselective Gold(I)-Catalyzed Addition to 2-Alkynyl Enones as a Case Study, *Eur. J. Org. Chem.* **2022**, *2022*, e202200518.

**Synthesis of Achiral Gold(I)-Cavitand Complexes**

After the different attempts to form a novel family of chiral gold(I)-cavitands, we decided to target a new methodology to induce enantioselectivity with such type of catalysts. For that, we pictured that the combination of the cavity effect and the H-bonded counteranion-directed catalysis approaches could be both present in a single system. On one hand, we would benefit from the cavity ligand shape to adapt the substrate position in a determined manner inside the ligand core that would not need to carry the chiral information. At the same time, the skeleton would have the suitable moiety to be able to bind a chiral anion by H-bond interactions to direct the reaction in an enantioselective manner (Figure 4). In this context, we envisioned that the introduction of a urea moiety as part of one wall of the cavitand core would offer the possibility to produce H-bonding interactions with the chiral silver salt upon chloride abstraction. We reasoned that the optimal position for the urea within the cavitand would be on the same wall that has the gold(I) center, since it would bring the chiral counteranion into close proximity to the reaction site, resulting in more efficient enantioinduction.

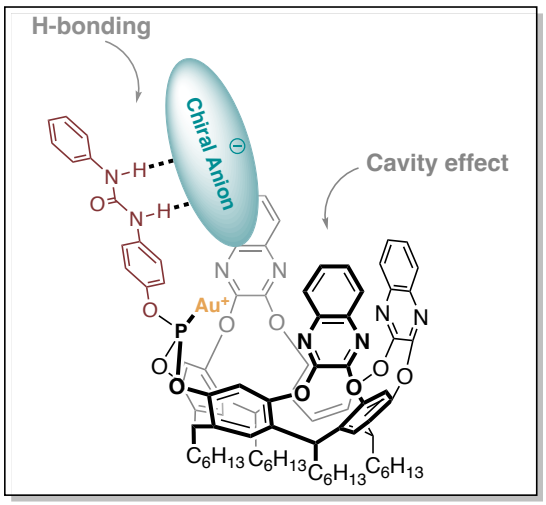


**Figure 4**. Design of the novel gold(I)-cavitand H-bonding system.

The synthetic approach started from diphenol **36** bearing the three quinoxaline walls in its skeleton which was treated with $PCl_3$ in basic conditions, followed by the addition of the corresponding *para*-, *meta*- or *ortho*-hydroxyurea **U** to afford phosphites **101a**, **101b** and **101c**, respectively (Scheme 34). Then, reaction of the phosphites with $AuCl{\cdot}SMe_2$, delivered the corresponding complexes in moderate to good yields.

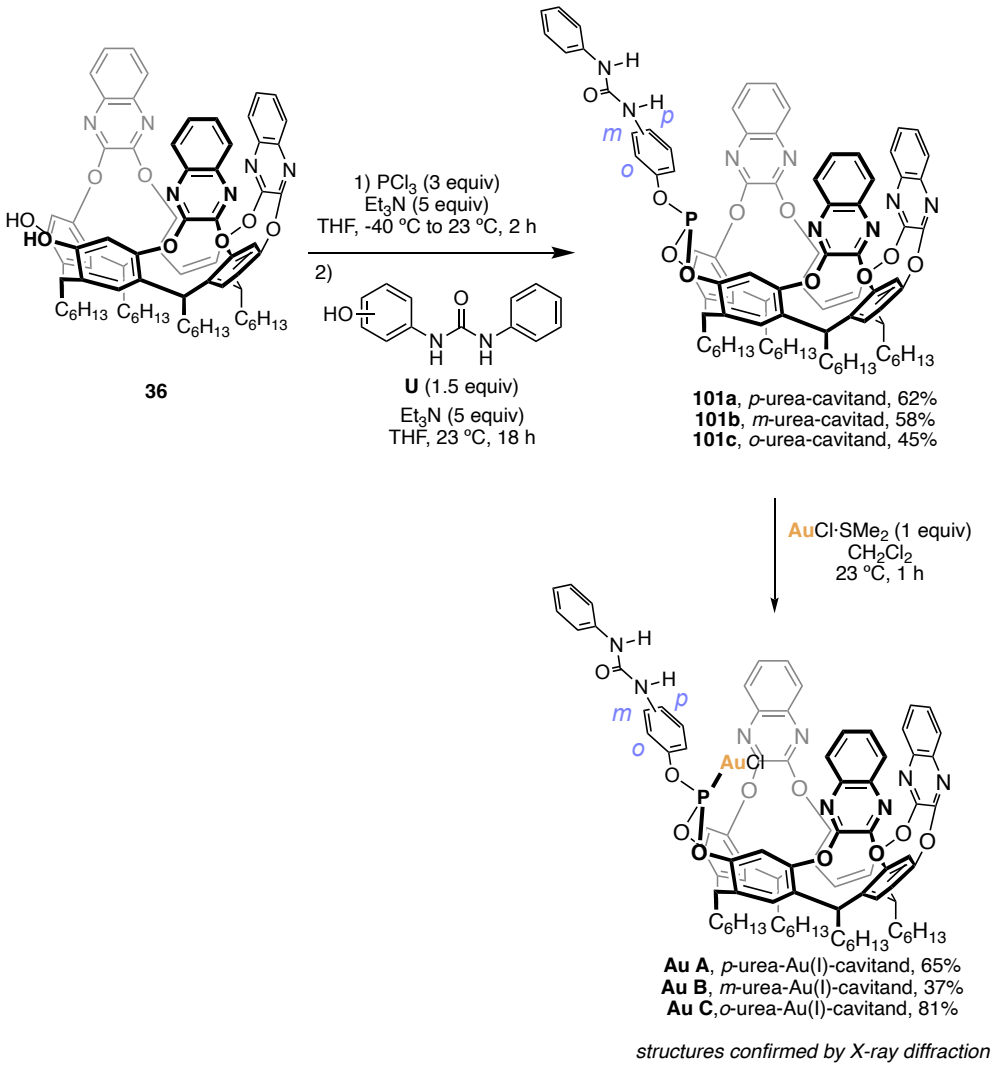


**Scheme 34**. Synthesis of achiral gold(I)-cavitand complexes **Au A**, **Au B** and **Au C**.

Crystals of the three gold(I)-cavitand complexes were obtained to confirm the structures. However, only the crystals from complex **Au C**, bearing the *ortho*-urea moiety, could be measured by X-ray diffraction (Figure 5). The structure shows how the gold(I) nucleus is located inside the cavity, flanked by the three quinoxaline walls.

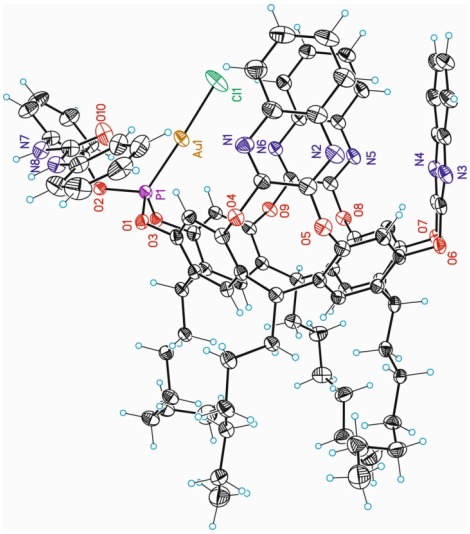


**Figure 5**. X-Ray structure of gold(I)-cavitand complex **Au C**.

The use of these achiral gold(I)-cavitand complexes in asymmetric gold(I) catalysis was explored in combination with a family of chiral silver salts (Figure 6).[48]

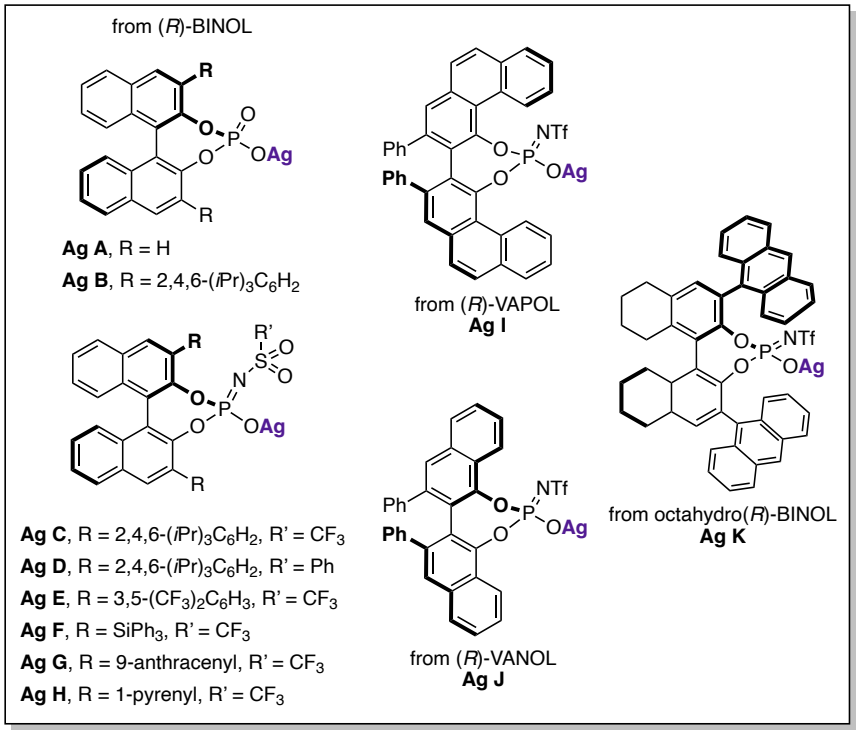


**Figure 6**. Library of chiral silver salts.

48 All the described synthesis of the chiral silver salts used can be found in the supporting information of references 45 and 47.

**Reaction Discovery and Optimization**

The performance of the new synthesized gold(I) complexes **Au A**, **Au B** and **Au C** was first explored in combination with chiral silver salt **Ag G** (Figure 7).

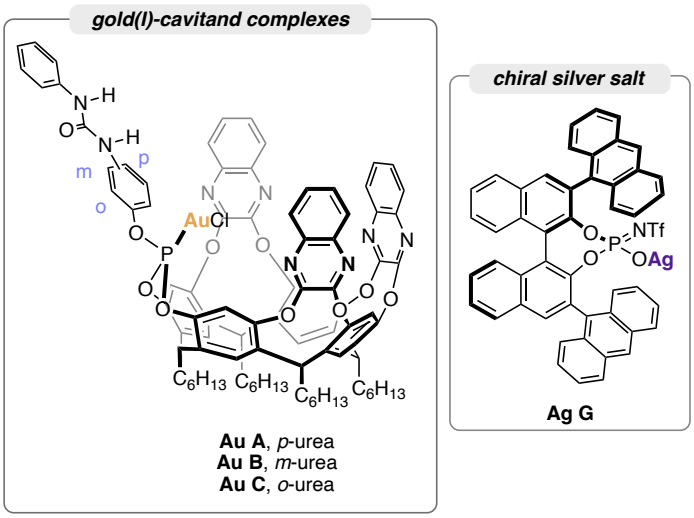


**Figure 7**. New gold(I)-cavitand complexes **Au A**, **Au B** and **Au C**, and **Ag G** used on the first reactivity studies.

The first enantioselective test was the alkoxycyclization reaction of 1,6-enyne **30a** using ethanol as external nucleophile. We applied the optimized conditions previously used for the first generation of the cavitands catalysts, considering the results achieved with the most effective chiral catalyst (Table 1, entry 1).[13] Product **31a** was obtained in moderate to good yields using the three different precatalysts. However, low *er* values were observed in all cases (Table 1, entries 2–4).

**Table 1**. Evaluation of the performance of **Au A**, **AuB** and **Au C** in combination with (*R*)-**Ag G** in the alkoxycyclization reaction of **31a**.

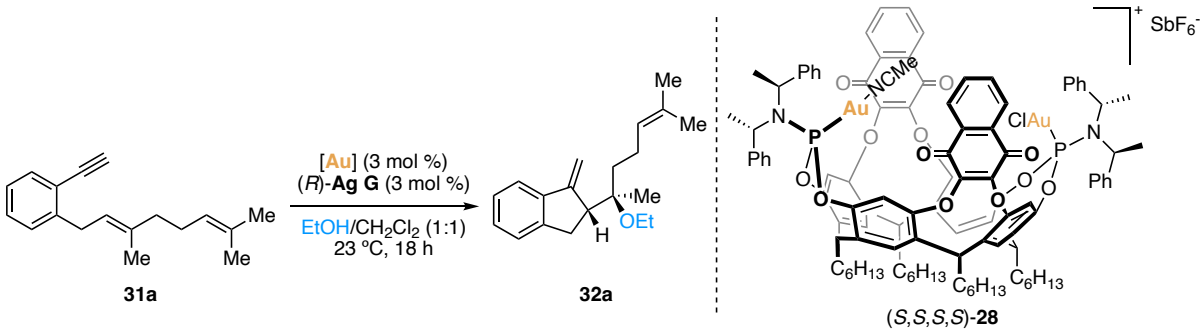


| Entry | [Au] | Yield (%)[a] | *er* (%)[b] |
|---|---|---|---|
| 1[c] | (*S*,*S*,*S*,*S*)-**28** | 90[d] | 96:4 |
| 2 | **Au A** | 66 | 43:57 |
| 3 | **Au B** | 56 | 54:46 |
| 4 | **Au C** | 48 | 47:52 |

[a] Determined by $^1$H NMR using $Ph_2CH_2$ as internal standard. [b] Determined by HPLC on chiral stationary phase. [c] Results previously reported.[13] [d] Isolated yield.

Our second trial involved the study of the developed complexes on the formal [4+2] cycloaddition of 1,6-arylenyne **95**. We applied the optimized conditions published earlier in the group,[45] where a H-bonded methodology involving gold(I) complex **96** and the same chiral silver salt (*R*)-**Ag G** proved to be the best catalytic system. However, in none of the cases the formation of product **97** was detected, presumably because the substrate does not fit inside the cavity pocket of the gold(I)-cavitand complexes (Scheme 35).

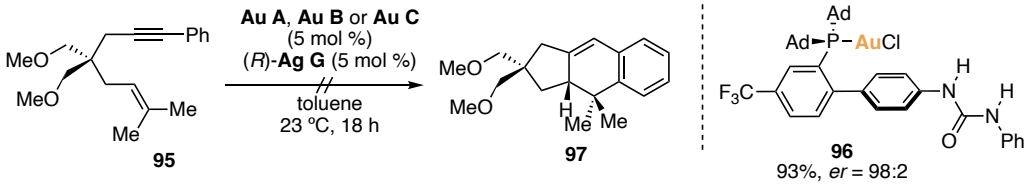


**Scheme 35**. Test of gold(I)-cavitand complexes **Au A**, **Au B** and **Au C** in combination with (*R*)-**Ag G** in the formal [4+2] cycloaddition of 1,6-arylenyne **95**.

Next, to explore the potential of the new HCDC system involving the novel gold(I)-cavitand complexes, we run a reaction discovery experiment in the HTE laboratory. Twelve different inter- and intramolecular gold(I) cyclization reactions involving potential substrates of interest that would render

useful transformations were screened against the three novel gold (I)-cavitand catalysts in combination with five chiral silver salts (Scheme 36).[5c,13,49]

49 (a) Yeom, H.-S.; Koo, J.; Park, H.-S.; Wang, Y.; Liang, Y.; Yu, Z.-X.; Shin, S. Gold-Catalyzed Intermolecular Reactions of Propiolic Acids with Alkenes: [4 + 2] Annulation and Enyne Cross Metathesis, *J. Am. Chem. Soc.* **2012**, *134*, 208–211. (b) Johansson, M. J.; Gorin, D. J.; Staben, S. T.; Toste, F. D. Gold(I)-Catalyzed Stereoselective Olefin Cyclopropanation, *J. Am. Chem. Soc.* **2005**, *127*, 18002–18003. (c) Zheng, H.; Wang, K.; Angelis, L. D.; Arman, H. D.; Doyle, M. P. Brønsted Acid Catalyzed Oxocarbenium-Olefin Metathesis/Rearrangements of 1H-Isochromene Acetals with Vinyl Diazo Compounds, *J. Am. Chem. Soc.* **2021**, *143*, 15391–15399. (d) Zi, W.; Toste, F. D. Gold(I)-Catalyzed Enantioselective Carboalkoxylation of Alkynes, *J. Am. Chem. Soc.* **2013**, *135*, 12600–12603. (e) Ruch, A. A.; Ellison, M. C.; Nguyen, J. K.; Kong, F.; Handa, S.; Nesterov, V. N.; Slaughter, L. M. Highly Sterically Encumbered Gold Acyclic Diaminocarbene Complexes: Overriding Electronic Control in Regiodivergent Gold Catalysis, *Organometallics* **2021**, *40*, 1416–1433. (f) Rauniyar, V.; Wang, Z. J.; Burks, H. E.; Toste, F. D. Enantioselective Synthesis of Highly Substituted Furans by a Copper(II)-Catalyzed Cycloisomerization–Indole Addition Reaction, *J. Am. Chem. Soc.* **2011**, *133*, 8486–8489. (g) Zuccarello, G.; Nannini, L. J.; Arroyo-Bondía, A.; Fincias, N.; Arranz, I.; Pérez-Jimeno, A. H.; Peeters, M.; Martín-Torres, I.; Sadurní, A.; García-Vázquez, V.; Wang, Y.; Kirillova, M. S.; Montesinos-Magraner, M.; Caniparoli, U.; Núñez, G. D.; Maseras, F.; Besora, M.; Escofet, I.; Echavarren, A. M. Enantioselective Catalysis with Pyrrolidinyl Gold(I) Complexes: DFT and NEST Analysis of the Chiral Binding Pocket, *JACS Au* **2023**, *3*, 1742–1754. (h) Mauleón, P.; Krinsky, J. L.; Toste, F. D. Mechanistic Studies on Au(I)-Catalyzed [3,3]-Sigmatropic Rearrangements Using Cyclopropane Probes, *J. Am. Chem. Soc.* **2009**, *131*, 4513–4520. (i) Zanini, M.; Cataffo, A.; Echavarren, A. M. Synthesis of Cyclobutanones by Gold(I)-Catalyzed [2 + 2] Cycloaddition of Ynol Ethers with Alkenes, *Org. Lett.* **2021**, *23*, 8989–8993.

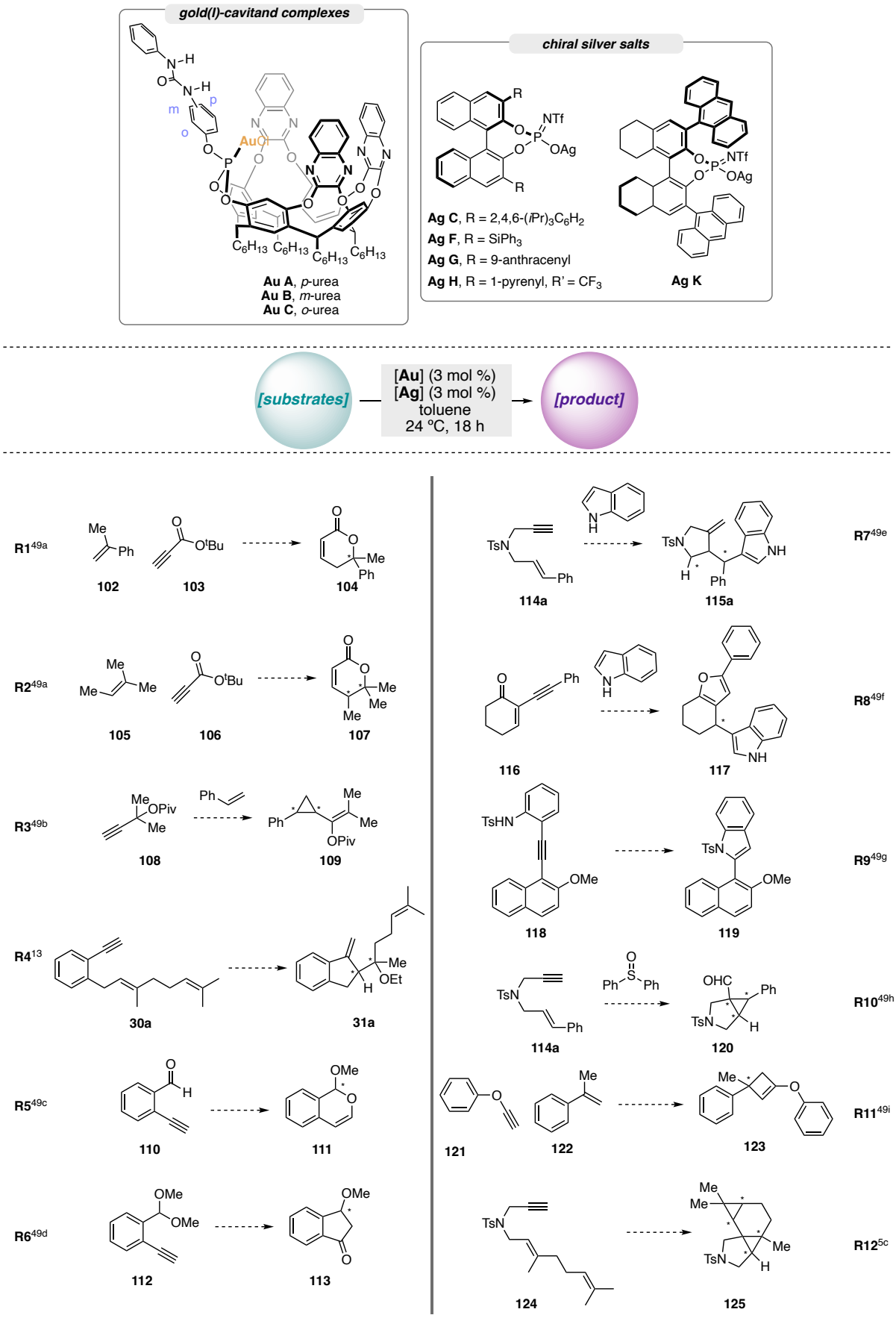


**Scheme 36**. HTE experiment of reaction discovery.

This initial exploratory screening led us to select the indole addition to 1,6-enyne **114a** as a promising reaction that we wanted to further study (Scheme 37). This reaction is a case study for an addition of indole as an electron-rich arene nucleophiles to 1,6-enynes and has been already explored in different catalytic systems.[50,49e]

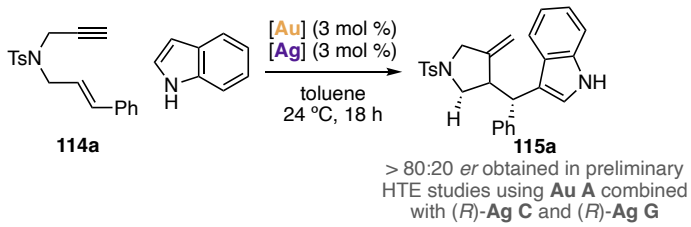


**Scheme 37**. Indole addition to 1,6-enyne **114a**.

Since we were dealing with a key H-bonding interaction, a system where the solvation and the environment present in the reaction mixture have a significant impact, we started the optimization process by exploring the solvent effect. This was achieved through another HTE experiment that allowed us to test several conditions in the indole addition to 1,6-enyne **114b** (Figure 8). Keeping constant the silver salt (*R*)-**Ag G** used, we screened the three gold(I)-cavitand complexes (**Au A** to **Au C**). A total of 18 reactions were set up, being able to test six different solvent systems for each gold(I)-complex/silver*-salt combination. In terms of yields, we observed that most of the combinations performed well, delivering product **115b** with moderate to good yields (Figure 8a). However, in the case of complex **Au C**, the reaction did not proceed to full conversion. This was presumably caused by the inability for the substrate to fit in its cavity in the case of this complex due to the proximity of the *ortho*-urea moiety to the reaction center. Regarding the solvent system, chloroform was discarded at this point, as it gave consistently the lowest yields (Figure 8a, column 4).

Then, the enantioselectivity was studied revealing a significant influence of the nature of the solvent (Figure 8b). The low *ee* values obtained with both 1,2-dichloroethane and *α*,*α*,*α*-trifluorotoluene allowed us to rule out any halogenated solvent for the transformation (Figure 8b; columns 1 and 3,

50 (a) Amijs, C. H. M.; Ferrer, C.; Echavarren, A. M. Gold(I)-Catalysed Arylation of 1,6-Enynes: Different Site Reactivity of Cyclopropyl Gold Carbenes, *Chem Commun* **2007**, *7*, 698–700. (b) Fourmy, K.; Mallet-Ladeira, S.; Dechy-Cabaret, O.; Gouygou, M. Platinum(II)–Phosphole Complexes: Synthesis and Evaluation as Enyne Cycloisomerisation Catalysts, *Dalton Trans* **2014**, *43*, 6728–6734. (c) Arumugam, K.; Varghese, B.; Brantley, J. N.; Konda, S. S. M.; Lynch, V. M.; Bielawski, C. W. 1,6-Enyne Cyclizations Catalyzed by N-Heterocyclic Carbene Supported Gold Complexes: Deconvoluting Sterics and Electronics, *Eur. J. Org. Chem.* **2014**, 493–497. (d) Teci, M.; Hueber, D.; Pale, P.; Toupet, L.; Blanc, A.; Brenner, E.; Matt, D. Metal Confinement through N-(9-Alkyl)Fluorenyl-Substituted N-Heterocyclic Carbenes and Its Consequences in Gold-Catalysed Reactions Involving Enynes, *Chem. Eur. J.* **2017**, *23*, 7809–7818. (e) Pedrazzani, R.; Kiriakidi, S.; Monari, M.; Lazzarini, I.; Bertuzzi, G.; López, C. S.; Bandini, M. Fluorinated Biphenyl Phosphine Ligands for Accelerated [Au(I)]-Catalysis, *ACS Catal.* **2024**, *14*, 6128–6136.

respectively). Best performances were achieved with **Au A**, with the urea in the *para*-position using 1,4-dioxane giving the desired product **115b** with 98% yield and 88% *ee* (Figure 8, A6).

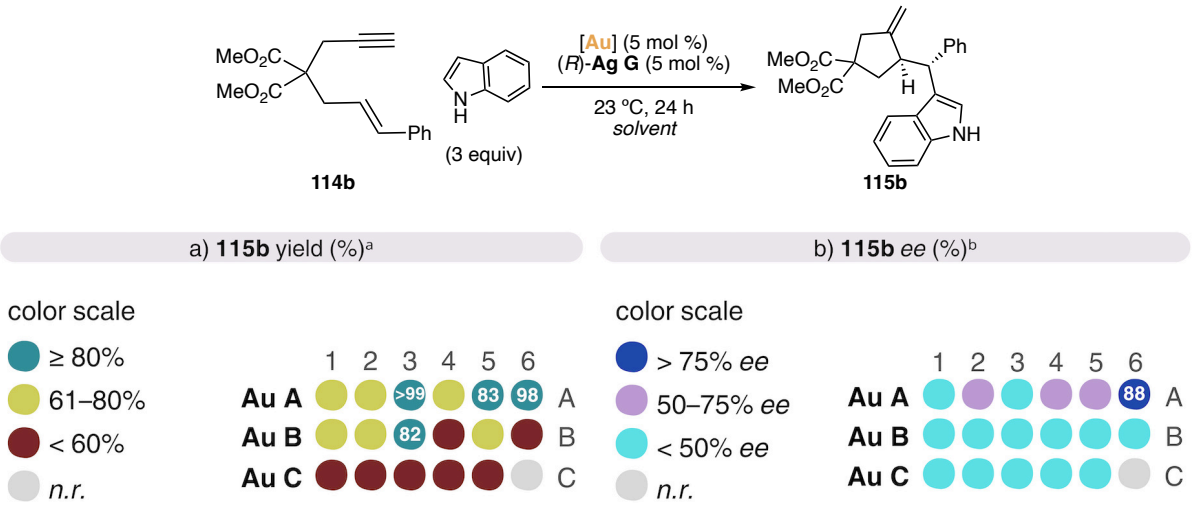


**Figure 8**. HTE results in the solvent screening for the indole addition to 1,6-enyne **114b**. 1: *α,α,α*-trifluorotoluene; 2: toluene; 3: 1,2-dichloroethane; 4: chloroform; 5: cyclopentyl methyl ether; 6: 1,4-dioxane. [a] Product yields determined by SFC analysis using naphthalene as internal standard. [b] *ee* values determined by SFC analysis. All reactions were carried out at 10 µmol scale. *n.r.* = no reaction.

Thus, even though cyclopentyl methyl ether (CPME) showed reactions with very good yield and promising enantioselectivities, 1,4-dioxane was selected as the best solvent among six tested in this HTE studies for this reaction (Figure 8).

Next, a second HTE experiment was designed using 1,4-dioxane to screen a variety of chiral silver salts and to find the best gold(I)-cavitand complex/silver*-salt combination for the reaction. We used ten phosphoramidate silver salts: eight accessed from (*R*)-BINOL with various groups in the 3,3'-position (**Ag A**–**Ag H**), one form (*R*)-VAPOL (**Ag I**) and one from (*R*)-VANOL (**Ag J**) scaffolds in combination with the three gold(I)-cavitand complexes **Au A–C** (Figure 9).

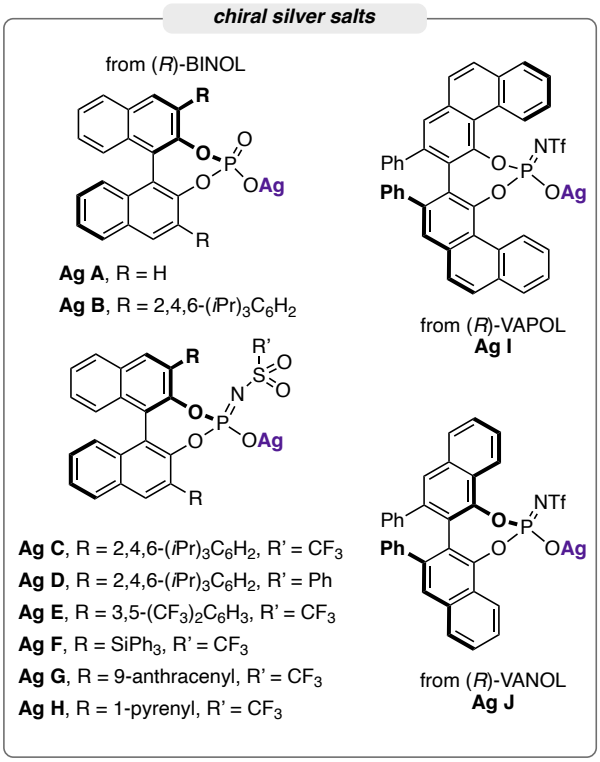


**Figure 9**. Library of chiral silver salts employed on the HTE experiment for the silver salt screening of the indole addition to 1,6-enyne **114b**.

As a result of all the combinations, a total of 30 reactions were set up in total in this study (Figure 10). The yield of the reactions was analyzed first (Figure 10a). Again, **Au C** was the complex achieving lower yields of **115b** due to steric hindrance (Figure 10, C1–C10). This time, we saw a more selective result from the three gold(I)-cavitand complexes since only **Au A** showed good yields giving 80% yield in combination with (*R*)-**Ag C** (Figure 10a, A3) and 70% with (*R*)-**Ag G** (Figure 10a, A7).

In terms of enantioselectivity (Figure 10b), the best performance was always observed with complex **Au A**, reaching *ee* up to 88%. In agreement with the highest yields observed, the best catalytic systems for the transformation were obtained by combining precatalyst **Au A** with either (*R*)-**Ag C** (80%, 82% *ee*; Figure 10b, A3) or (*R*)-**Ag G** (70%, 88% *ee*; Figure 10b, A7).

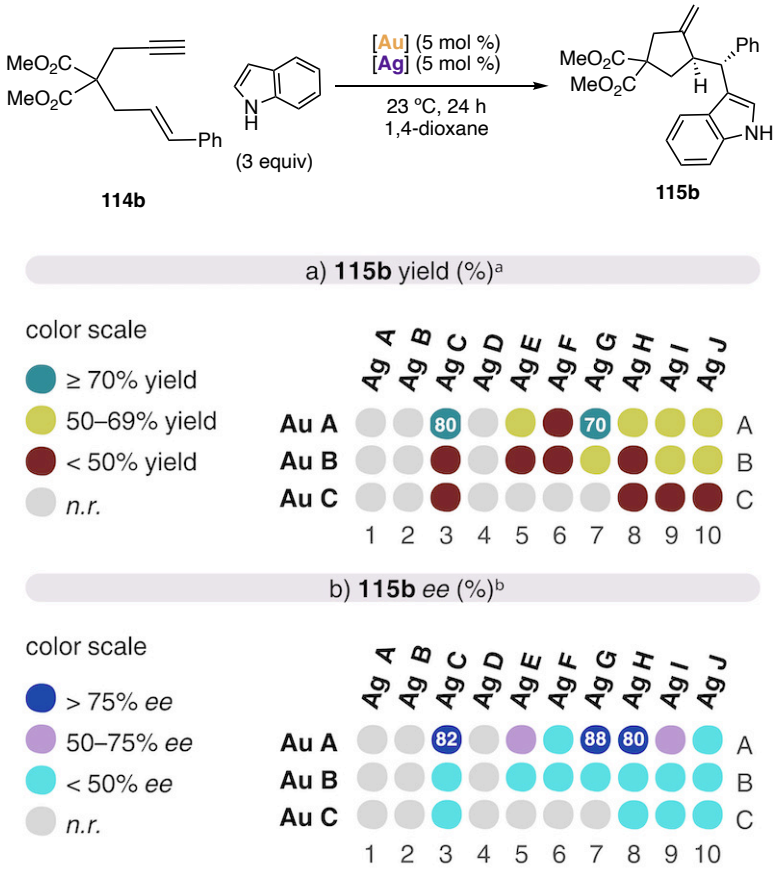


**Figure 10**. HTE results in the silver salt screening for the indole addition to 1,6-enyne **115b**. [a] Product yields determined by SFC analysis using naphthalene as internal standard. [b] *ee* values determined by SFC. All reactions were carried out at 10 µmol scale. *n.r.* = no reaction.

The best hit obtained from the HTE studies are shown in Table 2. During the first HTE plate, in the solvent screening, the two best solvents were CPME and 1,4-dioxane (Table 2, entries 1 and 2), the last offering better er and thus, used later for the silver salt screening THE study. Next, in the second HTE plate, the most suitable gold(I)-cavitand complex for the transformation was found to be **Au A** for all cases, with the *para*-urea moiety. Then, three chiral silver salts stood out from the seven tested in the second HTE experiment (Table 2, entries 2–4). Finally, the best one was found to be (*R*)-**Ag G**, with the anthracenyl moieties in the 3,3'-positions (Table 2, entry 2).

**Table 2**. Best HTE results obtained.

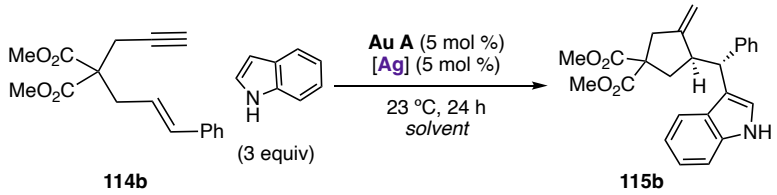


114b 115b

| Entry | [Ag] | Solvent | Yield (%)[a] | *er* (%)[b] |
|---|---|---|---|---|
| 1 | (*R*)-**Ag G** | CPME | 83 | 88:12 |
| 2 | (*R*)-**Ag G** | 1,4-dioxane | 70 | 94:6 |
| 3 | (*R*)-**Ag C** | 1,4-dioxane | 80 | 91:9 |
| 4 | (*R*)-**Ag H** | 1,4-dioxane | 62 | 90:10 |

[a] Yields determined by SFC analysis using naphthalene as internal standard. [b] *er* determined by SFC analysis. CPME = cyclopentyl methyl ether.

Next, we decided to continue the optimization experiments at the laboratory scale. First, the best HTE result was reproduced in the laboratory at a larger scale in a reduced time, affording moderate yields and very good enantioselectivities (Table 3, entry 2). Lowering the catalyst loading resulted in a lower yield but similar *er* (Table 3, entry 3). Moreover, lowering the amount of nucleophile to 1.5 equiv also delivered the product in good yield and *er* (Table 3, entry 4). At -50 °C, the reaction did not take place and when warming to -20 °C, poor yield and lower enantioselectivity were obtained (Table 3, entries 5 and 6). When no nucleophile was added, remaining starting material was observed together with a mixture of the 5- and 6-membered ring cyclized products (Table 3, entry 8).[14,51] With a larger excess of indole was added (10 equiv), a slight increase in yield was observed (Table 3, entry 9). Finally, control experiments showed that neither **Au A** nor (*R*)-**Ag G** were active on its own to form **115b** (Table 3, entries 10 and 11).

51 (a) Cabello, N.; Jiménez-Núñez, E.; Buñuel, E.; Cárdenas, D. J.; Echavarren, A. M. On the Mechanism of the Puzzling "Endocyclic" Skeletal Rearrangement of 1,6-Enynes, *Eur. J. Org. Chem.* **2007**, *2007*, 4217–4223. (b) Bartolomé, C.; Ramiro, Z.; Pérez-Galán, P.; Bour, C.; Raducan, M.; Echavarren, A. M.; Espinet, P. Gold(I) Complexes with Hydrogen-Bond Supported Heterocyclic Carbenes as Active Catalysts in Reactions of 1,6-Enynes, *Inorg. Chem.* **2008**, *47*, 11391–11397.

**Table 3**. Optimization of the reaction conditions.

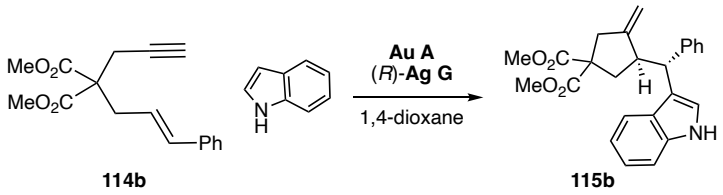


**114b** **115b**

| Entry[a] | catalyst loading (mol %) | indole (equiv) | T (°C) | t (h) | Yield (%)[b] | *er* (%)[c] |
|---|---|---|---|---|---|---|
| 1[d] | 5 | 3 | 23 | 24 | 70 | 94:6 |
| 2 | 5 | 3 | 23 | 18 | 68 | 94:6 |
| 3[e] | 3 | 3 | 23 | 18 | 61 | 91:9 |
| 4 | 3 | 3 | 23 | 18 | 41 | 95:5 |
| 5 | 5 | 1.5 | 23 | 18 | 74 | 94:6 |
| 6[f] | 5 | 1.5 | -50 | 18 | - | - |
| 7[f] | 5 | 1.5 | -20 | 48 | 40 | 90:10 |
| 8[g] | 5 | - | 23 | 18 | - | - |
| 9 | 5 | 10 | 23 | 18 | 78 | 95:5 |
| 10 | - | 1.5 | 23 | 18 | - | - |
| 11[h] | 5 | 1.5 | 23 | 18 | - | - |

[a] Reactions carried out at (0.07 mmol). [b] Isolated yields. [c] *er* determined by SFC using a chiral stationary phase. [d] Best HTE result obtained.[e] (*R*)-**Ag C** (5 mol %) was used. [f] toluene (0.1 M) was used as solvent. [g] Cyclized products without nucleophilic attack detected. [h] No silver salt added.

**Scope of the Enantioselective Nucleophilic Addition to 1,6-Enynes**

With the optimized conditions, we investigated the reaction scope (Scheme 38). The possibility of introducing different nucleophiles was studied using **Au A** and (*R*)-**Ag G** using 1,6-enynes of type **114**. Different substituents in the indole were tested. 5-Bromoindole performed well giving adduct **115c** with very good yield and *er*. However, the analogue 5-methoxyindole, resulted in a significant drop in the yield but maintaining the good *er* (**115d**, 94:6). 1-Methylindole reacted satisfactorily (**115e**; 65%, 95:5 *er*) while 2-methyl indole gave good *er* but very poor yield, probably due to steric effects (**115f**; 34%, 92:8 *er*). The electron rich arene 1,3,5-trimethoxybenzene could also be incorporated although in moderate yield and poorer *er* than previously observed, leading to **115g** in 18:82 *er*. Smaller nucleophiles such as water and ethanol performed better in terms of yield forming **115h** and **115i** in 89 and 78% yield, respectively. However, we observed a drop in the *er* values for both cases with values of 77:23 and 87:13 *er*, respectively. *E*-1,6-Enynes with different substitutions at the alkene also gave the corresponding adducts **115j**–**115n** with good yields, except for those with a *para*-electron-withdrawing group such as *para*-Cl that gave **115m** in 46% yield and *para*-$NO_2$ group that gave **115l**

in 26% yield. Nonetheless, the enantioselectivities were not affected, being 96:4 *er* and 95:5 *er*, respectively. Finally, modifications on the tether moiety of the substrates were applied. Changing the malonate by increasing the size of the ester from methyl to isopropyl produced **115o** in excellent yield and it did not affect the *er* outcome of the reaction. On the contrary, the *N*-tosyl group led to a drop in both yield and enantioselectivity, providing **115b** in 30% yield and 19:81 *er*, suggesting that the tether plays an important role in the folding of the substrate in the chiral pocket of the catalyst.

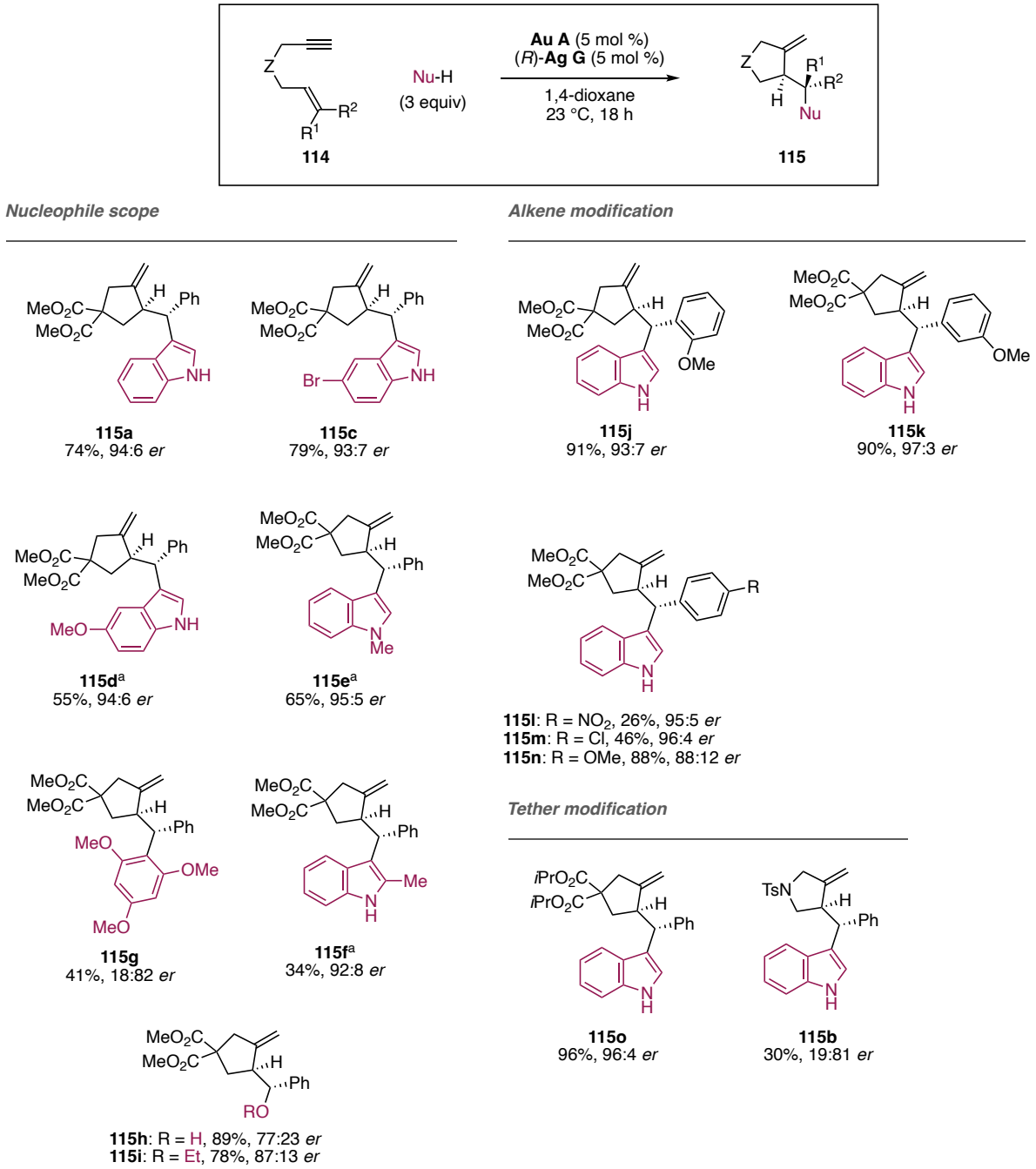


**Scheme 38**. Scope of the enantioselective nucleophilic addition to 1,6-enyne **114**.[a] 1.5 equiv of NuH added.

The configuration of **115m** (*S*,*S*) was assigned by X-ray diffraction (Figure 11).

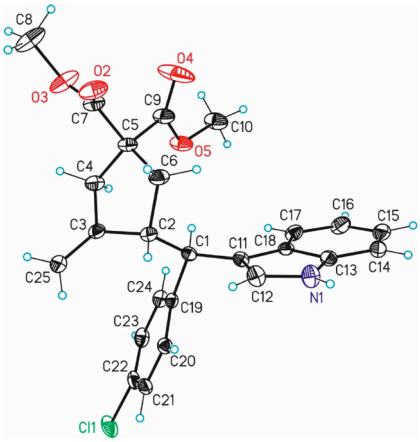


**Figure 11**. X-Ray structure of **115m**.

Some of the tested reactions during the scope studies did not form the desired product (Scheme 39). For instance, no reaction towards the formation of **115p** was observed when a sulfone-based tether on the substrate was present. The fact that no conversion of the starting enyne was observed strongly suggests that the substrate did not fit in the reaction site cavity. On the other hand, four of the tested nucleophiles proved not to be suitable for the reaction and adducts **115q**–**115t** were not observed. Instead, once again, mixtures of the 5- and 6-membered ring cyclization products were observed, without the occurrence of a nucleophilic attack.[14,51]

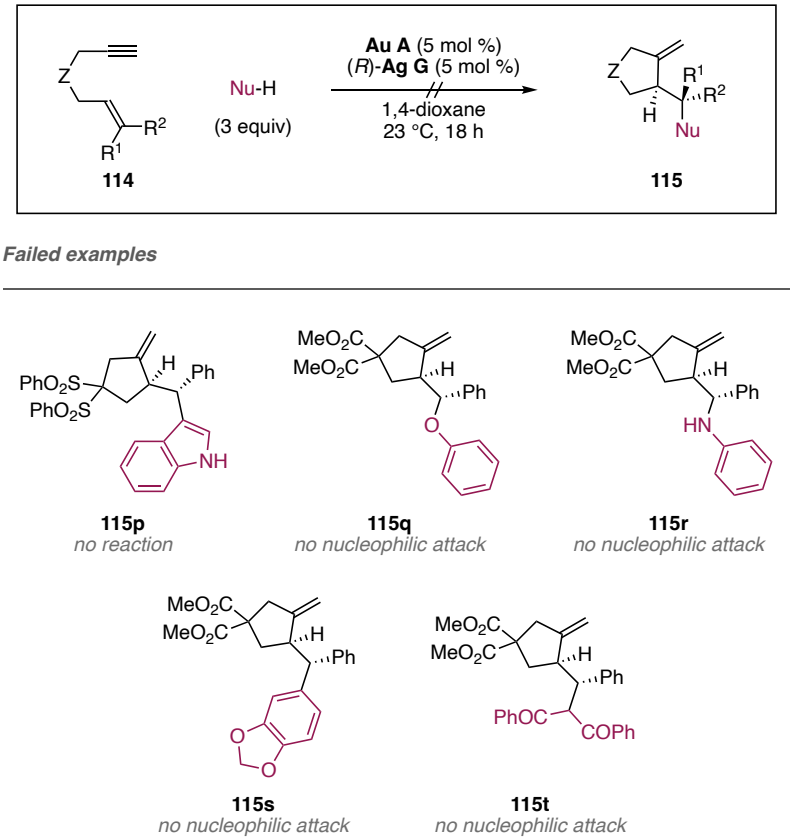


**Scheme 39**. Failed examples in the scope of the enantioselective nucleophilic addition to 1,6-enyne **114**.

## Application of Gold(I)-Cavitand Complexes: Towards the Total Synthesis of Renifolins[52]

### Introduction

### Renifolin Polyketides Family

Indane-based scaffolds are commonly found in various biologically active molecules[53] and are prevalent in several classes of secondary metabolites, including polyketides, terpenes, and alkaloids.[54] In particular, indidenes[55] and renifolins[56] prenylated polyketides isolated from the Southeast Asian plants

52 Work done in collaboration with Gabrielle Giovanardi.

53 Prasher, P.; Sharma, M. Medicinal Chemistry of Indane and Its Analogues: A Mini Review, *Chemistry Select* **2021**, *6*, 2658–2677.

54 Ahmed, N. Synthetic Advances in the Indane Natural Product Scaffolds as Drug Candidates: A Review, *Stud. Nat. Prod. Chem.* **2016**, *51*, 383–434.

55 He, R.; Huang, X.; Zhang, Y.; Wu, L.; Nie, H.; Zhou, D.; Liu, B.; Deng, S.; Yang, R.; Huang, S.; Nong, Z.; Li, J.; Huang, Y. Structural Characterization and Assessment of the Cytotoxicity of 2,3-Dihydro-1 *H*-Indene Derivatives and Coumarin Glucosides from the Bark of *Streblus Indicus*, *J. Nat. Prod.* **2016**, *79*, 2472–2478.

56 Li, Y.-P.; Yang, Y.-C.; Li, Y.-K.; Jiang, Z.-Y.; Huang, X.-Z.; Wang, W.-G.; Gao, X.-M.; Hu, Q.-F. Five New Prenylated Chalcones from *Desmodium Renifolium*, *Fitoterapia* **2014**, *95*, 214–219.

*Streblus indicus* and *Desmodium renifolium*, respectively, have been found to exhibit mild cytotoxicity against cancer cell lines in vitro.

Baudoin's group reported in 2023 the divergent synthesis of two indane polyketides of the indidene family: (+/–)-indidene A and (+)-(*S*,*R*)-indidine C (aka indidine B), in 11 and 13 steps, respectively (Figure 12). This work allowed the structure revision of indidenes B and C, which were previously missassigned.[54]

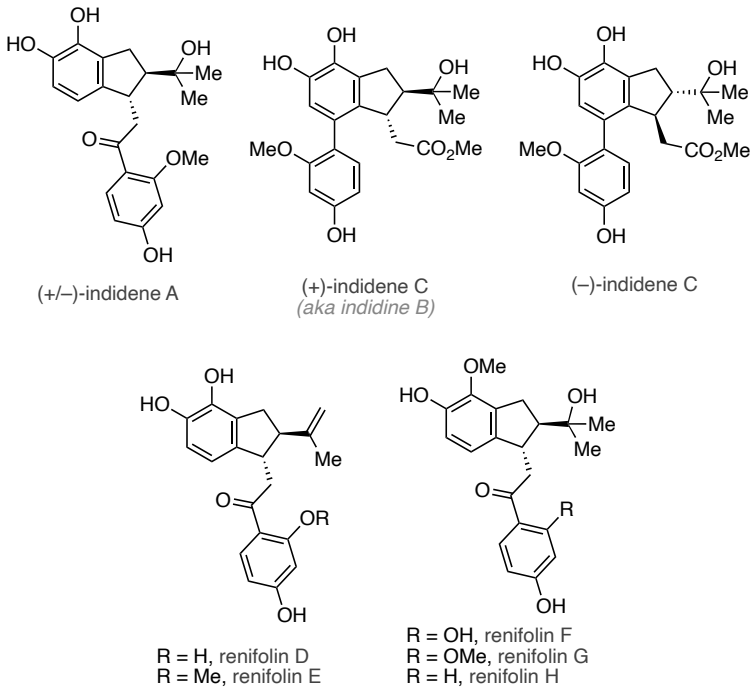


**Figure 12.** Selected members of the indidene renifolin polyketides.

**The alkoxycyclization reaction**

The first examples of alkoxycyclization reactions were reported using $PtCl_2$ as catalyst,[57] followed by the enantioselective version of such system, developed by Genêt's group.[58] The methodologies later

57 (a) Méndez, M.; Muñoz, M. P.; Echavarren, A. M. Platinum-Catalyzed Alkoxy- and Hydroxycyclization of Enynes, *J. Am. Chem. Soc.* **2000**, *122*, 11549–11550. (b) Méndez, M.; Muñoz, M. P.; Nevado, C.; Cárdenas, D. J.; Echavarren, A. M. Cyclizations of Enynes Catalyzed by $PtCl_2$ or Other Transition Metal Chlorides: Divergent Reaction Pathways, *J. Am. Chem. Soc.* **2001**, *123*, 10511–10520.

58 Charruault, L.; Michelet, V.; Taras, R.; Gladiali, S.; Genêt, J.-P. Functionalized Carbo- and Heterocycles via Pt-Catalyzed Asymmetric Alkoxycyclization of 1,6-Enynes, *Chem. Commun.* **2004**, *7*, 850–851.

extended to the use of gold(I) complexes. In 2003, the first reproducible results obtained with $AuCl_3$ for the 6-*endo-dig* cyclization of enyne **126** were published (Scheme 40).[59]

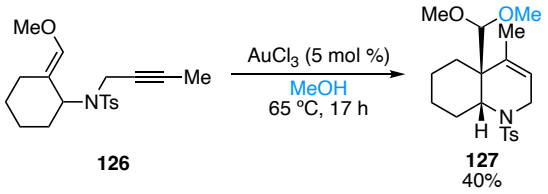


**Scheme 40**. First gold(I)-catalyzed alkoxycyclization reaction.

The first enantioselective alkoxycyclization reaction was reported in 2005, achieving enantioinduction with the use of a chiral phosphine ligand with 1,6 enynes (Scheme 41).[60] The levels of enantioinduction varied significantly depending on the substrate, as the system performed well with sulfone derivative **129b** but was ineffective with malonate **129a**.

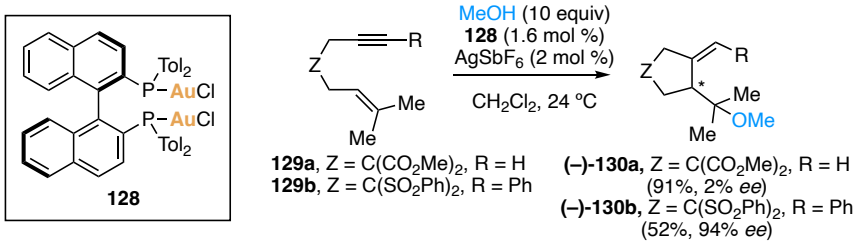


**Schem 41**. First examples on gold(I)-catalyzed enantioselective alkoxycyclization of 1,6-enynes.

Since then, several strategies were developed for this reaction to obtain enantioselective outcomes. Specifically, NHC-Au(I)-catalyzed methodologies showed promising results over the past year,[61] most works showed the correlation between the bulkiness of the ligand and the enantioselectivities observed.

---

59 Nevado, C.; Cárdenas, D. J.; Echavarren, A. M. Reaction of Enol Ethers with Alkynes Catalyzed by Transition Metals: 5-*exo-dig* versus 6-*endo-dig* Cyclizations *via* Cyclopropyl Platinum or Gold Carbene Complexes, *Chem. Eur. J.* **2003**, *9*, 2627–2635.

60 Muñoz, M. P.; Adrio, J.; Carretero, J. C.; Echavarren, A. M. Ligand Effects in Gold- and Platinum-Catalyzed Cyclization of Enynes: Chiral Gold Complexes for Enantioselective Alkoxycyclization, *Organometallics* **2005**, *24*, 1293–1300.

61 (a) Matsumoto, Y.; Selim, K. B.; Nakanishi, H.; Yamada, K.; Yamamoto, Y.; Tomioka, K. Chiral Carbene Approach to Gold-Catalyzed Asymmetric Cyclization of 1,6-Enynes, *Tetrahedron Lett.* **2010**, *51*, 404–406. (b) Gung, B. W.; Holmes, M. R.; Jones, C. A.; Ma, R.; Barnes, C. L. Structure–Enantioselectivity Correlation in NHC–Au(I) Catalysis for 1,6-Enynecyclizations, *Tetrahedron Lett.* **2016**, *57*, 3912–3915. (c) Okitsu, N.; Yoshida, T.; Usui, K.; Nakada, M. Synthesis of a New Chiral $C_2$-Symmetric NHC-AuCl Complex, *Heterocycles* **2016**, *92*, 720–732. (d) Zhang, J.-Q.; Liu, Y.; Wang, X.-W.; Zhang, L. Synthesis of Chiral Bifunctional NHC Ligands and Survey of Their Utilities in Asymmetric Gold Catalysis, *Organometallics* **2019**, *38*, 3931–3938. (e) Tugny, C.; del Rio, N.; Koohgard, M.; Vanthuyne, N.; Lesage, D.; Bijouard, K.; Zhang, P.; Meijide Suárez, J.; Roland, S.; Derat, E.; Bistri-Aslanoff, O.; Sollogoub, M.; Fensterbank, L.; Mouriès-Mansuy, V. *β*-Cyclodextrin–NHC–

In this context, in 2021 our group reported the enantioselective alkoxycyclization of 1,6-enynes catalyzed by chiral gold(I)-cavitand complexes.[13] As previously shown, we could afford good to excellent yields and enantioselectivities thanks to the strained cavity shape offered by the gold(I)-cavitand catalyst. Moreover, the methodology could be used for the first synthesis of (+)-mafaicheenamine C (Scheme 42).

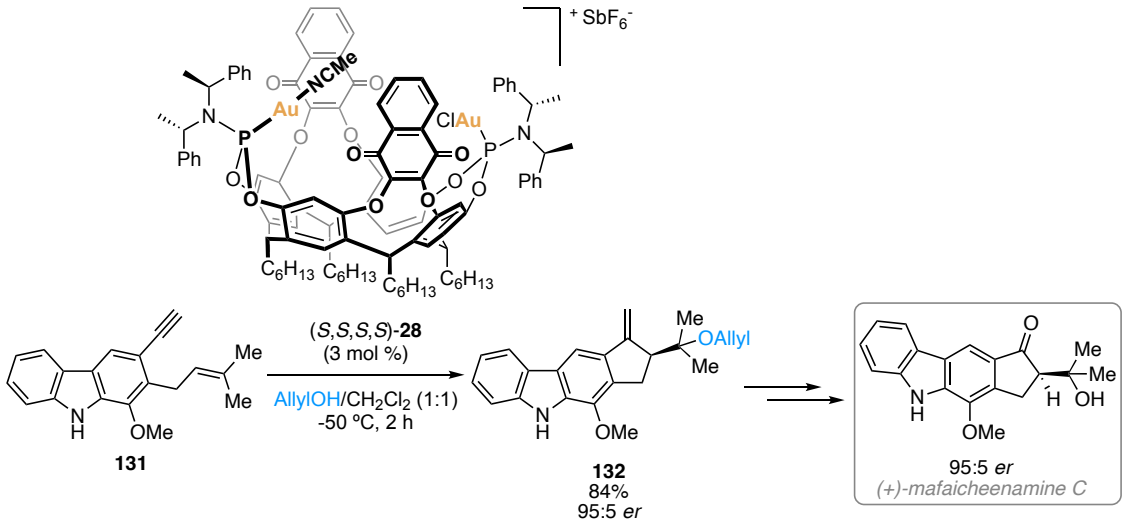


**Scheme 42**. Application of the enantioselective alkoxycyclization catalyzed by chiral gold(I)-cavitand catalyst (*S*,*S*,*S*,*S*)-**28** for the total synthesis of (+)-mafaicheenamine C.

Within this framework, we envisioned that we could afford the synthesis of renifolin natural products *via* a gold(I)-catalyzed alkoxycyclization reaction using a gold(I)-cavitand complex (Scheme 43).

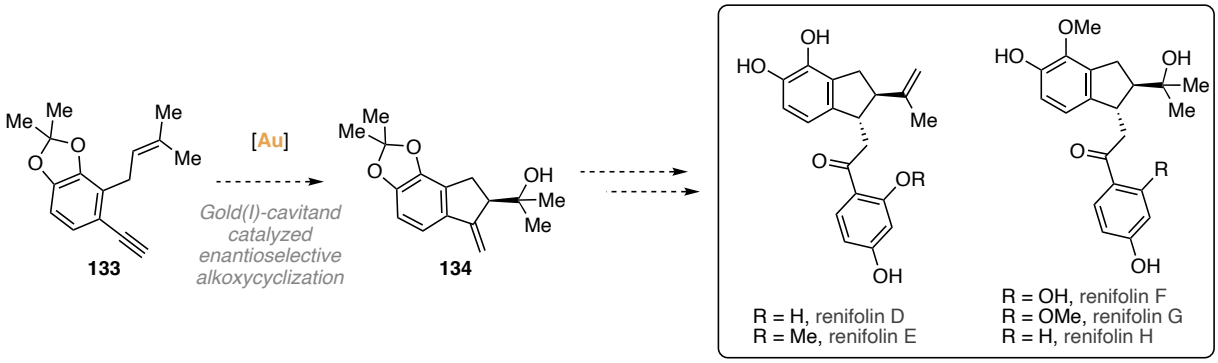


**Scheme 43**. Proposed pathway for the synthesis of renifolin *via* gold(I)-cavitand catalyzed enantioselective alkoxycyclization.

Gold(I) Complex (*β*-ICyD)AuCl: A Chiral Nanoreactor for Enantioselective and Substrate-Selective Alkoxycyclization Reactions, *ACS Catal.* **2020**, *10*, 5964–5972.

**Synthesis of the Building Block for the Gold(I)-Cavitand Catalyzed Alkoxycyclization**

Our work commenced by synthesizing the desired building block **133** (Scheme 44). The prenylation of commercially available 5-bromo-1,3-benzodioxole **135** with prenyl bromide produced **136** in 84% yield. Then, halogen exchange reaction afforded the iodinated compound **137**, which reacted with trimethylsilylacetylene to form **138**. After desilylation, we obtained the desired enyne **133**.

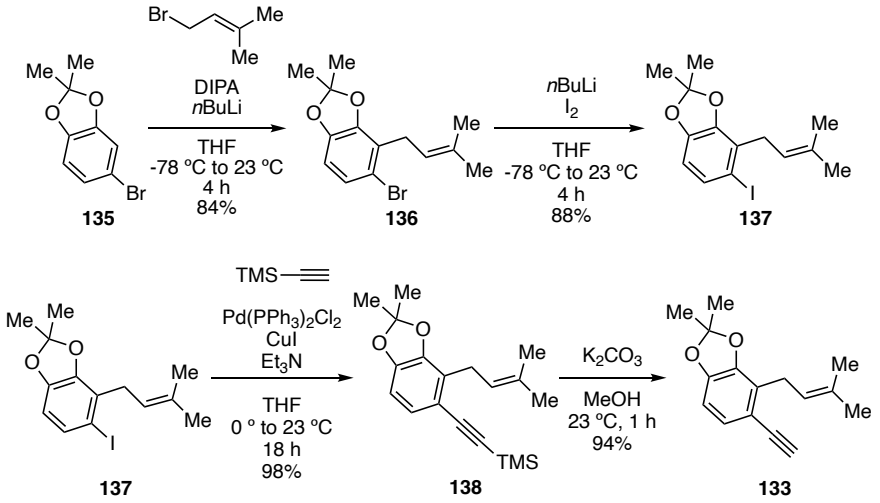


**Scheme 44**. Synthesis of key enyne **133**.

**Optimization of the Alkoxycyclization Reaction**

With the targeted enyne **133** in hand, we tested the alkoxycyclization reaction (Table 4). First, JohnPhos-gold(I) catalyst and complex **140**, which was prepared to mimic the active site of the gold(I)-cavitands, were selected to prove the reactivity towards the desired product **134**. First, using allylic alcohol as nucleophile, we compared the performance of cationic JohnPhos catalyst **139** and complex **140** to see that the first was forming product **134a** in higher yield (Table 4, entries 1 and 2). Then, we confirmed that the reaction does not proceed unless the alcohol is used as a cosolvent (Table 4, entries 3 and 4). Finally, we tested the binuclear complex (*S*,*S*,*S*,*S*)-**28'** using allylic alcohol to obtain **134a** in 57% yield and 73:27 *er* (Table 4, entry 6). Simultaneously, the analogue active catalyst (*S*,*S*,*S*,*S*)-**28** was tested in the reaction using water as nucleophile to obtain **134b** in 61% yield and 89:11 *er* (Table 4, entry 7).

**Table 4**. First experiments for the alkoxycyclization of enyne **133**.

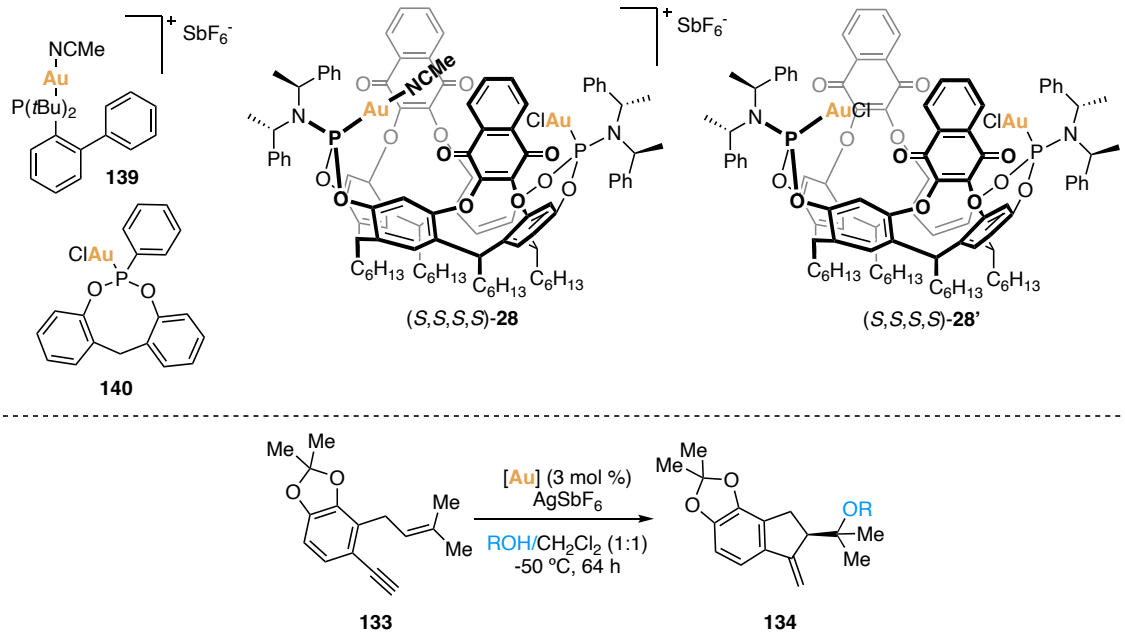


| Entry | [Au] | R | $AgSbF_6$ (mol %) | Yield (%)[a] | *er* (%)[b] |
|---|---|---|---|---|---|
| 1 | [(JohnPhos)Au(MeCN)]$SbF_6$ | allyl | - | 54 | - |
| 2 | **140** | allyl | 3 | 10 | - |
| 3[c] | [(JohnPhos)Au(MeCN)]$SbF_6$ | allyl | - | - | - |
| 4[c] | **140** | allyl | 3 | - | - |
| 5[d] | [(JohnPhos)Au(MeCN)]$SbF_6$ | H | - | 59 | - |
| 6 | (*S*,*S*,*S*,*S*)-**28'** | allyl | 6 | 57 | 73:27 |
| 7[d] | (*S*,*S*,*S*,*S*)-**28** | H | - | 61 | 89:11 |

[a] Isolated yields. [b] Enantiomeric ratios determined by HPLC. [c] Reaction run in $CH_2Cl_2$ (0.25 M) and 3 equiv of allylic alcohol and at 0 °C. [d] Acetone used instead of $CH_2Cl_2$ as solvent at 0 °C.

Based on these results, we conducted an HTE experiment to explore the possibility of improving the *er* by using a different catalytic setup. In total, we screened ten chiral gold(I)-cavitand systems (Figure 13). These included, chiral complex (*R*)-**80** (previously introduced in the second section of this chapter) and nine ACDC systems (described earlier in the third section of this chapter) using gold(I) complexes **Au A**–**Au C**, in combination with chiral silver salts (*R*)-**Ag C**, (*R*)-**Ag G** and (*R*)-**Ag K**. Finally, we also employed complexes from the first gold(I)-cavitand family:[13] mononuclear chiral complexes (*S*,*S*)-**141** and (*S*,*S*)-**142**, binuclear gold(I)-cavitand complexes (*S*,*S*,*S*,*S*)-**143a**, (*S*,*S*,*S*,*S*)-**143b**, (*S*,*S*,*S*,*S*)-**28'** and

the binuclear cationic gold(I)-cavitand catalyst (*S,S,S,S*)-**144**. Additionally, five different commercially available chloride scavengers were tested.

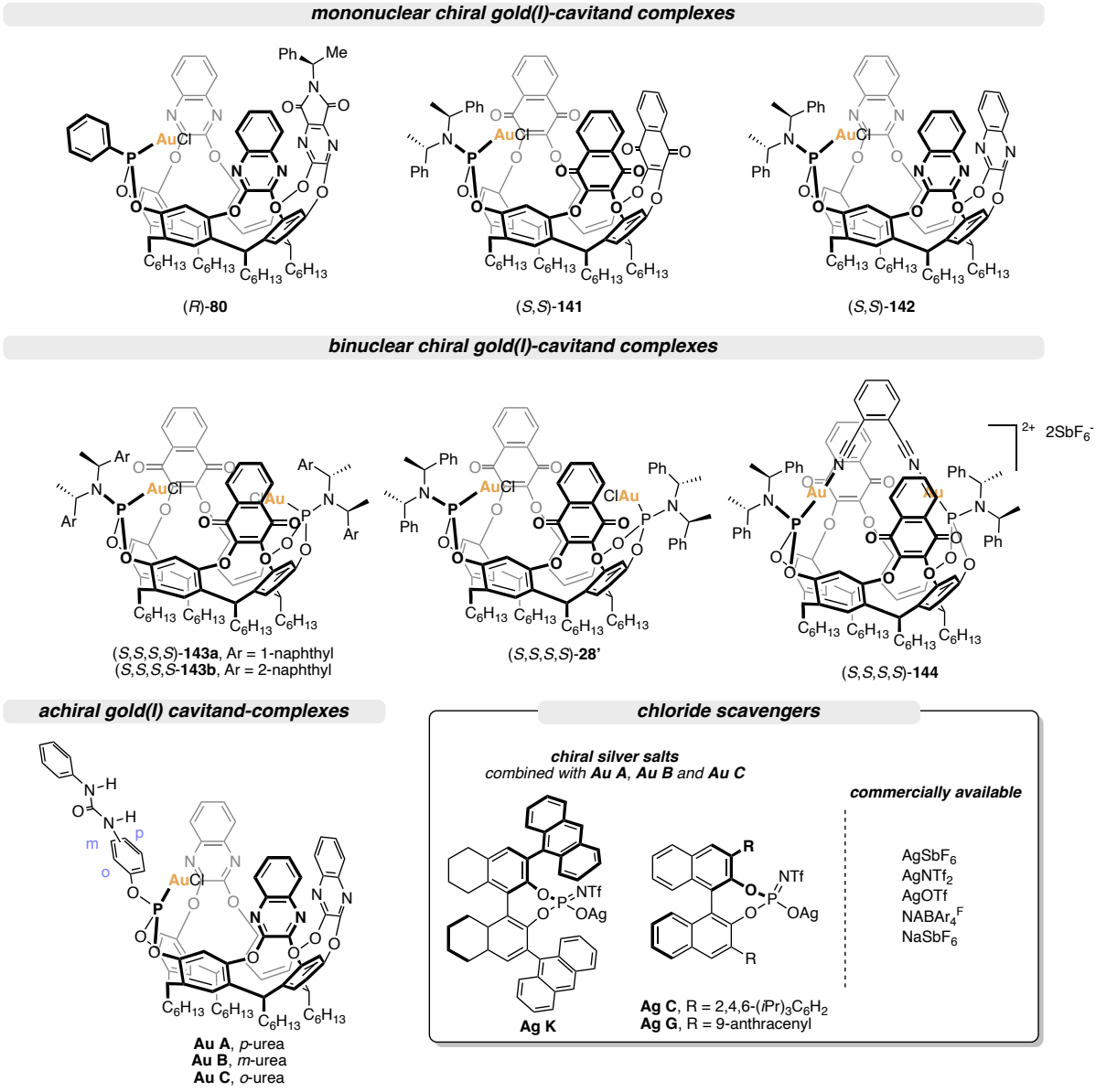


**Figure 13**. Gold(I)-cavitand complexes and chloride scavengers used in HTE experiment.

From the 50 tested reactions, we evaluated both the yield and the *ee* values (Figure 14). Four chiral gold(I)-cavitand complexes gave >70% yield towards the formation of **134b** with one or more of the five chloride scavengers used (Figure 14a, reactions B1, B4, B5, C3, E1, E2, E4, E5, F1 and F5). Then, we evaluated the *ee* values (Figure 14b). Three out of the four complexes with the highest yields also achieved the best *ee* values (Figure 14b, reactions C1–C5, E1-E5 and F1–F5). Regarding the nine tests performed using the ACDC system (Figure 13b, G6–G8, H6–H8 and I6–I8), none of them delivered **134b** in good yields and *ee*, in accordance with the result obtained in the first alkoxycyclization test performed with these systems (Table 1, page 82). Finally, five control experiments were set up to

observe that if no gold(I) complex was added in the reaction mixture no conversion of the starting material was detected (Figure 14, reactions K1–K5). Overall, the best result was observed with (*S*,*S*,*S*,*S*)-**28'** in combination with $AgSbF_6$, which gave **134b** in 83% yield and 80:20 *er* (Figure 14, reaction F1). Notably, this combination had been previously tested at 0 °C, resulting in a lower yield but a higher *ee*, producing **134b** in 61% yield and 89:11 *er* (Table 4, entry 7).

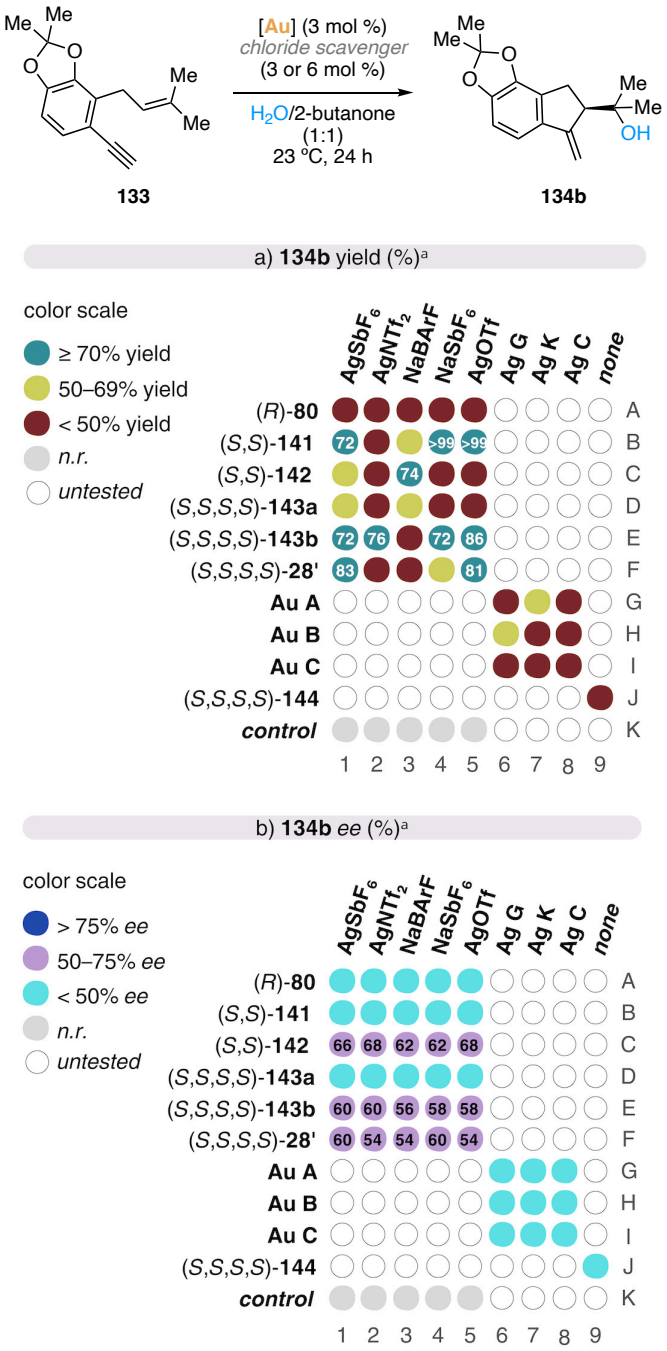


**Figure 14**. HTE results for the gold(I)-cavitand complexes and chloride scavenger screening in the alkoxycyclization reaction of **134b**. [a] Yields determined by UHPLC analysis using biphenyl as internal standard. [b] *ee* values determined by SFC analysis. All reactions were carried out at 10 µmol scale. *control*: no gold(I) complex added. *n.r.* = no reaction.

### Attempts for the Synthesis of Renifolin

Using the most effective catalytic system currently available to afford **134b**, we proceed with the synthesis towards the natural product by attempting the direct functionalization of the terminal alkene present in the molecule (Scheme 45). Our initial approach involved an intermolecular hydroacylation

to generate **146** using a rhodium catalyst and 2-hydroxylbenzaldehyde **145**,[62] but no product was obtained. Next, we explored a method utilizing benzoic acid and aniline as cocatalysts in a Rh system to afford **146**,[63] though again, no product was detected. Additionally, we tested other three conditions in the high-pressure laboratory. First, we attempted two Rh-catalyzed hydroformylations to yield the corresponding aldehyde **147** using syngas at 30 atm, but no conversion was observed.[64] Lastly, we intended to perform a hydrocarboxylation methodology for synthesizing cycloalkylacetic acids, initially using Alper's approach with a Pd-catalyzed system,[65] followed by a radical methodology which relies on the photocatalytic formate activation for the functionalization of unactivated alkenes.[66] Unfortunately, no formation of carboxylic acid **148** occurred by these methods either.

62 Kokubo, K.; Matsumasa, K.; Nishinaka, Y.; Miura, M.; Nomura, M. Reaction of 2-Hydroxybenzaldehydes with Alkynes, Alkenes, or Allenes via Cleavage of the Aldehyde C–H Bond Using a Rhodium Catalyst System, Bull. Chem. Soc. Jpn. **1999**, *72*, 303–311.

63 Jun, C.-H.; Lee, D.-Y.; Lee, H.; Hong, J.-B. A Highly Active Catalyst System for Intermolecular Hydroacylation, Angew. Chem. Int. Ed. **2000**, *39*, 3070–3072.

64 Wang, P.; Shi, H.; Feng, B.; Zhao, D.; Yang, D. Highly Selective and Recyclable Homogeneous Hydroformylation of Olefins with $[Rh(Cod)Cl]_2/PPh_3$ Regulated by $Et_3N$ as Additive, Mol. Catal. **2023**, *548*, 113459.

65 El Ali, B.; Alper, H. Palladium Acetate Catalyzed Synthesis of Cycloalkylacetic Acids by Regioselective Hydrocarboxylation of Methylenecycloalkanes with Formic Acid and 1,4-Bis(Diphenylphosphino)Butane, J. Org. Chem. **1993**, *58*, 3595–3596.

66 Alektiar, S. N.; Han, J.; Dang, Y.; Rubel, C. Z.; Wickens, Z. K. Radical Hydrocarboxylation of Unactivated Alkenes via Photocatalytic Formate Activation, *J. Am. Chem. Soc.* **2023**, *145*, 10991–10997.

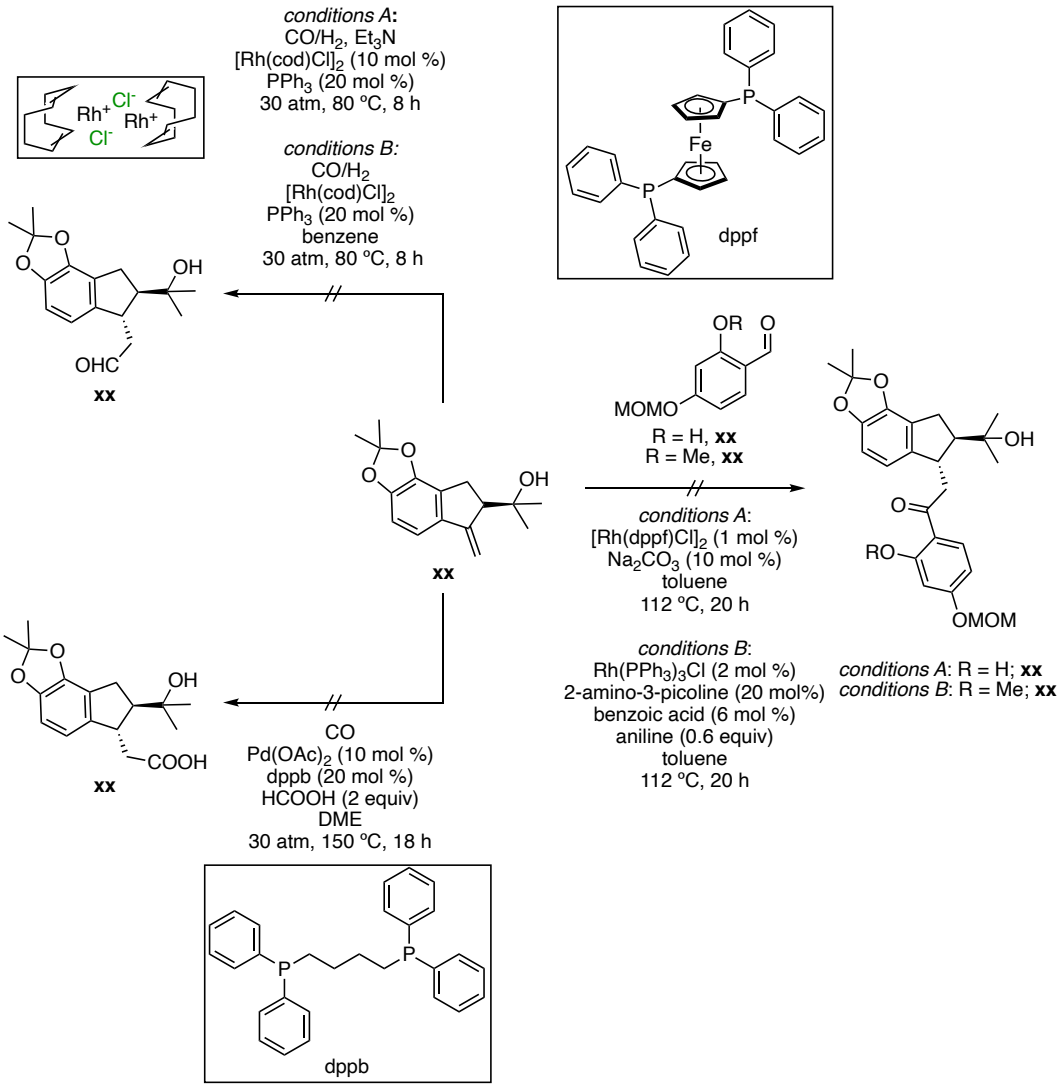


**Scheme 45**. Attempts towards the direct functionalization of terminal alkene **134b**.

**Conclusions**

Following the recent strategies developed in our group, we have explored three different approaches for the expansion of the use of gold(I)-cavitands in enantioselective transformations.

- The inclusion of amino acid moieties in the cavitand, in which the ligands could not be obtained.
- The introduction of a chiral moiety in one of the cavitand walls. This approach was accomplished by the synthesis of a new gold(I)-cavitand complex with a chiral phthalimide-type structure. Considering the results obtained while using these new compounds as catalysts, it was concluded that the adopted shape of the chiral wall in the complex was not close enough to the reaction center for efficient enantioinduction.
- The synthesis of three achiral gold(I)-cavitand complexes to be combined with chiral silver salts in an HCDC system for enantioinduction. Here, the catalytic framework achieved very good results in the enantioselective addition of several nucleophile species to 1,6-enynes.
- Finally, the use of gold(I)-cavitand complexes was applied in the alkoxycyclization reaction for the synthesis of a possible precursor for the synthesis of renifolin natural product.

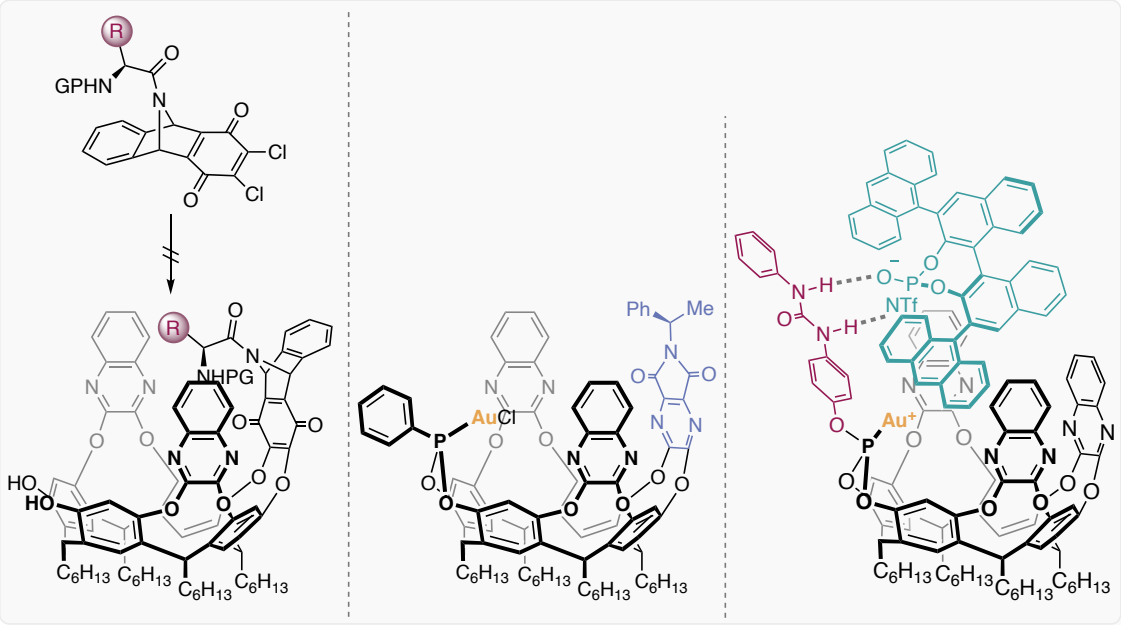

## Experimental Section

### General Methods

The synthesis of the ligands and gold(I) complexes was carried out under argon in solvents dried by passing through an activated alumina column on a PureSolvTM Solvent Purification System (SPS, Innovative Technologies, Inc., MA). Yields refer to chromatographically and spectroscopically pure ($^1$H NMR) homogeneous material, unless otherwise stated. Thin layer chromatography was carried out using TLC aluminum sheets coated with 0.2 mm of silica gel (Merck Gf234) using short-wave UV light as visualizing agent and, $KMnO_4$ or acidic vanillin followed by heat as developing agents. UHPLC-MS was performed in Agilent Technologies 1290 Infinity II, LC-MS with single-squad detector InfinityLab (APCI ionization source). Chromatographic purifications were carried out using flash grade silica gel (SDS Chromatogel 60 ACC, 40-60 μm) as the stationary phase manually, or using a CombiFlash®Rf instrument with normal phase disposable columns of different sizes (Teledyne Isco). Reactions were monitored by TLC and UHPLC (Agilent Technologies 1290 Infinity II, LC/MS with single-quad detector InfinityLab (APCI ionization source). Melting points were determined using a MP70 Melting Point System (Mettler Toledo). NMR spectra were recorded at 298 K on BrukerAvance Ultrashield NMR spectrometers (300 MHz, 400 MHz, 500 MHz and 500 MHz with CryoProbe). Chemical shifts (δ) are reported in parts per million (ppm) and referenced to residual solvent (for $^1$H NMR: $CDCl_3$ at 7.26 ppm, $CD_2Cl_2$ at 5.31 ppm, $(CD_3)_2SO$ at 2.50 ppm, $C_2D_2Cl_4$ at 6.0 ppm, $(CD_3)_2CO$ at 2.95 ppm; for $^{13}$C NMR: $CDCl_3$ at 77.16 ppm, $CD_2Cl_2$ at 54.00 ppm, $(CD_3)_2SO$ at 39.52 ppm, $C_2D_2Cl_4$ at 73.78 ppm, $(CD_3)_2CO$ at 29.92 ppm). The following abbreviations were used to explain multiplicities: s = singlet, d = doublet, t = triplet, q = quartet, p = "pentet" (quintet), m = multiplet, bs = broad singlet. $^{13}$C, $^{31}$P and $^{19}$F NMR spectra were always acquired with proton decoupling, even when not explicitly written. Coupling constants (*J*) are reported in Hertz (Hz). Two-dimensional NMR spectroscopy experiments (COSY, HSQC and HMBC) were used to assist in the assignment of signals in $^1$H and $^{13}$C spectra and data are reported only on selected compounds. Mass spectra were recorded on a Waters LCT Premier Spectrometer (ESI and APCI) or on an Autoflex Broker Daltonics (MALDI and LDI). Elemental analyses were performed on a LECO CHNS 932 micro- analyzer at the Universidad Complutense de Madrid. Specific optical rotation measurements were carried out on a Jasco P-1030 model polarimeter equipped with a PMT detector using the sodium line at 589 nm. Chiral HPLC analyses were performed on an Agilent Technologies 1200 series. SFC analyses were performed on an Agilent Technologies 1260 Infinity II, a Waters ACQUITY UPC2 System with diode array detector and by Chiral Technologies Europe analytical service. X-ray diffraction data were collected at 100 K on a Rigaku MicroMax-007HF, Mo *Kα* rotating anode, equipped with a Pilatus 200 K detector or on a Bruker APEX DUO, Mo *Kα* Microfocus source E025 IuS anode, equipped with an APEX DUO detector using omega scans.

Unless otherwise stated, reagents were obtained from commercial sources and used without further purification.

**Synthetic Procedures and Analytical Data**

**General procedure GP1: gold complexation**

Under an argon atmosphere, $(Me_2S)AuCl$ was added to a solution of the corresponding phosphonite or phosphite in anhydrous $CH_2Cl_2$ (0.05 M) at 23 °C. The reaction mixture was stirred at that temperature for 1 h and then concentrated under reduced pressure. The crude was purified by flash column chromatography on silica gel to obtain the gold(I) complexes.

**Resorcin[4]arene 34**

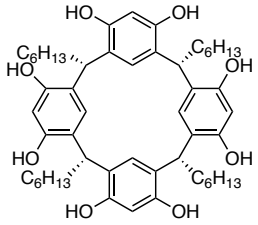


A reported procedure was followed.[67] Resorcinol (20 g, 0.181 mol, 1.0 equiv) was dissolved in $EtOH/H_2O$ (95:5 ratio, 120 mL, 0.99 M) and 36 mL of 37% aqueous HCl. The solution was cooled in an ice bath and of heptaldehyde (25.3 mL, 0.181 mol, 1.0 equiv) was added dropwise over a period of 1 h with an addition funnel. The mixture was allowed to slowly warm to 23 °C. The reaction mixture was then maintained at 80 °C for 12 h, and the yellow needles that separated were collected by filtration and washed with cold 1:1 $EtOH/H_2O$ until the material was pale yellow, and neutral to pH paper. Drying under vacuum at 100 °C for 16 h. Product **34** was used without further purification. Off-orange solid (28.6 g, 34.7 mmol, 77% yield).

**$^1$H NMR** (400 MHz, DMSO) δ 8.86 (s, 8H), 7.14 (s, 4H), 6.14 (s, 4H), 4.21 (t, $J$ = 7.8 Hz, 4H), 2.00 (m, 8H), 1.35 – 1.09 (m, 32H), 0.83 (t, $J$ = 6.9 Hz, 12H) ppm.

The spectral data were fully consistent with those previously reported.

67 Dueno, E. E.; Bisht, K. S. Synthesis of Polyhydroxy Cavitands and Intramolecular Inclusion of Their Octaester Derivatives, Tetrahedron **2004**, *60*, 10859–10868.

**Tetraquinoxaline 1a**

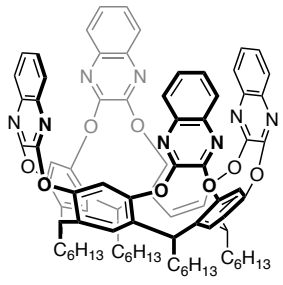

A reported procedure was followed.[68] Resorcin[4]arene **34** (20.2 g, 24.4 mmol, 1.0 equiv) and 2,3 dichloroquinoxaline (19.5 g, 97.7 mmol, 4.0 equiv) were suspended in anhydrous DMSO (287.4 mL, 0.085 M) and heated to 60 °C for 1 h. Then, K2CO3 (40.5 g, 293.2 mmol, 12.0 equiv) was then added in portions and the resulting mixture heated at 60 °C for 18 h. The reaction was cooled to room temperature, poured onto H2O (400 mL) and filtered. The solid was washed with H2O (3 x 100 mL) and dried under vacuum. The crude material was then crystallized from hot CH2Cl2 (*ca.* 40 mL) and AcOEt (*ca.* 80 mL). The resulting solid was filtered and washed with cold AcOEt (3 x 30 mL). White solid (19.5 g, 14.7 mmol, 60% yield).

**$^1$H NMR** (500 MHz, $CDCl_3$) δ 8.12 (s, 4H), 7.88 – 7.75 (m, 8H), 7.62 – 7.42 (m, 8H), 7.20 (s, 4H), 5.51 (bs, 4H), 2.21 – 2.31 (m, 4H), 1.52 – 1.30 (m, 32H), 0.93 (t, $J$ = 6.6 Hz, 12H) ppm.

The spectral data were fully consistent with those previously reported.

**Tetranaphtoquinone 1b**

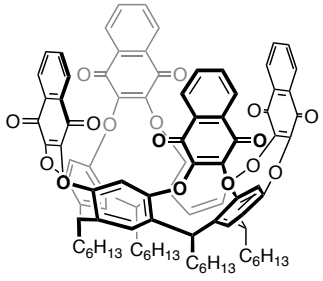

To a solution of resorcin[4]arene **34** (10 g, 12 mmol, 1.0 equiv) and 2,3-dichloronaphtalene-1,4-dione (12 g, 51 mmol, 4.2 equiv) in DMSO (180 mL, 0.067 M) at 50 ºC, $K_2CO_3$ (11 g, 82 mmol, 6.8 equiv) was added. The mixture was vigorously stirred for 18 h at 50 °C, then poured into $H_2O$. The resulting precipitate was collected by filtration, washed with $H_2O$ (x3), and dried under reduced pressure. The residue was purified by flash column chromatography ($SiO_2$, CH2Cl2/AcOEt 100:00 to 99:1). Yellow solid (9.5 g, 6.6 mmol, 54% yield).

68 Knighton, R. C.; Chaplin, A. B. Synthesis, Structure and Binding Properties of a Series of Dissymmetric Resorcin[4]Arene-Based Cavitands, *Tetrahedron* **2017**, *73*, 4591–4596.

**$^1$H NMR** (400 MHz, $CDCl_3$) δ 8.16 (ddt, *J* = 9.5, 7.3, 3.0 Hz, 8H), 7.72 (dd, *J* = 5.8, 3.2 Hz, 8H), 7.64 (s, 2H), 7.15 (s, 2H), 7.10 (s, 2H), 6.23 (s, 2H), 4.3 – 4.36 (m, 4H), 1.95 – 2.25 (m, 8H), 1.15 – 1.39 (m, 32H), 0.92 – 0.80 (m, 12H).

The spectral data were fully consistent with those previously reported.

**Biphenol 36**

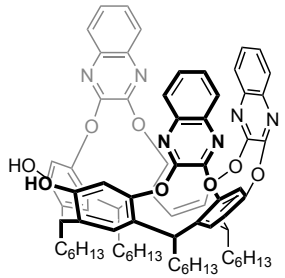


A reported procedure was followed.[69] Tetraquinoxaline **1a** (2.7 g, 2.03 mmol, 1.0 equiv) and CsF (6.2 g, 40.7 mmol, 20.0 equiv) were dissolved in anhydrous DMF (101.7 m, 0.02 M). The mixture was heated at 80 °C and catechol (246.4 mg, 2.24 mmol, 1.1 equiv) was added. After 45 min, the reaction was quenched by pouring the mixture into 250 mL of brine. The residue was purified by flash column chromatography ($SiO_2$, CH2Cl2/AcOEt 95:5). Off-white solid (1.5 g, 1.2 mmol, 61% yield).

**$^1$H NMR** (500 MHz, CDCl3) δ 8.23 (bs, 2H), 7.92 (dd, *J* = 1.0, 8.0 Hz, 2H), 7.83 (dt, *J* = 3.4, 3.4, 6.8 Hz, 2H), 7.76 – 7.71 (m, 2H), 7.66 (dd, *J* = 1.0, 8.0 Hz, 2H), 7.57 – 7.48 (m, 2H), 7.46 – 7.41 (m, 2H), 7.28 (s, 2H), 7.13 (s, 2H), 7.08 (s, 2H,), 5.58 (t, *J* = 8.0 Hz, 1H), 5.50 (t, *J* = 8.0 Hz, 2H), 4.25 (t, *J* = 8.0 Hz, 1H), 2.29 – 2.16 (m, 8H), 1.46 – 1.24 (m, 32H), 0.93 (t, *J* = 7.0 Hz, 12H) ppm.

The spectral data were fully consistent with those previously reported.

69 Ballistreri, F. P.; Brancatelli, G.; Demitri, N.; Geremia, S.; Guldi, D. M.; Melchionna, M.; Pappalardo, A.; Prato, M.; Tomaselli, G. A.; Trusso Sfrazzetto, G. Recognition of $C_{60}$ by Tetra- and Tri-Quinoxaline Cavitands, *Supramol. Chem.* **2016**, *28*, 601–607.

**Tetraphenol 37a**

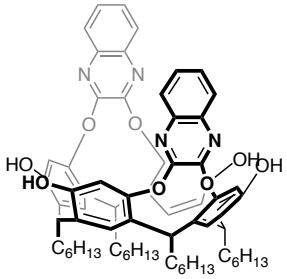

A reported procedure was followed.[68] A suspension of teatraquinoxaline **1a** (6.00 g, 4.51 mmol, 1.0 equiv) and CsF (13.71 g, 90.25 mmol, 20.0 equiv) in anhydrous DMF (600 mL, 0.0075 M) was heated to 80 °C. Catechol (1.59 g, 14.44 mmol, 3.2 equiv) was added and the reaction stirred at that temperature for 45 min. The reaction was poured onto iced brine (-10 °C; ca. 300 mL), filtered, and washed with $H_2O$. The crude material was co-evaporated with toluene (x2) to remove traces of DMF. The residue was purified by flash column chromatography ($SiO_2$, CH2Cl2/AcOEt 100:0 to 90:10). Off-white solid (4.9 g, 2.0 mmol, 41% yield).

**$^1$H NMR** (400 MHz, $(CD_3)_2CO$) δ 7.72 (s, 4H), 7.70 (dd, *J* = 6.3, 3.4 Hz, 4H), 7.48 (dd, *J* = 6.4, 3.4 Hz, 4H), 7.17 (s, 4H), 5.50 (t, *J* = 8.3 Hz, 2H), 4.44 (t, *J* = 7.9 Hz, 2H), 2.30 – 2.19 (m, 8H), 1.49 – 1.27 (m, 12H), 0.95 – 0.86 (m, 12H) ppm.

The spectral data were fully consistent with those previously reported.

**Tetraphenol 37b**

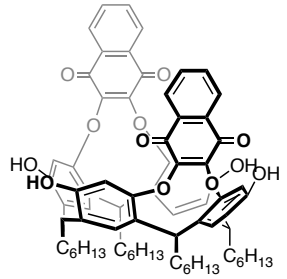

A reported procedure was followed.[70] Tetranaphthoquinone **1b** (3.51 g, 2.43 mmol, 1.0 equiv), pyrocatechol (670 mg, 6.1 mmol, 2.5 equiv) and CsF (7.4g, 48.7 mmol, 20.0 equiv) were dissolved in anhydrous DMF (356 mL, 0.7 M) at 23 ºC. The mixture was stirred for 25 min at 70 ºC before it was poured into ice-brine solution filtered, and washed with $H_2O$. The crude material was co-evaporated with toluene (x2) to remove traces of DMF. The residue was purified by flash column chromatography ($SiO_2$, CH2Cl2/AcOEt 100:0 to 80:20). Orange solid (1.1 g, 0.97 mmol, 40% yield).

70 Pochorovski, I.; Ebert, M.-O.; Gisselbrecht, J.-P.; Boudon, C.; Schweizer, W. B.; Diederich, F. Redox-Switchable Resorcin[4]Arene Cavitands: Molecular Grippers, *J. Am. Chem. Soc.* **2012**, *134*, 14702–14705.

**$^1$H NMR** (400 MHz, $(CD_3)_2CO$) δ 8.36 (s, 4H), 8.02 (dd, *J* = 5.7, 3.3 Hz, 4H), 7.82 (td, *J* = 5.8, 3.4 Hz, 4H), 7.17 (s, 4H), 6.84 (s, 4H), 4.80 (t, *J* = 7.8 Hz, 2H), 4.56 (bs, 2H), 2.20 (q, *J* = 7.5 Hz, 4H), 1.98 – 1.93 (m, 4H), 1.41 – 1.22 (m, 32H), 0.91 – 0.81 (m, 12H) ppm.

The spectral data were fully consistent with those previously reported.

**Attempted Synthesis of Chiral Amino Acid-Cavitand Gold(I) Complex**

**9-(Pyridin-2-ylsulfonyl)-1,4-dihydro-1,4-epiminonaphthalene (51a)**

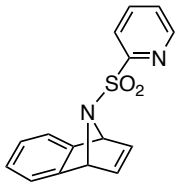


A reported procedure was followed.[71] To a solution of salicyl *N*-(2'-pyridylsulfonyl)pyrrole **50** (340 mg, 1.63 mmol, 1.0 equiv) and 2-((trimethylsilyl)oxy)phenyl trifluoromethanesulfonate **49** (667 mg, 2.12 mmol, 1.3 equiv) in acetonitrile (20.4 mL, 0.08 M) was added CsF (620 mg, 4.08 mmol, 2.5 equiv) in one portion. After stirring at 25 °C for 5 h, the reaction mixture was poured into aqueous $Na_2CO_3$ solution (10%, 5 mL). The resulting mixture was extracted with AcOEt (x3). The combined extracts were dried over $MgSO_4$, filtered and concentrated under reduced pressure. The residue was purified by flash column chromatography ($SiO_2$, CyH/AcOEt 95:5). Off-white solid (464 mg, 1.36 mmol, 83% yield).

**$^1$H NMR** (400 MHz, $CDCl_3$) δ 8.54 (dt, *J* = 4.7, 1.4 Hz, 1H), 7.72 – 7.66 (m, 2H), 7.29 (ddd, *J* = 5.8, 4.7, 3.1 Hz, 1H), 7.04 (dd, *J* = 5.1, 3.0 Hz, 2H), 6.79 (t, *J* = 1.6 Hz, 2H), 6.75 (dd, *J* = 5.2, 3.0 Hz, 2H), 5.60 (t, *J* = 1.6 Hz, 2H) ppm.

**$^{13}$C NMR** (101 MHz, $CDCl_3$) δ 155.9, 150.1, 147.4, 142.7, 137.7, 125.2, 123.6, 121.3, 68.1 ppm.

**HRMS** (ESI+) calculated for m/z $[C_{15}H_{12}N_2NaO_2S]^+$, $[M+Na]^+$: 307.0512, found: 307.0514.

The spectral data were fully consistent with those previously reported.

71 Lu, S.-S.; Lu, C.-D. Efficient Synthesis of *N*-(9-Xanthyl)-4-Toluenesulfonamides Enabled by an Addition-Cyclization Cascade of Arynes, Synlett **2013**, *24*, 640–644.

**11-(Pyridin-2-ylsulfonyl)-4a,9,9a,10-tetrahydro-9,10-epiminoanthracene-1,4-dione (53a)**

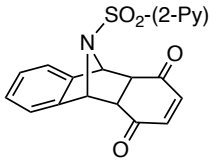


*Note: 1,4-benzoquinone was purified every time before use under vacuum sublimation at 100 °C using a cold finger set up.*

To a solution of **51a** (200 mg, 0.7 mmol, 1.0 equiv) in chloroform (2.4 mL, 0.3 M) were added 1,4-benzoquinone (76 mg, 0.7 mmol, 1.0 equiv) and 3,6-di(pyridin-2-yl)-1,2,4,5-tetrazine **52** (166.2 mg, 0.7 mmol, 1.0 equiv). The mixture was heated to 65 ºC and kept stirring at that temperature for 2 h. Then, evaporation of the solvent followed by purification of the crude mixture by flash column chromatography ($SiO_2$, CyH/AcOEt 90:10). Off-white solid (129 mg, 0.35 mmol, 50% yield).

**M.p.** = 130 °C.

**$^1$H NMR** (400 MHz, $CDCl_3$) δ 8.39 (ddd, *J* = 4.7, 1.7, 0.9 Hz, 1H), 7.72 – 7.67 (m, 1H), 7.62 (td, *J* = 7.7, 1.7 Hz, 1H), 7.21 (ddd, *J* = 7.5, 4.7, 1.3 Hz, 1H), 6.88 (s, 4H), 6.07 (s, 2H), 5.65 (dd, J = 3.1, 1.8 Hz, 2H), 3.85 (dd, J = 3.2, 1.7 Hz, 2H) ppm.

**$^{13}$C NMR** (101 MHz, $CDCl_3$) δ 195.3, 155.8, 150.2, 140.4, 140.3, 137.7, 127.7, 126.6, 123.0, 122.1, 66.9, 49.2 ppm.

**HRMS** (ESI+) calculated for m/z $[C_{19}H_{14}N_2NaO_4S]^+$, $[M+Na]^+$: 389.0566, found: 389.0581.

***tert*-Butyl 1,4-dihydro-1,4-epiminonaphthalene-9-carboxylate (51b)**

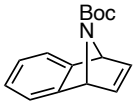


A reported procedure was adapted.[32] To a solution of *N*-(*tert*-butoxycarbonyl) pyrrole **57** (1.4 g, 8.4 mmol, 1.0 equiv) in DME (3.3 mL, 2.5 M) at 50 °C in a three-neck flask fitted with a reflux condenser and two addition funnels, was simultaneously and dropwise added a solution of anthranilic acid **56** (1.3 g, 9.2 mmol, 1.1 equiv) in DME (9.4 mL, 0.97 M) and a solution of isoamylnitrite (1.5 mL, 11 mmol, 1.3 equiv) in DME (5 mL, 2.2 M) separately. After the slow addition the reaction was stirred at 50 °C for 2 h. The mixture was concentrated, and the residue was dissolved in diethyl ether and washed with saturated $K_2CO_3$ (x3). The aqueous layer was extracted with $Et_2O$ (x2) and the combined organic layers were washed with brine (x2). The combined organic layer was dried over $MgSO_4$, filtered and concentrated under reduced pressure. The residue was purified by flash column chromatography ($SiO_2$, CyH/AcOEt 95:5). Off-white solid (1.64 g, 6.74 mmol, 80% yield).

**$^{1}$H NMR** (300 MHz, $CDCl_3$) δ 7.21 – 7.29 (m, 2H), 6.98 – 6.95 (m, 4H), 5.48 (bs, 1H), 1.38 (s, 9H) ppm.

**$^{13}$C NMR** (126 MHz, $CDCl_3$) δ 155.1, 148.4, 143.0, 125.0, 120.7, 80.5, 66.5, 28.2 ppm.

The spectral data were fully consistent with those previously reported.

**2,3-Dichlorobenzene-1,4-diol (59a)**

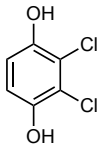


*Note: 1,4-benzoquinone was purified every time before use under vacuum sublimation at 100 °C using a cold finger set up.*

A reported procedure was followed.[72] A suspension of 1,4-benzoquinone (4.5 g, 41.6 mmol, 1.0 equiv) in anhydrous $Et_2O$ (36.5 mL, 1.14 M) was treated with $SO_2Cl_2$ (6.77 mL, 83.3 mmol, 2.0 equiv), and stirred for 18 h at 25 °C. The mixture was cooled in an ice bath and filtered. The collected solid was washed with cold $Et_2O$ (10 mL), and dried in vacuo. A suspension of the solid in AcOH (20 mL) was treated with conc. $H_2SO_4$ (2 mL), stirred for 24 h at 60 °C, and poured into ice. The mixture was extracted with $Et_2O$ (x2), the combined organic layers were washed with brine, dried over $MgSO_4$, filtered and concentrated under reduced pressure. The crude product was purified by flash column chromatography ($SiO_2$, CyH/AcOEt 70:30). Off-white solid (2.5 g, 14 mmol, 34% yield).

**$^{1}$H NMR** (400 MHz, $CDCl_3$) δ 6.93 (s, 2H), 5.23 (s, 2H) ppm.

**$^{13}$C NMR** (101 MHz, $CDCl_3$) δ 146.2, 118.3, 146.2 ppm.

The spectral data were fully consistent with those previously reported.

**2,3-Dichlorocyclohexa-2,5-diene-1,4-dione (59b)**

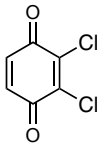


A reported procedure was followed.[72] A solution of 2,3-dichlorobenzene-1,4-diol (2.0 g, 11.17 mmol) in $Et_2O$ (164.3 mL, 0.068 M) was treated with $Ag_2O$ (6.5 g, 27.93 mmol, 2.5 equiv) for 30 min at 25

72 Pochorovski, I.; Boudon, C.; Gisselbrecht, J.-P.; Ebert, M.-O.; Schweizer, W. B.; Diederich, F. Quinone-Based, Redox-Active Resorcin[4]Arene Cavitands, *Angew. Chem. Int. Ed.* **2012**, *51*, 262–266.

°C. The mixture was filtered, and the solvent was evaporated. The crude product was purified by flash column chromatography ($SiO_2$, CyH/AcOEt 90:10). Yellow solid (1.56 g, 8.81 mmol, 79% yield).

**$^1$H NMR** (400 MHz, $CDCl_3$) δ 7.00 (s, 2H) ppm.

**$^{13}$C NMR** (101 MHz, $CDCl_3$) δ 177.4, 136.2, 141.2 ppm.

The spectral data were fully consistent with those previously reported.

***tert*-Butyl 2,3-Dichloro-1,4-dioxo-1,4,4a,9,9a,10-hexahydro-9,10-epiminoanthracene-11-carboxylate (55b)**

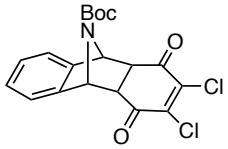


To a solution of **51b** (1.1 g, 4.52 mmol, 1.0 equiv) in chloroform (15.07 mL, 0.3 M) were added **59b** (800.1 mg, 4.52 mmol, 1.0 equiv) and 3,6-di(pyridin-2-yl)-1,2,4,5-tetrazine **52** (1.07 g, 4.52 mmol, 1.0 equiv). The mixture was heated to 65 ºC and kept stirring at that temperature for 2 h. Then, evaporation of the solvent followed by purification of the crude mixture by flash column chromatography ($SiO_2$, CyH/AcOEt 90:10). Off-white solid (1.24 g, 3.15 mmol, 70% yield).

**M.p.** = 151 °C.

**$^1$H NMR** (500 MHz, $CDCl_3$) δ 7.19 (dd, $J$ = 5.5, 3.1 Hz, 2H), 7.14 (dd, $J$ = 5.4, 3.1 Hz, 2H), 5.59 – 5.55 (m, 2H), 3.88 – 3.71 (m, 2H), 1.45 (s, 9H) ppm.

**$^{13}$C NMR** (126 MHz, $CDCl_3$) δ 185.9, 153.8, 140.1, 128.8, 128.6, 121.8, 82.2, 65.6, 49.2, 28.3 ppm.

**1,4-Dihydro-1,4-epiminonaphthalene**

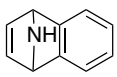


A reported procedure was adapted.[73] Under an argon atmosphere, acetyl chloride (1.7 mL, 23.6 mmol, 6.0 equiv) was added dropwise to 13.6 mL of MeOH at 0 °C. The resulting solution was stirred for 5 min at 0 °C and tert-butyl 1,4-dihydro-1,4-epiminonaphthalene-9-carboxylate (0.96 g, 3.93 mmol, 1.0 equiv) was added. The solution was allowed to warm to 23 °C and stirred for additional 2 h. Water was added, and the mixture was extracted with $Et_2O$ (x2). The aqueous layer was subsequently adjusted to pH ~ 10 with $K_2CO_3$ and extracted with $Et_2O$ (x3). The combined organic layers were dried over

73 Prenzel, A. H. G. P.; Deppermann, N.; Maison, W. Azabicycloalkenes as Synthetic Intermediates: Application to the Preparation of Diazabicycloalkane Scaffolds, *Org. Lett.* **2006**, *8*, 1681–1684.

$MgSO_4$, filtered, and the solvent was removed in vacuo (~ 400 mbar, *careful: volatile!*) to afford free amine as a brown oil, used on the next step without further purification.

**$^1$H NMR** (500 MHz, $CDCl_3$) δ 7.23 (dd, *J* = 5.1, 3.0 Hz, 2H), 7.00 (t, *J* = 1.4 Hz, 2H), 6.92 (dd, *J* = 5.1, 3.0 Hz, 2H), 4.98 (t, *J* = 1.3 Hz, 2H), 3.48 (bs, 1H) ppm.

**$^{13}$C NMR** (126 MHz, $CDCl_3$) δ 151.1, 144.5, 124.8, 120.9, 66.3 ppm.

The spectral data were fully consistent with those previously reported.

***tert*-Butyl ((2*S*)-1-(1,4-Dihydro-1,4-epiminonaphthalen-9-yl)-3-methyl-1-oxobutan-2-yl)carbamate (51c)**

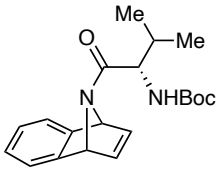


Compound **51b** (0.92 g, 6.43 mmol, 1.0 equiv) was added to a solution of *N*-Boc-$_L$-valine (1.4 g, 6.43 mmol, 1.0 equiv) in DMF (12.9 mL, 0.5 M), then into which HATU (2.93 g, 7.71 mmol, 1.2 equiv) and DIEA (1.66 g, 12.85 mmol, 2.0 equiv) were added. Reaction system was stirred for 18 h at 23 °C. Reaction solution was poured into water and extracted with AcOEt (x2). Organic phase was washed with $H_2O$ and brine each once, then dried over $MgSO_4$, filtered, and concentrated under reduced pressure. The crude product was purified by flash column chromatography ($SiO_2$, CyH/AcOEt 80:20). Off-white foam (1.25 g, 3.64 mmol, 93% yield over two steps).

**M.p.** = 132 °C.

*Note: Due to the presence of rotamers mixture (1:1), NMR studies were performed at 393 K, see compound **62c** where a T slope study was performed to demonstrate its presence and behaviour over T.*

**$^1$H NMR** (500 MHz, $C_2D_2Cl_4$, 393 K) δ 7.31 (td, *J* = 5.7, 3.1 Hz, 2H), 7.10 – 7.02 (m, 2H), 7.02 – 6.99 (m, 2H), 5.86 (s, 2H), 4.94 (d, *J* = 9.2 Hz, 1H), 4.21 (dd, *J* = 9.5, 6.6 Hz, 1H), 1.99 (h, *J* = 6.7 Hz, 1H), 1.48 (s, 9H), 1.11 – 0.83 (m, 6H).

**$^{13}$C NMR** (126 MHz, $C_2D_2Cl_4$, 393 K) δ 154.8, 147.6, 147.4, 124.6, 124.6, 120.3, 78.9, 56.1, 30.4, 27.8, 18.7, 17.0 ppm.f

**$[\alpha]^{22.4}_D$** +21.9 (c 0.03, $CH_2Cl_2$).

**HRMS** (ESI+) calculated for m/z $[C_{20}H_{26}N_2NaO_3]^+$, $[M+Na]^+$: 365.1836; found: 365.1843.

**_tert_-Butyl ((2*S*)-1-(2,3-Dichloro-1,4-dioxo-1,4,4a,9,9a,10-hexahydro-9,10-epiminoanthracen-11-yl)-3-methyl-1-oxobutan-2-yl)carbamate (55c)**

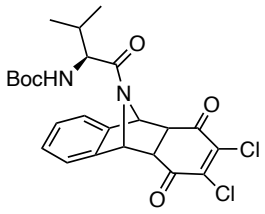


A mixture of tert-butyl **51c** (1.1 g, 4.52 mmol, 1.0 equiv), 3,6-di(pyridine-2-yl)-1,2,4,5-tetrazine **52** (1.07 g, 4.52 mmol, 1.0 equiv), and 2,3-dichlorocyclohexa-2,5-diene-1,4-dione **59b** (800.1 mg, 4.52 mmol, 1.0 equiv) in chloroform (15.1 mL, 0.3 M) was refluxed for 2 h. The solvent was removed in vacuo and the crude was purified by flash column chromatography ($SiO_2$, CyH/AcOEt 90:10). Off-white solid (1.24 g, 3.15 mmol, 70% yield).

**M.p.** = decomposition at 115 °C.

*Note: Due to the presence of rotamers mixture (1:1), NMR studies were performed at 393 K, see compound **62c** where a T slope study was performed to demonstrate its presence and behaviour over T.*

$^1$H NMR (500 MHz, $CD_2Cl_2$) δ 6.63 – 6.56 (m, 4H), 5.33 (dd, *J* = 5.1, 1.4 Hz, 1H), 5.25 (dd, *J* = 5.0, 1.4 Hz, 1H), 4.27 (d, *J* = 9.2 Hz, 1H), 3.58 (dd, *J* = 9.2, 7.1 Hz, 1H), 3.34 (dd, *J* = 9.1, 4.9 Hz, 1H), 3.17 (dd, *J* = 9.1, 5.0 Hz, 1H), 1.37 (dt, *J* = 13.6, 6.8 Hz, 1H), 0.86 (s, 9H), 0.34 (dd, *J* = 10.8, 6.8 Hz, 6H).

**$^{13}$C NMR** (126 MHz, $C_2D_2Cl_4$, 393 K) δ 176.4, 175.5, 140.7, 139.9, 135.5, 128.4, 128.1, 127.4, 127.3, 123.1, 114.6, 80.9, 80.7, 78.2, 77.9, 65.6, 64.6, 48.8, 47.9, 31.0, 27.9, 17.6, 17.2, 16.0 ppm.

**HRMS** (ESI+) calculated for m/z $[C_{24}H_{26}Cl_2N_2NaO_5]^+$, $[M+Na]^+$: 515.1111; found: 515.1113.

**$[\alpha]^{23.8}_D$** +114.4 (c 0.01, $CH_2Cl_2$).

**_tert_-Butyl ((2*S*)-1-(2,3-Dichloro-1,4-dihydroxy-9,10-dihydro-9,10-epiminoanthracen-11-yl)-3-methyl-1-oxobutan-2-yl)carbamate (61c)**

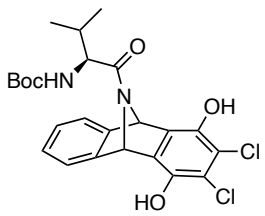


Under an argon atmosphere, **55c** (170.0 mg, 0.34 mmol, 1.0 equiv) was dissolved in anhydrous THF (21.5 mL, 0.016 M) and $K_2CO_3$ (95.2 mg, 0.69 mmol, 2.0 equiv) was added to the above solution. The reaction flask was stirred at 25 °C for 18 h. Consumption of the starting material was confirmed by TLC

analysis. The reaction mixture was washed with $H_2O$ and extracted with AcOEt (x3). The combined organic layer was dried over $MgSO_4$, filtered, and concentrated under reduced pressure. The crude was purified by flash column chromatography ($SiO_2$, CyH/AcOEt 80:20). Beige solid (98 mg, 0.20 mmol, 58% yield).

**M.p. =** decomposition at 160 °C.

*Note: Due to the presence of rotamers mixture (1:1), NMR studies were performed at 393 K, see compound **62c** where a T slope study was performed to demonstrate its presence and behaviour over T.*

**$^1$H NMR** (500 MHz, $CD_2Cl_2$) δ 6.84 (dq, *J* = 6.6, 3.2 Hz, 2H), 6.63 – 6.43 (m, 2H), 6.10 – 5.84 (m, 2H), 4.34 (d, *J* = 9.6 Hz, 1H), 3.69 (dd, *J* = 9.6, 7.1 Hz, 1H), 1.42 (dq, *J* = 13.6, 6.8 Hz, 1H), 0.86 (bs, 9H), 0.33 (dd, *J* = 6.7, 4.1 Hz, 6H).

**$^{13}$C NMR** (126 MHz, $C_2D_2Cl_4$, 393 K) δ 146.9, 146.6, 140.6, 134.1, 126.8, 126.7, 121.6, 118.5, 80.5, 57.5, 31.4, 28.8, 18.1 ppm.

**HRMS** (ESI+) calculated for m/z $[C_{24}H_{26}Cl_2N_2NaO_5]^+$, $[M+Na]^+$: 515.1111; found: 515.1118.

**$[\alpha]^{22.8}_D$** +56.3 (c 0.03, $CH_2Cl_2$).

***tert*-Butyl ((2*S*)-1-(2,3-Dichloro-1,4-dioxo-1,4,9,10-tetrahydro-9,10-epiminoanthracen-11-yl)-3-methyl-1-oxobutan-2-yl)carbamate (62c)**

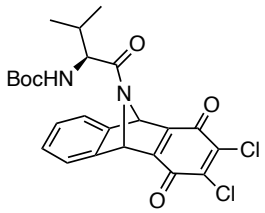


DDQ (245.12 mg, 1.08 mmol, 1.2 equiv) was added to a solution of **61c** (367.0 mg, 0.93 mmol, 1.0 equiv) in AcOEt (93 mL, 0.01 M) at 25 °C. After 24 h, consumption of the starting material is confirmed by TLC analysis. Reaction is quenched by addition of $NaHCO_3$ aqueous saturated solution followed by extraction with AcOEt (x3). The combined organic layer was dried over $MgSO_4$, filtered, and concentrated under reduced pressure. The crude was purified by flash column chromatography ($SiO_2$, CyH/AcOEt 80:20). Orange solid (222 mg, 0.57 mmol, 61% yield). In this case, a $^1$H NMR T slope experiment was performed to define the signals of the product, which had split signals due to the presence of rotamers (65:35 mixture at 298 K) (Figure 14).

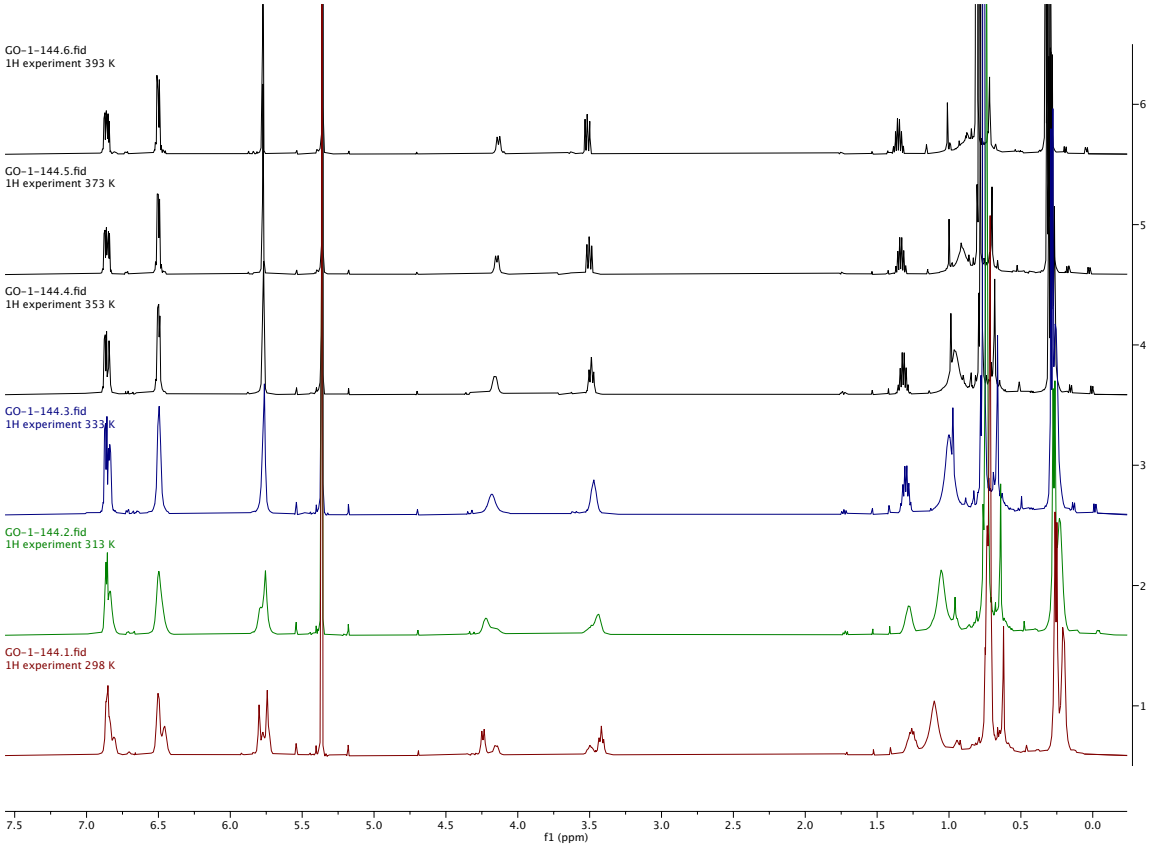


**Figure S1**. $^{1}$H NMR ($C_2D_2Cl_4$); Temperature slope from 298 to 393K to evidence the rotamers mixture of **62c**.

**M.p.** = decomposition at 100 °C.

**$^{1}$H NMR** (500 MHz, $C_2D_2Cl_4$, 393 K) δ 7.59 – 7.41 (m, 2H), 7.20 – 7.08 (m, 2H), 6.42 (s, 2H), 4.78 (d, *J* = 9.2 Hz, 1H), 4.16 (dd, *J* = 9.2, 7.3 Hz, 1H), 1.99 (dq, *J* = 13.6, 6.8 Hz, 1H), 1.45 (s, 9H), 0.95 (dd, *J* = 11.0, 6.7 Hz, 6H) ppm.

**$^{13}$C NMR** (126 MHz, $C_2D_2Cl_4$, 120 °C) δ 172.1, 171.9, 158.2, 155.4, 144.5, 144.1, 140.0, 139.8, 126.7, 126.6, 122.6, 122.4, 80.1, 57.0, 30.5, 28.1, 19.0, 17.7 ppm.

**HRMS** (ESI+) calculated for m/z $[C_{24}H_{24}Cl_2N_2NaO_5]^+$, $[M+Na]^+$: 513.0954; found: 513.0971.

**$[\alpha]^{22.5}_D$** +60.9 (c 0.05, $CH_2Cl_2$).

**Gold(I)-Cavitand Complex Bearing a Phthalimide Chiral Wall**

**5,6-Dichloropyrazine-2,3-dicarboxylic acid (69)**

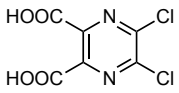


A reported procedure was followed.[34] To 400 mL of vigorously boiling water was added 2,3-dichloroquinoxaline (5 g, 25.1 mol, 1.0 equiv) and $KMnO_4$ (26.6 g, 168.3 mmol, 6.7 equiv) in portions over 30 min. The mixture was stirring at 98 °C for 2 h. The solid $MnO_2$ formed was removed by filtration from the hot suspension. The solid $MnO_2$ was boiled with 50 mL of water and filtered, and this procedure was repeated. The warm combined aqueous filtrate was acidified with 16 mL of concentrated aqueous HCl. The acidic filtrate was concentrated by rotary evaporator, and the residue was completely dried in vacuo. The solid residue was extracted with acetone (x2). The product was used without further purification. Beige solid (3.2 g, 14 mmol, 54% yield).

**$^{13}$C NMR** (101 MHz, Acetone) δ 164.2, 148.7, 143.6 ppm.

The spectral data were fully consistent with those previously reported.

**2,3-Dichlorofuro[3,4-*b*]pyrazine-5,7-dione (70)**

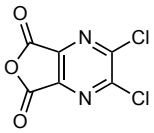


A reported procedure was followed.[34] A mixture of 5,6-dichloropyrazine-2,3-dicarboxylic acid (2.5 g, 10.55 mmol, 1.0 equiv) in $SOCl_2$ (5.4 mL,73.84 mmol, 7.0 equiv) was refluxed for 30 min. The excess $SOCl_2$ was evaporated, and the crystalline residue was dried in vacuo. The residue was dissolved in 50 mL of EtOAc and decolorized with charcoal. After removing the charcoal by filtration, the filtrate gave was dried to obtain the product which was used without further purification. Beige solid (1.65 g, 7.55 mmol, 71% yield).

**$^{13}$C NMR** (75 MHz, $(CD_3)_2CO$) δ 158.6, 155.7, 144.3 ppm.

The spectral data were fully consistent with those previously reported.

**(*R*)-2,3-dichloro-6-(1-phenylethyl)-5H-pyrrolo[3,4-b]pyrazine-5,7(6H)-dione ((*R*)-72)**

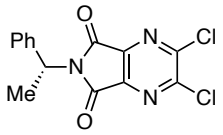

To a solution of 2,3-dichlorofuro[3,4-*b*]pyrazine-5,7-dione (1.0 g, 4.6 mmol, 1.0 equiv) in anhydrous THF (15.2 mL, 0.3 M) was added *R*-(+)-alpha-phenylethylamine (553.4 mg, 4.6 mmol, 1.0 equiv). The mixture was stirred at 23 ºC for 2 h. Then, oxalyl chloride (0.44 mL, 5.0 mmol, 1.1 equiv) and pyridine (0.81 mL, 10.1 mmol, 2.2 equiv) were added to the reaction mixture which was heated to 50 ºC and stirred for 18 h. After filtration and concentration under reduced pressure, the residue was co-evaporated with heptane (x3) to remove traces of pyridine. The residue was purified by flash column chromatography ($SiO_2$, CyH/$CH_2Cl_2$ 80:20 to 50:50). Off-white solid (611 mg, 1.9 mmol, 42% yield).

**M.p.** = 164 ºC.

**$^1$H NMR** (300 MHz, $CDCl_3$) δ 7.53 – 7.47 (m, 2H), 7.38 – 7.28 (m, 3H), 5.66 (q, *J* = 7.3 Hz, 1H), 1.97 (d, *J* = 7.4 Hz, 3H) ppm.

**$^{13}$C NMR** (126 MHz, $CDCl_3$) δ 162.1, 153.7, 143.4, 139.1, 128.9, 128.5, 127.7, 51.3, 17.5 ppm.

**$[\alpha]^{22.5}_D$** +82.6 (c 0.03, $CH_2Cl_2$).

**HRMS** (APCI+) calculated for $[C_{14}H_{10}Cl_2N_3O_2]^+$, $[M+H]^+$: 3222.0145 m/z; found: 322.0150 m/z.

**Biphenol 76**

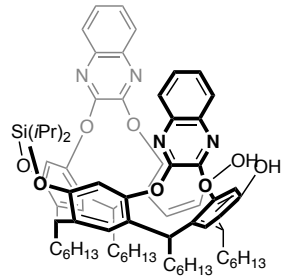

Under an argon atmosphere, to a solution of **37a** (300 mg, 0.28 mmol, 1.0 equiv) and dichlorodiisopropylsilane (54.1 mg, 0.29 mmol, 1.05 equiv) in anhydrous toluene (5.57 mL, 0.05 M), $Et_3N$ (93 µL, 0.67 mmol, 2.4 equiv) was added. The mixture was left stirring for 2 h at 23 ºC. Then, the reaction mixture was filtered through a pad of cotton and concentrated under reduced pressure. The residue was purified by flash column chromatography ($SiO_2$, CyH/AcOEt 90:10 to 60:40). White solid (152 mg, 0.13 mmol, 46% yield).

**M.p.** = 248–251 ºC.

**$^1$H NMR** (500 MHz, $CDCl_3$) δ 7.83 – 7.76 (m, 2H), 7.75 – 7.68 (m, 2H), 7.56 – 7.49 (m, 4H), 7.38 (s, 2H), 7.24 (s, 2H), 7.20 (d, *J* = 3.5 Hz, 4H), 5.62 (t, *J* = 8.2 Hz, 2H), 4.57 (t, *J* = 8.0 Hz, 1H), 4.32 (t, *J* = 7.8 Hz, 1H), 2.68 – 2.52 (m, 2H), 2.29 – 2.19 (m, 12H), 1.49 – 1.25 (m, 38H), 0.93 – 0.88 (m, 8H), 0.74 (d, *J* = 7.5 Hz, 6H) ppm.

**$^{13}$C NMR** (126 MHz, $CDCl_3$) δ 153.4, 153.2, 152.6, 152.2, 151.2, 150.6, 139.9, 139.5, 134.3, 132.7, 131.6, 129.5, 129.4, 128.7, 127.8, 127.7, 124.5, 122.6, 116.0, 110.6, 34.7, 34.1, 33.9, 33.9, 32.7, 32.4, 32.1, 32.0, 32.0, 29.6, 29.3, 28.2, 28.1, 28.0, 27.1, 22.9, 17.3, 16.7, 14.2, 11.5, 10.8 ppm.

**HRMS** (ESI+) calculated for $[C_{74}H_{88}N_4NaO_8Si]^+$, $[M+H]^+$: 1211.6264 m/z; found: 1211.6277 m/z.

**Cavitand (*R*)-77**

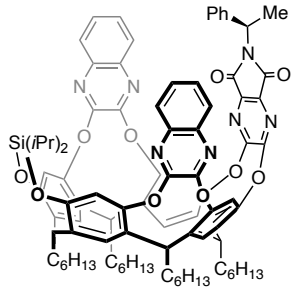


To a solution of biphenol **76** (111 mg, 0.1 mmol, 1.0 equiv) and (*R*)-**72** (31.6 mg, 0.1 mmol, 1.05 equiv) in anhydrous THF (6.2 mL, 0.015 M), $Cs_2CO_3$ (66.9 mg, 0.21 mmol, 2.2 equiv) was added. The mixture was vigorously stirred for 16 h at 70 ºC, then solvent was removed under vacuum. The residue was purified by column chromatography ($SiO_2$, CyH/AcOEt 100:00 to 70:30). Off-white solid (125 mg, 0.09 mmol, 93% yield).

**M.p.** = 310 ºC.

**$^1$H NMR** (500 MHz, $CDCl_3$) δ 8.26 (s, 1H), 8.20 (s, 1H), 8.10 – 8.03 (m, 1H), 8.00 (dd, *J* = 8.4, 1.3 Hz, 1H), 7.65 – 7.58 (m, 2H), 7.42 (ddd, *J* = 8.2, 6.9, 1.3 Hz, 1H), 7.40 – 7.36 (m, 2H), 7.30 (d, *J* = 8.1 Hz, 2H), 7.27 (s, 2H), 7.23 (ddd, *J* = 8.4, 7.0, 1.4 Hz, 1H), 7.19 – 7.15 (m, 1H), 7.13 (d, *J* = 9.3 Hz, 2H), 7.10 – 7.07 (m, 2H), 7.03 (t, *J* = 7.7 Hz, 2H), 5.73 – 5.61 (m, 3H), 5.55 (q, *J* = 7.3 Hz, 1H), 4.52 (t, *J* = 8.0 Hz, 1H), 2.27 – 2.23 (m, 10H), 1.88 (d, *J* = 7.3 Hz, 3H), 1.54 – 1.21 (m, 32H), 0.95 – 0.91 (m, 12H), 0.77 (t, *J* = 7.9 Hz, 6H).

**$^{13}$C NMR** (126 MHz, $CDCl_3$) δ 162.6, 162.2, 158.7, 158.7, 153.1, 153.0, 153.0, 152.8, 152.7, 152.5, 152.5, 152.2, 152.1, 150.6, 150.6, 142.0, 140.0, 140.0, 139.9, 139.8, 139.7, 137.7, 137.7, 135.9, 135.8, 134.4, 134.3, 132.1, 132.1, 129.6, 129.5, 129.4, 129.4, 129.1, 128.5, 127.6, 127.2, 126.9, 124.4, 123.9, 122.9, 122.7, 118.7, 118.6, 116.1, 116.1, 50.1, 34.6, 34.3, 34.1, 34.0, 32.7, 32.7, 32.6, 32.4, 32.1, 32.0, 32.0, 30.5, 29.5, 29.5, 29.3, 28.1, 27.9, 22.8, 22.8, 17.7, 17.2, 17.2, 16.7, 14.2, 11.4, 11.1 ppm.

**$[\alpha]^{23.5}_D$** +24.1 (c 0.01, $CH_2Cl_2$).

**HRMS** (MALDI) calculated for $[C_{88}H_{96}N_7O_{10}Si]^+$, $[M+H]^+$: 1438.6988 m/z; found: 1438.6947 m/z.

**Biphenol (*R*)-78**

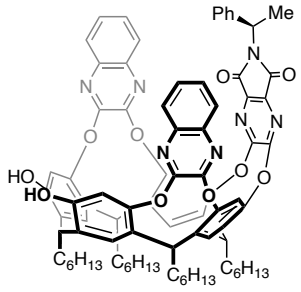


Under an argon atmosphere, to a solution of cavitand (*R*)-**77** (50 mg, 0.035 mmol, 1.0 equiv) in anhydrous THF (0.39 mL, 0.09 M), $Et_3N$ (9.7 µL, 0.07 mmol, 2.0 equiv) and $Et_3N{\cdot}3HF$ (20.4 µL, 0.13 mmol, 3.6 equiv) were added. The reaction was stirred for 1 h at 23 ºC. Then, volatiles were removed under reduced pressure. The residue was purified by column chromatography ($SiO_2$, CyH/AcOEt 90:10 to 60:40). White solid (35 mg, 0.04 mmol, 76% yield).

**M.p.** = 210 ºC.

**$^1$H NMR** (500 MHz, $CDCl_3$) δ 8.29 (s, 1H), 8.24 (s, 1H), 8.14 (dd, *J* = 8.3, 1.5 Hz, 1H), 8.06 (dd, *J* = 8.4, 1.3 Hz, 1H), 7.66 (d, *J* = 8.5 Hz, 2H), 7.46 (ddd, *J* = 8.4, 7.0, 1.5 Hz, 1H), 7.44 – 7.39 (m, 2H), 7.30 (t, *J* = 8.6 Hz, 3H), 7.18 – 7.11 (m, 7H), 7.05 (t, *J* = 7.6 Hz, 2H), 5.74 – 5.43 (m, 4H), 4.34 (t, *J* = 7.8 Hz, 1H), 2.39 – 2.14 (m, 8H), 1.88 (d, *J* = 7.4 Hz, 3H), 1.64 – 1.20 (m, 32H), 0.93 (ddt, *J* = 9.6, 7.1, 3.0 Hz, 12H) ppm.

**$^{13}$C NMR** (126 MHz, $CDCl_3$) δ 162.7, 162.4, 158.4, 158.4, 153.0, 152.9, 152.7, 152.6, 152.4, 152.4, 152.2, 151.6, 151.3, 141.7, 141.4, 139.9, 139.7, 139.4, 139.3, 137.5, 137.4, 135.7, 135.5, 130.7, 130.6, 129.7, 129.6, 129.5, 129.2, 129.0, 128.9, 128.5, 127.7, 127.1, 127.0, 126.9, 124.1, 123.9, 123.7, 123.4, 118.7, 110.7, 110.6, 50.1, 34.5, 34.2, 34.2, 33.9, 33.7, 32.7, 32.6, 32.0, 32.0, 29.6, 29.5, 28.1, 28.1, 28.1, 22.8, 22.8, 17.6, 14.2 ppm.

**$[\alpha]^{23.5}_D$** +20.8 (c 0.03, $CH_2Cl_2$).

**HRMS** (MALDI+) calculated for $[C_{82}H_{84}N_7O_{10}]^+$, $[M+H]^+$: 1326.6274 m/z; found: 1326.6279 m/z.

**Complex (*R*)-80**

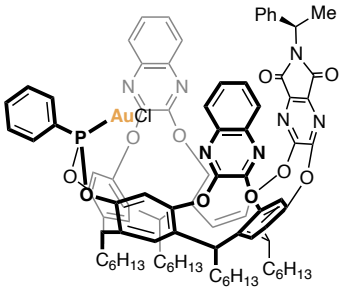


To a solution of biphenol (*R*)-**78** (38 mg, 29 µmol, 1.0 equiv) in anhydrous toluene (0.57 mL, 0.05 M), pyridine (11.6 µL, 0.03 mmol, 5.0 equiv) was added. After allowing the solution to stir during a period of 10 min, $PhPCl_2$ (5.8 µL, 0.04 mmol, 1.5 equiv) was added. After stirring for 2 h, the solvent was removed under vacuum. Due to rapid decomposition under air, the compound was used without further purification in the next step. Complex (*R*)-**80** was prepared following **GP1**, using $(Me_2S)AuCl$ (7.2 mg, 25 µmol, 1.1 equiv) and the crude phosphonite (*R*)-**78**. The crude was purified by flash column chromatography ($SiO_2$, CyH 100% to CyH/AcOEt 70:30). White solid (37.2 mg, 22 µmol, 90% yield over two steps).

**M.p** = 198 ºC.

**$^1$H NMR** (500 MHz, $CDCl_3$) δ 8.23 – 8.15 (m, 3H), 8.12 (d, *J* = 0.8 Hz, 1H), 8.05 – 7.99 (m, 1H), 7.88 (d, *J* = 8.3 Hz, 1H), 7.84 – 7.74 (m, 3H), 7.69 (td, *J* = 7.6, 3.1 Hz, 2H), 7.55 – 7.50 (m, 2H), 7.45 – 7.34 (m, 3H), 7.34 – 7.25 (m, 4H), 7.23 (d, *J* = 7.4 Hz, 1H), 7.16 – 7.06 (m, 3H), 6.94 (d, *J* = 7.7 Hz, 2H), 5.75 (dt, *J* = 15.7, 8.1 Hz, 2H), 5.68 (t, *J* = 8.1 Hz, 1H), 5.53 (q, *J* = 7.2 Hz, 1H), 4.69 (td, *J* = 8.0, 2.9 Hz, 1H), 2.48 – 2.12 (m, 8H), 1.87 (d, *J* = 7.3 Hz, 3H), 1.58 – 1.14 (m, 32H), 1.07 – 0.87 (m, 12H) ppm.

**$^{13}$C NMR** (126 MHz, $CDCl_3$) δ 162.8, 162.1, 158.4, 153.3, 153.2 (d, *J* = 2.1 Hz), 153.2, 153.1 (d, *J* = 2.1 Hz), 152.9, 152.6, 152.2, 152.0, 151.9 (d, *J* = 3.4 Hz), 147.7 (t, *J* = 7.9 Hz), 142.2, 141.6, 140.2 (d, *J* = 4.1 Hz), 139.4, 137.7 (dd, *J* = 7.2, 2.0 Hz), 136.3, 136.3, 136.2, 136.2, 136.0 (dd, *J* = 4.7, 2.9 Hz), 134.5, 132.4, 131.6, 131.4, 131.3, 130.0, 129.8, 129.4, 129.3, 128.9, 128.7, 128.5, 128.3, 128.1, 127.8, 126.3, 124.5, 123.7, 122.7, 122.5, 118.9, 117.7, 49.7, 35.9, 34.2, 34.2, 33.0, 32.9, 32.7, 32.1, 32.0, 30.7, 29.5, 29.5, 29.4, 28.6, 28.1, 28.0, 27.2, 22.8, 22.8, 22.8, 17.6, 14.2, 14.2, 14.2 ppm.

**$^{31}$P NMR** (203 MHz, $CDCl_3$) δ 135.8 ppm.

**$[\alpha]^{22.3}_D$** +21.8 (c 0.004, $CH_2Cl_2$).

**HRMS** (MALDI+) calculated for $[C_{88}H_{87}AuClN_7O_{10}P]^+$, $[M+H]^+$: 1666.0933 m/z; found: 1666.5550 m/z.

**Gold(I)-Cavitand Complexes in Hydrogen-bonded Ion Pair Catalysis**

Chiral silver salts (**Ag A–Ag K**) were prepared starting from the corresponding diols following literature procedures.[45,47]

**General Procedure GP2: phosphite synthesis**

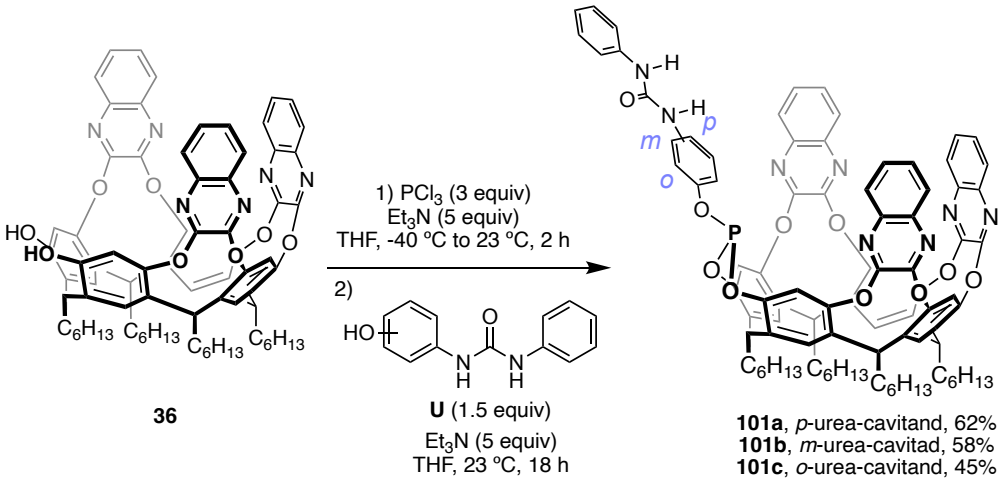


**Scheme S1**. General procedure GP2 for the phosphite synthesis.

Under an argon atmosphere, an oven dried Schlenk tube equipped with a stir bar was charged with biphenol **36** (1.0 equiv). Anhydrous THF was added and the solid was dissolved before cooling it to -40 ºC. A solution of PCl3 (3.0 equiv) in anhydrousTHF (0.12 M final concentration) was then added dropwise. After stirring for 10 min, anhydrous Et3N (5.0 equiv) was added at the same temperature. The mixture was allowed to warm up to room temperature and stirred for 2 h. The reaction was moved inside the glovebox where it was filtered through a celite pad (rinsing with THF). The filtrate was concentrated under reduced pressure, treated with toluene (1 mL) and evaporated. The obtained crude was dissolved in anhydrous THF (0.04 M) and $Et_3N$ (5.0 equiv) was added followed by the corresponding hydroxyurea **U** (2.0 equiv). The resulting mixture was left stirring 18 h at room temperature. Next day, the volatiles were removed under vacuum and the crude was purified by flash column chromatography ($SiO_2$, CyH/AcOEt ) providing the desired phosphite ligand (**101a–101c**).

Note: phosphites were found to readily oxidize under air. Flash column chromatography were carried out using $N_2$. Compounds had to be stored in the glovebox or quickly coordinated to gold.

**1-(4-Hydroxyphenyl)-3-phenylurea (U1)**

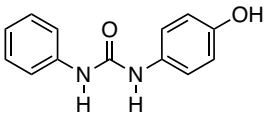


To an oven-dried 50 mL flask was added 4-aminophenol (0.88 mL, 9.16 mmol, 1.0 equiv) and dissolved in anhydrous MeCN (18 mL). The system was cooled to 0 ºC with an ice/water bath and isocyanatobenzene (1.0 mL, 9.16 mmol, 1.0 equiv) was added dropwise and the mixture was left stirring at the same temperature for 2 h. The solvent was evaporated obtaining hidroxyurea **U1** as a white solid (2.08 g, 9.11 mmol, 99% yield) which was used as it is without further purification.

**$^1$H NMR** (500 MHz, $(CD_3)_2SO$) δ 9.06 (s, 1H), 8.52 (s, 1H), 8.31 (s, 1H), 7.43 (dt, *J* = 8.7, 1.6 Hz, 2H), 7.31 – 7.24 (m, 2H), 7.24 – 7.19 (m, 2H), 6.94 (tt, *J* = 7.5, 1.1 Hz, 1H), 6.75 – 6.63 (m, 2H) ppm.

Spectroscopic data matched those reported in the literature.[74]

**1-(3-Hydroxyphenyl)-3-phenylurea (U2)**

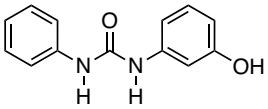


To an oven-dried 50 mL flask was added 3-aminophenol (0.500 g, 4.58 mmol, 1.0 equiv) and dissolved in anhydrous MeCN (9 mL). The system was cooled to 0 ºC with an ice/water bath and isocyanatobenzene (0.50 mL, 4.58 mmol, 1.0 equiv) was added dropwise. The mixture was left stirring at the same temperature for 1 h. The solvent was evaporated and the crude was purified by flash column chromatography (CyH/AcOEt 70:30 to 50:50) obtaining hidroxyurea U2 as a white solid (0.98 g, 4.30 mmol, 94% yield).

**$^1$H NMR** (500 MHz, $(CD_3)_2SO$) δ 9.31 (s, 1H), 8.56 (d, *J* = 18.3 Hz, 2H), 7.44 (dd, *J* = 8.6, 1.1 Hz, 2H), 7.30 – 7.24 (m, 2H), 7.07 – 7.00 (m, 2H), 6.99 – 6.91 (m, 1H), 6.79 (s, 1H), 6.37 (ddd, *J* = 8.1, 2.3, 0.8 Hz, 1H) ppm.

Spectroscopic data matched those reported in the literature.[74]

74 Velappan, A. B.; Charan Raja, M. R.; Datta, D.; Tsai, Y. T.; Halloum, I.; Wan, B.; Kremer, L.; Gramajo, H.; Franzblau, S. G.; Kar Mahapatra, S.; Debnath, J. Attenuation of *Mycobacterium* Species through Direct and Macrophage Mediated Pathway by Unsymmetrical Diaryl Urea, *Eur. J. Med. Chem.* **2017**, *125*, 825–841.

**1-(2-Hydroxyphenyl)-3-phenylurea (U3)**

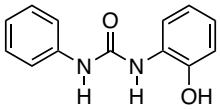

To an oven-dried 50 mL flask was added 2-aminophenol (0.500 g, 4.58 mmol) and dissolved in anhydrous MeCN (9 mL). The system was cooled to 0 ºC with an ice/water bath and isocyanatobenzene (0.50 mL, 4.58 mmol, 1.0 equiv) was added dropwise. The mixture was left stirring at the same temperature for 1 h. The solvent was evaporated and the crude was purified by flash column chromatography (CyH/AcOEt 70:30 to 50:50) obtaining hidroxyurea **U3** as a white solid (0.963 g, 4.22 mmol, 92% yield).

**$^1$H NMR** (500 MHz, $(CD_3)_2SO$) δ 9.93 (s, 1H), 9.29 (s, 1H), 8.16 (s, 1H), 8.03 (dd, *J* = 7.9, 1.7 Hz, 1H), 7.44 (dt, *J* = 8.7, 1.6 Hz, 2H), 7.31 – 7.23 (m, 2H), 6.95 (tt, *J* = 7.5, 1.1 Hz, 1H), 6.84 (dd, *J* = 7.8, 1.6 Hz, 1H), 6.76 (dtd, *J* = 23.8, 7.4, 1.7 Hz, 2H) ppm.

**$^{13}$C NMR** (126 MHz, $(CD_3)_2SO$) δ 153.0, 146.1, 140.4, 129.3, 128.3, 122.2, 122.1, 119.6, 119.0, 118.3, 114.8 ppm.

Spectroscopic data matched those reported in the literature.[74]

**Phosphite 101a**

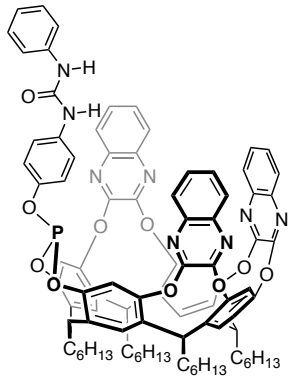

Prepared following general procedure **GP2**, using biphenol **36** (200 mg, 0.17 mmol, 1.0 equiv) and hidroxyurea **U1** (76 mg, 0.331 mmol, 2.0 equiv). Phosphite **101a** was obtained as a beige solid (158 mg, 0.11 mmol, 65% yield) after purification by flash column chromatography ($SiO_2$, CyH/AcOEt 90:10).

**M.p.** = 247–250 °C.

**$^1$H NMR** (500 MHz, $CDCl_3$) δ 8.32 (s, 2H), 8.00 – 7.96 (m, 2H), 7.78 (dd, *J* = 6.3, 3.5 Hz, 2H), 7.72 (dd, *J* = 8.4, 1.4 Hz, 2H), 7.60 – 7.55 (m, 2H), 7.50 – 7.48 (m, 2H), 7.47 – 7.44 (m, 2H), 7.37 – 7.30 (m, 8H), 7.23 (d, *J* = 3.9 Hz, 6H), 7.13 – 7.09 (m, 1H), 6.78 (s, 1H), 5.71 (t, *J* = 8.2 Hz, 3H), 4.47 (td,

*J* = 9.3, 2.0 Hz, 1H), 2.34 – 2.23 (m, 6H), 2.18 (q, *J* = 8.0 Hz, 2H), 1.52 – 1.23 (m, 32H), 1.04 – 0.85 (m, 12H) ppm.

**$^{13}$C NMR** (126 MHz, $CDCl_3$) δ 153.6 (d, *J* = 4.7 Hz), 153.0 (d, *J* = 6.0 Hz), 152.8 (d, *J* = 4.9 Hz), 152.6 (d, *J* = 7.0 Hz), 147.9, 146.5 (d, *J* = 5.8 Hz), 139.9, 139.9, 138.0, 137.3 (d, *J* = 2.6 Hz), 136.1, 135.7, 134.6, 129.5, 129.3, 129.1, 128.1, 128.0 (d, *J* = 4.0 Hz), 124.6, 123.5, 122.9, 122.7, 122.0 (d, *J* = 5.2 Hz), 121.5, 119.1, 117.7, 36.0, 34.4, 34.2, 32.8, 32.2, 32.1, 32.0, 32.0, 31.7, 22.8, 14.2 ppm.

**$^{31}$P NMR** (203 MHz, $CDCl_3$) δ 131.5 ppm.

**HRMS** (ESI+) calculated for m/z $[C_{89}H_{88}N_8O_{10}P]^+$, $[M+H]^+$: 1459.6356; found 1459.6358.

**Phosphite 101b**

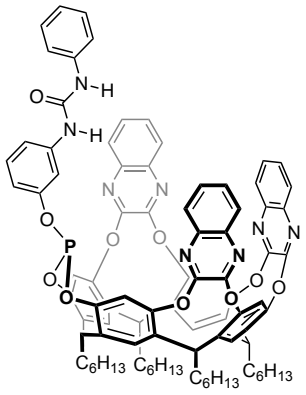

Prepared following general procedure **GP2**, using biphenol **36** (400 mg, 0.33 mmol, 1.0 equiv) and hidroxyurea **U2** (152 mg, 0.66 mmol, 2.0 equiv). Phosphite **101b** was obtained as a beige solid (296 mg, 0.20 mmol, 61% yield) after flash column chromatography ($SiO_2$, CyH/AcOEt 90:10).

**M.p.** = 270–273 °C.

**$^{1}$H NMR** (500 MHz, $CDCl_3$) δ 8.32 (d, *J* = 1.6 Hz, 2H), 7.96 (dd, *J* = 8.3, 1.4 Hz, 2H), 7.78 (dd, *J* = 6.3, 3.5 Hz, 2H), 7.71 (d, *J* = 8.3 Hz, 2H), 7.56 (td, *J* = 9.0, 1.2 Hz, 2H), 7.44 (td, *J* = 6.3, 2.6 Hz, 5H), 7.37 (s, 3H), 7.36 – 7.32 (m, 3H), 7.25 – 7.22 (m, 6H), 7.08 – 7.02 (m, 1H), 7.00 – 6.94 (m, 1H), 5.71 (t, *J* = 8.2 Hz, 3H), 4.48 (t, *J* = 7.9 Hz, 1H), 2.32 – 2.25 (m, 7H), 2.17 (q, *J* = 7.9 Hz, 2H), 1.54 – 1.29 (m, 33H), 0.97 – 0.84 (m, 12H) ppm.

**$^{13}$C NMR** (126 MHz, $CDCl_3$) δ 153.0, 153.0, 152.8, 152.7, 152.6, 152.5, 151.9, 146.5 (d, *J* = 5.9 Hz), 139.9, 139.8, 138.0, 137.4 (d, *J* = 2.6 Hz), 136.1 (d, *J* = 1.9 Hz), 135.7, 130.3, 129.6, 129.5, 129.4, 129.3, 129.1, 128.0, 124.4, 123.5, 123.0, 121.1, 119.1, 117.7 (d, *J* = 3.0 Hz), 116.5, 116.2, 112.9 (d, *J* = 4.7 Hz), 36.0, 34.4, 34.2, 32.8, 32.2, 32.1, 32.0, 31.7, 29.9, 29.6, 29.5, 28.2, 28.1, 27.9, 22.8 (d, *J* = 2.9 Hz), 14.2, 14.2 ppm.

**$^{31}$P NMR** (203 MHz, $CDCl_3$) δ 132.0 ppm.

**HRMS** (ESI +) calculated for m/z $[C_{89}H_{87}N_8O_{10}P]^+$, $[M+H]^+$: 1459.6356; found 1459.6341.

**Phosphite 101c**

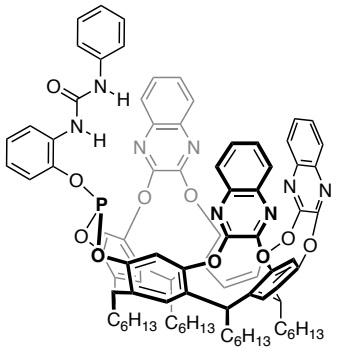

Prepared following general procedure **GP2,** using biphenol **36** (150 mg, 0.13 mmol, 1.0 equiv) and hidroxyurea **U3** (57 mg, 0.25 mmol, 2.0 equiv). Phosphite **101c** was obtained as a beige solid (101 mg, 0.07 mmol, 56% yield) after flash column chromatography ($SiO_2$, CyH /EtOAc 90:10).

**M.p.** 259–261 °C.

**$^1$H NMR** (500 MHz, $CDCl_3$) δ 8.31 (d, *J*= 2.5 Hz, 2H), 8.25 (t, *J* = 6.9 Hz, 1H), 7.96 (d, *J* = 8.3 Hz, 2H), 7.81 – 7.77 (m, 2H), 7.68 – 7.64 (m, 2H), 7.56 (ddd, *J* = 8.4, 7.0, 1.4 Hz, 2H), 7.50 – 7.42 (m, 5H), 7.41 – 7.37 (m, 2H), 7.32 (d, *J* = 3.7 Hz, 2H), 7.30 – 7.26 (m, 2H), 7.25 – 7.22 (m, 4H), 7.22 – 7.17 (m, 1H), 7.08 – 7.01 (m, 2H), 5.72 (td, *J* = 6.8, 4.2 Hz, 3H), 4.44 (t, *J* = 7.9 Hz, 1H), 2.36 – 2.24 (m, 6H), 2.18 (q, *J* = 8.0 Hz, 2H), 1.61 – 1.30 (m, 32H), 0.99 – 0.88 (m, 12H) ppm.

**$^{13}$C NMR** (126 MHz, $CDCl_3$) δ 153.0, 152.9, 152.7 (d, *J* = 3.6 Hz), 152.6, 146.0 (d, *J* = 5.5 Hz), 141.1 (d, *J* = 2.9 Hz), 139.9, 139.8, 138.0 (d, *J* = 5.2 Hz), 137.2 (d, *J* = 2.6 Hz), 136.1, 136.1, 136.0, 130.7, 129.6 (d, *J* = 2.8 Hz), 129.3, 129.1, 128.0, 128.0 (d, *J* = 3.1 Hz), 125.4, 124.7 (d, *J* = 5.8 Hz), 123.5, 123.3, 123.0, 121.9, 120.2 (d, *J* = 8.2 Hz), 119.2, 117.7, 36.0, 34.3, 34.2, 32.8, 32.3, 32.1, 32.0, 31.7, 29.9, 29.6, 29.5, 28.2 (d, *J* = 2.7 Hz), 28.0, 22.8, 14.2 ppm.

**$^{31}$P NMR** (203 MHz, $CDCl_3$) δ 134.8 ppm.

**HRMS** (ESI +) calculated for m/z $[C_{89}H_{87}N_8NaO_{10}P]^+$, $[M+H]^+$: 1481.6175; found 1481.6167.

**Complex Au A**

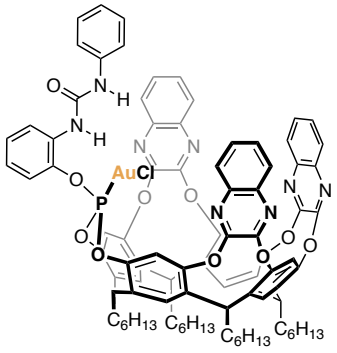


Prepared following general procedure **GP1**, using phosphite **101a** (76 mg, 0.05 mmol, 1.0 equiv). Complex **Au A** was obtained as a white solid (71 mg, 0.042 mmol, 81% yield) after flash column chromatography ($SiO_2$, CyH/AcOEt 100:0 to 80:20).

**M.p.** = 169–173 °C.

**$^1$H NMR** (500 MHz, $CDCl_3$) δ 8.51 (d, *J* = 8.3 Hz, 1H), 8.21 (s, 2H), 7.95 (s, 2H), 7.85 – 7.79 (m, 2H), 7.75 (d, *J* = 8.3 Hz, 2H), 7.58 (s, 2H), 7.52 (dd, *J* = 6.2, 3.6 Hz, 3H), 7.46 – 7.40 (m, 4H), 7.34 (t, *J* = 8.0 Hz, 1H), 7.30 (s, 2H), 7.22 (s, 2H), 7.15 (s, 6H), 7.09 (td, *J* = 7.9, 1.6 Hz, 1H), 5.76 (t, *J* = 8.2 Hz, 1H), 5.70 (t, *J* = 8.2 Hz, 2H), 4.18 (t, *J* = 7.1 Hz, 1H), 2.30 (q, *J* = 8.0 Hz, 2H), 2.27 – 2.16 (m, 6H), 1.56 – 1.31 (m, 32H), 0.98 – 0.90 (m, 12H) ppm.

**$^{13}$C NMR** (126 MHz, $CDCl_3$) δ 153.0, 153.0, 152.8, 152.6, 152.6, 152.3, 151.9, 143.4, 134.0 (d, *J* = 6.5 Hz), 139.6, 139.0 (d, *J* = 12.4 Hz), 138.3, 138.3, 136.4, 135.7, 135.3, 131.6, 129.7, 129.5, 129.4, 129.3, 127.9, 127.6, 127.4, 123.6, 123.0, 122.9, 122.3, 121.9, 118.9, 117.7, (d, *J* = 3.9 Hz), 35.3, 34.2, 34.2, 32.8, 32.6, 32.1, 32.0, 31.9, 30.0, 29.9, 29.5, 28.8, 28.1, 28.1, 27.4, 22.8, 22.8, 22.7, 14.2, 14.2 ppm.

**$^{31}$P NMR** (203 MHz, $CDCl_3$) δ 105.6 ppm.

**HRMS (ESI +)** calculated for m/z $[C_{89}H_{87}AuClN_8NaO_{10}P]^+$, $[M+Na]^+$: 1713.5529; found 1713.5519.

**Complex Au B**

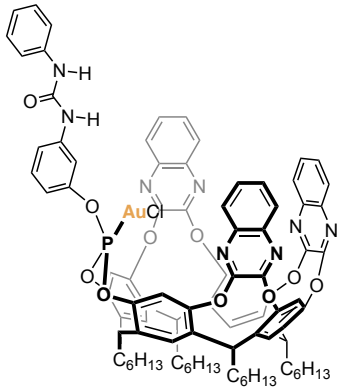


Prepared following general procedure **GP2**, using phosphite **101b** (296 mg, 0.20 mmol, 1.0 equiv). Complex **Au B** was obtained as a white solid (126 mg, 0.08 mmol, 37% yield) after flash column chromatography ($SiO_2$, CyH/AcOEt 100:0 to 80:20).

**M.p.** = 176–177 °C.

**$^1$H NMR** (500 MHz, $CDCl_3$) δ 8.19 (s, 2H), 7.85 (dd, *J* = 8.3, 1.4 Hz, 2H), 7.79 – 7.75 (m, 2H), 7.73 (dd, *J* = 8.4, 1.4 Hz, 2H), 7.64 (s, 1H), 7.51 – 7.48 (m, 5H), 7.47 (d, *J* = 1.4 Hz, 1H), 7.44 – 7.39 (m, 4H), 7.33 – 7.29 (m, 5H), 7.27 (s, 1H), 7.25 – 7.21 (m, 1H), 7.19 (s, 1H), 7.13 – 7.01 (m, 3H), 5.78 (t, *J* = 8.2 Hz, 1H), 5.73 (t, *J* = 8.2 Hz, 2H), 4.55 (td, *J* = 7.9, 3.0 Hz, 1H), 2.39 – 2.18 (m, 8H), 1.59 – 1.28 (m, 32H), 0.98 – 0.89 (m, 12H) ppm.

**$^{13}$C NMR** (126 MHz, $CDCl_3$) δ 153.0, 153.0 (d, *J* = 1.8 Hz), 152.9, 152.7, 152.6, 152.3, 152.1, 149.8 (d, *J* = 3.6 Hz), 143.6 (d, *J* = 2.8 Hz), 140.7, 140.1 (d, *J* = 5.1 Hz), 139.8, 138.3 (d, *J* = 2.1 Hz), 137.9, 136.5, 136.0 (d, *J* = 2.9 Hz), 135.3, 130.8, 129.7, 129.6, 129.5, 129.3, 128.5, 127.9, 127.5, 124.5, 123.8, 122.9, 121.1, 119.0, 117.8 (d, *J* = 3.9 Hz), 117.5, 115.7 (d, *J* = 4.7 Hz), 112.4 (d, *J* = 5.0 Hz), 66.0, 36.0, 34.2, 32.8, 32.1, 32.0, 30.6, 29.6, 29.5, 29.5, 28.2, 28.1, 28.0, 22.8, 22.8, 22.8, 15.4, 14.2, 14.2 ppm.

**$^{31}$P NMR** (203 MHz, $CDCl_3$) δ 109.4 ppm.

**HRMS** (ESI+) calculated for m/z $[C_{89}H_{87}AuClN_8NaO_{10}P]^+$, $[M+Na]^+$: 1713.5529; found 1713.5512.

**Complex Au C**

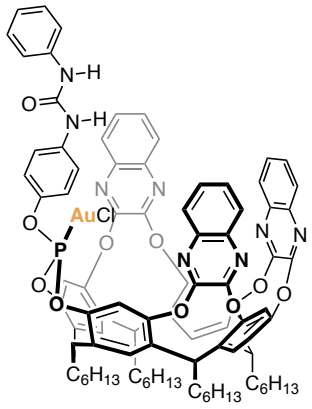


Prepared following general procedure **GP1**, using phosphite **101c** (480 mg, 0.33 mmol, 1.0 equiv). Complex **Au C** was obtained as a white solid (466 mg, 0.28 mmol, 84% yield) after flash column chromatography ($SiO_2$, CyH/AcOEt 100:0 to 80:20).

**M.p.** = 234–240 °C.

**$^1$H NMR** (500 MHz, $CDCl_3$) δ 8.18 (s, 2H), 7.85 (dd, *J* = 8.3, 1.5 Hz, 2H), 7.80 – 7.76 (m, 3H), 7.76 – 7.73 (m, 1H), 7.51 – 7.48 (m, 4H), 7.47 (dd, *J* = 4.8, 2.1 Hz, 4H), 7.43 (td, *J* = 8.4, 7.7 Hz, 2H), 7.40 – 7.35 (m, 4H), 7.33 – 7.30 (m, 5H), 7.18 – 7.14 (m, 1H), 6.94 (s, 1H), 6.79 (s, 1H), 5.77 (t, *J* = 8.2 Hz, 1H), 5.72 (t, J = 8.2 Hz, 2H), 4.52 (td, *J* = 8.0, 3.0 Hz, 1H), 2.38 – 2.17 (m, 8H), 1.54 – 1.30 (m, 33H), 0.98 – 0.91 (m, 12H) ppm.

**$^{13}$C NMR** (126 MHz, $CDCl_3$) δ 153.1, 153.0, 152.8, 152.6, 152.3, 152.1, 145.1 (d, *J* = 4.7 Hz), 143.6 (d, *J* = 3.0 Hz), 140.1 (d, *J* = 6.4 Hz), 139.8, 138.3 (d, *J* = 1.9 Hz), 137.8, 137.1, 136.5, 135.9 (d, *J* = 2.9 Hz), 135.2, 129.7, 129.6, 129.6, 129.3, 128.6, 127.9, 127.5, 124.9, 123.8, 122.8, 122.2 (d, *J* = 4.5 Hz), 121.9, 121.8, 35.9, 34.2, 32.8, 32.8, 32.1, 32.0, 30.5, 29.8, 29.6, 29.5, 29.4, 28.2, 28.1, 27.9, 22.8, 22.8, 22.8, 14.2 ppm.

**$^{31}$P NMR** (202 MHz, $CDCl_3$) δ 109.7 ppm.

**HRMS** (ESI+) calculated for m/z $[C_{89}H_{87}AuClN_8NaO_{10}P]^+$, $[M+Na]^+$: 1713.5529; found 1713.5519.

**Enantioselective Alkoxycyclization of 31a**

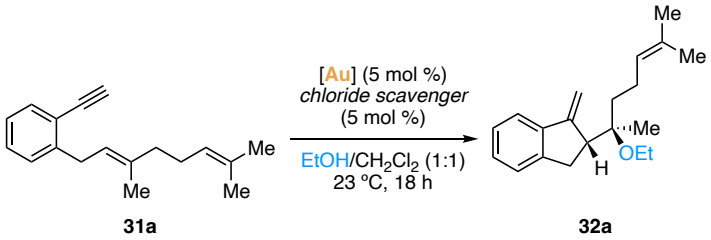


**Scheme S2**. Alkoxycyclization reaction of 1,6-enyne **31a**.

The procedure for this reaction was previously optimized in the group.[13] 1,6-Enyne **31a** (1.0 equiv) and the corresponding gold(I) complex (5 mol %) were dissolved in $CH_2Cl_2$/EtOH (1:1, 0.25 M) at 23 ºC. Then, the corresponding chloride scavenger was added (3–10 mol %). The mixture was stirred for 18 h. The reaction was quenched by the addition of $Et_3N$ (*ca.* 3 drops) and concentrated under reduced pressure. Yield was determined by $^1H$ NMR using $Ph_2CH_2$ as internal standard. The spectral data were fully consistent with those previously reported.

**Formal [4+2] cycloaddition of 1,6-arylenyne 95**

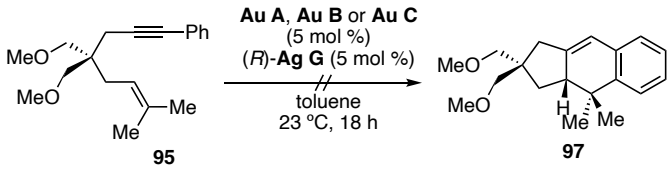


**Scheme S3**. Formal [4+2] cycloaddition of 1,6-enyne **96**.

The procedure for this reaction was previously optimized in the group.[45] 1,6-Enyne **95** (1.0 equiv) and the corresponding gold(I) complex (5 mol %) were dissolved in anhydrous toluene and a solution of (*R*)-**Ag G** (5 mol %) was added. The reaction was stirred for 18 h before being quenched by the addition of $Et_3N$ (*ca.* 3 drops) and concentrated. Yield was determined by $^1H$ NMR using $Ph_2CH_2$ as internal standard. The spectral data were fully consistent with those previously reported.

**Substrates Synthesis for the Nucleophilic addition to 1,6-Enynes 114**

Enynes **114** were prepared from the corresponding allyl bromides and commercially available propargyl malonate. Allyl bromides were not stable and were prepared from the corresponding allyl alcohols and immediately used or stored in the freezer for a short period of time.

**General procedure GP3: 1,6-enyne 114 preparation**

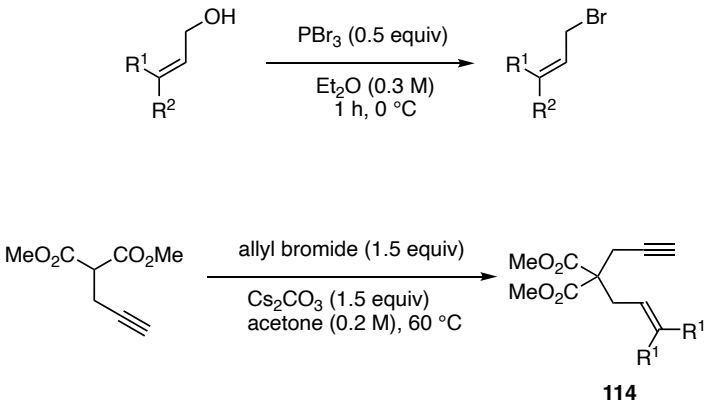


**Scheme S3**. General procedure GP3 for the substrates **114** preparation.

*Allyl bromide preparation:* To a flame-dried flask charged with a stirring bar and the corresponding allyl alcohol was added anhydrous $Et_2O$ (0.3 M). The solution was cooled to 0 °C with an ice/$H_2O$ bath and $PBr_3$ (0.5 equiv) was added dropwise. The mixture was allowed to warm up to room temperature and was stirred until starting material consumption (monitored by GC-MS and TLC). The reaction was then quenched by dropwise addition of $H_2O$, the aqueous phase is then extracted with $Et_2O$ (x2). The combined organic layers are washed with brine, dried over $MgSO_4$, filtered, and evaporated. The crude was used as such in the next step without further purification.

*Alkylation propargyl malonate:* To a flask equipped with a stirring bar and charged with $Cs_2CO_3$ (1.5 equiv) was added HPLC-grade acetone. Then propargyl malonate was added dropwise (1.0 equiv) and the system was stirred for 5 min. Finally, all bromide (1.5 equiv) was added as a solution in acetone (0.2 M final concentration). The system was heated to reflux and left stirring until starting material consumption (monitored by GC-MS and TLC). The reaction was filtered, and the solvent was evaporated under reduced pressure. The crude was purified by flash column chromatography ($SiO_2$, CyH/AcOEt ) affording the corresponding 1,6-enyne.

**Dimethyl 2-cinnamyl-2-(prop-2-yn-1-yl)malonate (114a)**

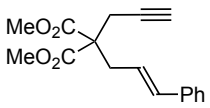


Prepared following general procedure **GP3**, using (*E*)-cinnamyl alcohol (2.69 g, 20.8 mmol). Cinnamyl bromide was obtained as a colorless oil (3.30 g, 16.8 mmol, 83% yield) and was used in the following step with propargyl malonate (1.70 mL, 11.2 mmol, 1.0 equiv). Enyne **114a** was obtained as a white solid (2.90 g, 10.1 mmol, 91% yield) after flash column chromatography ($SiO_2$, CyH/AcOEt 100:0 to 90:10).

**$^1$H NMR** (300 MHz, $CDCl_3$) δ 7.37 – 7.26 (m, 4H), 7.25 – 7.18 (m, 1H), 6.52 (dt, *J* = 15.6, 1.3 Hz, 1H), 6.00 (dt, *J* = 15.5, 7.7 Hz, 1H), 3.76 (s, 6H), 2.97 (dd, *J* = 7.7, 1.3 Hz, 2H), 2.85 (d, *J* = 2.7 Hz, 2H), 2.06 (t, *J* = 2.7 Hz, 1H) ppm.

**$^{13}$C NMR** (75 MHz, $CDCl_3$) δ 170.3, 137.1, 134.8, 128.7, 127.7, 126.4, 123.2, 79.0, 71.8, 57.4, 53.0, 36.0, 23.1 ppm.

The spectral data were fully consistent with those previously reported.[75]

***N*-(*E*)-Cinnamyl-4-methyl-*N*-(prop-2-yn-1-yl)benzenesulfonamide (114b)**

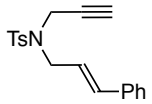


A reported procedure was adapted.[76] To a flame-dried flask equipped with a stirring bar were sequentially added triphenyl phosphine (1.95 g, 7.45 mmol, 2.0 equiv), 4-methyl-N-(prop-2-yn-1-yl)benzenesulfonamide (936 mg, 4.47 mmol, 1.2 equiv), anhydrous THF (12 mL, 0.28 M) and cinnamyl alcohol (0.48 mL, 3.37 mmol, 1.0 equiv). The mixture was cooled to 0 ºC and diethyl azodicarboxylate (2.9 mL, 7.45 mmol, 2.0 equiv) was added dropwise. Then the reaction was stirred at 23 °C for 16 h. After complete conversion of the starting material, the solvent was removed under reduced pressure and the residue was re-dissolved in AcOEt, washed with brine, dried over $MgSO_4$, filtered and evaporate. The crude was purified by flash column chromatography (CyH/AcOEt, 9:1) and the product was obtained as an off-white solid. The columned fraction was then recrystallized from refluxing CyH obtaining enyne **114b** as a white solid (762 mg, 2.34 mmol, 63 % yield).

**$^1$H NMR** (300 MHz, $CDCl_3$) δ 7.83 – 7.72 (m, 2H), 7.37 – 7.22 (m, 7H), 6.58 (d, *J* = 15.8 Hz, 1H), 6.08 (dt, *J* = 15.8, 6.9 Hz, 1H), 4.13 (d, *J* = 2.4 Hz, 2H), 4.00 (dd, *J* = 6.9, 1.1 Hz, 2H), 2.44 (s, 3H), 2.05 (t, *J* = 2.5 Hz, 1H) ppm.

**$^{13}$C NMR** (75 MHz, $CDCl_3$) δ 143.6, 136.1, 134.9, 129.5, 128.6, 128.1, 127.8, 126.6, 122.9, 73.8, 48.6, 35.9, 21.6 ppm.

The spectral data were fully consistent with those previously reported.

75 Vaghi, L.; Benincori, T.; Cirilli, R.; Alberico, E.; Mussini, P. R.; Pierini, M.; Pilati, T.; Rizzo, S.; Sannicolò, F. Ph-tetraMe-Bithienine, the First Member of the Class of Chiral Heterophosphepines: Synthesis, Electronic and Steric Properties, Metal Complexes and Catalytic Activity, *Eur. J. Org. Chem.* **2013**, *2013*, 8174–8184.

76 Zhao, S.; Zang, Z.-L.; Li, S.; Wen, X.; Wang, C.; Guo, J.; He, Y. Iridium-Catalyzed Cycloisomerization of N-Tethered 1,7-Enynes: Construction of an Azabicyclo[5.1.0]Octene System, *J. Org. Chem.* **2020**, *85*, 9321–9330.

**Dimethyl (*E*)-2-(3-(2-Methoxyphenyl)allyl)-2-(prop-2-yn-1-yl)malonate (114j)**

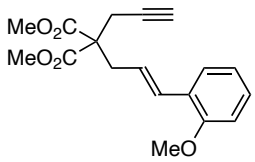


Prepared following general procedure **GP3**, using (*E*)-3-(2-methoxyphenyl)prop-2-en-1-ol (300 mg, 1.83 mmol). Allyl bromide was obtained as a pale-yellow oil (380 mg, 1.67 mmol, 82% yield) and was used in the following step with propargyl malonate (170 µL, 1.12 mmol, 1.0 equiv). Enyne **79j** was obtained as a colorless oil (342 mg, 1.08 mmol, 97% yield) after purification ($SiO_2$, CyH/AcOEt 100:0 to 90:10).

**M.p.** = 60 °C.

**$^1$H NMR** (300 MHz, $CDCl_3$) δ 7.36 (dd, *J* = 7.6, 1.7 Hz, 1H), 7.24 – 7.16 (m, 1H), 6.93 – 6.77 (m, 3H), 5.99 (dt, *J* = 15.6, 7.7 Hz, 1H), 3.82 (s, 3H), 3.76 (s, 6H), 2.98 (dd, *J* = 7.7, 1.3 Hz, 2H), 2.85 (d, *J* = 2.7 Hz, 2H), 2.05 (t, *J* = 2.7 Hz, 1H) ppm.

**$^{13}$C NMR** (75 MHz, $CDCl_3$) δ 170.4, 156.7, 129.8, 128.7, 127.0, 126.4, 123.8, 120.7, 111.0, 79.0, 71.7, 57.6, 55.6, 52.9, 36.4, 23.1 ppm.

**HRMS** (ESI+) calculated for m/z $[C_{18}H_{20}NaO_5]^+$, $[M+Na]^+$: 339.1203; found 339.1218.

**Dimethyl (*E*)-2-(3-(3-Methoxyphenyl)allyl)-2-(prop-2-yn-1-yl)malonate (114k)**

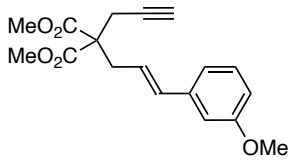


Prepared following general procedure **GP3**, using (*E*)-3-(3-methoxyphenyl)prop-2-en-1-ol (871 mg, 5.30 mmol). Allyl bromide was obtained as a colorless oil (995 mg, 5.30 mmol, 83% yield) and was used in the following step with propargyl malonate (152 µL, 0.999 mmol, 1.0 equiv). Enyne **114k** was obtained as a colorless oil (239 mg, 0.755 mmol, 44% yield) after purification by flash column chromatography ($SiO_2$, CyH/AcOEt 100:0 to 90:10).

**M.p.** = 58 °C.

**$^1$H NMR** (500 MHz, $CDCl_3$) δ 7.21 (t, *J* = 7.9 Hz, 1H), 6.93 (dt, *J* = 7.6, 1.3 Hz, 1H), 6.86 (dd, *J* = 2.6, 1.6 Hz, 1H), 6.78 (ddd, *J* = 8.2, 2.6, 0.9 Hz, 1H), 6.49 (dt, *J* = 15.8, 1.4 Hz, 1H), 6.00 (dt, *J* = 15.5, 7.7 Hz, 1H), 3.81 (s, 3H), 3.76 (s, 6H), 2.96 (dd, *J* = 7.7, 1.3 Hz, 2H), 2.85 (d, *J* = 2.7 Hz, 2H), 2.06 (t, *J* = 2.7 Hz, 1H) ppm.

**$^{13}$C NMR** (126 MHz, $CDCl_3$) δ 170.3, 159.9, 138.6, 134.7, 129.6, 123.6, 119.1, 113.2, 112.0, 79.0, 71.8, 57.4, 55.4, 53.0, 36.0, 23.1 ppm.

**HRMS** (ESI+) calculated for m/z $[C_{18}H_{20}NaO]^+$, $[M+Na]^+$: 339.1203; found 339.1203.

**Dimethyl (*E*)-2-(3-(4-nitrophenyl)allyl)-2-(prop-2-yn-1-yl)malonate (114l)**

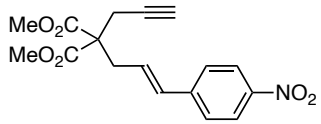


Prepared following general procedure **GP3**, using (*E*)-3-(4-nitrophenyl)prop-2-en-1-ol (400 mg, 2.23 mmol). Allyl bromide was obtained as a yellow oil (410 mg, 1.69 mmol, 76% yield) and was used in the following step with propargyl malonate (170 μL, 1.11 mmol, 1.0 equiv). Enyne **114l** was obtained as a yellow solid (230 mg, 0.69 mmol, 62% yield) after purification by flash column chromatography ($SiO_2$, CyH/AcOEt 100:0 to 90:10).

**M.p.** = 68 °C

**$^1$H NMR** (300 MHz, $CDCl_3$) δ 8.21 – 8.09 (m, 2H), 7.51 – 7.37 (m, 2H), 6.59 (d, *J* = 15.8 Hz, 1H), 6.33 – 6.14 (m, 1H), 3.77 (s, 6H), 3.01 (dd, *J* = 7.6, 1.2 Hz, 2H), 2.85 (d, *J* = 2.7 Hz, 2H), 2.08 (t, *J* = 2.7 Hz, 1H) ppm.

**$^{13}$C NMR** (75 MHz, $CDCl_3$) δ 170.1, 147.1, 143.4, 132.8, 128.8, 127.0, 124.1, 78.6, 72.1, 57.2, 53.1, 36.3, 23.4 ppm.

**HRMS** (ESI+) calculated for m/z $[C_{17}H_{17}NNaO_6]^+$, $[M+Na]^+$: 354.0948; found 354.0950.

The spectral data were fully consistent with those previously reported.[¡Error! Marcador no definido.c]

**Dimethyl (*E*)-2-(3-(4-chlorophenyl)allyl)-2-(prop-2-yn-1-yl) (114m)**

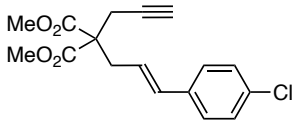


Prepared following general procedure **GP3**, using (*E*)-3-(4-chlorophenyl)prop-2-en-1-ol (200 mg, 1.19 mmol). Allyl bromide was obtained as a colorless oil (200 mg, 0.864 mmol, 76% yield) and was used in the following step with propargyl malonate (89 μL, 0.588 mmol, 1.0 equiv). Enyne **114m** was obtained as a white solid (150 mg, 0.468 mmol, 80% yield) after purification by flash column chromatography ($SiO_2$, CyH/AcOEt 100:0 to 90:10).

**M.p.** = 84–86 °C.

**$^1$H NMR** (300 MHz, $CDCl_3$) δ 7.26 – 7.24 (m, 4H), 6.47 (dt, *J* = 15.7, 1.3 Hz, 1H), 5.99 (dt, *J* = 15.5, 7.7 Hz, 1H), 3.76 (s, 6H), 2.95 (dd, *J* = 7.7, 1.3 Hz, 2H), 2.84 (d, *J* = 2.7 Hz, 2H), 2.06 (t, *J* = 2.6 Hz, 1H) ppm.

**$^{13}$C NMR** (75 MHz, $CDCl_3$) δ 170.2, 135.6, 133.6, 133.3, 128.8, 127.6, 124.1, 78.9, 71.9, 57.3, 53.0, 36.0, 23.2 ppm.

The spectral data were fully consistent with those previously reported.[77]

**Dimethyl (*E*)-2-(3-(4-Methoxyphenyl)allyl)-2-(prop-2-yn-1-yl)malonate (114n)**

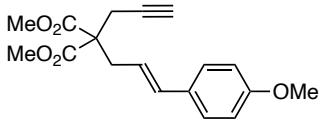


Prepared following general procedure **GP3**, using (*E*)-3-(4-methoxyphenyl)prop-2-en-1-ol (300 mg, 1.83 mmol). Allyl bromide was obtained as a colorless oil (350 mg, 1.54 mmol, 84% yield) and was used in the following step with propargyl malonate (152 µL, 0.999 mmol, 1.0 equiv). Enyne **114n** was obtained as a colorless oil (200 mg, 0.632 mmol, 63% yield) after purification by flash column chromatography ($SiO_2$, CyH/AcOEt 100:0 to 90:10).

**$^1$H NMR** (300 MHz, $CDCl_3$) δ 7.31 – 7.26 (m, 1H), 7.25 – 7.23 (m, 1H), 6.87 – 6.79 (m, 2H), 6.46 (d, *J* = 15.7 Hz, 1H), 5.84 (dt, *J* = 15.5, 7.6 Hz, 1H), 3.80 (s, 3H), 3.76 (s, 6H), 2.94 (dd, *J* = 7.7, 1.2 Hz, 2H), 2.84 (d, *J* = 2.7 Hz, 2H), 2.05 (t, *J* = 2.7 Hz, 1H) ppm.

**$^{13}$C NMR** (75 MHz, $CDCl_3$) δ 170.4, 134.2, 127.6, 120.9, 114.1, 79.0, 71.7, 57.4, 55.4, 53.0, 36.0, 23.0 ppm.

The spectral data were fully consistent with those previously reported.[78]

77 Wang, G.; Wang, Y.; Li, Z.; Li, H.; Yu, M.; Pang, M.; Zhao, X. Gold-Catalyzed Cyclization/Hydroboration of 1,6-Enynes: Synthesis of Bicyclo[3.1.0]hexane Boranes *Org. Lett.* **2022**, *24* (51), 9425–9430.

78 Nieto-Oberhuber, C.; Muñoz, M. P.; López, S.; Jiménez-Núñez, E.; Nevado, C.; Herrero-Gómez, E.; Raducan, M.; Echavarren, A. M. Gold(I)-Catalyzed Cyclizations of 1,6-Enynes: Alkoxycyclizations and *exo*/*endo* Skeletal Rearrangements, *Chem. Eur. J.* **2006**, *12*, 1677–1693.

**Diisopropyl (*E*)-2-Cinnamyl-2-(prop-2-yn-1-yl)malonate (114o)**

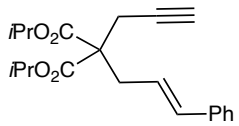


Prepared following a modified literature procedure.[79] Under argon, to a solution of **114a** (400 mg, 1.40 mmol) in *i*-PrOH (2.3 mL, 0.6 M) was added, at room temperature, Ti(O*i*-Pr)$_4$ (0.83 mL, 2.80 mmol, 2.0 equiv). The mixture was warmed to 80 °C and stirred overnight. After 14 h, the reaction was diluted with water (5 mL) and $Et_2O$ (10 mL). The aqueous phase was extracted with $Et_2O$ (3 x 10 mL). The combined organic layers were washed with brine, dried over $Na_2SO_4$, filtered, and solvent was removed under reduced pressure. The crude was purified by flash column chromatography (CyH/AcOEt, 100:0 to 98:2) enyne **114o** as a colorless oil (306 mg, 0.894 mmol, 64% yield).

**$^1$H NMR** (300 MHz, $CDCl_3$) δ 7.38 – 7.25 (m, 4H), 7.27 – 7.16 (m, 1H), 6.51 (d, *J* = 15.7 Hz, 1H), 6.03 (dt, *J* = 15.5, 7.7 Hz, 1H), 5.09 (hept, *J* = 6.3 Hz, 2H), 2.94 (dd, *J* = 7.6, 1.2 Hz, 2H), 2.82 (d, *J* = 2.7 Hz, 2H), 2.04 (t, *J* = 2.7 Hz, 1H), 1.25 (d, *J* = 2.5 Hz, 6H), 1.23 (d, *J* = 2.5 Hz, 6H) ppm.

**$^{13}$C NMR** (75 MHz, $CDCl_3$) δ 169.4, 137.2, 134.6, 128.6, 127.6, 126.4, 123.5, 79.2, 71.6, 69.3, 57.0, 35.8, 22.9, 21.8, 21.7 ppm.

Spectroscopic data matched those reported in the literature.[80]

79 Hungerbühler, E.; Naef, R.; Schnurrenberger, P.; Weidmann, B.; Züger, M.; Seebach, D. Titanate-Mediated Transesterifications with Functionalized Substrates. *Synthesis,* **1982**, *2*, 138–141.

80 Chao, C.-M.; Vitale, M. R.; Toullec, P. Y.; Genêt, J.-P.; Michelet, V. Asymmetric Gold-Catalyzed Hydroarylation/Cyclization Reactions, *Chem. Eur. J.* **2009**, *15*, 1319–1323.

**HTE experiments for the indole addition to 1,6-enyne 114b**

To benefit from the two-component combinatorial nature of the HCDC approach, HTE experiments were performed to screen for the best solvent and combination of gold(I) complex and chiral metal salt (Figure S2).

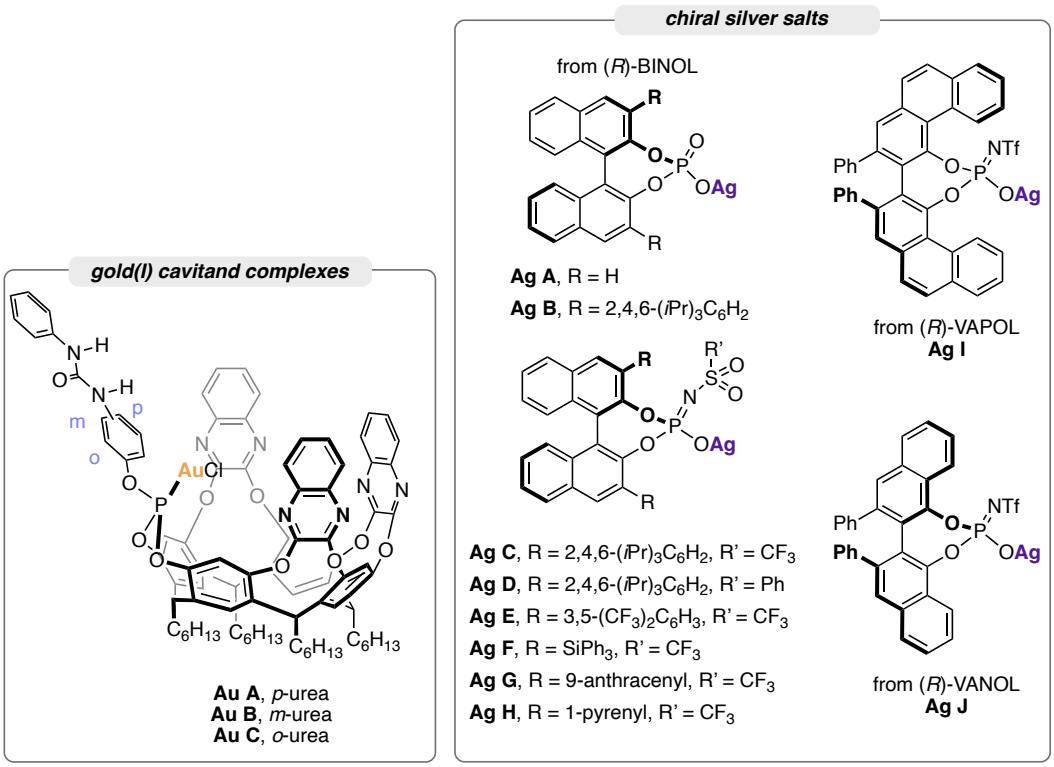


**Figure S2**. Library of gold(I)-cavitand complexes and chiral silver salts used in the HTE experiments.

**HTE procedure used for solvent screening in the indole addition to 1,6-enyne 114b**

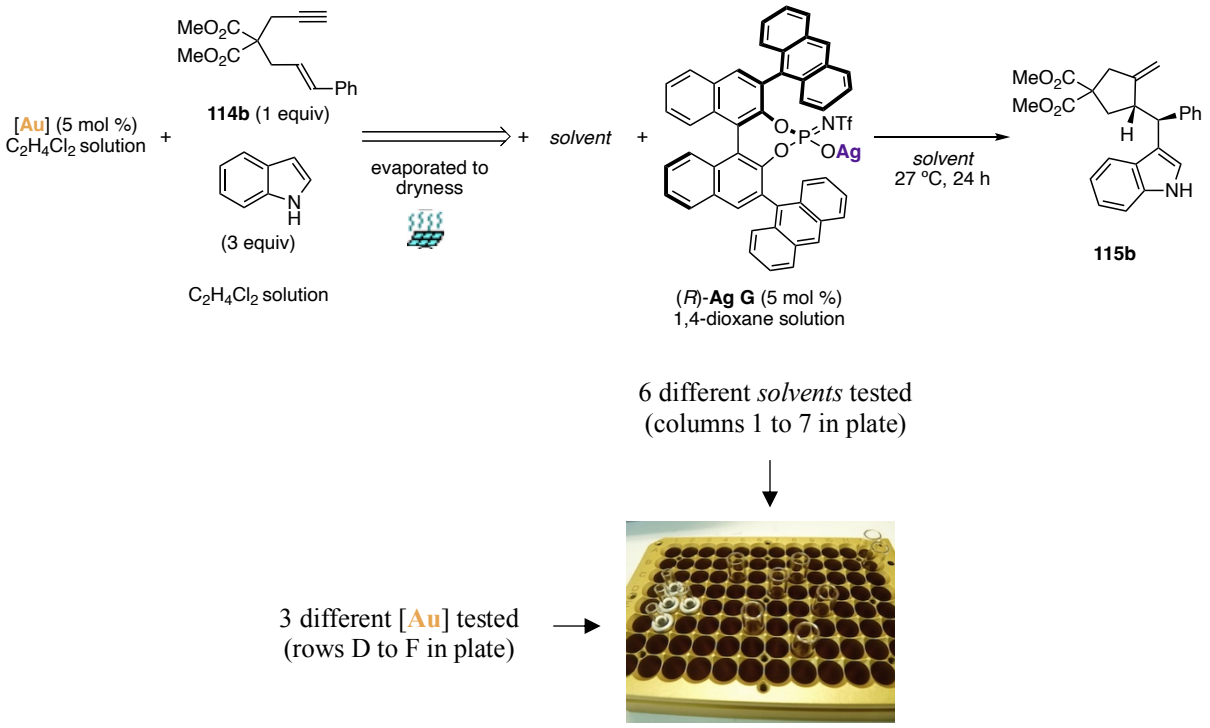


**Scheme S4**. HTE setup for the solvent screening.

The gold(I) complexes were each dissolved in anhydrous $C_2H_4Cl_2$ in a 0.005 M solution. A 70 µL aliquot of each solution (7 mol %, 0.7 µmol) was added to the corresponding 0,75 mL glass vials charged with a parylene-coated stainless-steel micro stir bar, positioned within a 96-well block assembly. To the reaction vials containing the gold(I) complexes were added 100 µL of a stock $C_2H_4Cl_2$ solution of 1,6-enyne **114b** (0.1 M, 10 µmol, 1 equiv) and indole (0.3 M, 30 µmol, 3 equiv). The solvent was evaporated in a centrifuge under vacuum (Genevac EZ-2 apparatus). Then, 65 µL of the corresponding anhydrous solvent was added to each column of the reaction plate. Finally, 35 µL of the solution of silver salt (*R*)-**Ag G** in the corresponding reaction solvent (0.02 M, 7 mol %, 0.7 µmol) were added. The reaction plate was capped, and the reactions were left stirring at 27 °C for 24 h in a Tumble Stirrer apparatus. After this time, 500 µL of a stock solution containing naphthalene as internal standard (0.005 M solution, 2.5 µmol, 0.25 equiv) and $Et_3N$ (0.004 M, 2 µmol, 0.2 equiv) were added to each reaction vial. To prepare the samples for SFC analysis, 20 µL of each diluted reaction solution was transferred to a 96-well analysis plate containing 500 µL of $CH_3CN$ in each well.

**Table S1**. High-throughput screening of solvents for the gold(I)-catalyzed indole addition to 1,6-enyne **114b**. Product yields (calculated using naphthalene as internal standard) and *er* values were determined by SFC on chiral stationary phase. IB column (150 × 4.6 mm, 3 µm), $CO_2$:MeOH gradient method (100:0 for 1 min, then increasing to 60:40 over 4 min, hold for 1 min at 60:40, then decreasing to 100:0 over 0.25 min and hold for 1.25 min), 3.0 mL/min, T = 35 °C, ABPR 150 bar, 230 nm): naphtalene (2.39 min), **114b** (2.49 min), indole (3.60 min), **115b** en1 (4.55 min), **115b** en2 (4.69 min).

**Table S1a**. **115b** Yield (%) shown.[a]

| | | 1 | 2 | 3 | 4 | 5 | 6 |
|---|---|---|---|---|---|---|---|
| | | **$CF_3C_6H_5$** | **toluene** | **DCE** | **$CHCl_3$** | **CPME** | **1,4-dioxane** |
| A | **Au A** | 73 | 78 | >99 | 69 | 83 | 98 |
| B | **Au B** | 74 | 69 | 82 | 41 | 78 | 53 |
| C | **Au C** | 46 | 36 | 57 | 8 | 37 | - |

CPME = cyclopentyl methyl ether. [a] Color code: ≥ 70%, dark green; 50–69%, olive green; < 50% dark red; grey = no reaction.

**Table S1b**. **115b** *er* (%) shown.[a]

| | | 1 | 2 | 3 | 4 | 5 | 6 |
|---|---|---|---|---|---|---|---|
| | | **$CF_3C_6H_5$** | **toluene** | **DCE** | **$CHCl_3$** | **CPME** | **1,4-dioxane** |
| A | **Au A** | 66:34 | 85:15 | 73:27 | 78:22 | 88:12 | 94:6 |
| B | **Au B** | 48:52 | 47:53 | 49:51 | 53:47 | 53:47 | 44:56 |
| C | **Au C** | 48:52 | 41:59 | 53:47 | 48:52 | 37:63 | - |

CPME = cyclopentyl methyl ether. [a] Color code: ≥ 90:10, electric blue; 75:25–90:10, violet; < 75:25, cyan; grey = no reaction

**HTE procedure used silver salt screening in the indole addition to 1,6-enyne 114b**

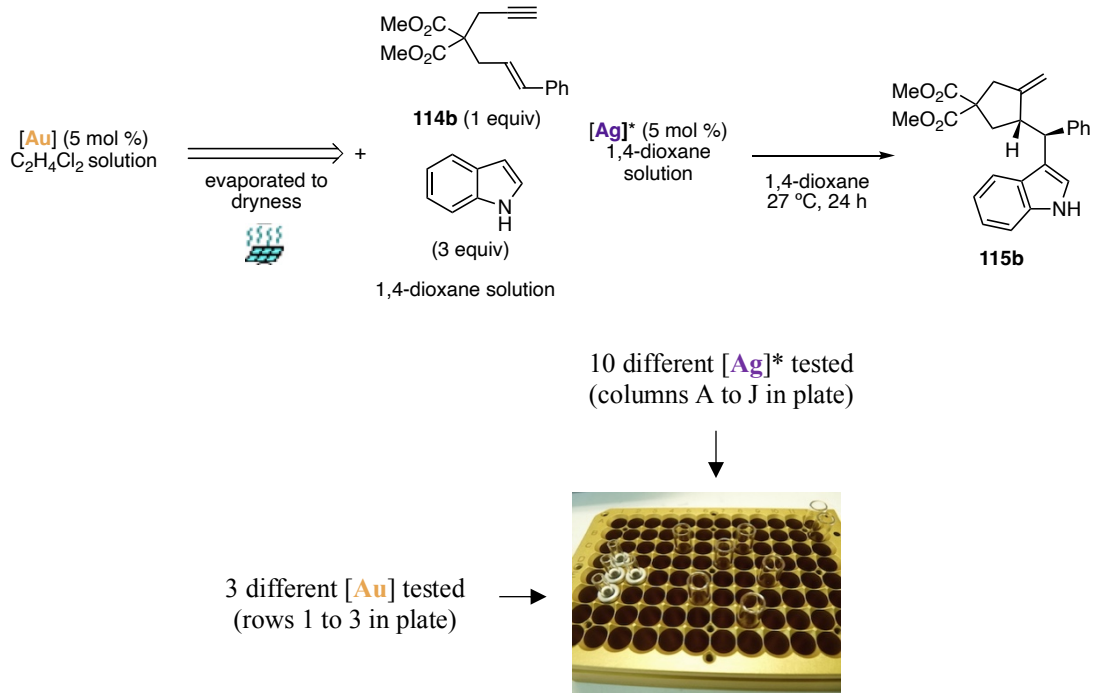


**Scheme S5**. HTE setup for the chiral silver salt screening.

The gold(I) complexes were each dissolved in anhydrous $C_2H_4Cl_2$ to give a 0.005 M solution (3.5 µmol). A 50 µL of each solution (5 mol %, 0.25 µmol) was added to the corresponding 0.75 mL glass vials charged with a parylene-coated stainless-steel micro stir bar, positioned within a 96-well block assembly. The solvent was evaporated in a centrifuge under vacuum (Genevac EZ-2 apparatus). To the reaction vials containing the gold(I) complexes were added 20 µL of a stock dioxane solution of 1,6-enyne **114b** (0.250 M, 5 µmol, 1 equiv) and indole (0.75 M, 15 µmol, 3 equiv) in 1,4-dioxane. Finally, 30 µL of a solution of the corresponding silver salt in anhydrous dioxane (0.008 M, 5 mol %, 0.25 µmol) were added to each column of the reaction plate. The reaction plate was capped, and the reactions were left stirring at 27 °C for 24 h in a Tumble Stirrer apparatus. After this time, 463 µL of a stock solution containing naphthalene as internal standard (0.0027 M solution, 1.25 µmol, 0.25 equiv) and $Et_3N$ (0.002 M, 1 µmol, 0.2 equiv) were added to each reaction vial. To prepare the samples for SFC analysis 20 µL of each diluted reaction solution was transferred to a 96-well analysis plate containing 500 µL of $CH_3CN$ in each well.

**Table S2**. High-throughput screening of gold (I) complexes and chiral silver salts for the gold(I)-catalyzed indole addition to 1,6-enyne **114b**. Product yields (calculated using naphthalene as internal standard) and *er* values were determined by SFC on chiral stationary phase. IB column (150 × 4.6 mm, 3 µm), $CO_2$:MeOH gradient method (100:0 for 1 min, then increasing to 60:40 over 4 min, hold for 1 min at 60:40, then decreasing to 100:0 over 0.25 min and hold for 1.25 min), 3.0 mL/min, T = 35 °C, ABPR 150 bar, 230 nm): naphtalene (2.39 min), **114b** (2.49 min), indole (3.60 min), **115b** en1 (4.55 min), **115b** en2 (4.69 min).

**Table S2a**. **114b**, yield (%) shown.[a]

| | | 1 | 2 | 3 | 4 | 5 | 6 | 7 | 8 | 9 | 10 |
|---|---|---|---|---|---|---|---|---|---|---|---|
| | | **Ag A** | **Ag B** | **Ag C** | **Ag D** | **Ag E** | **Ag F** | **Ag G** | **Ag H** | **Ag I** | **Ag J** |
| A | **Au A** | - | - | 80 | - | 50 | 44 | 70 | 62 | 66 | 64 |
| B | **Au B** | - | - | 17 | - | 12 | 16 | 61 | 36 | 66 | 60 |
| C | **Au C** | - | - | 3 | - | - | - | - | 4 | 5 | 10 |

[a] Color code: ≥ 70%, dark green; 50–69%, olive green; < 50% dark red; grey (*n.r.*) = no reaction.

**Table S2b**. **114b**, *er* (%) shown.[a]

| | | 1 | 2 | 3 | 4 | 5 | 6 | 7 | 8 | 9 | 10 |
|---|---|---|---|---|---|---|---|---|---|---|---|
| | | **Ag A** | **Ag B** | **Ag C** | **Ag D** | **Ag E** | **Ag F** | **Ag G** | **Ag H** | **Ag I** | **Ag J** |
| A | **Au A** | - | - | 91:9 | - | 84:16 | 30:70 | 94:6 | 90:10 | 81:19 | 65:35 |
| B | **Au B** | - | - | 52:49 | - | 62:38 | 36:64 | 47:53 | 34:66 | 64:36 | 55:45 |
| C | **Au C** | - | - | 52:48 | - | - | - | - | 42:58 | 45:55 | 30:70 |

[a] Color code: ≥ 90:10, electric blue; 75:25 – 90:10, violet; < 75:25, cyan; grey (*n.r.*) = no reaction.

**General procedure GP4: enantioselective nucleophile addition to 1,6-enynes 114**

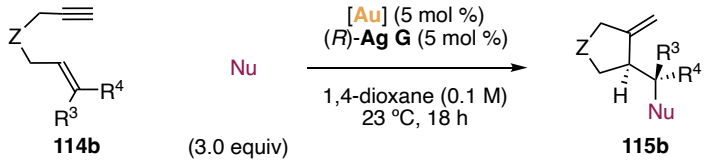


**Scheme S6**. General procedure GP4.

To a GMCS or MW vial containing a solution of enyne (1.0 equiv) and nucleophile (3.0 equiv) in anhydrous 1,4-dioxane was added respectively a solution of complex **Au A** (5 mol %) and a solution of *(R)*-**Ag G** (5 mol %) in 1,4-dioxane (0.1 M final concentration) at 23 °C. The resulting mixture was stirred until starting material consumption, determined by TLC or GCMS analysis. The reaction was then quenched by addition of $Et_3N$ (*ca.* 3 drops) and filtered through a silica-filled glass pipette. Volatiles were removed under reduced pressure and the crude product was purified by flash column chromatography or preparative TLC ($SiO_2$, CyH/AcOEt).

The absolute configuration of the compounds **115** was assigned by comparison to **115m** and assuming a uniform stereochemical mechanism.

**Dimethyl (*R*)-3-((*R*)-(1H-indol-3-yl)(phenyl)methyl)-4-methylenecyclopentane-1,1-dicarboxylate (115a)**

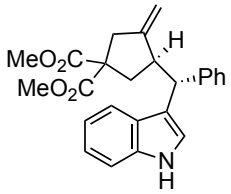


Prepared following general procedure **GP4** using **114a** (30.0 mg, 0.99 mmol, 1.0 equiv) and indole (34.6 mg, 0.29 mmol, 3.0 equiv) as a nucleophile in 1,4-dioxane (1.0 mL, 0.1 M), at 25 °C for 16 h. The crude product was purified by flash column chromatography ($SiO_2$, CyH/AcOEt 90:10 to 80:20). Compound **115a** was obtained as a white solid (29.5 mg, 0.98 mmol, 74% yield, 94:6 *er*).

**$^1$H NMR** (300 MHz, $CDCl_3$) δ 8.06 (bs, 1H), 7.54 (d, *J* = 8.0 Hz, 1H), 7.37 – 7.28 (m, 3H), 7.25 – 7.18 (m, 2H), 7.18 – 7.08 (m, 3H), 7.05 (td, *J* = 7.5, 1.1 Hz, 1H), 4.80 (s, 1H), 4.22 – 4.10 (m, 2H), 3.72 (s, 3H), 3.64 (s, 3H), 3.61 – 3.45 (m, 1H), 3.13 (dq, *J* = 15.9, 2.4 Hz, 1H), 2.97 – 2.85 (m, 1H), 2.76 (ddd, *J* = 13.6, 7.9, 1.5 Hz, 1H), 1.98 (dd, *J* = 13.7, 8.5 Hz, 1H) ppm.

**$^{13}$C NMR** (75 MHz, $CDCl_3$) δ 172.4, 172.2, 149.0, 144.5, 136.3, 128.6, 128.2, 127.3, 126.2, 122.1, 121.5, 119.5, 119.5, 118.7, 111.2, 110.2, 58.6, 52.9, 52.8, 48.1, 46.9, 41.9, 40.0 ppm.

**SFC** (IG (100 × 3 mm, 3 μm), 80:20 $CO_2$:*i*-PrOH, 1.5 mL/min, 35 ºC, BPR 150 bar, 280 nm): $t_R$ en1 (minor) 1.25 min; $t_R$ en2 (major) 1.53 min.

**[α]$^{24.6}_{D}$** +2.8 (c 1.28, $CHCl_3$).

The spectral data were fully consistent with those previously reported.[81]

**3-((*R*)-((*R*)-4-methylene-1-tosylpyrrolidin-3-yl)(phenyl)methyl)-1H-indole (115b)**

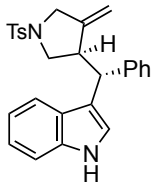


Prepared following general procedure **GP4**, using **114b** (20 mg, 61.5 μmol, 1.0 equiv) and indole (21.6 mg, 0.18 mmol, 3.0 equiv) as a nucleophile in toluene (1.0 mL, 0.1 M), at 25 °C for 16 h. The crude product was purified by flash column chromatography ($SiO_2$, CyH/AcOEt 80:20). Compound **115b** was obtained as an off-white solid (9 mg, 20 μmol, 30% yield, 19:81 *er*).

**$^1$H NMR** (300 MHz, $CDCl_3$) δ 8.06 (s, 1H), 7.60 (d, *J* = 8.2 Hz, 2H), 7.33 (d, *J* = 8.2 Hz, 2H), 7.24 (d, *J* = 8.1 Hz, 2H), 7.20 – 6.99 (m, 7H), 4.79 – 4.70 (m, 1H), 4.28 – 4.19 (m, 1H), 3.96 (d, *J* = 10.2 Hz, 1H), 3.91 – 3.79 (m, 2H), 3.50 – 3.30 (m, 3H), 2.43 (s, 4H) ppm.

**$^{13}$C NMR** (75 MHz, $CDCl_3$) δ 145.2, 143.7, 143.3, 136.5, 132.9, 129.8, 128.4, 128.3, 127.9, 127.0, 126.4, 122.4, 121.2, 119.6, 119.4, 118.1, 111.3, 110.3, 53.2, 52.5, 47.9, 45.9, 21.7 ppm.

**SFC** (IC (100 × 3 mm, 3 μm), 80:20 $CO_2$:EtOH, 1.2 mL/min, 35 °C, BPR 150 bar, 210 nm): $t_R$ en1 (minor) 4.66 min; $t_R$ en2 (major) 5.11 min.

**[α]$^{24.6}_{D}$** –38.4 (c 0.54, $CHCl_3$).

The spectral data were fully consistent with those previously reported.[49e]

81 Toullec, P. Y.; Genin, E.; Leseurre, L.; Genêt, J.-P.; Michelet, V. Room-Temperature Au(I)-Catalyzed C-C Bond Formation through a Tandem Friedel-Crafts-Type Addition/Carbocyclization Reaction, *Angew. Chem. Int. Ed Engl.* **2006**, *45*, 7427–7430.

**Dimethyl (*R*)-3-((*R*)-(5-bromo-1H-indol-3-yl)(phenyl)methyl)-4-methylenecyclopentane-1,1-dicarboxylate (115c)**

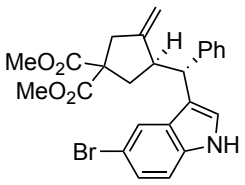


Prepared following general procedure **GP4** using **114a** (28.6 mg, 0.1 mmol, 1.0 equiv) and 5-bromoindole (58.8 mg, 0.3 mmol, 3.0 equiv) as a nucleophile in 1,4-dioxane (1.0 mL, 0.1 M), at 25 °C for 16 h. The crude product was purified by flash column chromatography ($SiO_2$, CyH/AcOEt 90:10 to 80:20). Compound **115c** was obtained as a white solid (38 mg, 0.079 mmol, 79% yield, 93:7 *er*).

**$^1$H NMR** (300 MHz, $CDCl_3$) δ 8.16 (s, 1H), 7.65 (dt, *J* = 1.4, 0.7 Hz, 1H), 7.36 – 7.09 (m, 8H), 4.80 (t, *J* = 1.7 Hz, 1H), 4.11 (d, *J* = 2.3 Hz, 1H), 4.08 (d, *J* = 10.4 Hz, 1H), 3.73 (s, 3H), 3.65 (s, 3H), 3.57 – 3.35 (m, 1H), 3.17 – 2.99 (m, 1H), 2.91 (dd, *J* = 16.0, 1.5 Hz, 1H), 2.78 – 2.60 (m, 1H), 1.93 (dd, *J* = 13.7, 8.5 Hz, 1H) ppm.

**$^{13}$C NMR** (75 MHz, $CDCl_3$) δ 172.4, 172.2, 148.7, 144.0, 134.8, 129.0, 128.5, 128.4, 126.4, 125.0, 122.7, 121.9, 118.5, 112.8, 112.7, 110.3, 58.5, 53.0, 52.9, 47.9, 46.9, 41.8, 39.9 ppm.

**HRMS** (ESI+) calculated for m/z $[C_{25}H_{25}BrNO_4]^+$, $[M+H]^+$: 482.0961; found 482.0959.

**SFC** (IB-N (100 × 3 mm, 3 μm), 60:40 $CO_2$:MeOH, 1.2 mL/min, 35 °C, BPR 150 bar, 210 nm): $t_R$ en1 (major) 0.99 min; $t_R$ en2 (minor) 1.27 min.

**$[\alpha]^{24.6}_D$** +38.7 (c 1.74, $CHCl_3$).

**Dimethyl (*R*)-3-((*R*)-(5-Methoxy-1H-indol-3-yl)(phenyl)methyl)-4-methylenecyclopentane-1,1-dicarboxylate (115d)**

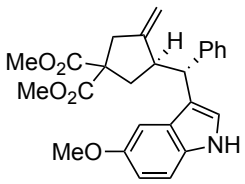


Prepared following general procedure **GP4** using **114a** (28.6 mg, 0.1 mmol, 1.0 equiv) and 5-methoxyindole (22.1 mg, 0.15 mmol, 1.5 equiv) as a nucleophile in 1,4-dioxane (1.0 mL, 0.1 M), at 25 °C for 16 h. The crude product was purified by flash column chromatography ($SiO_2$, CyH/AcOEt 90:10 to 80:20). Compound **115d** was obtained as a white solid (24 mg, 0.055 mmol, 55% yield, 94:6 *er*).

**M.p.** = 52 °C.

**$^1$H NMR** (300 MHz, $CDCl_3$) δ 7.95 (bs, 1H), 7.34 – 7.28 (m, 2H), 7.26 – 7.07 (m, 5H), 6.95 (d, *J* = 2.4 Hz, 1H), 6.80 (dd, *J* = 8.8, 2.4 Hz, 1H), 4.80 (s, 1H), 4.18 – 4.07 (m, 2H), 3.79 (s, 3H), 3.72 (s, 3H), 3.64 (s, 3H), 3.50 (qd, *J* = 8.3, 1.8 Hz, 1H), 3.11 (dd, *J* = 15.9, 2.1 Hz, 1H), 2.89 (d, *J* = 15.9 Hz, 1H), 2.77 (ddd, *J* = 13.6, 7.9, 1.4 Hz, 1H), 1.98 (dd, *J* = 13.7, 8.5 Hz, 1H) ppm.

**$^{13}$C NMR** (75 MHz, $CDCl_3$) δ 172.4, 172.2, 154.0, 149.1, 144.4, 131.5, 128.6, 128.2, 127.8, 126.2, 122.4, 118.5, 112.2, 111.8, 110.1, 101.6, 58.6, 56.0, 52.9, 52.8, 48.1, 46.9, 41.9, 39.9 ppm.

**HRMS** (ESI+) calculated for m/z $[C_{26}H_{27}NNaO_5]^+$, $[M+Na]^+$:456.1781; found 456.1783.

**SFC** (IB-N (100 x 3 mm, 3 μm), 80:30 $CO_2$:MeOH, 1.2 mL/min, 35 °C, BPR 150 bar, 210 nm): $t_R$ en1 (major) min 1.25; $t_R$ en 2 (minor) 1.82 min.

**$[\alpha]^{24.6}_D$** +26.7 (c 1.13, $CHCl_3$).

**Dimethyl (*R*)-3-((*R*)-(1-Methyl-1H-indol-3-yl)(phenyl)methyl)-4-methylenecyclopentane-1,1-dicarboxylate (115e)**

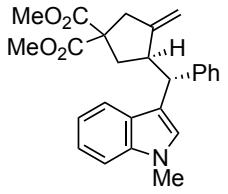


Prepared following general procedure **GP4** using **114a** (28.6 mg, 0.1 mmol, 1.0 equiv) and N-methylindole (19.68 mg, 0.15 mmol, 1.5 equiv) as a nucleophile in 1,4-dioxane (1.0 mL, 0.1 M), at 25 °C for 16 h. The crude product was purified by flash column chromatography ($SiO_2$, CyH/AcOEt 90:10 to 80:20). Compound **115e** was obtained as a white solid (41.8 mg, 0.065 mmol, 65% yield, 95:5 *er*).

**$^1$H NMR** (300 MHz, $CDCl_3$) δ 7.56 – 7.49 (m, 1H), 7.35 – 7.29 (m, 2H), 7.24 – 7.15 (m, 3H), 7.15 – 7.07 (m, 1H), 7.06 – 7.01 (m, 1H), 7.00 (d, *J* = 1.9 Hz, 1H), 4.77 (s, 1H), 4.12 (d, *J* = 10.7 Hz, 2H), 3.76 (s, 3H), 3.72 (s, 3H), 3.63 (s, 3H), 3.57 – 3.45 (m, 1H), 3.18 – 3.04 (m, 1H), 2.93 – 2.83 (m, 1H), 2.81 – 2.67 (m, 1H), 1.94 (dd, *J* = 13.7, 8.5 Hz, 1H) ppm.

**$^{13}$C NMR** (75 MHz, $CDCl_3$) δ 172.4, 172.2, 149.1, 144.7, 137.0, 128.6, 128.2, 127.7, 126.3, 126.1, 121.7, 119.5, 119.0, 117.3, 110.1, 109.2, 58.5, 52.9, 52.8, 48.2, 46.9, 41.9, 40.1, 32.9 ppm.

**SFC** (OD (100 x 3 mm, 3 μm), 80:20 $CO_2$:MeOH, 1.2 mL/min, 35 °C, BPR 150 bar, 210 nm): $t_R$ en1 (major) 1.12 min; $t_R$ en2 (minor) 1.23 min.

**$[\alpha]^{24.6}_D$** –7.25 (c 1.49, $CHCl_3$).

The spectral data were fully consistent with those previously reported.[81]

**dimethyl (*R*)-3-((*R*)-(2-methyl-1*H*-indol-3-yl)(phenyl)methyl)-4-methylenecyclopentane-1,1-dicarboxylate (115f)**

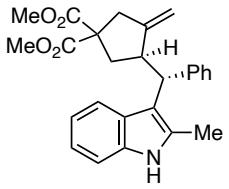


Prepared following general procedure **GP4** using **114a** (28.6 mg, 0.99 mmol, 1.0 equiv) and 2-methyl-1H-indole (19.7 mg, 0.15 mmol, 1.5 equiv) as a nucleophile in 1,4-dioxane (1.0 mL, 0.1 M), at 25 °C for 16 h. The crude product was purified by flash column chromatography ($SiO_2$, CyH/AcOEt 90:10 to 80:20). Compound **115f** was obtained as a white solid (14 mg, 0.34 mmol, 34% yield, 92:8 *er*).

**M.p.** 61–66 ºC.

**$^1$H NMR** (300 MHz, $CDCl_3$) δ 7.79 – 7.68 (m, 2H), 7.41 (d, *J* = 7.3 Hz, 2H), 7.25 – 7.17 (m, 3H), 7.14 – 7.03 (m, 3H), 4.89 – 4.78 (m, 1H), 4.31 – 4.23 (m, 1H), 4.04 (s, 1H), 3.99 – 3.82 (m, 1H), 3.72 (s, 3H), 3.62 (s, 3H), 3.20 – 3.08 (m, 1H), 3.05 – 2.93 (m, 1H), 2.57 – 2.46 (m, 1H), 2.41 (s, 3H), 1.84 (dd, *J* = 13.5, 9.2 Hz, 1H) ppm.

**$^{13}$C NMR** (75 MHz, $CDCl_3$) δ 172.5, 172.4, 150.2, 144.8, 135.4, 131.3, 128.3, 128.2, 127.8, 125.9, 120.9, 119.6, 119.4, 114.5, 110.4, 109.6, 58.0, 52.8, 52.8, 47.9, 45.1, 41.8, 39.9, 12.7 ppm.

**HRMS (ESI +)** calculated for $[C_{26}H_{27}NNaO_4]^+$ $[M+Na]^+$ 440.1830 m/z; found 440.1830 m/z**.**

**SFC** (IB-N (100 × 3 mm, 3 μm), 80:20 $CO_2$:*i*-PrOH, 1.2 mL/min, 35 ºC, BPR 150 bar, 210 nm): en2 (major, 100%) 3.33 min.

**$[\alpha]^{24.6}_D$** –9.49 (c 1.08, $CHCl_3$).

**Dimethyl (*R*)-3-Methylene-4-((*R*)-phenyl(2,4,6-trimethoxyphenyl)methyl)cyclopentane-1,1-dicarboxylate (115g)**

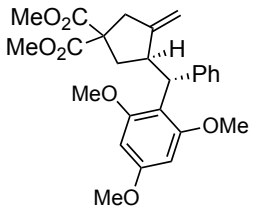


Prepared following general procedure **GP4**, using **114a** (20 mg, 69.8 μmol, 1.0 equiv) and 1,3,5-trimethoxybenzene (35.24 mg, 0.21 mmol, 3.0 equiv) as a nucleophile in 1,4-dioxane (1.0 mL, 0.1 M), at 23 °C for 16 h. The crude product was purified by flash column chromatography ($SiO_2$, CyH/AcOEt 90:10 to 80:20). Compound **115g** was obtained as a white solid (13 mg, 29 μmol, 41% yield, 18:82 *er*).

**M.p.** = 74 °C.

**$^1$H NMR** (500 MHz, $CDCl_3$) δ 7.48 – 7.44 (m, 2H), 7.19 (t, *J* = 7.7 Hz, 2H), 7.09 (t, *J* = 7.3 Hz, 1H), 6.08 (s, 2H), 4.73 (q, *J* = 2.2 Hz, 1H), 4.50 (d, *J* = 11.0 Hz, 1H), 4.26 (qd, *J* = 2.2, 0.8 Hz, 1H), 3.99 (tdt, *J* = 11.9, 7.5, 2.4 Hz, 1H), 3.81 (s, 6H), 3.76 (s, 3H), 3.74 (s, 3H), 3.66 (s, 3H), 3.09 (dq, *J* = 16.5, 2.2 Hz, 1H), 3.01 (dq, *J* = 16.6, 1.9 Hz, 1H), 2.37 (ddd, *J* = 12.9, 7.5, 1.6 Hz, 1H), 1.68 (dd, *J* = 13.0, 10.8 Hz, 1H) ppm.

**$^{13}$C NMR** (126 MHz, $CDCl_3$) δ 172.6, 172.5, 159.6, 151.5, 144.7, 128.8, 127.8, 125.6, 113.7, 108.2, 91.1, 57.8, 55.7, 55.3, 52.8, 52.7, 44.3, 43.1, 41.8, 40.1 ppm.

**SFC** (IG-3 (150 × 4.6 mm, 3 μm), 93:7 $CO_2$:*i*-PrOH, 2.0 mL/min, 35 °C, BPR 140 bar, 230 nm): $t_R$ en1 (minor) 4.33 min; $t_R$ en2 (major) 4.72 min.

**$[\alpha]^{24.6}_D$** +80.9 (c 1.79, $CHCl_3$).

The spectral data were fully consistent with those previously reported.[82]

**Dimethyl (*S*)-3-((*R*)-hydroxy(phenyl)methyl)-4-methylenecyclopentane-1,1-dicarboxylate (115h)**

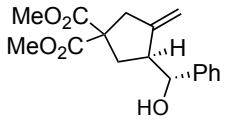


Prepared following general procedure **GP4**, **114a** (20 mg, 69.8 μmol, 1.0 equiv) and water (3.4 μL, 0.21 mmol, 3.0 equiv) as a nucleophile in HPLC-grade 1,4-dioxane (1.0 mL, 0.1 M), at 25 °C for 16 h. The crude product was purified by flash column chromatography ($SiO_2$, CyH/AcOEt 90:10 to 80:20). Compound **115h** was obtained as a white solid (19 mg, 62 μmol, 89% yield, 77:23 *er*).

**$^1$H NMR** (500 MHz, $CDCl_3$) δ 7.42 – 7.33 (m, 4H), 7.30 – 7.26 (m, 1H), 5.16 (q, *J* = 2.2 Hz, 1H), 5.01 (t, *J* = 3.5 Hz, 1H), 4.94 (q, *J* = 2.3 Hz, 1H), 3.75 (s, 3H), 3.71 (s, 3H), 3.11 – 3.03 (m, 1H), 3.03 – 3.00 (m, 2H), 2.32 (dd, *J* = 13.5, 9.4 Hz, 1H), 2.24 (dd, *J* = 13.6, 8.5 Hz, 1H), 2.17 (d, *J* = 2.9 Hz, 1H) ppm.

**$^{13}$C NMR** (75 MHz, $CDCl_3$) δ 172.2, 172.2, 149.1, 142.5, 128.4, 127.4, 126.0, 108.5, 74.2, 58.4, 52.92, 52.9, 49.9, 42.2, 33.8 ppm.

**SFC** (IG (100 × 3 mm, 3 μm), 85:15 $CO_2$:MeOH, 1.2 mL/min, 35 ºC, BPR 150 bar, 210 nm): $t_R$ en1 (major) 1.31 min; $t_R$ en2 (minor) 1.49 min.

**$[\alpha]^{24.6}_D$** +70.8 (c 0.70, $CHCl_3$).

[82] Leseurre, L.; Chao, C.-M.; Seki, T.; Genin, E.; Toullec, P. Y.; Genêt, J.-P.; Michelet, V. Synthesis of Functionalized Carbo- and Heterocycles via Gold-Catalyzed Cycloisomerization Reactions of Enynes, *Tetrahedron* **2009**, *65*, 1911–1918.

The spectral data were fully consistent with those previously reported.[58]

**Dimethyl (*S*)-3-((*R*)-ethoxy(phenyl)methyl)-4-methylenecyclopentane-1,1-dicarboxylate (115i)**

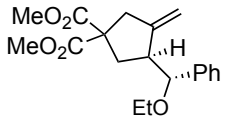


Prepared following general procedure **GP4**, using **114a** (20 mg, 69.8 μmol, 1.0 equiv) and anhydrous EtOH (12.2 μL, 0.21 mmol, 3.0 equiv) as a nucleophile in 1,4-dioxane (1.0 mL, 0.1 M), at 25 °C for 16 h. The crude product was purified by flash column chromatography ($SiO_2$, CyH/AcOEt 100:0 to 90:10). Compound **115i** was obtained as a white solid (18 mg, 54 μmol, 78% yield, 87:13 *er*).

**$^1$H NMR** (500 MHz, CDCl3) δ 7.37 – 7.33 (m, 2H), 7.32 – 7.29 (m, 2H), 7.24 – 7.19 (m, 1H), 4.93 (q, J = 2.1 Hz, 1H), 4.54 – 4.47 (m, 1H), 4.28 (d, J = 6.1 Hz, 1H), 3.76 (s, 3H), 3.70 (s, 3H), 3.42 (dq, J = 9.4, 7.1 Hz, 1H), 3.30 (dq, J = 9.4, 7.0 Hz, 1H), 3.01 (dq, J = 15.9, 2.6 Hz, 1H), 2.95 – 2.87 (m, 2H), 2.47 (ddd, J = 13.5, 8.1, 1.7 Hz, 1H), 2.37 (dd, J = 13.5, 8.7 Hz, 1H), 1.16 (t, J = 7.0 Hz, 3H) ppm.

**$^{13}$C NMR** (75 MHz, $CDCl_3$) δ 172.3, 172.3, 148.7, 141.5, 128.3, 127.6, 127.3, 108.6, 83.9, 64.8, 58.8, 52.8, 49.5, 42.3, 35.5, 15.3 ppm.

**HPLC** (OJ-H (250 × 4.6 mm, 5 μm), 99:1 n-hexane:*i*-PrOH, 1.0 mL/min, 25 °C, 210 nm): $t_R$ en1 (major) 20.48 min; $t_R$ en2 (minor) 25.91 min.

**$[\alpha]^{24.6}_D$** +74.6 (c 1.12, $CHCl_3$).

The spectral data were fully consistent with those previously reported.[58]

**Dimethyl (*R*)-3-((*R*)-(1H-indol-3-yl)(2-methoxyphenyl)methyl)-4-methylenecyclopentane-1,1-dicarboxylate (114j)**

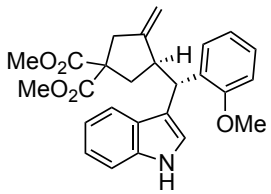


Prepared following general procedure **GP4** using **114j** (31.6 mg, 0.1 mmol, 1.0 equiv) and indole (35.1 mg, 0.3 mmol, 3.0 equiv) as a nucleophile in 1,4-dioxane (1.0 mL, 0.1 M), at 25 °C for 16 h. The crude product was purified by flash column chromatography ($SiO_2$, CyH/AcOEt 90:10 to 85:15). Compound **115j** was obtained as a white solid (39 mg, 90 μmol, 90% yield, 93:7 *er*).

**M.p.** = 54–60 °C.

**$^1$H NMR** (300 MHz, $CDCl_3$) δ 8.01 (s, 1H), 7.56 (d, *J* = 7.9 Hz, 1H), 7.30 (d, *J* = 8.0 Hz, 1H), 7.23 (dd, *J* = 7.5, 1.6 Hz, 1H), 7.19 – 6.99 (m, 4H), 6.80 (t, *J* = 7.7 Hz, 2H), 4.78 (d, *J* = 10.8 Hz, 1H), 4.69 (s, 1H), 4.04 (s, 1H), 3.85 (s, 3H), 3.72 (s, 3H), 3.64 (s, 3H), 3.45 (q, *J* = 8.1 Hz, 1H), 3.21 (d, *J* = 15.7 Hz, 1H), 2.86 (d, *J* = 15.7 Hz, 1H), 2.77 (dd, *J* = 13.7, 7.9 Hz, 1H), 1.98 (dd, *J* = 13.7, 7.9 Hz, 1H) ppm.

**$^{13}$C NMR** (75 MHz, $CDCl_3$) δ 172.6, 172.3, 157.4, 149.4, 136.1, 133.1, 128.8, 127.8, 127.0, 122.0, 121.8, 120.6, 119.7, 119.4, 118.7, 111.0, 110.8, 108.9, 58.9, 55.6, 52.9, 52.8, 46.8, 41.8, 40.2, 39.5 ppm.

**HRMS** (ESI+) calculated for m/z $[C_{26}H_{27}NNaO_5]^+$, $[M+Na]^+$: 456.1781; found 456.1795.

**SFC** (IC (100 × 3 mm, 3 μm), 90:10 $CO_2$:EtOH, 1.2 mL/min, 35 °C, BPR 150 bar, 210 nm): $t_R$ en1 (minor) 2.13 min; $t_R$ en2 (major) 2.55 min.

**$[\alpha]^{24.6}_D$** –35.60 (c 1.10, $CHCl_3$).

**Dimethyl (*R*)-3-((R)-(1H-indol-3-yl)(3-methoxyphenyl)methyl)-4-methylenecyclopentane-1,1-dicarboxylate (115k)**

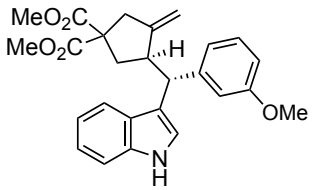


Prepared following general procedure **GP4** using **114k** (17.5 mg, 55.3 μmol, 1.0 equiv) and indole (19.4 mg, 0.17 mmol, 3.0 equiv) as a nucleophile in 1,4-dioxane (1.0 mL, 0.1 M), at 25 °C for 16 h. The crude product was purified by flash column chromatography ($SiO_2$, CyH/AcOEt 90:10 to 85:15). Compound **115k** was obtained as a white solid (21.5 mg, 49.6 μmol, 90% yield, 97:3 *er*).

**M.p.** = 67 °C.

**$^1$H NMR** (500 MHz, $CDCl_3$) δ 8.09 (s, 1H), 7.57 (dq, *J* = 8.0, 0.8 Hz, 1H), 7.30 (dt, *J* = 8.1, 0.9 Hz, 1H), 7.17 – 7.10 (m, 3H), 7.05 (ddd, *J* = 8.0, 7.0, 1.0 Hz, 1H), 6.94 (dt, *J* = 7.7, 1.3 Hz, 1H), 6.89 (dd, *J* = 2.6, 1.6 Hz, 1H), 6.67 (ddd, *J* = 8.2, 2.6, 0.9 Hz, 1H), 4.81 (dt, *J* = 2.5, 1.4 Hz, 1H), 4.20 (h, *J* = 1.0 Hz, 1H), 4.15 – 4.09 (m, 1H), 3.74 (s, 3H), 3.72 (s, 3H), 3.63 (s, 3H), 3.52 (dq, *J* = 8.3, 1.9 Hz, 1H), 3.12 (dq, *J* = 16.0, 2.4 Hz, 1H), 2.90 (dq, *J* = 15.9, 1.5 Hz, 1H), 2.74 (ddd, *J* = 13.7, 7.9, 1.7 Hz, 1H), 1.96 (dd, *J* = 13.7, 8.5 Hz, 1H) ppm.

**$^{13}$C NMR** (126 MHz, $CDCl_3$) δ 172.4, 172.2, 159.5, 148.9, 146.2, 136.3, 129.1, 127.3, 122.1, 121.5, 121.2, 119.5, 119.5, 118.6, 114.8, 111.2, 111.1, 110.2, 58.5, 55.2, 52.9, 52.8, 48.1, 46.8, 41.9, 40.0 ppm.

**HRMS** (ESI+) calculated for m/z $[C_{26}H_{28}NO_5]^+$, $[M+H]^+$: 434.1962; found 434.194.

**SFC** (OD (100 × 3 mm, 3 μm), 85:15 $CO_2$:MeOH, 1.2 mL/min, 35 °C, BPR 150 bar, 210 nm): $t_R$ en1 (major) 2.67 min; $t_R$ en2 (minor) 3.32 min.

**$[\alpha]^{24.6}_D$** +4.64 (c 1.00, $CHCl_3$).

**Dimethyl (*R*)-3-((*R*)-(1H-indol-3-yl)(4-nitrophenyl)methyl)-4-methylenecyclopentane-1,1-dicarboxylate (115l)**

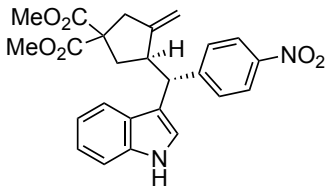

Prepared following general procedure **GP4** using **114l** (33.1 mg, 0.100 mmol, 1.0 equiv) and indole (35.1 mg, 0.3 mmol, 3.0 equiv) as a nucleophile in 1,4-dioxane (1.0 mL, 0.1 M), at 25 °C for 16 h. The crude product was purified by flash column chromatography ($SiO_2$, CyH/AcOEt 90:10 to 80:20). Compound **115l** was obtained as a yellow solid (11.5 mg, 25.6 μmol, 26% yield, 95:5 *er*).

**M.p.** = 75–77 °C.

**$^1$H NMR** (500 MHz, $CDCl_3$) δ 8.14 (bs, 1H), 8.11 – 8.05 (m, 2H), 7.46 (d, *J* = 8.7 Hz, 2H), 7.43 (d, *J* = 8.3 Hz, 1H), 7.35 (d, *J* = 8.2 Hz, 1H), 7.20 (d, *J* = 2.5 Hz, 1H), 7.17 (ddd, *J* = 8.2, 7.0, 1.1 Hz, 1H), 7.05 (ddd, *J* = 8.0, 7.0, 1.0 Hz, 1H), 4.80 (d, *J* = 1.6 Hz, 1H), 4.26 (d, *J* = 10.6 Hz, 1H), 4.07 (dt, *J* = 2.8, 1.5 Hz, 1H), 3.72 (s, 3H), 3.64 (s, 3H), 3.51 (dtd, *J* = 9.9, 7.9, 1.8 Hz, 1H), 3.15 (dq, *J* = 15.9, 2.3 Hz, 1H), 2.94 – 2.86 (m, 1H), 2.79 (ddd, *J* = 13.8, 7.9, 1.5 Hz, 1H), 2.00 (dd, *J* = 13.8, 7.9 Hz, 1H) ppm.

**$^{13}$C NMR** (101 MHz, CDCl3) δ 172.2, 172.1, 152.2, 148.5, 146.5, 136.4, 129.4, 126.9, 123.6, 122.6, 121.8, 119.9, 119.0, 117.1, 111.5, 110.7, 58.5, 53.0, 53.0, 48.0, 46.9, 41.6, 39.8 ppm.

**HRMS** (ESI+) calculated for m/z $[C_{25}H_{24}N_2NaO_6]^+$, $[M+Na]^+$: 471.1527; found 471.1527.

**SFC** (IA (100 × 3 mm, 3 μm), 80:20 $CO_2$:*i*-PrOH, 1.2 mL/min, 35 °C, BPR 150 bar, 210 nm): $t_R$ en1 (minor) 2.69 min; $t_R$ en2 (major) 3.08 min.

**$[\alpha]^{24.6}_D$** –5.45 (c 0.99, $CHCl_3$).

**Dimethyl (*R*)-3-((*R*)-(4-chlorophenyl)(1H-indol-3-yl)methyl)-4-methylenecyclopentane-1,1-dicarboxylate (115m)**

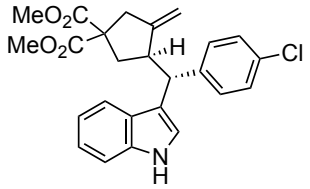

Prepared following general procedure **GP4** using **114m** (17.5 mg, 54.6 μmol, 1.0 equiv) and indole (19.2 mg, 0.16 mmol, 3.0 equiv) as a nucleophile in 1,4-dioxane (1.0 mL, 0.1 M), at 25 °C for 16 h.

The crude product was purified by flash column chromatography ($SiO_2$, CyH/AcOEt 90:10 to 80:20). Compound **115m** was obtained as a white solid (11 mg, 25 μmol, 46% yield, 96:4 *er*).

The absolute configuration was assigned by X-ray crystallography.

**M.p.** = 129 °C.

**$^1$H NMR** (500 MHz, $CDCl_3$) δ 8.11 (s, 1H), 7.47 (dq, *J* = 8.0, 0.8 Hz, 1H), 7.32 (dt, *J* = 8.1, 0.9 Hz, 1H), 7.25 – 7.22 (m, 2H), 7.20 – 7.17 (m, 2H), 7.15 (ddd, *J* = 8.2, 7.0, 1.1 Hz, 1H), 7.12 (d, *J* = 2.4 Hz, 1H), 7.05 (ddd, *J* = 8.0, 7.0, 1.0 Hz, 1H), 4.81 (dt, *J* = 3.0, 1.7 Hz, 1H), 4.18 – 4.08 (m, 2H), 3.72 (s, 3H), 3.63 (s, 3H), 3.46 (dtd, *J* = 10.1, 8.1, 1.9 Hz, 1H), 3.12 (dq, *J* = 15.9, 2.4 Hz, 1H), 2.89 (dq, *J* = 15.9, 1.5 Hz, 1H), 2.75 (ddd, *J* = 13.8, 7.9, 1.6 Hz, 1H), 1.96 (dd, *J* = 13.8, 8.2 Hz, 1H).

**$^{13}$C NMR** (75 MHz, $CDCl_3$) δ 172.3, 172.2, 148.7, 143.0, 136.3, 131.8, 130.0, 128.3, 127.1, 122.3, 121.5, 119.6, 119.3, 118.2, 111.3, 110.5, 58.6, 53.0, 52.9, 47.5, 46.9, 41.8, 39.9 ppm.

**HRMS** (ESI+) calculated for m/z $[C_{25}H_{24}ClNNaO_4]^+$, $[M+Na]^+$: 460.1286; found 460.1296.

**SFC** (OJ (100 × 3 mm, 3 μm), 80:20 $CO_2$:EtOH, 1.2 mL/min, 35 °C, BPR 150 bar, 210 nm): $t_R$ en1 (minor) 1.93 min; $t_R$ en2 (major) 2.43 min.

**$[\alpha]^{24.6}_D$** +2.41 (c 1.59, $CHCl_3$).

**Dimethyl (*R*)-3-((*R*)-(1H-indol-3-yl)(4-methoxyphenyl)methyl)-4-methylenecyclopentane-1,1-dicarboxylate (115n)**

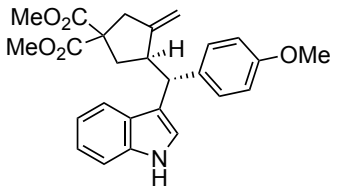


Prepared following general procedure **GP4** using **114n** (20.0 mg, 63.2 μmol, 1.0 equiv) and indole (22.2 mg, 0.19 mmol, 3.0 equiv) as a nucleophile in 1,4-dioxane (1.0 mL, 0.1 M), at 25 °C for 16 h. The crude product was purified by flash column chromatography ($SiO_2$, *n*-pentane/AcOEt 90:10 to 80:20). Compound **115n** was obtained as a colorless oil (24 mg, 55 μmol, 88% yield, 88:12 *er*).

**M.p.** = 50–54 °C.

**$^1$H NMR** (300 MHz, $CDCl_3$) δ 8.07 (bs, 1H), 7.55 (d, *J* = 7.9 Hz, 1H), 7.33 (d, *J* = 8.0 Hz, 1H), 7.27 – 7.20 (m, 2H), 7.19 – 7.10 (m, 2H), 7.10 – 7.03 (m, 1H), 6.84 – 6.72 (m, 2H), 4.83 (s, 1H), 4.19 (s, 1H), 4.14 (d, *J* = 10.3 Hz, 1H), 3.76 (s, 3H), 3.75 (s, 3H), 3.66 (s, 3H), 3.50 (q, *J* = 7.7 Hz, 1H), 3.13 (d, *J* = 15.9 Hz, 1H), 2.91 (d, *J* = 15.9 Hz, 1H), 2.76 (dd, *J* = 13.6, 8.0 Hz, 1H), 1.98 (dd, *J* = 13.6, 8.5 Hz, 1H) ppm.

**$^{13}$C NMR** (75 MHz, $CDCl_3$) δ 172.4, 172.2, 157.9, 149.0, 136.7, 136.3, 129.5, 127.3, 122.1, 121.4, 119.5, 119.5, 119.0, 113.6, 111.2, 110.2, 58.6, 55.3, 52.9, 52.8, 47.3, 47.0, 41.9, 40.0 ppm.

**HRMS** (ESI+) calculated for m/z $[C_{26}H_{27}NNaO_5]^+$, $[M+Na]^+$: 456.1781; found 434.1794.

**SFC** (IG (100 × 3 mm, 3 μm), 80:20 $CO_2$:*i*-PrOH, 1.2 mL/min, 35 °C, BPR 150 bar, 210 nm): $t_R$ en1 (minor) 1.58 min; $t_R$ en2 (major) 2.04 min.

**$[\alpha]^{24.6}_D$** +3.85 (c 1.28, $CHCl_3$).

**Diisopropyl (*R*)-3-((*R*)-(1H-indol-3-yl)(phenyl)methyl)-4-methylenecyclopentane-1,1-dicarboxylate (115o)**

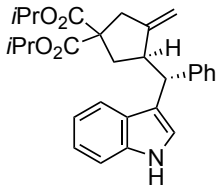


Prepared following general procedure **GP4**, using **114o** (34.2 mg, 0.1 mmol, 1.0 equiv) and indole (35.1 mg, 0.3 mmol, 3.0 equiv) as a nucleophile in 1,4-dioxane (1.0 mL, 0.1 M), at 25 °C for 16 h. The crude product was purified by flash column chromatography ($SiO_2$, CyH/AcOEt 90:10). Compound **115o** was obtained as a colorless oil (44 mg, 96 μmol, 96% yield, 96:4 *er*).

**$^1$H NMR** (300 MHz, $CDCl_3$) δ 8.08 (s, 1H), 7.54 (d, *J* = 7.9 Hz, 1H), 7.37 – 7.28 (m, 3H), 7.25 – 7.18 (m, 2H), 7.17 – 7.07 (m, 3H), 7.07 – 6.98 (m, 1H), 5.06 (hept, 1H), 4.95 (hept, *J* = 6.3 Hz, 1H), 4.78 (s, 1H), 4.17 (d, *J* = 10.3 Hz, 1H), 4.13 (s, 1H), 3.60 – 3.44 (m, 1H), 3.17 – 3.00 (m, 1H), 2.86 (dd, *J* = 15.9, 1.3 Hz, 1H), 2.71 (ddd, *J* = 13.5, 7.8, 1.4 Hz, 1H), 1.95 (dd, *J* = 13.6, 8.5 Hz, 1H), 1.21 (d, *J* = 6.3 Hz, 6H), 1.18 (d, *J* = 6.2 Hz, 3H), 1.09 (d, *J* = 6.3 Hz, 3H) ppm.

**$^{13}$C NMR** (75 MHz, $CDCl_3$) δ 171.4, 171.3, 149.3, 144.5, 136.2, 128.5, 128.1, 127.2, 126.0, 121.9, 121.4, 119.4, 119.3, 118.7, 111.0, 109.7, 68.9, 68.8, 58.5, 47.9, 46.8, 41.7, 39.6, 21.6, 21.5, 21.5 ppm.

**HRMS** (ESI+) calculated for m/z $[C_{29}H_{33}NNaO_4]^+$, $[M+Na]^+$: 482.2302; found 482.2312.

**SFC** (IB-N (100 × 3 mm, 3 μm), 85:15 $CO_2$:MeOH, 1.2 mL/min, 35 °C, BPR 150 bar, 210 nm): $t_R$ en1 (major) 2.14 min; $t_R$ en2 (minor) 2.70 min.

**$[\alpha]^{24.6}_D$** –0.4 (c 1.14, $CHCl_3$).

**Towards the Synthesis of Renifolins**

The preparation of the following complexes has been previously described:[13] (*S*,*S*,*S*,*S*)-**31,** (*S*,*S*,*S*,*S*)-**31'**, **120**, (*S*,*S*)-**122a**, (*S*,*S*)-**122b**, (*S*,*S*)-**123**, (*S*,*S*,*S*,*S*)-**124a**, (*S*,*S*,*S*,*S*)-**124b,** and (*S*,*S*,*S*,*S*)-**125**.

**5-Bromo-2,2-dimethyl-4-(3-methylbut-2-en-1-yl)benzo[*d*][1,3]dioxole (136)**

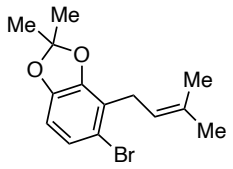


Under an argon atmosphere, DIPA (0.924 mL, 6.55 mmol, 1.5 equiv) was dissolved in 8.6 mL of THF (8.6 mL, 0.5 M) and cooled to -78 °C. *n*BuLi (2.14 M in hexane) (3.06 mL, 6.55 mmol, 1.5 eq.) was added and the solution was stirred at -78 ºC for 1 h. A solution of 5-bromo-2,2-dimethylbenzo[*d*][1,3]dioxole **135** (1.00 g, 4.36 mmol, 1.0 equiv) in 2 mL of THF (0.4 M, final concentration) was slowly added at -78 °C. The mixture was left under magnetic stirring at -78 °C for an additional 30 min. Finally, prenyl bromide (2.6 g, 4.37 mmol, 4.0 equiv) was slowly added dropwise. After 15 min, the cooling bath was removed, and the mixture was allowed to slowly warm up to room temperature. After 4 h, the reaction was quenched by addition of sat. $NH_4Cl$ aqueous solution. The resulting mixture was recovered with AcOEt, and the organic phase was separated, washed with water (x2) and brine (x2), dried over $Na_2SO_4$, filtered, and the volatiles were removed under reduced pressure. The crude was purified by flash column chromatography ($SiO_2$, CyH/AcOEt 95:5). Colorless oil (1.092 g, 3.67 mmol, 84% yield).

**$^1$H NMR** (500 MHz, $CDCl_3$) δ = 6.97 (d, *J* = 8.2 Hz, 1H), 6.48 (d, *J* = 8.3 Hz, 1H), 5.25 (ddq, *J* = 8.6, 5.8, 1.4 Hz, 1H), 3.38 (ddt, *J* = 7.3, 2.1, 1.0 Hz, 2H), 1.81 – 1.76 (m, 3H), 1.72 (q, *J* = 1.3 Hz, 3H), 1.69 (s, 6H) ppm.

**$^{13}$C NMR** (126 MHz, $CDCl_3$) δ = 146.5, 146.4, 132.9, 124.4, 123.1, 120.4, 118.4, 115.0, 107.2, 28.7, 25.8, 25.8, 18.1 ppm.

**HRMS** (APCI+) calculated for $[C_{14}H_{18}BrO_2]^+$, $[M+H]^+$: 297.0485 m/z; found: 297.0486 m/z.

**5-Iodo-2,2-dimethyl-4-(3-methylbut-2-en-1-yl)benzo[*d*][1,3]dioxole (137)**

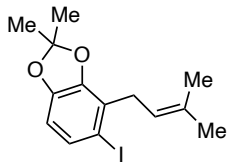


Under an argon atmosphere, **116** (1.1 g, 3.71 mmol, 1.0 equiv) was dissolved in 18.5 mL of THF (0.2 M) and cooled to -78 °C. *n*BuLi (2.36 M in hexane) (2.04 mL, 4.82 mmol, 1.3 equiv) was added and

the solution was stirred at -78 °C for 1 h. Iodine (1.22 g, 4.82 mmol, 1.3 equiv) was added at -78 °C. The cooling bath was removed, and the coloured solution was stirred at room temperature for 4 h. Then the reaction was quenched by addition of sat. $Na_2SO_3$ aqueous solution, the resulting mixture was recovered with AcOEt and the organic phase was separated, washed with water (x2) and brine (x2), dried over $Na_2SO_4$, filtered, and the volatiles were removed under reduced pressure. The crude was purified by flash column chromatography (SiO2, CyH/AcOEt 97:3). Colorless oil (1.12 g, 3.27 mmol, 88% yield).

**$^1$H NMR** (500 MHz, $CDCl_3$) δ = 7.22 (d, *J* = 8.2 Hz, 1H), 6.36 (d, *J* = 8.1 Hz, 1H), 5.20 (hept, *J* = 7.1, 1.4 Hz, 1H), 3.35 (dp, *J* = 7.2, 1.1 Hz, 2H), 1.78 (d, *J* = 1.4 Hz, 3H), 1.70 (q, *J* = 1.4 Hz, 3H), 1.66 (s, 6H) ppm.

**$^{13}$C NMR** (126 MHz, $CDCl_3$) δ = 147.4, 141.9, 132.9, 131.2, 126.0, 120.4, 118.3, 108.3, 88.7, 32.9, 25.9, 25.8, 18.4 ppm.

**HRMS** (ESI+) calculated for *m/z*, $[C_{14}H_{18}IO_2]^+$, $[M+H]^+$: 345.0346; found: 345.0340.

**((2,2-Dimethyl-4-(3-methylbut-2-en-1-yl)benzo[*d*][1,3]dioxol-5-yl)ethynyl)trimethylsilane (138)**

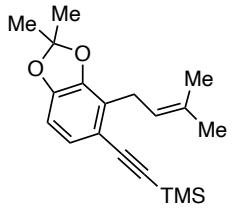


Under an argon atmosphere, a solution of $Pd(PPh_3)_2Cl_2$ (114.7 mg, 0.16 mmol, 0.05 equiv), CuI (62.2 mg, 0.33 mmol, 0.1 equiv) and **137** (1.12 g, 3.27 mmol, 1.0 equivl) in THF (6.5 mL, 0.5 M) was degassed with argon for 10 min. Then, $Et_3N$ (1.37 mL, 9.8 mmol, 3 equib) was added, and the mixture was cooled to 0 °C. Finally, trimethylsilylacetylene (0.51 mL, 3.59 mmol, 1.1 equiv) was added dropwise. The mixture was allowed to slowly warm to room temperature. and left after magnetic stirring for 18 h. Then, the reaction was quenched by addition of water and the organic layer was recovered, washed with water (x2) and brine (x2), dried over $Na_2SO_4$, filtered, and the volatiles were removed under reduced pressure. The crude was purified by flash column chromatography ($SiO_2$, CyH/AcOEt 95:5). Colorless oil (1.0 g, 3.2 mmol, 98 % yield).

**$^1$H NMR** (500 MHz, $CDCl_3$) δ = 6.98 (d, *J* = 8.1 Hz, 1H), 6.53 (d, *J* = 8.0 Hz, 1H), 5.35 (dddd, *J* = 8.7, 5.8, 2.9, 1.4 Hz, 1H), 3.43 (dt, *J* = 7.2, 1.1 Hz, 2H), 1.78 (d, *J* = 1.3 Hz, 3H), 1.71 (q, *J* = 1.3 Hz, 3H), 1.68 (s, 6H), 0.25 (s, 9H) ppm.

**$^{13}$C NMR** (126 MHz, $CDCl_3$) δ = 147.5, 145.1, 132.2, 126.6, 125.3, 121.3, 118.0, 115.6, 106.0, 104.2, 95.2, 27.2, 25.8, 25.7, 18.1, 0.1 ppm.

**HRMS** (ESI+) calculated for *m/z* $[C_{19}H_{27}O_2Si]^+$, $[M+H]^+$: 315.1775; found: 345.1769.

**5-Ethynyl-2,2-dimethyl-4-(3-methylbut-2-en-1-yl)benzo[*d*][1,3]dioxole (133)**

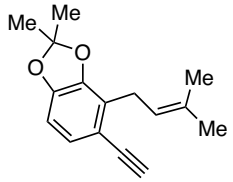

$K_2CO_3$ (0.90 g, 6.54 mmol, 2.05 equiv) was added to a solution of **138** (1.00 g, 3.19 mmol, 1.0 equiv) in MeOH (16.0 mL, 0.2 M) and was left under magnetic stirring at 23 °C for 1h. Then, the reaction was quenched with the addition of water and the mixture was recovered with AcOEt. The organic phase was separated, washed with water (x2) and brine (x2), dried over $Na_2SO_4$, filtered, and the volatiles were removed under reduced pressure. The crude was purified by flash column chromatography ($SiO_2$, CyH/AcOEt 95:5). Yellow oil (727.3 mg, 3.0 mmol, 94% yield).

**$^1$H NMR** (500 MHz, $CDCl_3$) δ = 7.01 (d, *J* = 8.1 Hz, 1H), 6.55 (d, *J* = 8.0 Hz, 1H), 5.32 (ddq, *J* = 8.7, 5.9, 1.4 Hz, 1H), 3.44 (dt, *J* = 7.2, 1.1 Hz, 2H), 3.13 (s, 1H), 1.78 (dd, *J* = 1.3, 0.4 Hz, 3H), 1.71 (q, *J* = 1.4 Hz, 3H), 1.69 (s, 6H) ppm.

**$^{13}$CNMR** (126 MHz, $CDCl_3$) δ = 147.7, 145.5, 132.4, 126.8, 125.6, 121.1, 118.2, 114.5, 106.1, 78.4, 27.1, 25.9, 25.7, 18.0 ppm.

**HRMS** (APCI+) calculated for *m/z* $[C_{16}H_{19}O_2]^+$, $[M+H]^+$: 243.1380 m/z; found: 243.1380 m/z.

**(*S*)-7-(2-(Allyloxy)propan-2-yl)-2,2-dimethyl-6-methylene-7,8-dihydro-6*H*-indeno[4,5-*d*][1,3]dioxole (134a)**

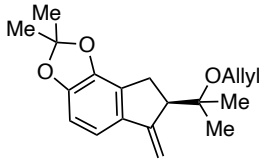

Under an argon atmosphere, a solution of **121** (15.00 mg, 0.062 mmol, 1.0 equiv) in $CH_2Cl_2$ (0.31 mL, 0.2 M) was added to a solution of catalyst (*S,S,S,S*)-**28'** (4.36 mg, 1.86 μmol, 3 mol %) in allyl alcohol (0.31 mL, 0.2 M) at -50 °C. The mixture was left under magnetic stirring at that temperature for 18 h. Then, the reaction was quenched by addition of $Et_3N$ (*ca.* 3 drops), the solvent was removed under reduced pressure and the crude purified by preparative TLC ($SiO_2$, CyH/$CH_2Cl_2$ 80:20). Colorless oil (10.6 mg, 35.3 μmol, 57% yield).

**$^1$H NMR** (500 MHz, $CDCl_3$) δ = 6.97 (d, *J* = 8.0 Hz, 1H), 6.63 (dt, *J* = 8.0, 0.8 Hz, 1H), 5.97 (ddt, *J* = 17.2, 10.5, 5.4 Hz, 1H), 5.48 (dd, *J* = 2.0, 0.6 Hz, 1H), 5.36 – 5.27 (dq, *J* = 10.5, 1.6 Hz, 1H), 5.15 (dq, *J* = 10.4, 1.5 Hz, 1H), 5.11 (d, *J* = 1.7 Hz, 1H), 3.99 (ddt, *J* = 5.4, 4.6, 1.6 Hz, 2H), 3.28 (ddt, *J* = 8.0, 4.1, 1.9 Hz, 1H), 2.98 – 2.94 (m, 2H), 1.71 (s, 3H), 1.69 (s, 3H), 1.29 (s, 3H), 1.03 (s, 3H) ppm.

**$^{13}$C NMR** (126 MHz, $CDCl_3$) δ = 150.0, 147.3, 137.4, 135.8, 125.4, 118.0, 115.8, 112.7, 107.2, 104.6, 62.5, 51.3, 28.9, 25.9, 25.9, 22.7, 22.7 ppm.

**HPLC** Chiralcel OD-H (250 mm x 4.6 mm, 5 μm) at 25 °C, flow 1.0 ml/min, isocratic hexane/*i*PrOH 100:0, 254 nm, $t_R$ (minor) 12.8; $t_R$ (major) 13.6.

**(*S*)-2-(2,2-Dimethyl-6-methylene-7,8-dihydro-6*H*-indeno[4,5-*d*][1,3]dioxol-7-yl)propan-2-ol (134b)**

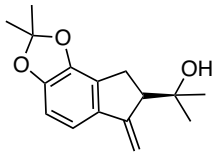


Under an argon atmosphere, catalyst (*S*,*S*,*S*,*S*)-**28'** (14.5 mg, 6.19 μmol, 3 mol %) was added to a suspension of **133** (50.00 mg, 0.206 mmol, 1.0 equiv) in acetone/water (1:1 ratio, 1.04 mL, 0.2 M) cooled to 0 °C, under vigorous magnetic stirring. The mixture was left under magnetic stirring at that temperature for 18 h. Then, the reaction was quenched by addition of $Et_3N$ (*ca.* 3 drops), the solvent was removed under reduced pressure and the crude purified by preparative TLC ($SiO_2$, CyH/AcOEt 85:15). Dark-orange oil (32.8 mg, 126 μmol , 61% yield).

**$^1$H NMR** (500 MHz, $CDCl_3$) δ = 6.98 (d, *J* = 8.0 Hz, 1H), 6.65 (dt, *J* = 8.0, 0.7 Hz, 1H), 5.51 (d, *J* = 1.5 Hz, 1H), 5.11 (d, *J* = 1.3 Hz, 1H), 3.08 – 2.99 (m, 2H), 2.84 – 2.75 (m, 1H), 1.96 (s, 1H), 1.71 (d, *J* = 0.7 Hz, 3H), 1.69 (d, *J* = 0.7 Hz, 3H), 1.24 (s, 3H), 1.05 (s, 3H) ppm.

**$^{13}$C NMR** (126 MHz, $CDCl_3$) δ = 150.3, 147.6, 143.0, 136.8, 125.4, 118.2, 112.9, 107.4, 104.7, 72.7, 55.0, 29.7, 27.4, 25.9, 25.9, 25.3 ppm.

**HRMS** calculated for *m/z* $[M+H]^+$, $[C_{16}H_{20}NaO_3]^+$: 283.1305; found: 283.1308.

**$[\alpha]^{25.9}_D$** -48.7 (c 0.95, $CH_2Cl_2$).

**HPLC** Chiralcel OD-H (250 mm x 4.6 mm, 5 μm) at 25 °C, flow 1.0 ml/min, isocratic hexane/*i*PrOH 98:2, 254 nm, $t_R$ (minor) 8.6; $t_R$ (major) 11.3.

**HTE procedure for the study of the alkoxycylization of 1,6-enyne 133 using different gold(I) catalysts**

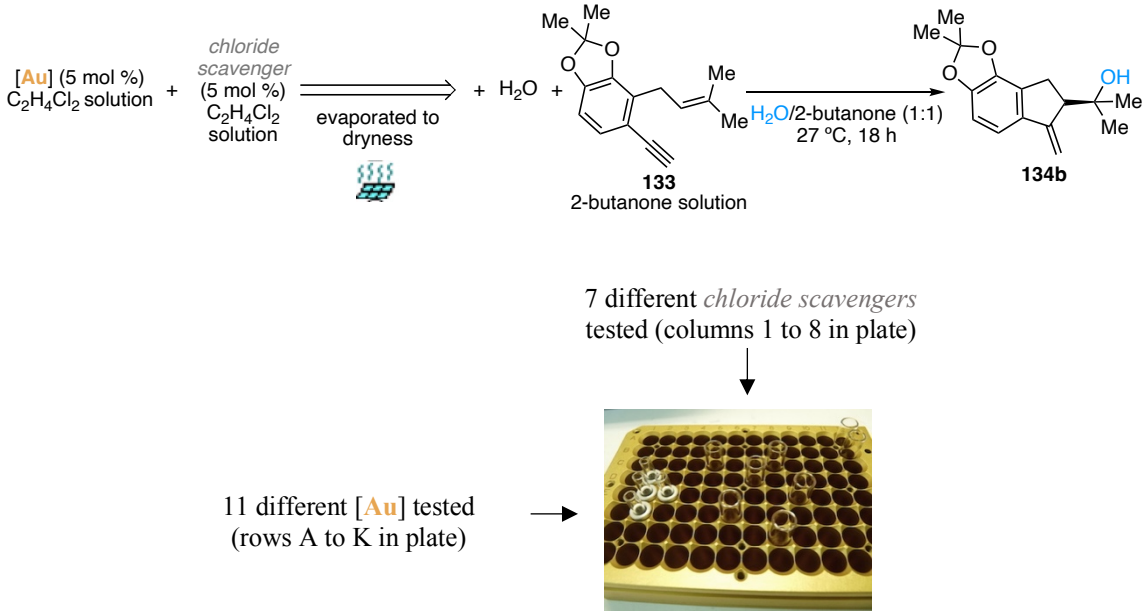


**Scheme S7**. HTE setup for the gold(I)-cavitand complexes and chloride scavenger screening in the alkoxycyclization reaction of 1,6-enyne **133**.

20 µL of a solution of each gold(I) complex in $C_2H_4Cl_2$ (3 mol %) was added to 20 µL of the corresponding scavenger solution (3.75 mol %) to the corresponding 0.75 mL glass vials charged with a parylene-coated stainless-steel micro stir bar, positioned within a 96-well block assembly. The mixture was left under magnetic stirring for 1 h and then the solvent was removed (Genevac EZ-2 apparatus). Then, 20 µL of distilled water was added to the resulting cationic complex formed followed by 20 µL of a solution of **133** in 2-butanone (0.4 M). The resulting mixture was left stirring at 25 °C for 18 hours in a Tumble Stirrer apparatus. The reaction mixture was diluted with 500 µL of a stock solution of internal standard (biphenyl, 0.005 M) and $Et_3N$ (0.002 M). To prepare the samples for UHPLC and SFC analysis, 20 µL of each diluted reaction solution was transferred to a 96-well analysis plate containing 500 µL of $CH_3CN$ in each well.

**Table S3**. High-throughput screening of solvents for the gold(I)-catalyzed alkoxycyclization of 1,6-enyne **133**, **134b** yield (%) shown.[a]

| | | 1 | 2 | 3 | 4 | 5 | 6 | 7 | 8 | 9 |
|---|---|---|---|---|---|---|---|---|---|---|
| | | **$AgSbF_6$** | **$AgNTf_2$** | **$NaBAr^F$** | **$NaSbF_6$** | **AgOTf** | **Ag G** | **Ag K** | **Ag C** | **none** |
| A | (*R*)-**80** | 16 | 18 | 30 | 3 | 9 | | | | |
| B | (*S*,*S*)-**141** | 72 | 31 | 62 | >99 | >99 | | | | |
| C | (*S*,*S*)-**142** | 63 | 26 | 74 | 13 | 32 | | | | |
| D | (*S*,*S*,*S*,*S*)-**143a** | 61 | 32 | 59 | 16 | 43 | | | | |
| E | (*S*,*S*,*S*,*S*)-**143b** | 72 | 76 | 41 | 72 | 86 | | | | |
| F | (*S*,*S*,*S*,*S*)-**28'** | 83 | 34 | 26 | 66 | 81 | | | | |
| G | **Au A** | | | | | | 18 | 6 | 16 | |
| H | **Au B** | | | | | | 51 | 25 | 7 | |
| I | **Au C** | | | | | | 30 | 17 | 1 | |
| J | (*S*,*S*,*S*,*S*)-**144** | | | | | | | | | 20 |
| K | *control* | *n.r.* | *n.r.* | *n.r.* | *n.r.* | *n.r.* | | | | |

[a] Product yields calculated using biphenyl as internal standard in the UHPLC. C18 column (1.7 µm, 2.1 x 50 mm), $H_2O$:$CH_3CN$ (+0.1% formic acid), gradient method (90:10 for 1 min, then increasing to 2:98 over 1.4 min, hold at 2:98 for 2.4 min, then decreasing to 90:10 over 0.6 min), 0.5 mL/min, T = 35 ºC, PDA 200 – 400 nm. Biphenyl (1.16 min), **133** (2.36 min), **134b** (1.98 min). Color code: ≥ 70%, dark green; 50–69%, olive green; < 50% dark red; grey (*n.r.*) = no reaction.

**Table S4.** High-throughput screening of solvents for the gold(I)-catalyzed alkoxycyclization of 1,6-enyne **133**, **134b** *er* (%) shown.[a]

| | | 1 | 2 | 3 | 4 | 5 | 6 | 7 | 8 | 9 |
|---|---|---|---|---|---|---|---|---|---|---|
| | | **$AgSbF_6$** | **$AgNTf_2$** | **$NaBAr^F$** | **$NaSbF_6$** | **AgOTf** | **Ag G** | **Ag K** | **Ag C** | **none** |
| A | (*R*)-**80** | 51:49 | 51:49 | 51:49 | 53:47 | 50:50 | | | | |
| B | (*S*,*S*)-**141** | 52:48 | 52:48 | 51:49 | 51:49 | 51:49 | | | | |
| C | (*S*,*S*)-**142** | 83:17 | 84:16 | 81:19 | 81:19 | 84:16 | | | | |
| D | (*S*,*S*,*S*,*S*)-**143a** | 36:64 | 36:64 | 36:64 | 39:61 | 37:63 | | | | |
| E | (*S*,*S*,*S*,*S*)-**143b** | 80:20 | 80:20 | 78:22 | 79:21 | 79:21 | | | | |
| F | (*S*,*S*,*S*,*S*)-**28'** | 80:20 | 77:23 | 77:23 | 80:20 | 77:23 | | | | |
| G | **Au A** | | | | | | 54:46 | 44:56 | 53:47 | |
| H | **Au B** | | | | | | 47:53 | 47:53 | 45:55 | |
| I | **Au C** | | | | | | 50:50 | 48:52 | 50:50 | |
| J | (*S*,*S*,*S*,*S*)-**144** | | | | | | | | | 51:49 |
| K | *control* | *n.r.* | *n.r.* | *n.r.* | *n.r.* | *n.r.* | | | | |

[a] *er* determined by SFC on chiral stationary phase. IB column (150 × 4.6 mm, 3 μm), $CO_2$:IPA gradient method (100:0 for 1 min, then increasing to 60:40 over 5 min, hold for 1 min at 60:40, then decreasing to 100:0 over 0.25 min and hold for 1.25 min), 3.0 mL/min, T = 35 °C, ABPR 150 bar, 230 nm): biphenyl (2.7 min), **133** ( 1.77 min), **134b** en1 (3.0 min), **134b** en2 (3.07 min). Color code: ≥ 90:10, electric blue; 75:25 – 90:10, violet; < 75:25, cyan; grey (*n.r.*)= no reaction.

## Crystallographic Data

### *tert*-Butyl ((2*S*)-1-(1,4-Dihydro-1,4-epiminonaphthalen-9-yl)-3-methyl-1-oxobutan-2-yl)carbamate (51c)

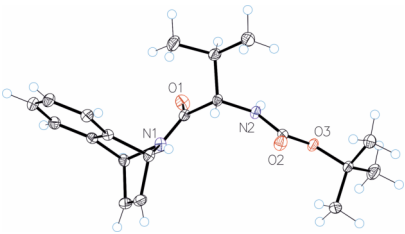


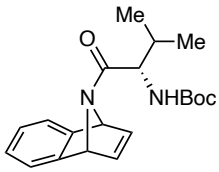


**Table S7**. Crystal data and structure refinement for **51c**.

| | |
|---|---|
| Identification code | mo_GO-1-259_0m_a |
| Empirical formula | $C_{20}H_{26}N_2O_3$ |
| Formula weight | 342.43 |
| Temperature/K | 99.68 |
| Crystal system | monoclinic |
| Space group | $P2_1$ |
| a/Å | 12.7261(10) |
| b/Å | 5.9276(5) |
| c/Å | 13.1305(11) |
| α/° | 90 |
| β/° | 108.380(2) |
| γ/° | 90 |
| Volume/Å$^3$ | 939.97(13) |
| Z | 2 |
| $\rho_{calc}$g/cm$^3$ | 1.210 |
| μ/mm$^{-1}$ | 0.081 |
| F(000) | 368.0 |
| Crystal size/mm$^3$ | 0.3 × 0.2 × 0.1 |
| Radiation | MoKα (λ = 0.71073) |
| 2Θ range for data collection/° | 3.372 to 63.23 |
| Index ranges | -18 ≤ h ≤ 18, -7 ≤ k ≤ 8, -15 ≤ l ≤ 19 |
| Reflections collected | 11715 |
| Independent reflections | 5420 [$R_{int}$ = 0.0426, $R_{sigma}$ = 0.0506] |
| Data/restraints/parameters | 5420/1/231 |
| Goodness-of-fit on F$^2$ | 1.038 |
| Final R indexes [I>=2σ (I)] | $R_1$ = 0.0399, $wR_2$ = 0.1053 |
| Final R indexes [all data] | $R_1$ = 0.0425, $wR_2$ = 0.1075 |
| Largest diff. peak/hole / e Å$^{-3}$ | 0.37/-0.20 |
| Flack parameter | 0.3(6) |

**Complex (*R*)-80**

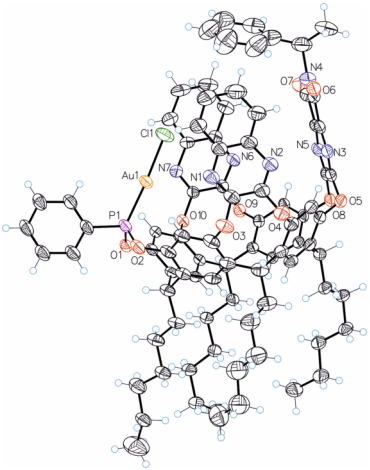


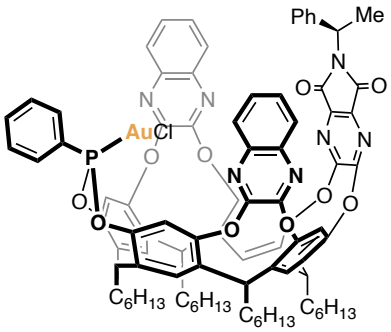


**Table S8**. Crystal data and structure refinement for complex (*R*)-**80**.

| | |
|---|---|
| Identification code | mo_GO1219_0m |
| Empirical formula | $C_{93.5}H_{97.51}AuCl_4N_7O_{10}P$ |
| Formula weight | 1849.03 |
| Temperature/K | 100.02 |
| Crystal system | triclinic |
| Space group | P-1 |
| a/Å | 11.6946(8) |
| b/Å | 14.2374(12) |
| c/Å | 28.029(2) |
| α/° | 101.572(2) |
| β/° | 93.758(2) |
| γ/° | 110.656(3) |
| Volume/Å$^3$ | 4230.5(6) |
| Z | 2 |
| $\rho_{calc}$g/cm$^3$ | 1.452 |
| μ/mm$^{-1}$ | 1.949 |
| F(000) | 1899.0 |
| Crystal size/mm$^3$ | 0.5 × 0.4 × 0.02 |
| Radiation | MoKα (λ = 0.71073) |
| 2Θ range for data collection/° | 3 to 54.384 |
| Index ranges | -11 ≤ h ≤ 14, -17 ≤ k ≤ 14, -35 ≤ l ≤ 35 |
| Reflections collected | 58923 |
| Independent reflections | 18040 [$R_{int}$ = 0.0854, $R_{sigma}$ = 0.0712] |
| Data/restraints/parameters | 18040/614/1214 |
| Goodness-of-fit on F$^2$ | 1.036 |
| Final R indexes [I>=2σ (I)] | $R_1$ = 0.0580, $wR_2$ = 0.1461 |
| Final R indexes [all data] | $R_1$ = 0.0835, $wR_2$ = 0.1613 |
| Largest diff. peak/hole / e Å$^{-3}$ | 1.36/-1.64 |

**Complex Au C (CCDC-2266408)**

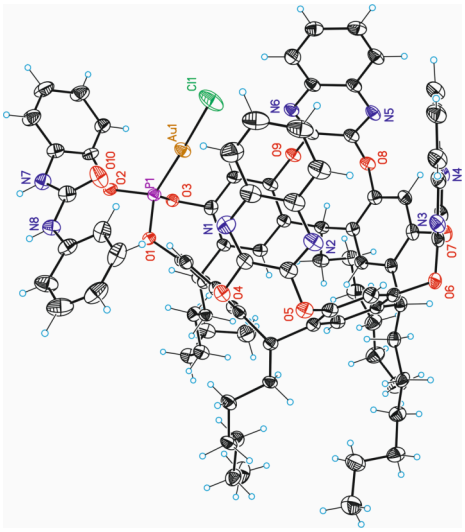

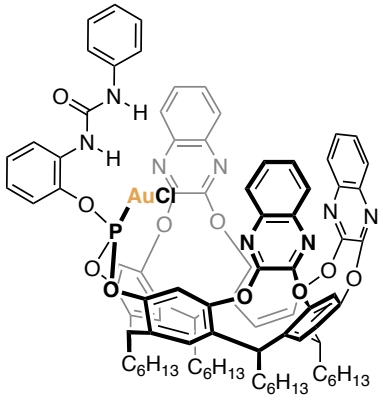


**Table S9**. Crystal data and structure refinement for complex **Au C**.

| | |
|---|---|
| Identification code | GO312LT_C2c |
| Empirical formula | $C_{96.70}H_{97.55}AuClN_{11.85}O_{10}P$ |
| Formula weight | 1849.10 |
| Temperature/K | 100(2) |
| Crystal system | monoclinic |
| Space group | C 2/c |
| a/Å | 35.9742(6) |
| b/Å | 13.3931(2) |
| c/Å | 40.3962(7) |
| α/° | 90 |
| β/° | 114.898(2) |
| γ/° | 90 |
| Volume/Å$^3$ | 17654.2(6) |
| Z | 8 |
| $\rho_{calc}$g/cm$^3$ | 1.391 |
| μ/mm$^{-1}$ | 1.782 |
| F(000) | 7614 |
| Crystal size/mm$^3$ | 0.500 x 0.500 x 0.400 |
| 2Θ range for data collection/° | 3.352 to 32.452 |
| Index ranges | -53<=h<=52,-20<=k<=19,-59<=l<=48 |
| Reflections collected | 149847 |
| Independent reflections | 29372[R(int) = 0.0782] |
| Data/restraints/parameters | 29372/ 833/ 1315 |
| Goodness-of-fit on F$^2$ | 1.079 |
| Final R indexes [I>=2σ (I)] | R1 = 0.0681, wR2 = 0.1612 |
| Final R indexes [all data] | R1 = 0.0957, wR2 = 0.1727 |
| Largest diff. peak/hole / e Å$^{-3}$ | 6.063 and -2.493 |

**Dimethyl (*R*)-3-((*R*)-(4-chlorophenyl)(1H-indol-3-yl)methyl)-4-methylenecyclopentane-1,1-dicarboxylate (115m) (CCDC-2266406)**

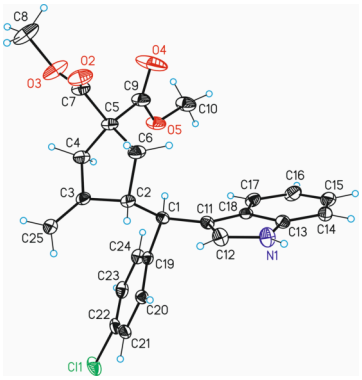


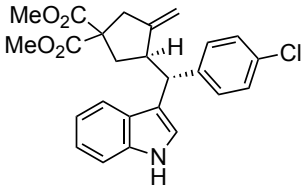


**Table S8**. Crystal data and structure refinement for for **115m**.

| | |
|---|---|
| Identification code | AMZ-04-364 |
| Empirical formula | $C_{25}H_{24}ClNO_4$ |
| Formula weight | 437.90 |
| Temperature/K | 100(2) |
| Crystal system | orthorhombic |
| Space group | P 21 21 21 |
| a/Å | 7.85740(13) |
| b/Å | 12.4594(2) |
| c/Å | 22.5242(4) |
| α/° | 90 |
| β/° | 90 |
| γ/° | 90 |
| Volume/Å$^3$ | 2205.07(7) |
| Z | 4 |
| $\rho_{calc}$g/cm$^3$ | 1.391 |
| μ/mm$^{-1}$ | 0.205 |
| F(000) | 920 |
| Crystal size/mm$^3$ | 0.200 x 0.100 x 0.050 |
| 2Θ range for data collection/° | 1.808 to 32.372 |
| Index ranges | -11<=h<=11,-18<=k<=18,-33<=l<=32 |
| Reflections collected | 49017 |
| Independent reflections | 7510[R(int) = 0.0301] |
| Data/restraints/parameters | 7510/ 0/ 285 |
| Goodness-of-fit on F$^2$ | 1.060 |
| Final R indexes [I>=2σ (I)] | R1 = 0.0314, wR2 = 0.0824 |
| Final R indexes [all data] | R1 = 0.0344, wR2 = 0.0840 |
| Largest diff. peak/hole / e Å$^{-3}$ | 0.361 and -0.169 |

UNIVERSITAT ROVIRA I VIRGILI
Novel Supramolecular Gold(I)-Cavitand Catalysts and Approach to the Total Synthesis of Monomarginine
Gala Ogalla Estévez

# Chapter II: *Towards the Total Synthesis of Monomarginine*

UNIVERSITAT ROVIRA I VIRGILI
Novel Supramolecular Gold(I)-Cavitand Catalysts and Approach to the Total Synthesis of Monomarginine
Gala Ogalla Estévez

## Introduction

### Gold Catalysis in Total Synthesis

The total synthesis of natural products often involves the construction of complex structures in very specific manners to achieve selective results. Methodologies that involve gold catalysis has been used in several examples over the last years, with strategies that emphasize the role of gold-catalyzed reactions.[1]

Different gold-catalyzed reactions have been reported for the preparation of natural products. For instance, a gold(I) catalyzed oxidative cyclization reaction was the key-step to afford the first enantioselective total synthesis of (–)-nardoaristolone B (Scheme 1). By using 1,5-enyne **1** and 3,5-dichloropyridine *N*-oxide **2** as the oxidant, the cycloisomerized product **3** was formed in 74% yield, which was followed by an allylic oxidation to afford the natural product.[2]

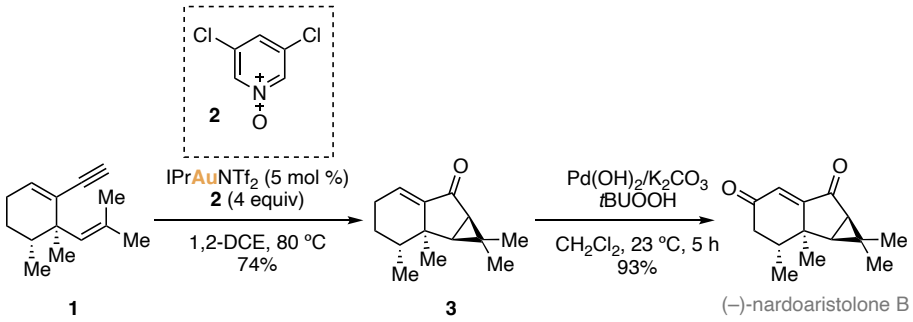


**Scheme 1**. Total synthesis of (–)-nardoaristolone B *via* gold(I)-catalyzed oxidative cyclization strategy.

Another interesting example of gold(I) catalysis is the of polyene cyclization, which happen in a cascade manner upon activation of the alkyne moiety, which initiates the cyclization process.[3] In 2009, Michelet reported the cascade phenoxycyclization reaction of 1,5-enyne **4** catalyzed by $PPh_3AuNTf_2$ under mild conditions (Scheme 2, top). Our group extended the methodology to the formation of up to four C–C

1 For selected reviews on the topic see: (a) Pflästerer, D.; Hashmi, A. S. K. Gold Catalysis in Total Synthesis – Recent Achievements, *Chem. Soc. Rev.* **2016**, *45*, 1331–1367. (b) Mayans, J. G.; Armengol-Relats, H.; Calleja, P.; Echavarren, A. M. Gold(I)-Catalysis for the Synthesis of Terpenoids: From Intramolecular Cascades to Intermolecular Cycloadditions, *Isr. J. Chem.* **2018**, *58*, 639–658. (c) Gu, Y.; Tan, C.; Gong, J.; Tany, Z. Diversity-Oriented Synthesis of Natural Products *via* Gold-Catalyzed Cascade Reactions, *Synlett* **2018**, *29*, 1552–1571. (d) De, S.; Dan, A. K.; Sahu, R.; Parida, S.; Das, D. Total Synthesis of Natural Products Using Gold Catalysis, *Chem. Asian J.* **2022**, *17*, e202200896.

2 Homs, A.; Muratore, M. E.; Echavarren, A. M. Enantioselective Total Synthesis of (−)-Nardoaristolone B via a Gold(I)-Catalyzed Oxidative Cyclization, *Org. Lett.* **2015**, *17*, 461–463.

3 (a) Toullec, P. Y.; Blarre, T.; Michelet, V. Mimicking Polyolefin Carbocyclization Reactions: Gold-Catalyzed Intramolecular Phenoxycyclization of 1,5-Enynes, *Org. Lett.* **2009**, *11*, 2888–2891. (b) Rong, Z.; M. Echavarren, A. Broad Scope Gold(I)-Catalysed Polyenyne Cyclisations for the Formation of up to Four Carbon–Carbon Bonds, *Org. Biomol. Chem.* **2017**, *15*, 2163–2167.

bonds and showed the application to polycyclic bromoalkynes, which could be further functionalized. For example, tetracycle **7** was obtained by cyclization of bromide substituted tetraenyne **6** through a cascade nucleophilic attack after the formation of the corresponding cyclopropyl gold(I) carbene (Scheme 2, bottom).

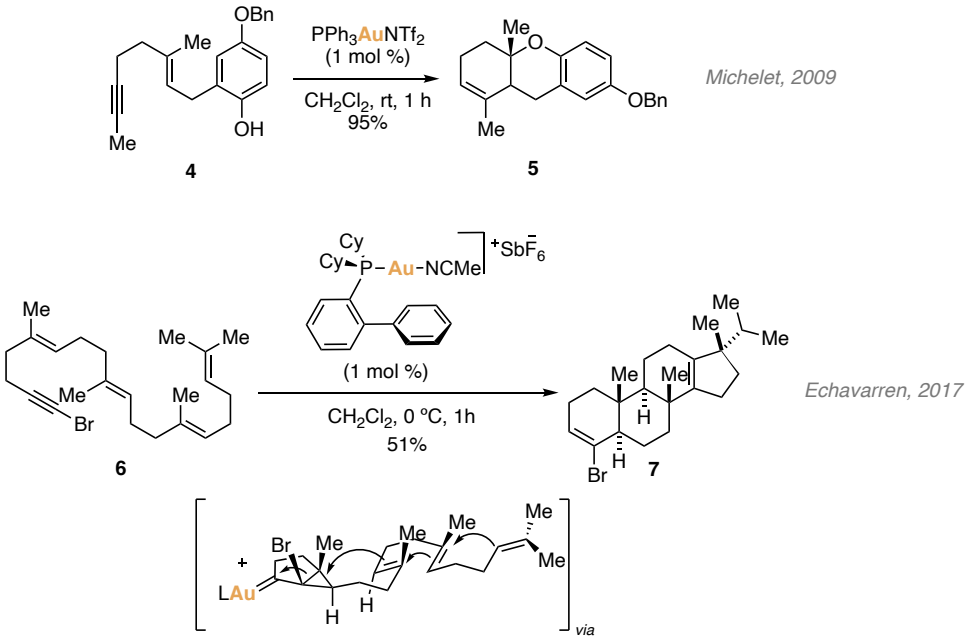


**Scheme 2**. Examples for polyenyne cyclizations catalyzed by gold.

Several terpenoids have been synthesized *via* gold catalysis. [4] For instance, by ring-expanding cycloisomerization methodologies[4a,c] or tandem reactions.[4b] More recently in our group, the sesquiterpene waitziacuminone was synthesized.[5] In this case, the use of acetylene gas, formed *in situ* from calcium carbide and water, in a gold(I) catalyzed reaction with geranyl acetone to form the natural product in one single step (Scheme 3).

4 (a) Sethofer, S. G.; Staben, S. T.; Hung, O. Y.; Toste, F. D. Au(I)-Catalyzed Ring Expanding Cycloisomerizations: Total Synthesis of Ventricosene, *Org. Lett.* **2008**, *10*, 4315. (b) Shi, H.; Fang, L.; Tan, C.; Shi, L.; Zhang, W.; Li, C.; Luo, T.; Yang, Z. Total Syntheses of Drimane-Type Sesquiterpenoids Enabled by a Gold-Catalyzed Tandem Reaction, *J. Am. Chem. Soc.* **2011**, *133*, 14944–14947. (c) Zheng, H.; Felix, R. J.; Gagné, M. R. Gold-Catalyzed Enantioselective Ring-Expanding Cycloisomerization of Cyclopropylidene Bearing 1,5-Enynes, *Org. Lett.* **2014**, *16*, 2272–2275.

5 Scharnagel, D.; Escofet, I.; Armengol-Relats, H.; de Orbe, M.E.; Korber, J. N.; Echavarren, A. M. Acetylene as a Dicarbene Equivalent for Gold(I) Catalysis: Total Synthesis of Waitziacuminonein One Step. *Angew. Chem., Int. Ed.* **2020**, *59*, 4888−4891.

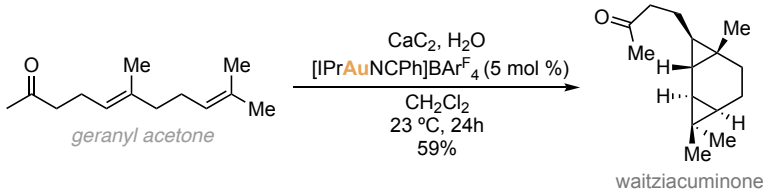


**Scheme 3**. Total synthesis of waitziacuminone using acetylene gas in a gold(I)-catalyzed system.

Finally, one last selected example is the 8-*endo-dig* hydroarylation as a key step in the synthesis of lundurines A–C (Scheme 4).[6]

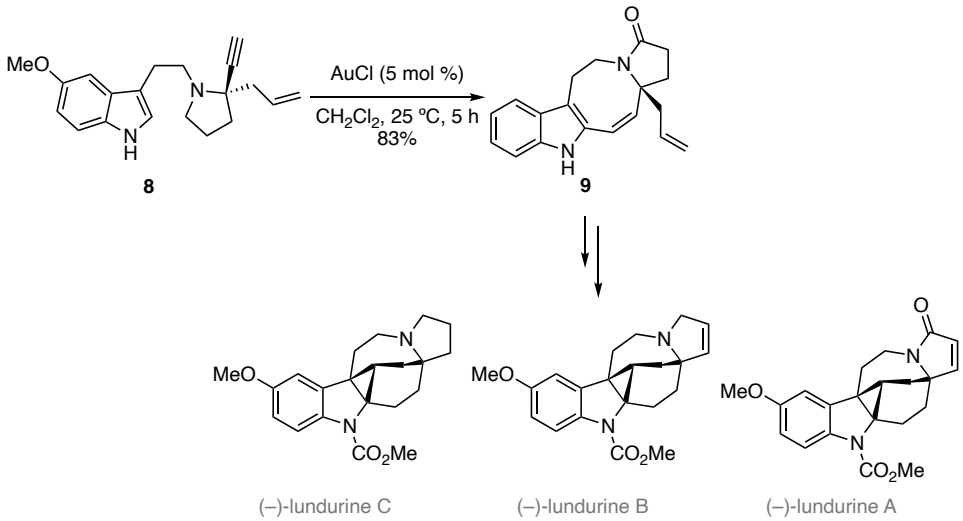


**Scheme 4**. Gold(I)-catalyzed hydroarylation of alkyne **8** for achieving common building block **9** for the total synthesis of lundurine A–C.

**Monocarpia Marginalis Species**

Malayan Annonaceae species, commonly known as the "custard apple family", is a group of flowering plants that includes trees, shrubs, and lianas. These plants are known for exhibiting a wide variety of pharmacological properties. Particullarly, *Monocarpia* is known to be represented in the family by a single known species, *Monocarpia marginalis*. This species belongs to a small genus of trees in the Annonaceae family, confined to the Malay Peninsula (Peninsular Thailand and Peninsular Malaysia), and the islands of Sumatra and Borneo (Figure 1, left).[7]

6 Kirillova, M. S.; Muratore, M. E.; Dorel, R.; Echavarren, A. M. Concise Total Synthesis of Lundurines A–C Enabled by Gold Catalysis and a Homodienyl Retro-Ene/Ene Isomerization, *J. Am. Chem. Soc*. **2016**, *138*, 3671–3674.

7 Turner, I. M. A New Combination in Momocarpia (Annonaceae), *Edinb. J. Bot.* **2012**, *69*, 95–98.


**Figure 1**. Georeferenced records for *Monocarpia marginalis* (left)[8] and *Monocarpia marginalis* sample extracted (right).[9]

In 1993, Guittet's group reported the isolation and identification of **10a**, an orange solid compound assigned as monomargine.[10a] Subsequently, in 2008, Kam's group published the isolation of an analogous tetracyclic lactam **10b** from the same species, as a red amorphous solid, which was named as monomarginine.[10b] Both compounds were isolated from the bark of *Monocarpia marginalis* (Figure 2). Formally, structure **10b** derives from the introduction of a methoxy group into structure **10a** at the C4 position.

Monomargine was described to be a weak inhibitor of topoisomerase I at 10 μg/mL, and both were cytotoxic towards drug-sensitive and vincristine-resistant human KB (VJ300) cells and Jurkat cells (monomargine with $IC_{50}$ 4.7, 3.0 and 0.7 μg/mL, and monomarginine with $IC_{50}$ 4.0, 2.6 and 0.4 μg/mL).[10]

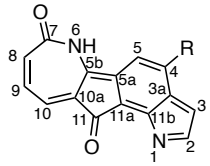


**10a**, R = H; *Assigned as monomargine in 1993*
**10b**, R = OMe; *Assigned as monomarginine in 2008*

**Figure 2**. Initial assigned structures for monomargine **10a** and monomarginine **10b**.

8 Data from the Global Biodiversity Information Facility.

9 From The New York Botanical Garden.

10 (a) Mahmood, K.; Païs, M.; Fontaine, C.; Ali, H. M.; Hamid, A.; Hadi, A.; Guittet, E. Monomargine, a Nitrogenous Cytotoxic Pigment from Monocarpia Marginalis, *Tetrahedron Lett.* **1993**, *34*, 1795–1796. (b) Lim, S.-H.; Mahmood, K.; Komiyama, K.; Kam, T.-S. A Cycloartane Incorporating a Fused Tetrahydrofuran Ring and a Cytotoxic Lactam from *Monocarpia Marginalis*, *J. Nat. Prod.* **2008**, *71*, 1104–1106.

The structure assignments were based mainly on 2D NMR analysis, which relied on the $^{1}H–^{13}C$ correlations pictured in Figure 3. Guittet's report was first relying on the molecular formula $C_{15}H_8N_2$, established by the high-resolution mass spectrometry. Additionally, they observed two absortion bands on the IR spectra at 1643cm$^{-1}$ and 1611 cm$^{-1}$, attributed to the presence of conjugated carbonyl functional groups (Figure 3a, **10a**). They first suggested that the proton observed at δ 13.00 ppm corresponded to an amide NH, based on the HMBC correlation with a carbonyl group at δ 164.5 ppm in the $^{13}C$ NMR (Figure 3c, **10a**). Additionally, they argued that the seven remaining protons at low field, between δ 9.2 and 7.2 ppm, corresponded to a highly conjugated system involving the second nitrogen atom. Analysing the HMBC spectrum, combined with the multiplicity and the chemical shifts observed in the $^{1}H$ NMR, they envisioned the amide as a part of a seven membered ring, including the C8-C10a dienic system (Figure 3b and 3c, **10a**).[10a] On the other side, in 2008, Kam's research reported the structure of **10b**, which relied on the previous observations by the group of Guttiet. The IR spectrum has three key absortions, one at 3434 cm$^{-1}$, attributed to secondary amide and two related to carbonyl functions, at 1639 and 1606 cm$^{-1}$, respectively (Figure 3a, **10b**). To specify the methoxy position in the structure, based on the HMBC correlation data, they assigned it bonded at the C4 position (observing three-bond correlations from H-C5 to C3a, C5b, C11a and from MeO to C4 (δ 150.0 ppm) (Figure 3c, **10b**).[10b]

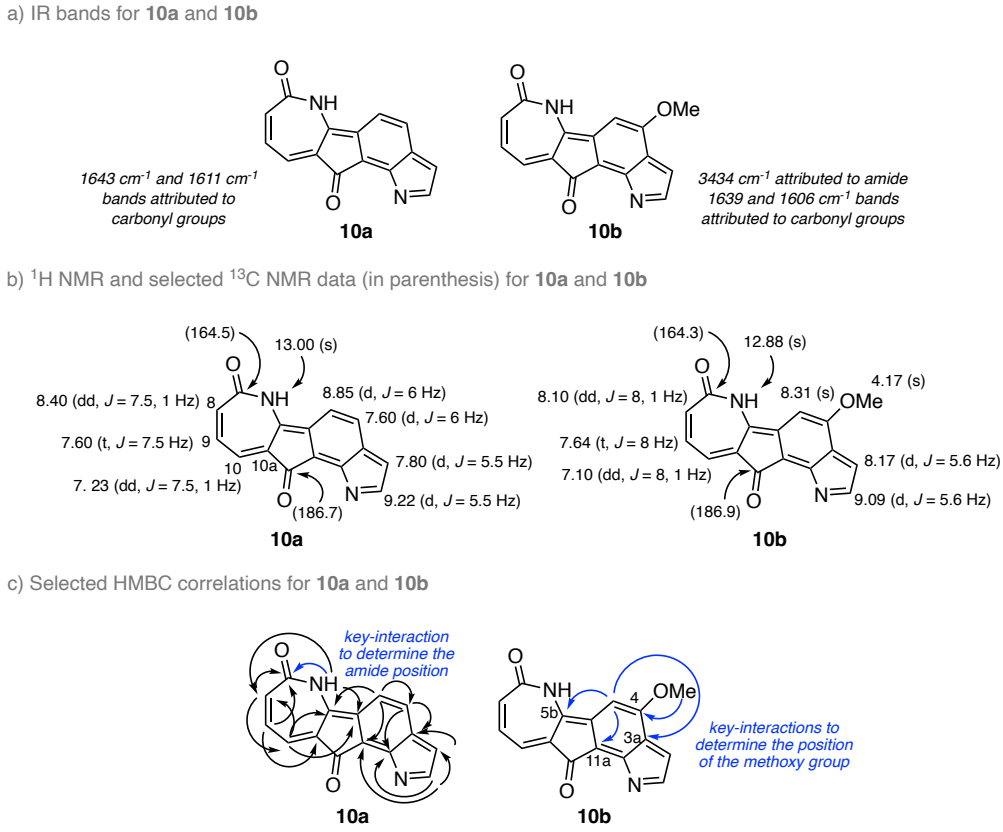


**Figure 3**. Selected data reported for **10a** and **10b**. HMBC correlations are shown from H to C.

## Objectives

The objective of the research summarized in this chapter starts with the structure revision of monomarginine, a natural product belonging to the Malayan Annonaceae species, isolated from *Monocarpia marginalis*. Then, the objective focused on the development of a methodology for the synthesis of this natural product. A gold(I)-catalyzed cyclization to form the azaanthraquinone core present in the skeleton of the structure was envisioned as a possible methodology.[11]

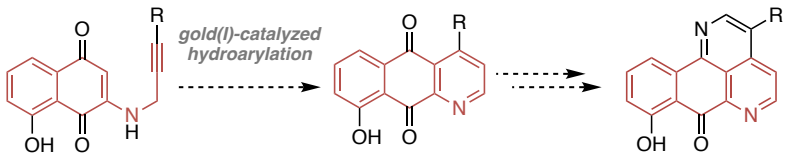


**Scheme 5**. Construction of azaanthraquinone core *via* a gold(I)-catalyzed cyclization.

11 Part of the experiments described in this section were performed jointly with Dr. Marc Paul Beller and were based upon preliminary work done in collaboration with Dr. Eduardo García Padilla.

## Results and Discussion

### Structure Elucidation

Methods for elucidating complex structures have advanced significantly due to the availability of high-field NMR magnets, cryogenic probes, and sophisticated two-dimensional pulse sequences, establishing NMR spectroscopy as the leading technique for structure determination.[12] One example is a case study reported by Herzon's group in 2023, focusing on secondary metabolites compounds and detailing the process of their structure determination.[13]

In this context, despite the mentioned reports in literature regarding monomarginine,[10] we were convinced that the assignment of its structure was wrong. For instance, we envisioned that structures such as **11a** or **11b**, containing an indole moiety would be more likely than **10b** monomarginine (Figure 4). Nonetheless, the structure elucidation was challenging owing to the high degree of unsaturation, with nine quaternary carbons in the molecule.

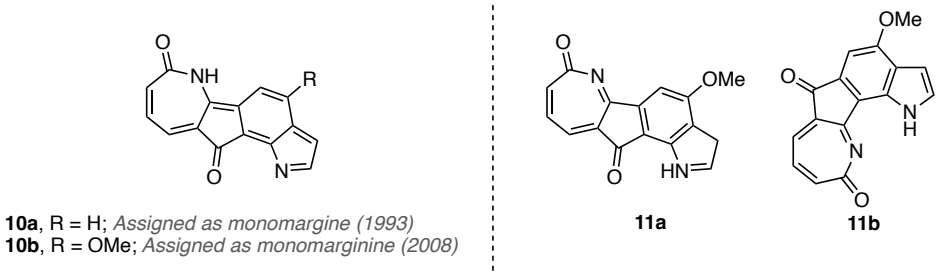


**Figure 4**. Proposed possible structures before reassignment.

Fortunately, we were pleased to receive 1.1 mg sample of monomarginine from the isolation team in Malaysia (Kam's group),[10b] who generously provided it for our study. We initiated our work with an in-depth NMR analysis of the molecule: the $^{1}H$, $^{13}C$ NMR, DEPT, GOESY as well as two-dimensional analysis (COSY, NOESY, HSQC, HMBC) were performed on a 500 MHz cryoprobe spectrometer.[14] The $^{1}H$ and $^{13}C$ NMR spectra were aligned with those reported, with minor variations likely attributed to differences in solution concentration or equipment. Regarding the two-dimensional spectra, some differences were noted (which will be addressed later in the chapter). However, the structure was only confirmed later when crystals of the molecule were obtained from the recovered NMR sample, revealing its complete framework, which is very different from that originally proposed (Figure 5).

12 Reynolds, W. F. In *Pharmacognosy*; Badal, S.; Delgoda, R., Eds.; Academic Press: Boston, **2017**; Chapter 29, *567*.

13 DiBello, M.; Healy, A. R.; Nikolayevskiy, H.; Xu, Z.; Herzon, S. B. Structure Elucidation of Secondary Metabolites: Current Frontiers and Lingering Pitfalls, *Acc. Chem. Res.* **2023**, *56*, 1656–1668.

14 For detailed on all the NMR spectras, see the experimental section of this chapter.

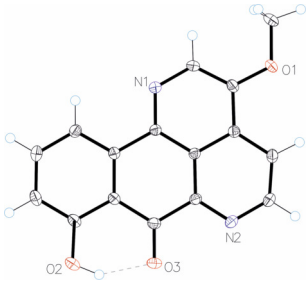


**Figure 5**. X-Ray structure of monomarginine **12**.

With this information in hand, we were able to fully compare both structures **10b** and **12** in detail, and specify the signals observed by NMR (Table 1).

**Table 1**. Comparison of $^{1}H$ and $^{13}C$ NMR shifts between the reported and the measured sample of monomarginine **12**.

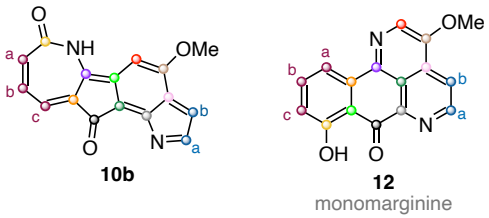


| Position | Reported $^{1}H$ NMR[a] | Measured $^{1}H$ NMR[b] | Reported $^{13}C$ NMR[a] | Measured $^{13}C$ NMR[b] |
|---|---|---|---|---|
| OMe | 4.17 (s) | 4.19 (s) | 56.7 | 57.7 |
| a | 9.09 (d, $J$ = 5.6 Hz) | 9.14 (d, $J$ = 5.5 Hz) | 148.1 | 148.1 |
| b | 8.17 (d, $J$ = 5.6 Hz) | 8.25 (d, $J$ = 5.6 Hz) | 119.2 | 119.3 |
| | - | - | 131.5 | 131.6 |
| | - | - | 150.0 | 150.0 |
| | 8.31 (s) | 8.41 (s) | 127.1 | 127.5 |
| | - | - | 116.1 | 116.3 |
| | - | - | 142.6 | 143.0 |
| NH | 12.88 (s) | - | - | - |
| | - | - | 164.3 | 164.4 |
| a | 8.10 (dd, $J$ = 8, 1 Hz) | 8.20 (dd, $J$ =7.7, 1 Hz) | 116.2 | 116.2 |
| b | 7.64 (t, $J$ = 8 Hz) | 7.69 (t, $J$ = 8.1 Hz) | 137.8 | 137.8 |
| c | 7.10 (dd, $J$ = 8, 1 Hz) | 7.14 (dd, $J$ = 8.4, 1.1 Hz) | 119.8 | 119.8 |
| | - | - | 135.7 | 136.2 |
| | - | - | 186.9 | 187.1 |
| | - | - | 119.6 | 119.8 |
| | - | - | 147.2 | 147.4 |
| OH | - | 12.93 (s) | - | - |

Chemical shifts given in ppm and solvent used $CDCl_3$. [a] Characterization data was carried out in a 400 MHz equipment for $^{1}H$ NMR and in a 100 MHz for $^{13}C$ NMR.[10b] [b] Characterization data was carried out in a 500 MHz equipment for $^{1}H$ NMR and in a 126 MHz for $^{13}C$ NMR.

Having the confirmed structure, rationalization of the HMBC interactions could be performed for the observed interaction signals in 2008[10b] and the ones we detected in our studies for **12**. Some HMBC key-interactions that reveal the main differences between the analogous structures are shown in Figure 6.

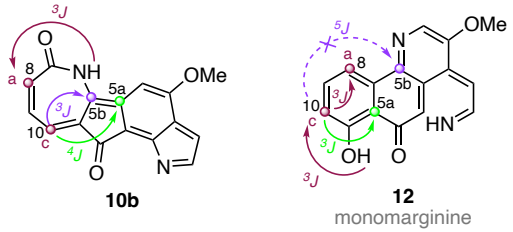


**Figure 6**. Selected HMBC key-interactions for **10b** and monomarginine **12**. Correlations are shown from H to C. The color of each arrow corresponds to the color of the carbon atom receiving the interaction. Full arrows are for correlations reported (for **10b**)[10b] or observed (for **12)**, while dashed arrows have not been observed.

On one side, the $^{3}J_{NH–C8}$ in **1b**, resulted to be $^{3}J_{OH–C10}$ coupling in **12** (Figure 7).

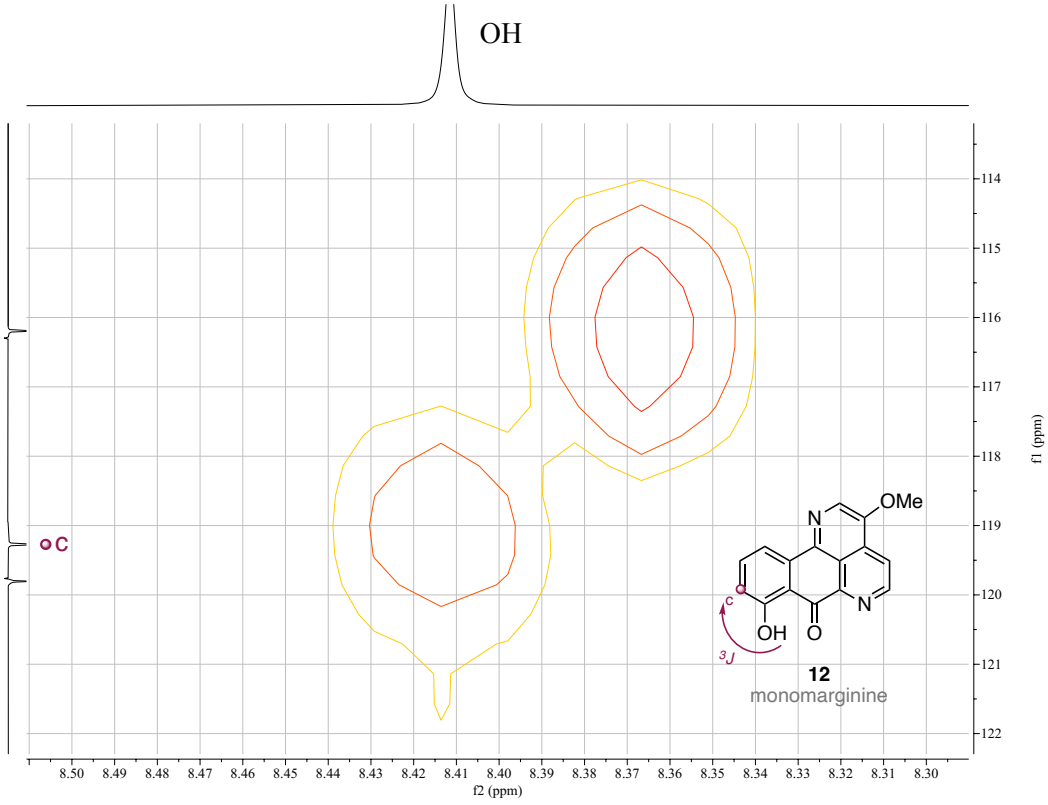


**Figure 7**. $^{3}J_{OH–C10}$ correlation in HMBC.

Then, the most intriguing part of the reassignment involved the quaternary carbon-atoms, as seven out of nine were missplaced in the skeleton of **10b**. For instance, $^{3}J_{H10–C5b}$ in **10b** would not be possible in **12** since they are five bond distances away ($^{5}J_{H10–C5b}$), which is not observed. Instead, $^{3}J_{H10–C5a}$ coupling, which is overlapping with $^{3}J_{H10–C8}$, corresponding to what the isolation team originally reported as $^{4}J_{H10–C5a}$ correlation in **10b** (Figure 8).

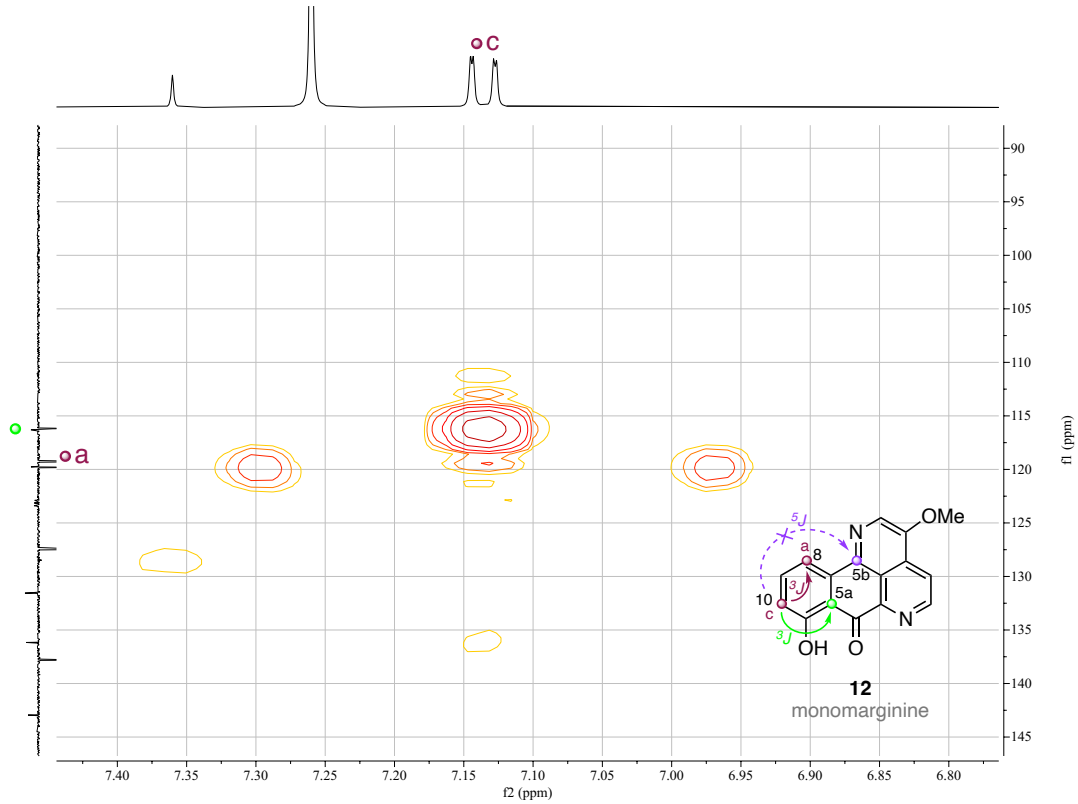


**Figure 8**. $^{3}J_{H10–C5a}$ and $^{3}J_{H10–C8}$ correlation in HMBC.

**First Approach for the Azaanthraquinone Core Synthesis**

Having the confirmed structure of the molecule, we started to target the synthesis of the natural product. The first retrosynthetic analysis we envisioned is shown in Scheme 6. The construction of key intermediate **33**, an anthraquinone assembly bearing a terminal alkyne. The terminal alkyne could be converted into a 1-sulfonyl-1,2,3-triazole following a copper(I)-catalyzed click-reaction[15] which would then be a suitable substrate for a rhodium-catalyzed denitrogenative hydration of the triazole moiety,[16] affording a direct monomarginine precursor **34**. To provide key intermediate **33**, we envisioned two possible paths. On one side, introducing the pyridine ring *via* a Diels-Alder reaction between an *α,β*-

15 (a) Raushel, J.; Fokin, V. V. Efficient Synthesis of 1-Sulfonyl-1,2,3-Triazoles, *Org. Lett.* **2010**, *12*, 4952–4955. (b) Yoo, E. J.; Ahlquist, M.; Kim, S. H.; Bae, I.; Fokin, V. V.; Sharpless, K. B.; Chang, S. Copper-Catalyzed Synthesis of *N*-Sulfonyl-1,2,3-triazoles: Controlling Selectivity, *Angew. Chem. Int. Ed.* **2007**, *46*, 1730–1733.

16 (a) Bennett, J. M.; Shapiro, J. D.; Choinski, K. N.; Mei, Y.; Aulita, S. M.; Reinheimer, E. W.; Majireck, M. M. Synthesis of Phthalan and Phenethylamine Derivatives *via* Addition of Alcohols to Rhodium(II)-Azavinyl Carbenoids, *Tetrahedron Lett.* **2017**, *58*, 1117–1122. (b) Chuprakov, S.; Worrell, B. T.; Selander, N.; Sit, R. K.; Fokin, V. V. Stereoselective 1,3-Insertions of Rhodium(II) Azavinyl Carbenes, *J. Am. Chem. Soc.* **2014**, *136*, 195–202. (c) Miura, T.; Biyajima, T.; Fujii, T.; Murakami, M. Synthesis of *α*-Amino Ketones from Terminal Alkynes *via* Rhodium-Catalyzed Denitrogenative Hydration of *N*-Sulfonyl-1,2,3-Triazoles, *J. Am. Chem. Soc.* **2012**, *134*, 194–196.

unsaturated *N*,*N*-dimethylhydrazone **16** and juglone, following pathway I.[17] On the other hand, a gold(I)-catalyzed 6-*endo-dig* cycloisomerization from the aminated juglone adduct **27a** could be expected to cyclize giving rise to intermediate **33**, following pathway II.[18]

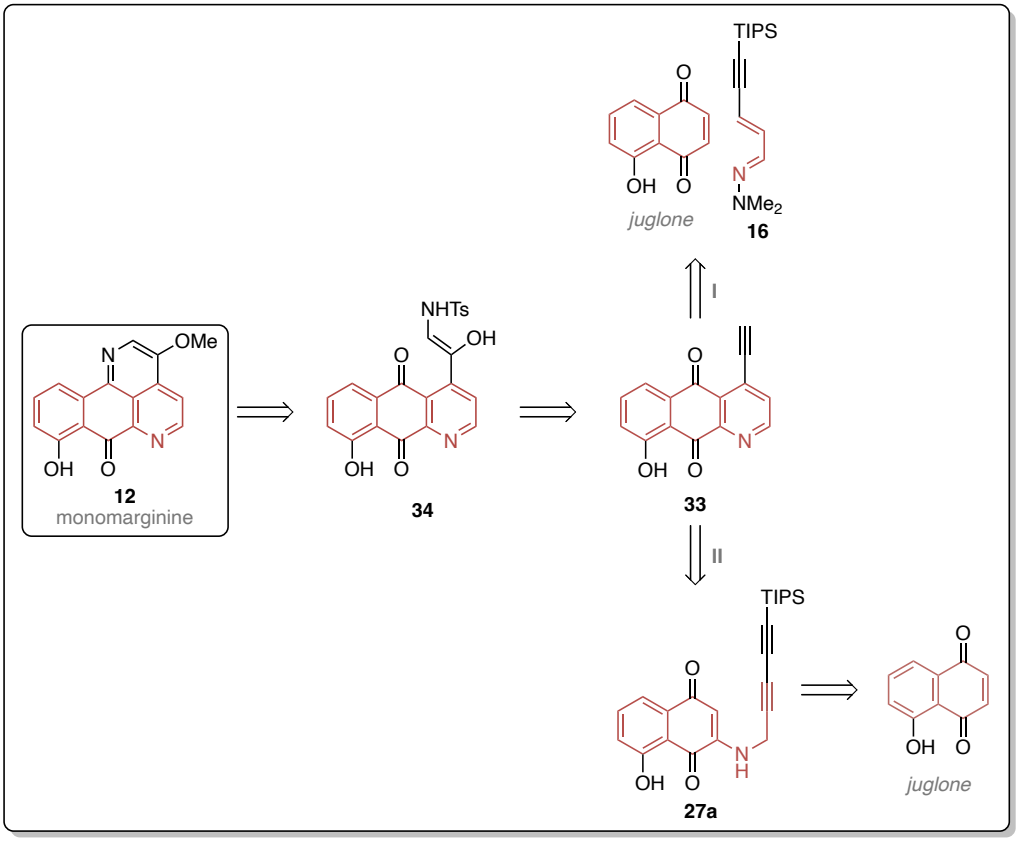


**Scheme 6**. First retrosynthetic analysis towards monomarginine **12**.

To test pathway I in Scheme 6, azadiene **16** was prepared in a two-sequence step. From acrylaldehyde **14** and bromo alkyne **12**, a palladium-catalyzed coupling reaction afforded aldehyde **6** in 61% yield. Then, a condensation under acidic conditions between aldehyde **15** and *N*,*N*-dimethylhydrazine, gave rise to the desired *N*,*N*-dimethylhydrazone **16** in 76% yield (Scheme 7).

17 Alvarez, F.; Taleb, A.; Gentili, J.; Nebois, P.; Terreux, R.; Domard, M.; Thozet, A.; Merle, D.; Fillion, H.; Walchshofer, N. A Diels–Alder Strategy for the Building of Imidazo[4,5-g]quinoline-4,9-dione Derivatives, *Eur. J. Org. Chem.* **2005**, *2005*, 1903–1908.

18 Jiang, C.; Xu, M.; Wang, S.; Wang, H.; Yao, Z.-J. Azaanthraquinone Assembly from *N*-Propargylamino Quinone *via* a Au(I)-Catalyzed 6-e*ndo-dig* Cycloisomerization, *J. Org. Chem.* **2010**, *75*, 4323–4325.

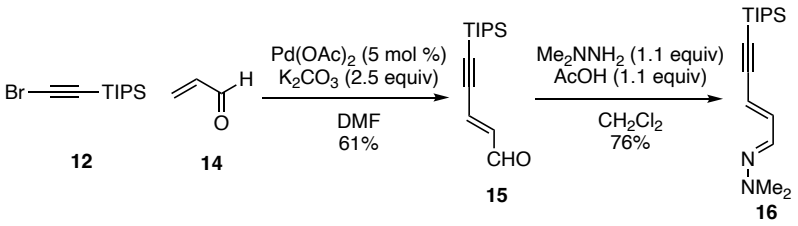


**Scheme 7**. Synthesis of *N*,*N*-dimethylhydrazone **16**.

As a starting point for the Diels-Alder reaction between *N*,*N*-dimethylhydrazone **16** and juglone, mild conditions were tested, which did not form the desired product (Table 2, entry 1). However, using $Ac_2O$ and heating to 80 ºC in acetonitrile, 20% of cycloadduct **17** could be isolated (Table 2, entry 2). Give **17** under similar conditions (Table 2, entries 3 and 4). Additionally, the mixture was exposed to microwave radiations but only starting materials were recovered (Table 2, entries 5 and 6).

**Table 2**. Efforts towards the Diels Alder between juglone and *N*,*N*-dimethylhydrazone **7**.

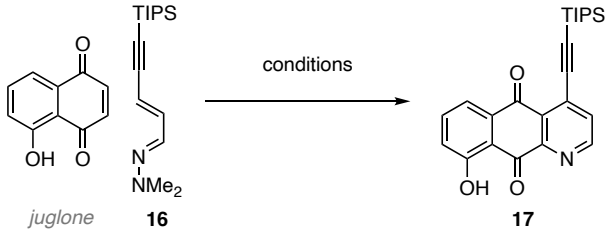


| Entry | Conditions | Yield (%) |
|---|---|---|
| 1 | EtOH, 23 ºC, 4 h | -[a] |
| 2 | $CH_3CN$, $Ac_2O$, 80 ºC, 18 h | 20 |
| 3 | $CH_3CN$, $Ac_2O$, $MnO_2$, 80 ºC, 18 h | -[a] |
| 4 | $CH_3CN$, $CeCl_3 \cdot 7H_2O$, $Ac_2O$, 80 ºC, 4 h | -[a] |
| 5 | $CH_3CN$, $Ac_2O$, 110 ºC, MW, 18 h | -[a] |
| 6 | $CH_3CN$, $Ac_2O$, 80 ºC. *Then*, MW, 110 ºC | -[a] |

[a] No conversion of the starting material was observed.

Unfortunately, multiple attempts to reproduce the conditions that first yielded desired product **17** (Table 2, entry 2) encountered significant reproducibility challenges, resulting in no formation of cycloadduct **17** again or complex mixtures when harsher conditions were applied.

Thus, another strategy to face the synthesis of the key intermediate **27** was envisioned following pathway II, where an aminated juglone derivative would be a precursor for the gold(I)-catalyzed cyclization reaction to afford **27** (Scheme 2, path II).

The preparation of dyine **20** was afforded by a Cadiot-Chodkiewicz reaction between bromoalkyne **12** and *N*-Bocpropargylamine **18**, followed by the *N*-Boc deprotection under acidic conditions (Scheme 8).

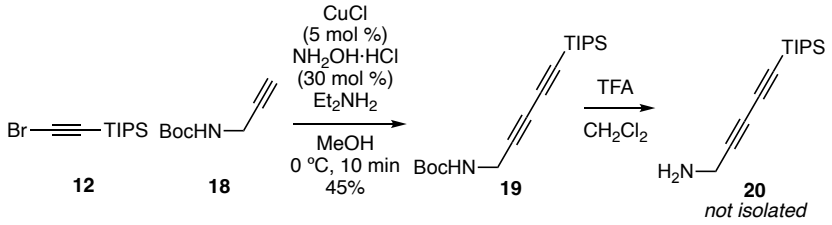


**Scheme 8**. Synthesis of dyine **20**.

To direct the amination for the synthesis of the desired precursor of the gold(I)-catalyzed cyclization **17a** (Scheme 2), a regioselective bromination of juglone was first performed, affording brominated juglone **21** in 39% yield (Scheme 9). Then, amination with freshly prepared amine **20** yielded the corresponding aminated juglone **22**, although with the unexpected regioselectivity. This unexpected regioselectivity was found after the gold(I)-catalyzed syclization of diyne **23** followed by *in situ* TIPS-deprotection, when crystals of tricycle **24** were obtained, revealing its structure by X-ray diffraction (Figure 9). Presumably the hydrogen-bonded phenol group, instead of the bromide, controls the regioselectivity of the amination reaction at C-3. Nonetheless, the next reaction for the functionalization of the terminal alkyne present in **23** was carried out as a proof of concept, giving rise to the expected triazole **24** in 40% yield.

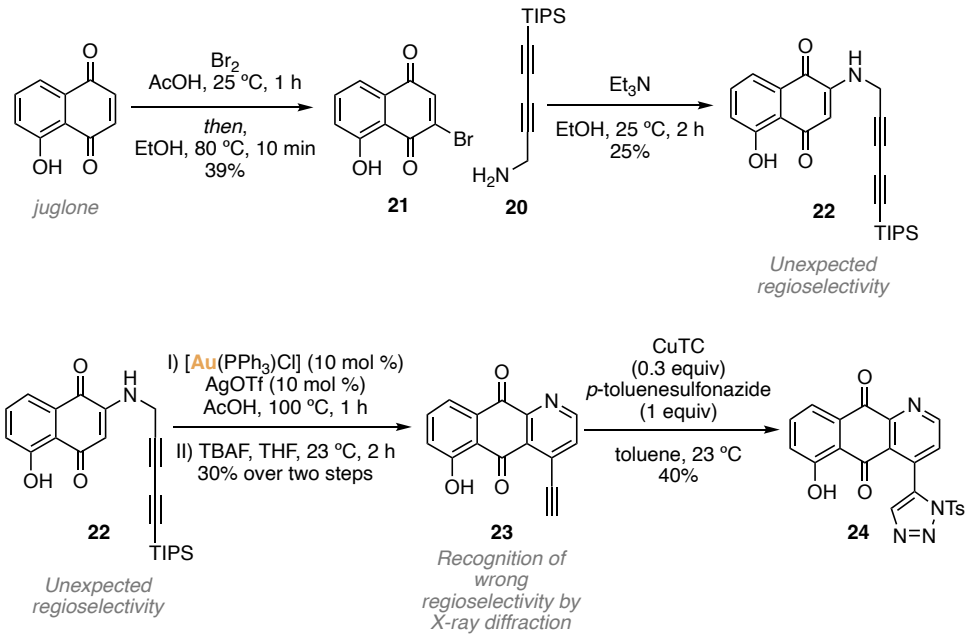


**Scheme 9**. First test for the gold(I)-catalyzed hydroarilation reaction of **22**.

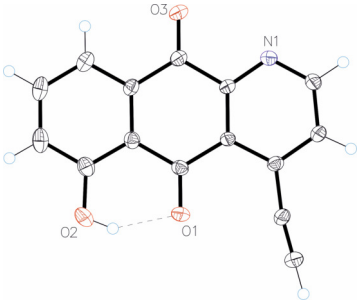


**Figure 9**. X-Ray structure of **23**.

The structure of **22** was carefully studied by HMBC, where the $^{3}J_{H3–C1}$ coupling could be observed, confirming the regioselectivity obtained (Figure 10).

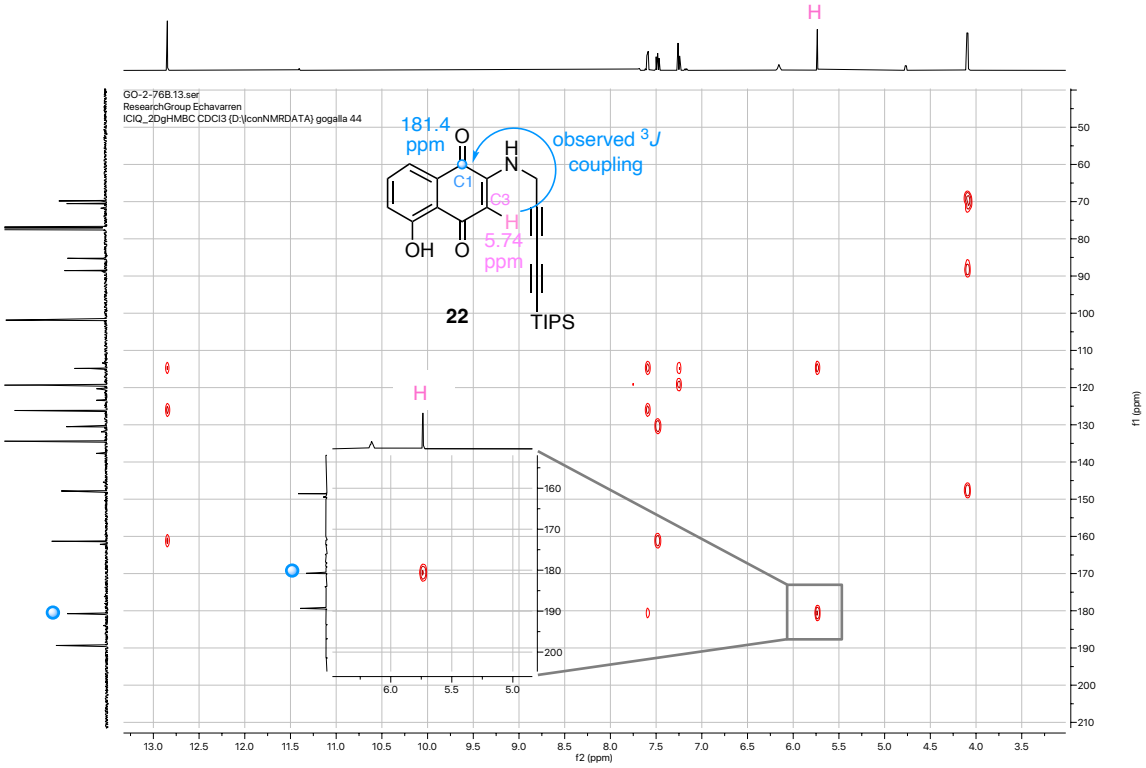


**Figure 10**. $^{3}J_{H3–C1}$ key-interaction observed in HMBC for **22**.

To reverse the observed regioselectivity, we attempted to functionalize juglone by changing the bromine position. Additionally, giving the influence of the phenol group, we hypothesized that its protection, could reverse the regiochemistry of the amination. Thus, the synthesis of compounds **26** was carried out from commercially available 1,5-diacetoxynaphtalene **25** following a reported two steps procedure for the bromination[19a] and the methylation[19b] reaction to afford **26a** and **26b**, respectively (Scheme 10).

19 (a) Grunwell, J. R.; Karipides, A.; Wigal, C. T.; Heinzman, S. W.; Parlow, J.; Surso, J. A.; Clayton, L.; Fleitz, F. J.; Daffner, M.; Stevens, J. E. The Formal Oxidative Addition of Electron-Rich Transoid Dienes to

Then, using identical amination reaction conditions, adducts **27** were formed with the expected structure. Nonetheless, the reaction was not totally regioselective and **28** was identified as a major byproduct in the crude reaction mixture (*ca.* 34%), which was confirmed by X-ray diffraction (Figure 11), which complicated the purification process, resulting in low yields of the desired products (Scheme 10, **27a** and **27b)**.

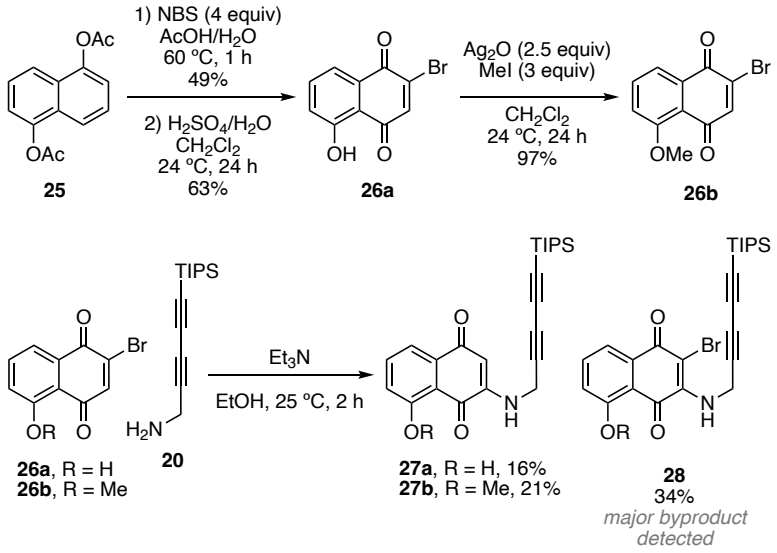


**Scheme 10**. Amination reaction from the modified brominated juglone **26a** and **26b**.

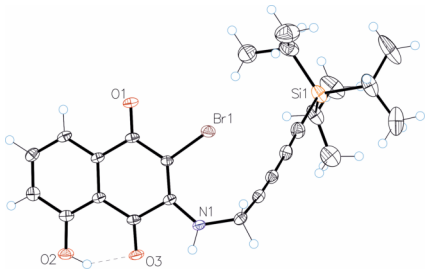


**Figure 11**. X-Ray structure of byproduct **28**.

The structure of **27a** was again confirmed by HMBC correlations analysis, where it could be observed the corresponding key-interaction $^{3}J_{H2–C4}$ (Figure 12).

Bromonaphthoquinones, *J. Org. Chem.* **1991**, *56*, 91–95. (b) Ngwira, K. J.; Rousseau, A. L.; Johnson, M. M.; de Koning, C. B. Reactions of [2-(2-Naphthyl)Phenyl]Acetylenes and 2-(2-Naphthyl)Benzaldehyde O-Phenyloximes: Synthesis of the Angucycline Tetrangulol and 1,10,12-Trimethoxy-8-Methylbenzo[c]Phenanthridine, *Eur. J. Org. Chem.* **2017**, *2017*, 1479–1488.

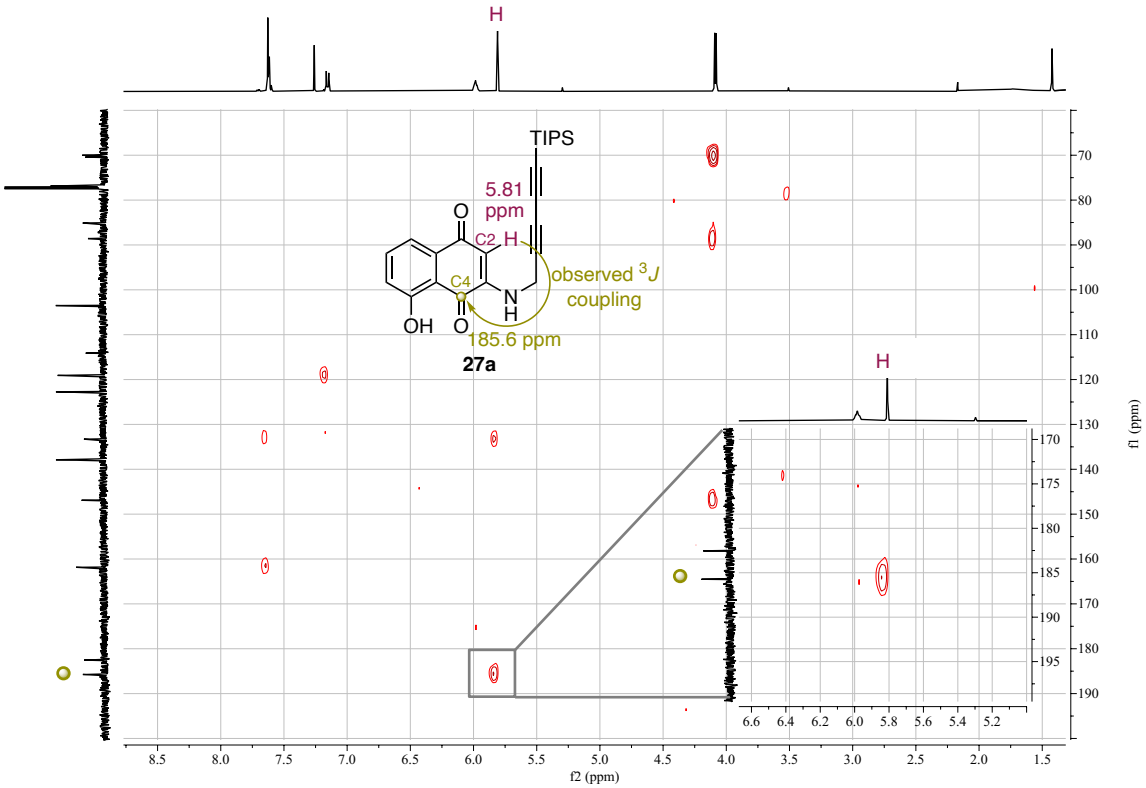


**Figure 12**. Key $^3J_{H2–C4}$ interaction observed in HMBC for **27a**.

Unfortunately, the gold(I)-catalyzed cyclization reaction was unsuccessful when either **27a** or **27b** were employed as substrates (Scheme 11). The reaction consistently let to either no reaction or decomposition, attributed to the unstability of the substrates.

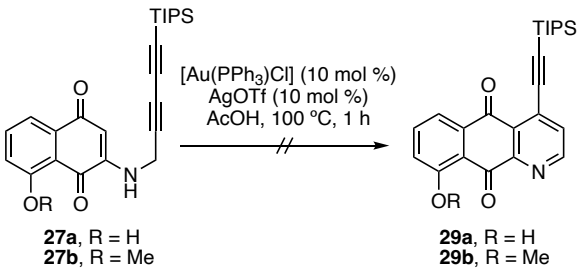


**Scheme 11**. Attempts for the gold(I)-catalyzed hydroaryation of **27a** and **27b**.

As an alternative approach, we considered a previous result obtained in the group.[20] Starting with the analogous diyne substrate **31**, synthesized in three steps from **30**, the gold(I)-catalyzed reaction unexpectedly occured on the carbon-atom bearing one of the methoxy groups, at the C4 position, yielding tricyclic compound **32** (Scheme 12). The structure of **32** was confirmed by NMR and X-ray diffraction (Figure 13).

20 Experiments performed by Dr. Marc Paul Beller.

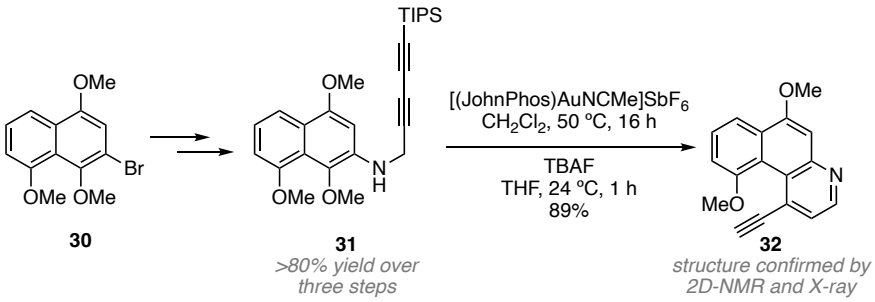


**Scheme 12**. Gold(I)-catalyzed cyclization of **31**.

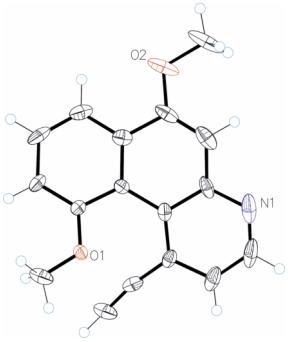


**Figure 13**. X-Ray structure of tricycle **32**.

To prevent the cyclization at the C4 position, a strategy was proposed to restrict the rotation of the amine by introducing cyclic carbamate **39** as precursor for the gold(I)-catalyzed cyclization (Scheme 13).

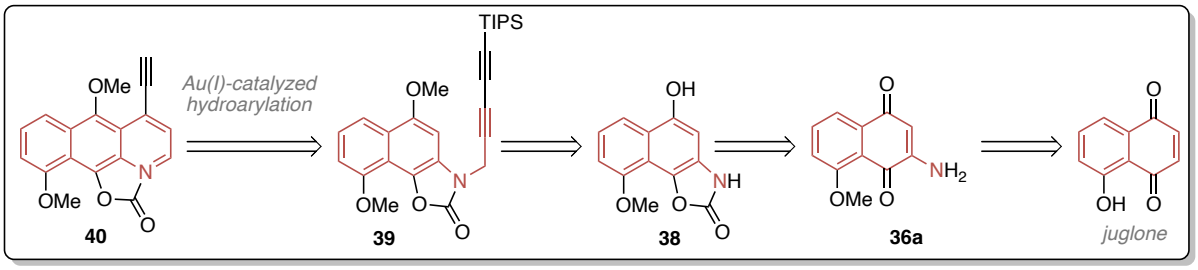


**Scheme 13**. Retrosynthetic analysis for new route *via* **39** as key intermediate.

Thus, commercially available 5-methoxy-1,4-naphthoquinone was exposed to hydroxylamine **35** under basic conditions to afford the corresponding primary amine **36a**,[21] which could be monoprotected to afford **36b** in 76% yield (Scheme 14). Then, treatment of the juglone-aminated derivatives **36a** or **36b** with sodium dithionite as reducing agent took place. However, none of the reduced intermediates reacted with 4-nitrophenylchloroformate **37** to yield desired cyclic carbamate **38** (Scheme 14).

21 Seong, W.-L; Jung, M.L.; Jung, K.B.; Cheul, T.-R.; Hoon, L.-S.; Dae, L.-K.; You-Hui, L.; Hwan, K.-T.; Canadian Patent; WO2015102369A1, **2015**.

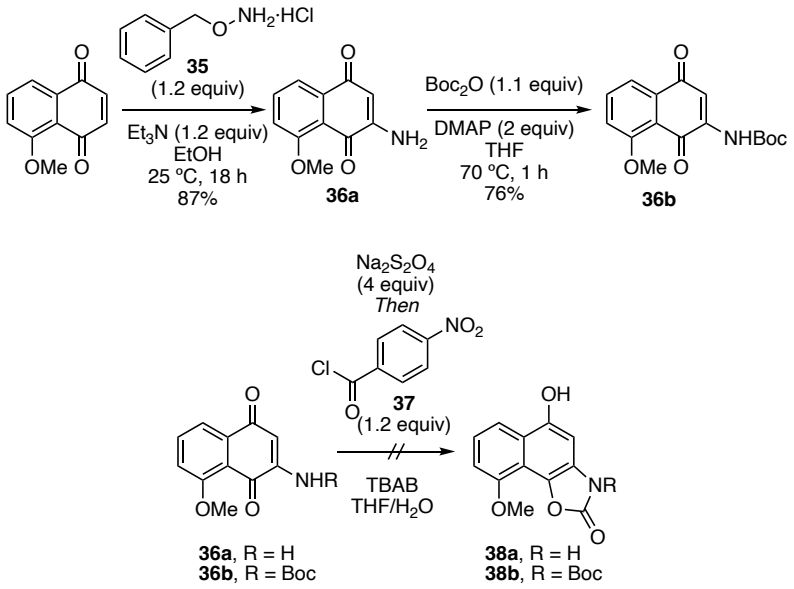


**Scheme 14**. Attempted synthesis of cyclic carbamate **38**.

**Second Approach for the Naphthyridine Core Synthesis**

Discarding the idea of starting the synthesis from juglone derivatives to form the azaanthraquinone skeleton, our next strategy was focused on intermediates **54**, bearing the pyridine cycle, aiming to functionalize this side of the molecule first, generating the naphthyridine-tricyclic ring system in **66** (Scheme 15).

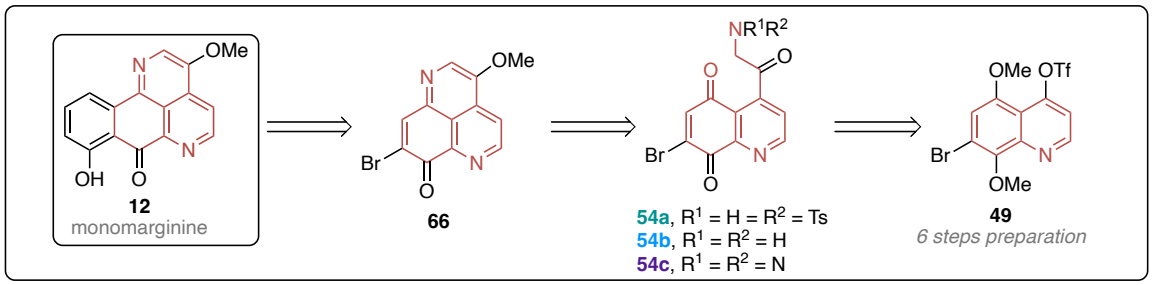


**Scheme 15**. Retrosynthetic analysis involving key-intermedates **54**.

The synthesis for target substrate **49** was performed in six steps by adapting reported procedures (Scheme 16).[22] First, *ortho*-bromination of the commercially available 4-methoxy-2-nitrophenol **41** yielded regioselectively 2-bromo-6-nitrohydroquinone **42** in 78% yield. Next, methylation of the phenol

22 (a) Cassis, R.; Tapia, R.; Valderrama, J. A. Synthesis of 4(1H)-Quinolones by Thermolysis of Arylaminomethylene Meldrum's Acid Derivatives, *Synth. Commun.* **1985**, *15*, 125–133. (b) Guay, V.; Brassard, P. The Regiospecific Synthesis of the A and B Rings of Phomazarin, *J. Heterocycl. Chem.* **1987**, *24*, 1649–1652. (c) Canova, S.; Bellosta, V.; Bigot, A.; Mailliet, P.; Mignani, S.; Cossy, J. Total Synthesis of Herbimycin A, *Org. Lett.* **2007**, *9*, 145–148. (d) Vedachalam, S.; Murugesh, N.; Chakraborty, P.; Karvembu, R.; Liu, X.-W. NHC Catalyzed Enantioselective Coates-Claisen Rearrangement: A Rapid Access to the Dihydropyran Core for Oleuropein Based Secoiridoids, *New J. Chem.* **2018**, *42*, 1832–1839.

was carried out, followed by the selective reduction of the nitro group in compound **43** using iron, yielding amine **44**. Then, the commercially available Meldrum's acid reacted with trimethyl orthoformate for 3 h at 95 ºC affording **45** in 85% yield. Amine **44** and methoxymethylen Meldrum's acid **45** reacted to afford enamine **46** in 70% yield.

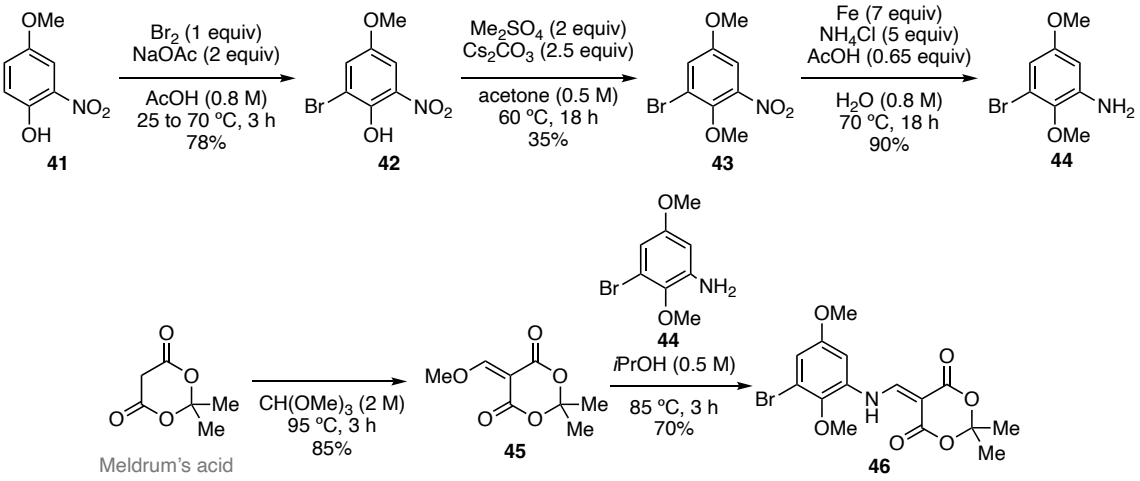


**Scheme 16**. Synthesis of **46**.

Next, by heating **46** in $Ph_2O$ at 235 ºC, ketene **47** is formed upon acetone loss and decarboxylation, to give the subsequent cyclization, yielding quinolone **48**. Finally, triflation of **48** formed desired compound **49** (Scheme 17).

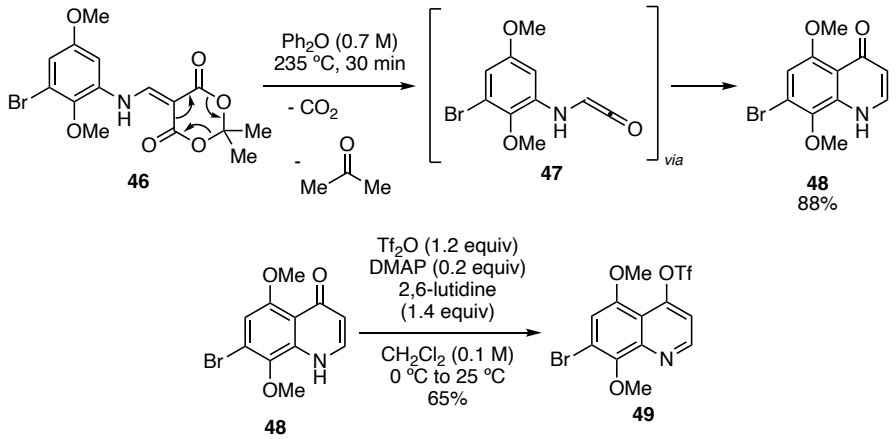


**Scheme 17**. Synthesis of triflate **49**.

We envisioned the functionalization of the triflate moiety in **49** for the introduction of the triazole group which would allow us to explore the Rh-catalyzed denitrogenative hydration strategy for the formation of amine **54a**.[16] Sonogashira coupling with TMS acetylene followed by the TMS-deprotection, afforded the desired terminal alkyne **51**, which proved to be a suitable substrate for the copper-catalyzed reaction. Finally, oxidation with cerium ammonium nitrate (CAN) yielded triazole **53** in 49% yield. Nonetheless,

our efforts for the formation of **54a** through this path were not successful and only starting material was recovered under the examined reaction conditions (Scheme 18).

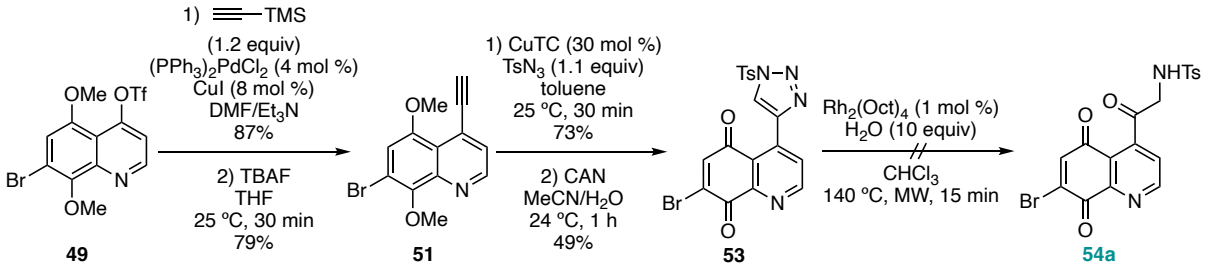


**Scheme 18**. Attempts for the synthesis of **54a**.

As an alternative, we targeted the synthesis of $\alpha$-haloketone **56**, which would later be converted into the corresponding $\alpha$-aminoketone **54b** (Scheme 18). Thus, halogenation of **51** with NBS[23] or NIS,[24] afforded the corresponding haloalkynes **55a** and **55b** in 65 and 76% yield, respectively (Scheme 19).

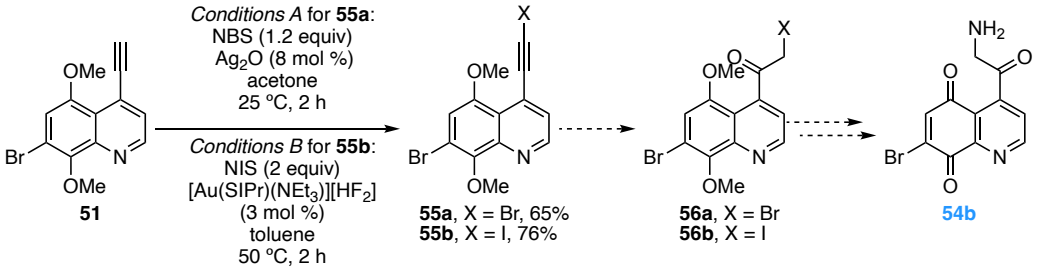


**Scheme 19**. Halogenation of terminal alkyne **51** and possible next steps towards **54b**.

Several attempts for the direct hydration of these compounds were performed (Table 3). However, decomposition of the starting materials was observed at the reaction conditions studied.

**Table 3**. Attempts for the hydrolysis of akynes **55a** and **55b**.

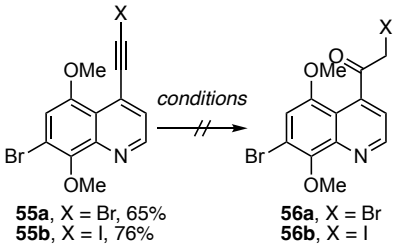


| Entry | Conditions | 56 Yield (%) |
|---|---|---|

23 Zatolochnaya, O. V.; Gevorgyan, V. Synthesis of Fluoro- and Perfluoroalkyl Arenes *via* Palladium-Catalyzed [4 + 2] Benzannulation Reaction, *Org. Lett.* **2013**, *15*, 2562–2565.

24 Gómez-Herrera, A.; Nahra, F.; Brill, M.; Nolan, S. P.; Cazin, C. S. J. Sequential Functionalization of Alkynes and Alkenes Catalyzed by Gold(I) and Palladium(II) N-Heterocyclic Carbene Complexes, *ChemCatChem* **2016**, *8*, 3381–3388.

| | | |
|---|---|---|
| 1 | $Ce(SO_4)_2$, $H_2O$, $H_2SO_4$, $CH_2Cl_2$, 80 ºC, 18 h | - |
| 2 | $HBF_4$, $F_3EtOH$, 80 ºC, 2 h | - |
| 3 | $In(OTf)_3$, $H_2O$, HOAc, 100 ºC, 18 h | - |
| 4 | $[(IPr)Au(NTf_2)]$, $H_2O$, MsOH, EtOH, 50 ºC, 18 h | - |

We then applied the well-known Stille coupling with tributyl(ethoxyvinyl)stannane **57** to triflate **49**, using Farina protocol, yielding **58** in 91% yield, without the bromine being affected (Scheme 20).[25]

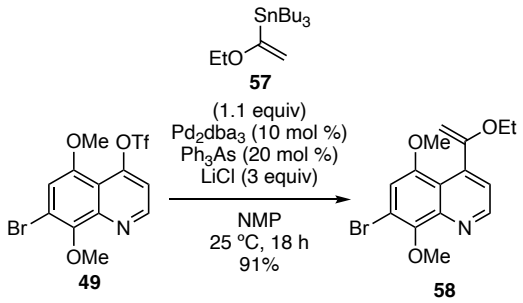


**Scheme 20**. Stille-Migita coupling to afford enol ether **58**.

Next, the bromination of enol ether **58** was tested under different conditions to afford the desired *α*-bromoketone **56a** (Table 4). Using NBS under mild conditions did not afford more than 15% yield of **56a** (Table 4, entry 1). Bromine was used on its own and in the presence of acid with no success (Table 4, entries 2 and 3). Then, Baran's recently developed reagent for electrophilic halogenations was tested using **59** as bromine source,[26] although product **56a** was not observed. Finally, under acidic conditions, we observed the formation of methyl ketone **60** (Table 4, entry 4). Thus, with subsequent addition of bromine, desired product **56a** was obtained in moderate yields (Table 4, entry 6). The structure of **56a** was confirmed by X-ray diffraction (Figure 14).

**Table 4**. Conditions tested for affording **46a** from enol ether **48**.

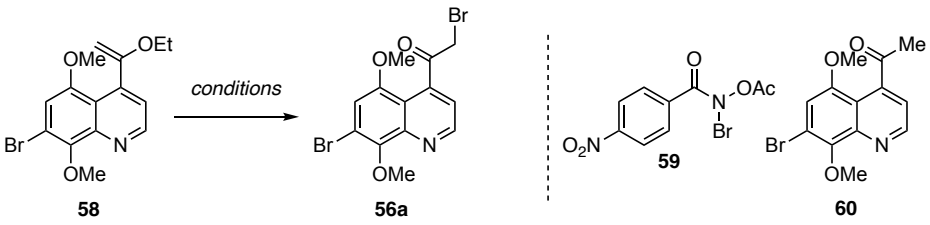


25 Farina, V.; Krishnan, B. Large Rate Accelerations in the Stille Reaction with Tri-2-furylphosphine and Triphenylarsine as Palladium Ligands: Mechanistic and Synthetic Implications, *J. Am. Chem. Soc.* **1991**, *113*, 9585–9595.

26 Wang, Y.; Bi, C.; Kawamata, Y.; Grant, L. N.; Samp, L.; Richardson, P. F.; Zhang, S.; Harper, K. C.; Palkowitz, M. D.; Vasilopoulos, A.; Collins, M. R.; Oderinde, M. S.; Tyrol, C. C.; Chen, D.; LaChapelle, E. A.; Bailey, J. B.; Qiao, J. X.; Baran, P. S. Discovery of N–X Anomeric Amides as Electrophilic Halogenation Reagents, *Nat. Chem.* **2024**, *16*, 1539–1545.

| Entry | Conditions | Yield (%) |
|---|---|---|
| 1 | NBS, $THF/H_2O$, 25 ºC, 30 min | 15 |
| 2 | $Br_2$, $CH_2Cl_2$, 25 ºC | - |
| 3 | $Br_2$, AcOH, $CH_2Cl_2$, 25 ºC | - |
| 4 | **59**, $Me_2CO_3$/HBr in AcOH 33%, 45 ºC, 1 h | -[a] |
| 5 | HBr in AcOH 33%, $THF/H_2O$, 0 ºC, 30 min. Then, NBS, 65 ºC, 1 h | -[a] |
| 6 | HBr/AcOH, 25 ºC, 1 h. Then, $Br_2$, 70 ºC | 57 |

[a] Methyl ketone **60** observed as only product.

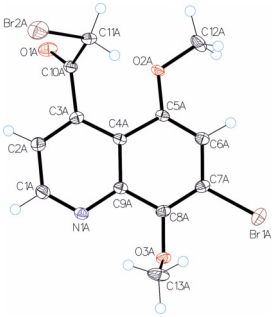


**Figure 14**. X-Ray structure of **56a**.

Having *α*-bromoketone **56a** in hand, its transformation to the corresponding *α*-aminoketone **62** was envisioned. One first trial, was testing the Delépine reaction using hexamethylenetetramine **52** (HMTE).[27] However, no conversion of **56a** was observed in this case (Scheme 21). In parallel, oxidation with cerium ammonium nitrate (CAN) of the hydroquinone afforded **54d** in 61% yield, which we aimed to use for further amination tests (Scheme 21).

27 Delépine, M. Sur l'hexamethylene-amine (suite). Solubilities, hydrate, bromure, sulfate, phosphate. *Bull. Soc. Chim. France* **1895**, *13*, 352–361.

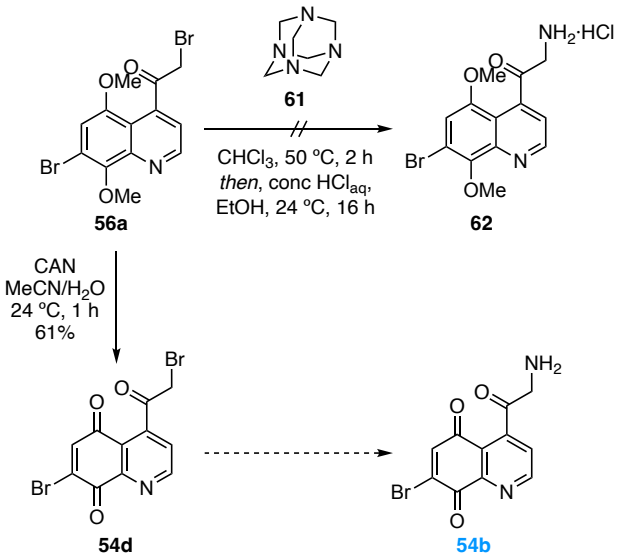


**Scheme 21**. Attempts for the transformation of **56a**.

However, despite trying several conditions with different amine sources to react with **54d**, no formation of *α*-aminoketone **54b** was observed (Table 5).

**Table 5**. Attempts for the *α*-aminoketone **54b** from oxidized *α*-bromoketone **54d**.

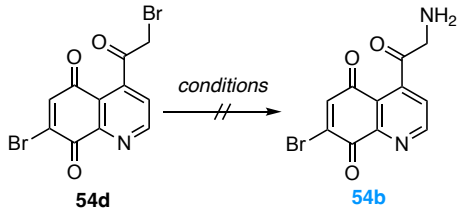


**54d** **54b**

| Entry | Conditions | Yield (%) |
|---|---|---|
| 1 | $NH_4Cl$, DMSO, 23 ºC, 2 h | -[a] |
| 2 | $NH_3$ in MeOH, 23 ºC, 1 h | -[a] |
| 3 | HMTE (**61**), $CHCl_3$, 50 ºC, 2 h. *Then*, conc $HCl_{aq}$, EtOH, 24 ºC, 16 h | -[a] |

[a] Recovery of **54d**.

At this point, we converted *α*-bromoketone **56a** into *α*-azidoketone **63**, which could also be oxidized to **54c** in good yields using CAN. We considered the possibility for an aza-Wittig reaction, but the conversion to phosphazide **64** failed. On the other hand, reduction of **63** to the primary amine **65** was also attempted but did not yield the desired product **65** (Scheme 22).

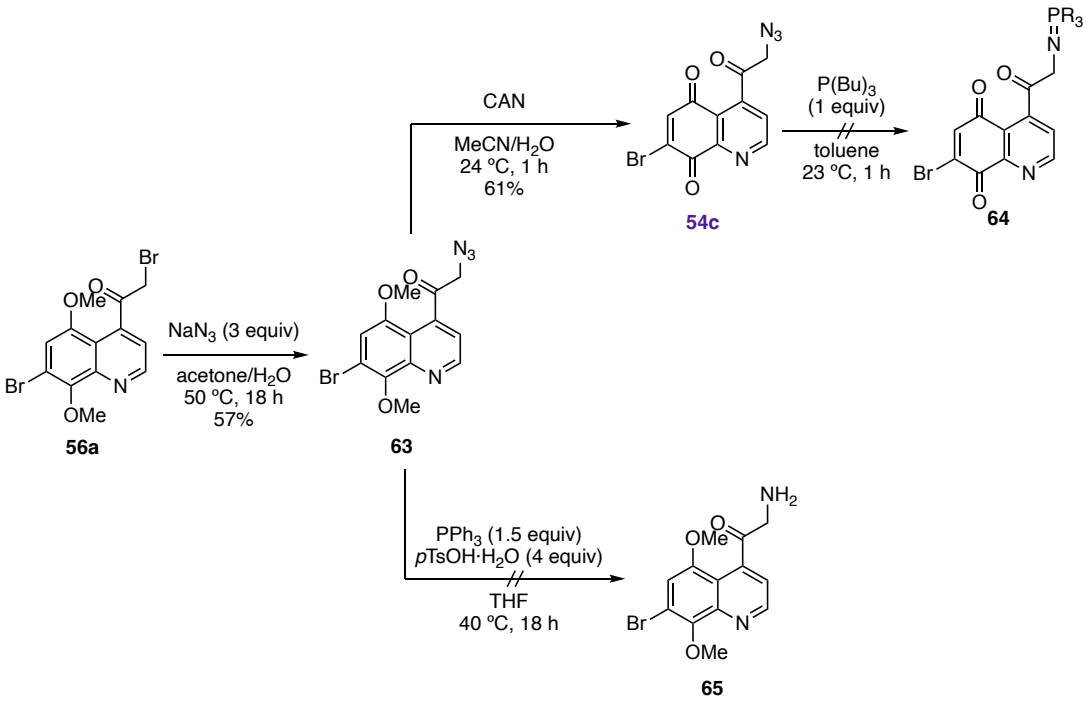


**56a** **63** **54c** **64** **65**

**Scheme 22**. Attempts for the functionalization of azide **63**.

**Third Approach for the Diels-Alder Reaction to Afford Azaanthraquinone Core**

At this point, we reconsidered a strategy that relies on the synthesis of the tricyclic azaanthroquinone structure. Now, a Diels-Alder reaction for the introduction of the phenol ring, using the previously synthesized brominated azanaphthoquinone derivatives **54** as dienophiles (Scheme 23).

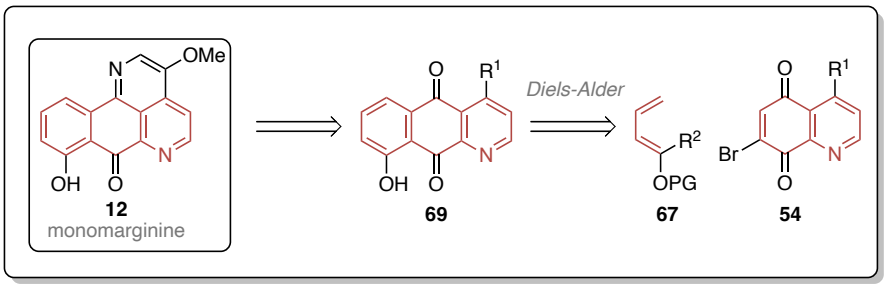


**Scheme 23**. Retrosynthetic analysis of the third approach, based on the Diels-Alder reaction for the construction of azaanthraquinone **69**. PG = protecting group.

First, inspired by Rawal's work using a ketene-equivalent 1,3-diene,[28] we tested the cycloaddition reaction using our previously synthesized $\alpha$-bromoketone **54d** as dienophile (Scheme 24). However, no consumption of the starting materials was observed for the formation of cycloadduct **68a**.

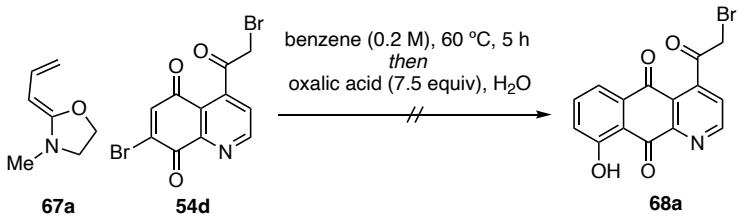


**Scheme 24**. First attempt of Diels-Alder reaction between diene **67a** and dienophile **54d**.

Therefore, the oxidation of previous synthesized intermediates **49** and **60** for the preparation of other possible dienophiles was executed (Scheme 25). Triflate **49** was oxidized under the conventional conditions using CAN, affording **42e** in a 47% yield. On the other hand, methyl ketone **60** was obtained by subjecting **58** to acid conditions, followed by oxidation to form **54f**.

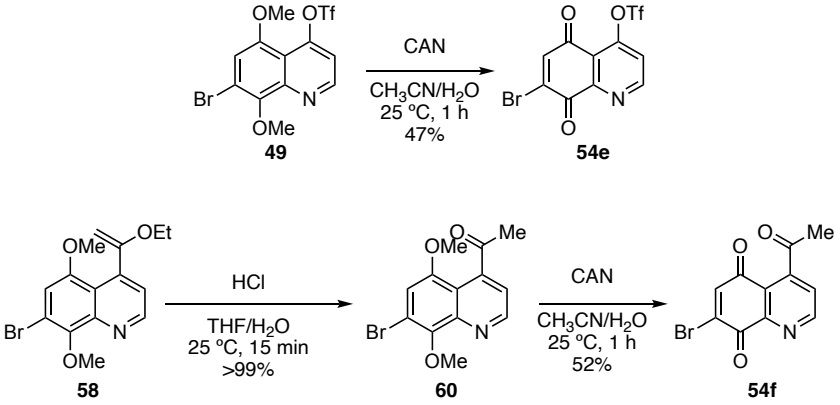


**Scheme 25**. Preparation of dienophiles **54e** and **54f**.

28 Elkin, P. K.; Durfee, N. D.; Rawal, V. H. Diels–Alder Reactions of 1-Alkoxy-1-amino-1,3-butadienes: Direct Synthesis of 6-Substituted and 6,6-Disubstituted 2-Cyclohexenones and 6-Substituted 5,6-Dihydropyran-2-ones, *Org. Lett.* **2021**, *23*, 5288–5293.

With a small library of 1,3-dienes and dienophiles prepared, we tested several Diels-Alder reactions (Table 6). Rawal's diene **67a** was also tested with **54c** in benzene at 60 ºC for five hours, with no success (Table 6, entry 1). Dienophile **54c** was also used in combination with diene **67b** at different temperature ranges, but cycloaddition product did not form either under these condtions (Table 6, entries 2 and 3). Diene **67b**, did not deliver the corresponding product **68** when exposed to other members of the available dienophile family (Table 6, entries 4 and 5). By slighthly modifiying the electronics on the diene, using instead **67c** with triflate **54e** did not afford the product either (Table 6, entry 6). Similarly, using more electron-deficient diene **67d**, which would lead to the free phenol, was not successful (Table 6, entry 7). Finally, we could observe the full conversion of the starting materials towards adducts **68** when mixing **67e** and dienophiles **54e** and **54d**, both at low or at room temperature (Table 6, entries 8 and 9). Nonetheless, we encountered challenges when trying to purify the cycloadducts formed, since they were very unstable under air or any treatment that we attempted for their isolation.

**Table 6**. Diels-Alder reaction attempts.

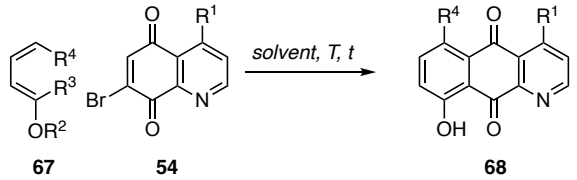


**67** **54** **68**

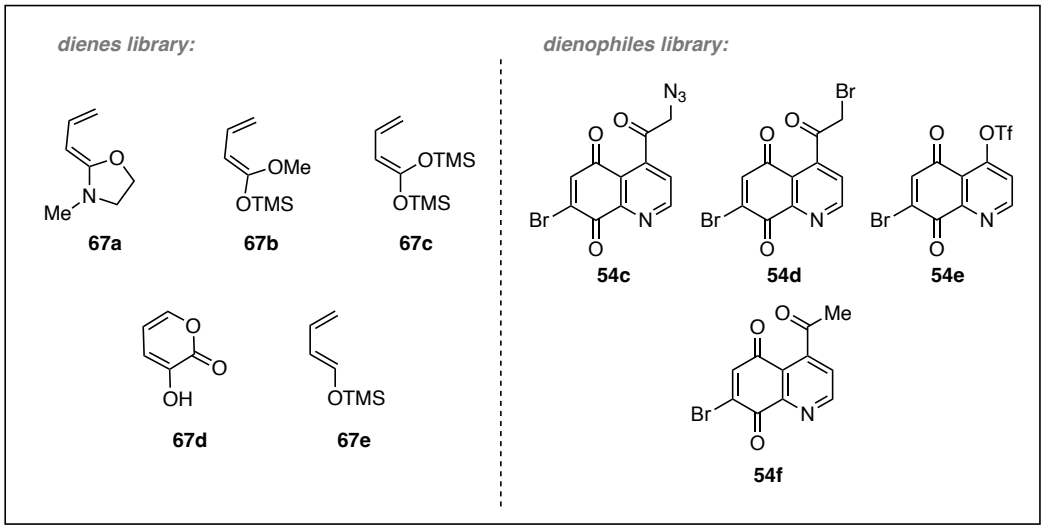


| Entry | diene | dienophile | solvent | T (ºC) | T (h) | 68 |
|---|---|---|---|---|---|---|
| 1 | **67a** | **54c** | benzene | 60 | 5 | n.d. |
| 2 | **67b** | **54c** | benzene | 23 | 0.5 | n.d. |
| 3 | **67b** | **54c** | toluene | -78 | 0.5 | n.d. |
| 4 | **67b** | **54f** | toluene | -78 | 0.5 | n.d. |
| 5 | **67b** | **54e** | $C_6D_6$ | 23 | 2 | n.d. |
| 6 | **67c** | **54e** | $C_6D_6$ | 23 | 2 | n.d. |
| 7 | **67d** | **54e** | $C_6D_6$ | 23 | 2 | n.d. |
| 8 | **67e** | **54e** | toluene-$d_8$ | -78 | 18 | Full conversion |
| 9 | **67e** | **54d** | toluene-$d_8$ | 23 | 1 | Full conversion |

n.d. = not detected.

Therefore, having identified a working combination for the cycloaddition reaction to form adducts **68a** and **68b**, we tried to find conditions for its subsequent aromatization (Scheme 26).

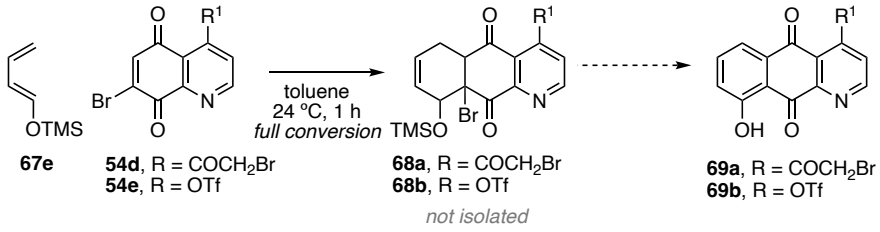


**Scheme 26**. Formation of **68a** and **68b** and its aromatization step towards **69** to be explored.

Thus, working in a one-pot system under an argon atmosphere, we attempted the treatment of cycloadduct **68b**, whose formation was detected formation by $^1$H NMR (Table 7). However, none of the assayed conditions tried were forming the desired azaanthraquinone product **69b**.

**Table 7**. Attempts for the direct aromatization of the Diels-Alder adduct **69b**.

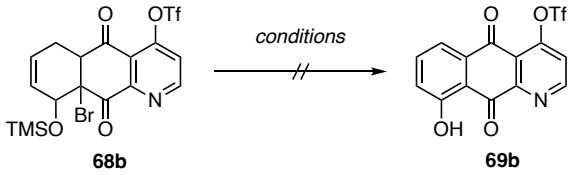


| Entry | conditions | 69b |
|---|---|---|
| 1 | THF, HCl, 23 ºC, 18 h | n.d. |
| 2 | $CrO_3$, AcOH, 118 ºC, 2 h | n.d. |
| 3 | $CrO_3$, acetone, 24 ºC, 2 h | n.d. |
| 4 | TBAF, THF, 23 ºC, 18 h | n.d. |
| 5 | $MnO_2$, TBAF, THF | n.d. |
| 6 | HF·$Et_3$N, THF, 23 ºC, 18 h | n.d. |
| 7[a] | $CrO_3$, AcOH, 23 ºC, 18 h | n.d. |

n.d. = not detected. [a] **54d** used instead

**Outlook**

To accomplish monomarginine's synthesis, the development of a new approach is currently under study in our group (Scheme 27). From substrate **30**, a Buchwald-Hartwig amination would be followed by a regioselective acetaldehyde addition. Then, the methyl ketone could be converted into its pyridone analogue using DMFDMA, followed by triflation and cross-coupling according to our previous strategy, to afford the corresponding methyl ketone. Finally, the enolate oxidation with *t*BuONO would form an oxime[29] which would be reduced to the corresponding acetamide. Finally, upon CAN oxidation, formation of the imine-containing ring in monomarginine could take place. Last, a selective methyl deprotection would be needed to afford the natural product.

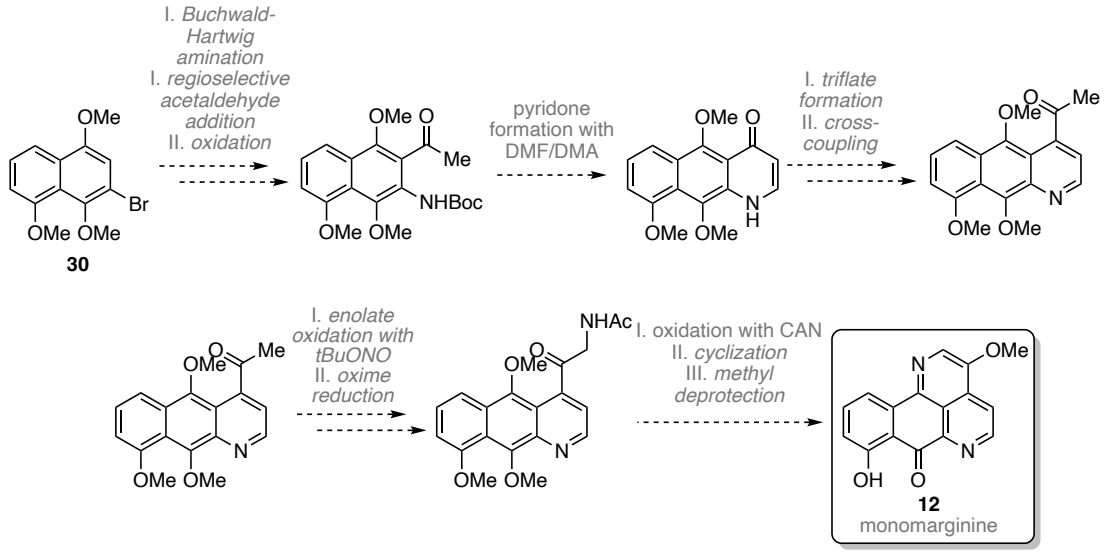


**Scheme 27**. Future work for the synthesis of monomarginine **12**.

29 (a) Zhu, J.; Kong, Y.; Lin, F.; Wang, B.; Chen, Z.; Liu, L. Copper-Catalyzed Direct Amination of 1,2,3-Triazole N-Oxides by C–H Activation and C–N Coupling, *Eur. J. Org. Chem.* **2015**, *2015*, 1507–1515. (b) Son, J.; Kim, K. H.; Mo, D.-L.; Wink, D. J.; Anderson, L. L. Single-Step Modular Synthesis of Unsaturated Morpholine N-Oxides and Their Cycloaddition Reactions, *Angew. Chem. Int. Ed.* **2017**, *56*, 3059–3063.

## Conclusions

The correct structure of monomarginine was determined through X-ray diffraction and detailed NMR analysis of a natural sample. Then, various synthetic methods have been explored in our laboratories. The construction of the azaanthraquinone core was targeted *via* a gold(I)-catalyzed hydroarylation or through a Diels-Alder reaction, utilizing different combinations of diene and dienophile partners. On the other side, the naphtyridine core was envisioned as an alternative trycylic framework to be constructed from an $\alpha$-aminoketone precursor following a condensation reaction to form the top ring. Although several analoguous intermediates were obtained during our attempts, the total synthesis of monomarginine has not yet been achieved. Efforts towards its completion are currently ongoing in our laboratories.

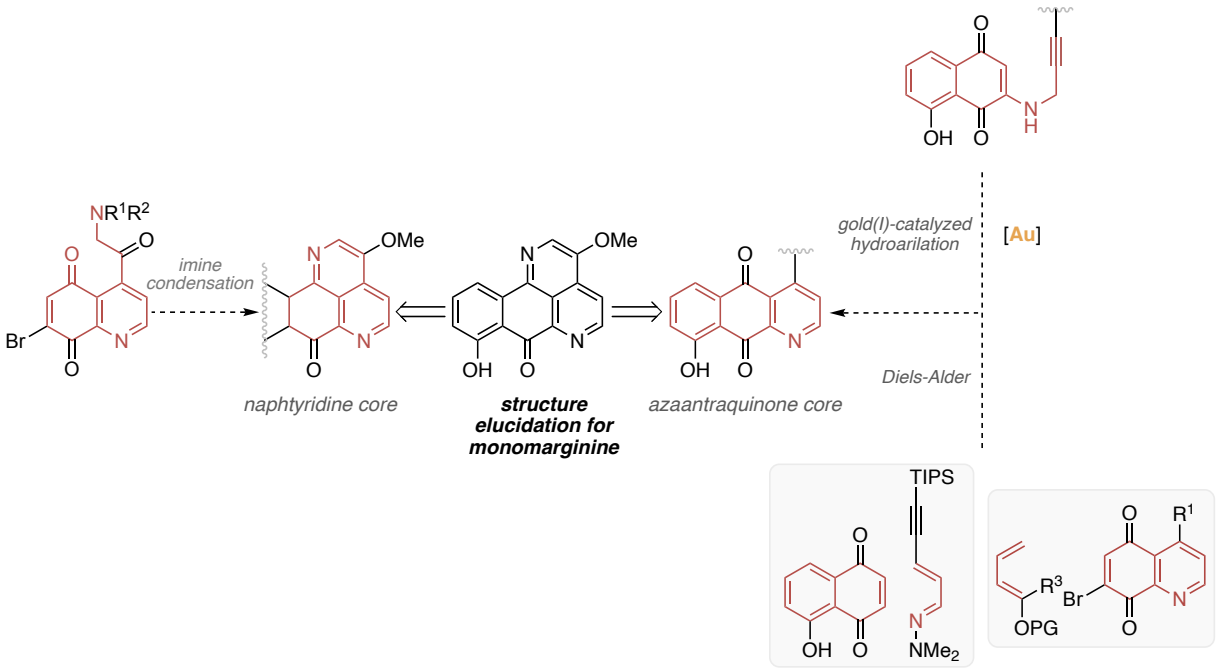


**Scheme 27**. Explored synthetic approaches for generating structures that incorporate the key cores of monomarginine precursors. PG = protecting group.

## Experimental Section

### General Methods

The general information has been provided in the experimental section of *Chapter I.*

### Synthetic Procedures and Analytical Data

Dienes **67a**,[28] **67b**,[30] **67c**,[31] **67d**[32] and **67e**[33] were synthesized as reported in literature. Baran's reagent **59** was synthesized as described.[26] Bromojuglone derivatives **26a**[19a] and **26b**[19b] were prepared following reported procedures.

### Monomarginine (12)

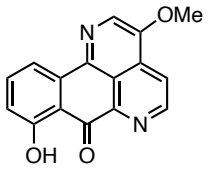


*A 1.1 mg of sample, provided by Professor Dr. Kam Toh Seok from the University of Malasya, was used for in-depth studies in structure determination.*

**$^1$H NMR** (500 MHz, $CDCl_3$) δ 12.93 (s, 1H), 9.14 (d, *J* = 5.5 Hz, 1H), 8.41 (s, 1H), 8.25 (d, *J* = 5.6 Hz, 1H), 8.20 (dd, *J* = 7.7, 1.1 Hz, 1H), 7.69 (t, *J* = 8.0 Hz, 1H), 7.14 (dd, *J* = 8.4, 1.0 Hz, 1H), 4.19 (s, 3H) ppm.

**$^{13}$C NMR** (126 MHz, $CDCl_3$) δ 187.1, 164.4, 150.0, 148.1, 147.4, 143.0, 137.8, 136.2, 131.6, 127.5, 119.8, 119.3, 116.3, 116.2, 56.7, 1.2 ppm.

**HRMS** (ESI+) calculated for m/z $[C_{16}H_{10}N_2NaO_3]^+$, $[M+Na]^+$: 301.0584, found: 301.0573.

30 Fleming, I. *Product Subclass 25: Acylsilanes*, 1st Edition.; Thieme Verlag, **2002**.

31 Welmaker, G. S. A Simple, Efficient Preparation of 1,1-Bis(trimethylsiloxy)-1,3-butadiene, *Org. Prep. Proced. Int.* **1993**, *25*, 595–597.

32 Points III, G. L.; Stout, K. T.; Beaudry, C. M. Regioselective Formation of Substituted Indoles: Formal Synthesis of Lysergic Acid, *Chem. Eur. J.* **2020**, *26*, 16655–16658.

33 Laina-Martín, V.; Humbrías-Martín, J.; Fernández-Salas, J. A.; Alemán, J. Asymmetric Vinylogous Mukaiyama Aldol Reaction of Isatins under Bifunctional Organocatalysis: Enantioselective Synthesis of Substituted 3-Hydroxy-2-oxindoles, *Chem. Commun.* **2018**, *54*, 2781–2784.

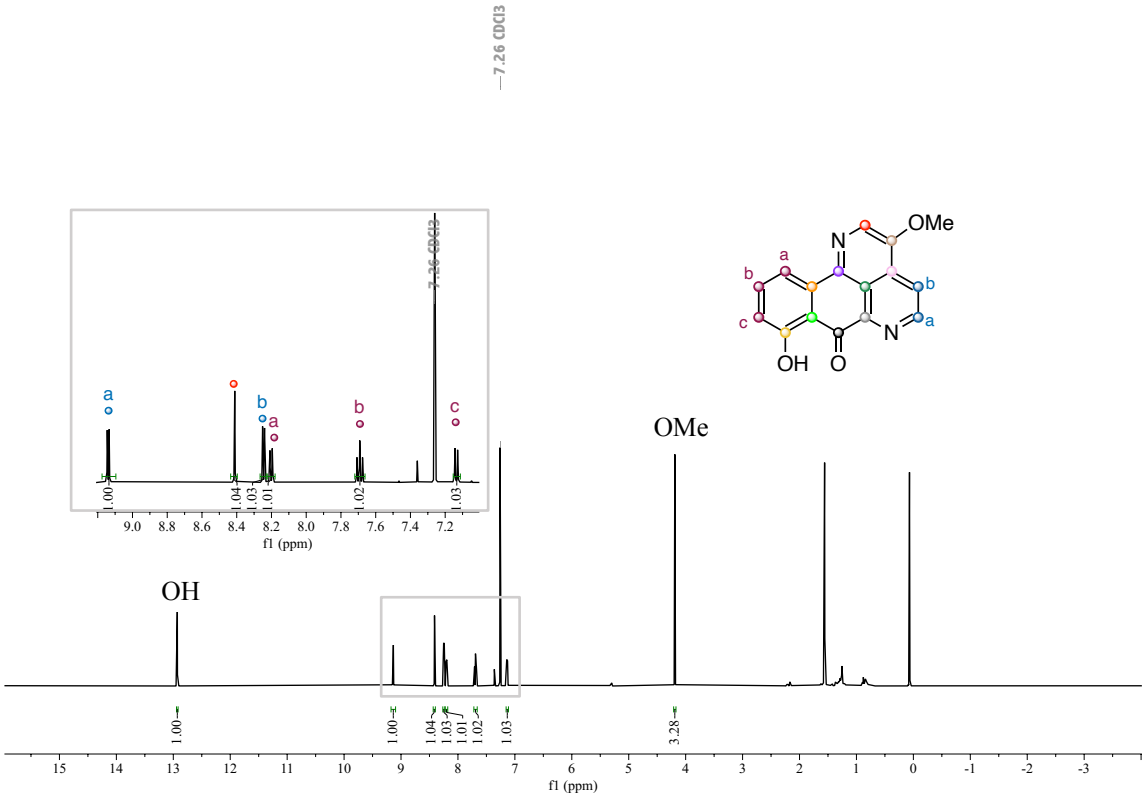


**Figure S1**. $^{1}H$ NMR ($CDCl_3$) for monomarginine **12**.

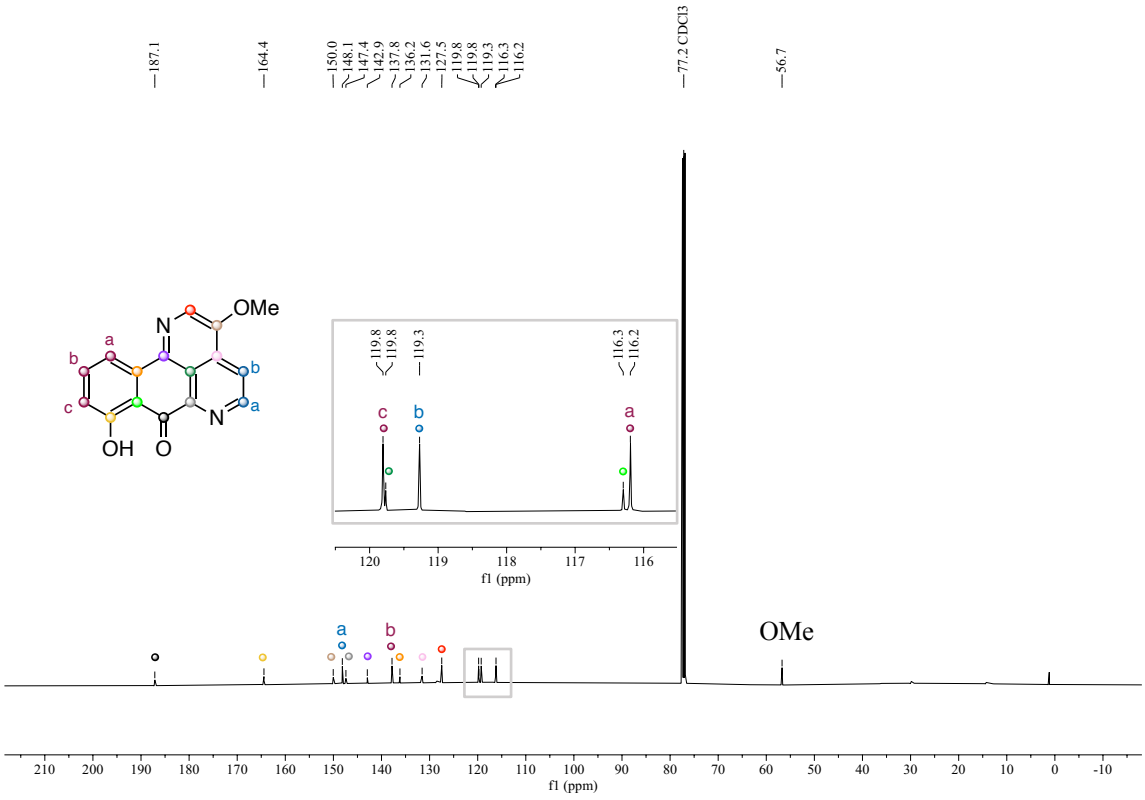


**Figure S2**. $^{13}C\{^{1}H\}$ NMR ($CDCl_3$) for monomarginine **12**.

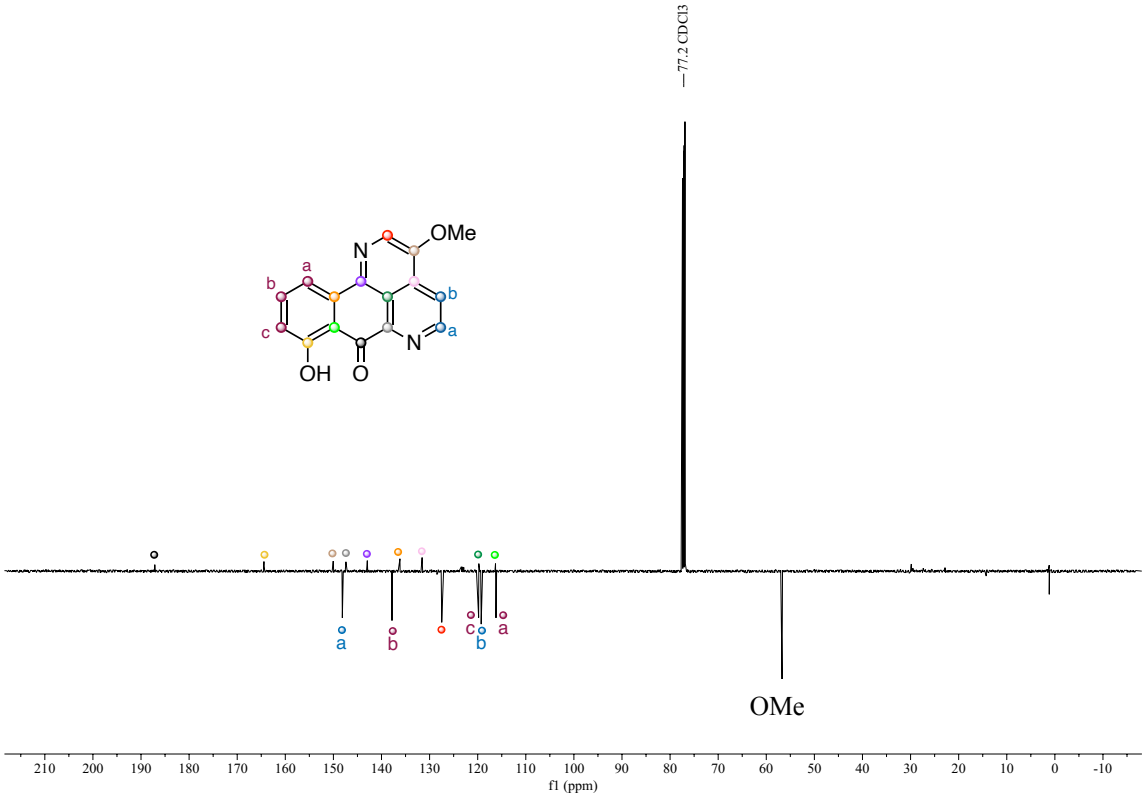


**Figure S3**. DEPTQ-135 NMR for monomarginine **12**. Quaternary carbons pointing upwards, CH and $CH_3$ pointing downwards.

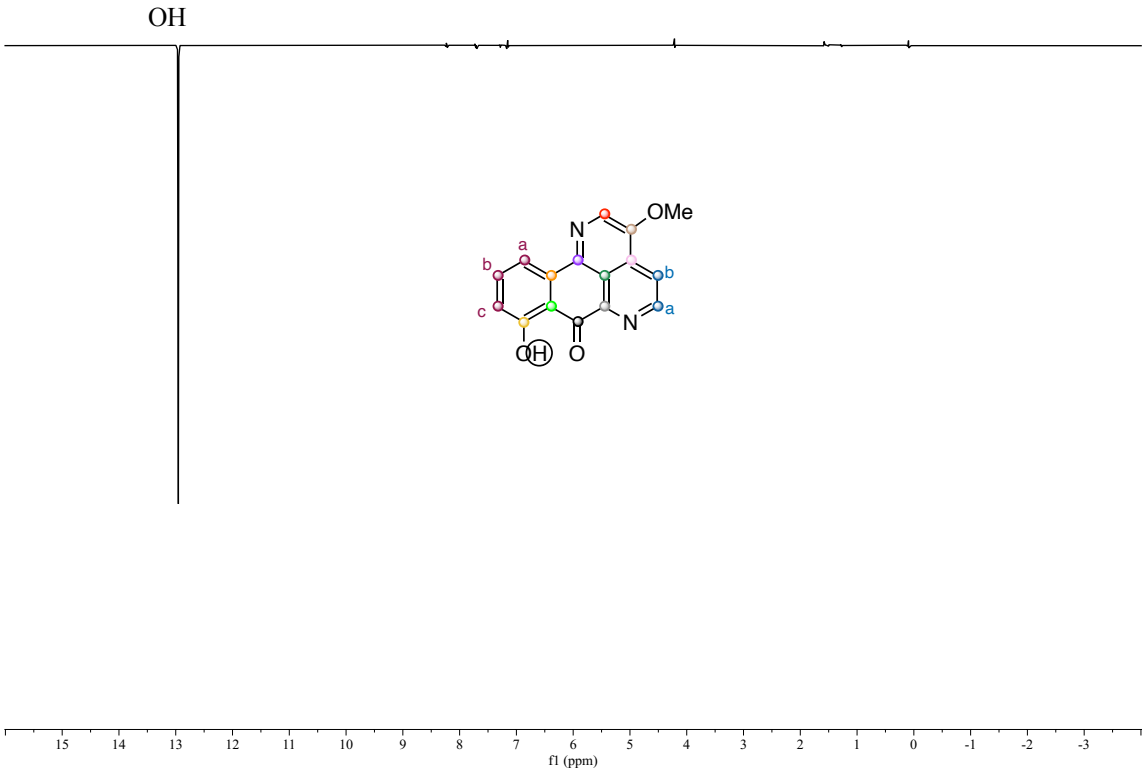


**Figure S4**. Goesy (nOe) NMR, irradiation on OH (12.93 ppm) in monomarginine **12**.

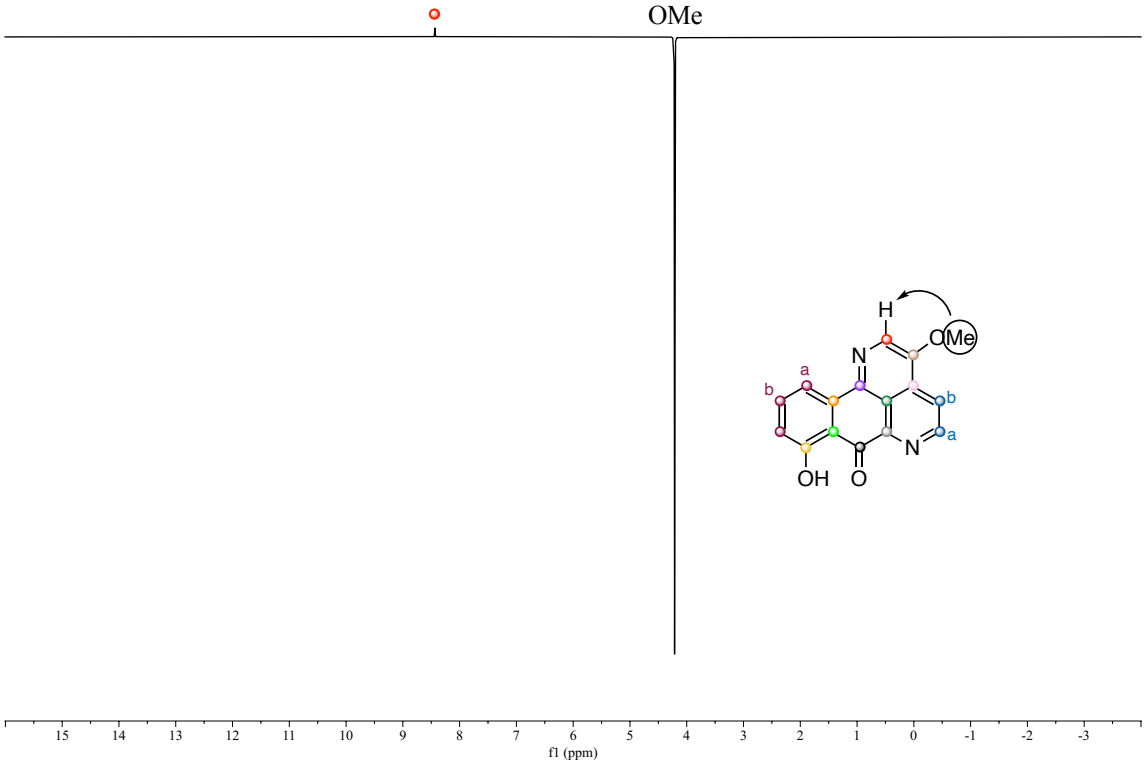


**Figure S5**. Goesy (nOe) NMR, irradiation on OMe (4.19 ppm) in monomarginine **12**.

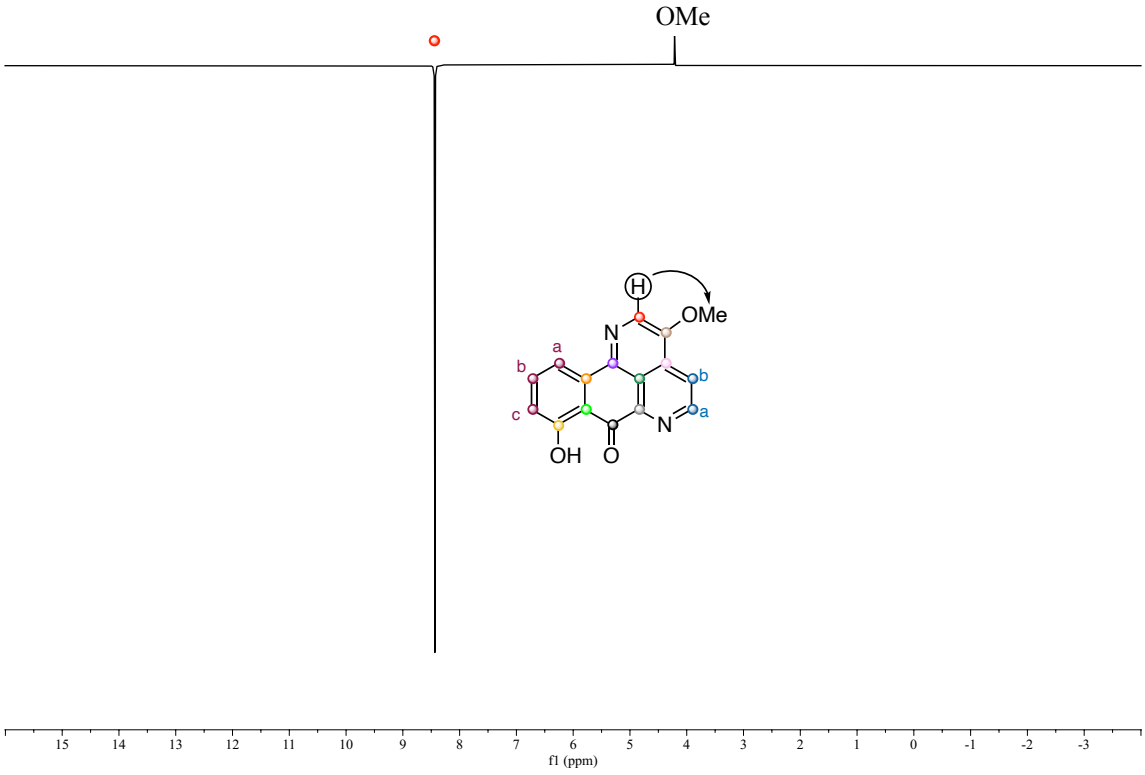


**Figure S6**. Goesy (nOe) NMR, irradiation on H-C5 (8.41 ppm) in monomarginine **12**.

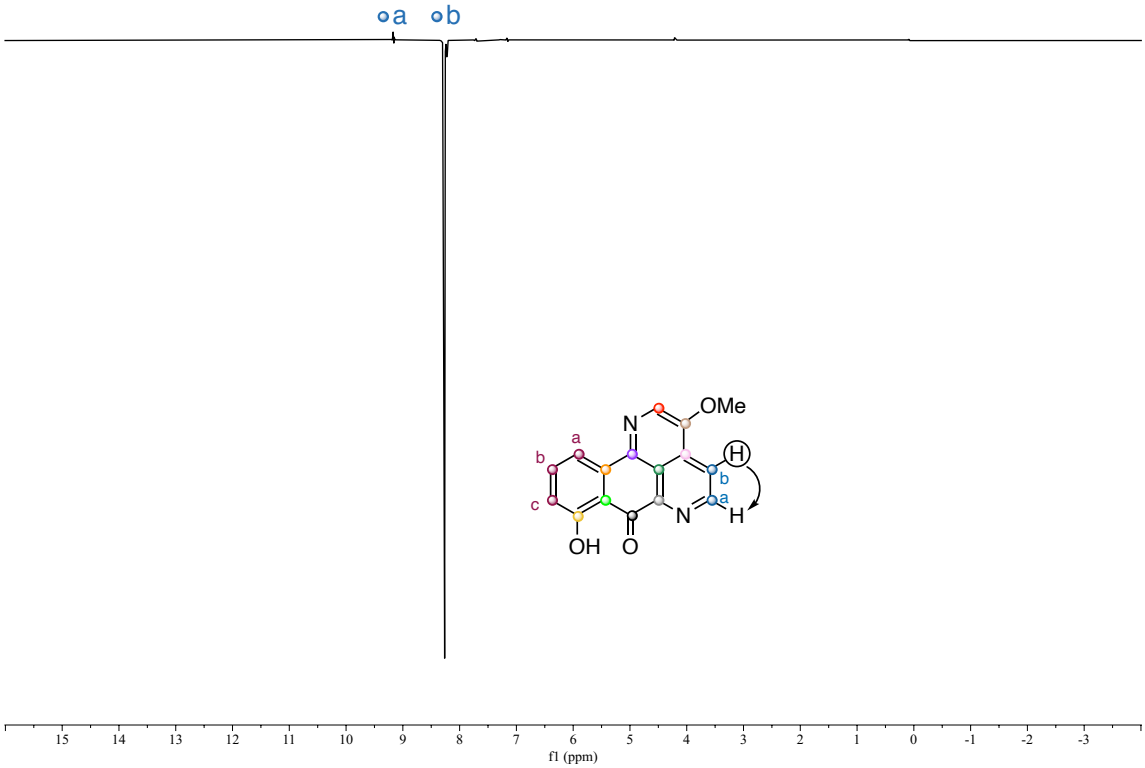


**Figure S7**. Goesy (nOe) NMR, irradiation on H-C3 (8.25 ppm) in monomarginine **12**.

## Two-dimensional analysis for monomarginine (12):

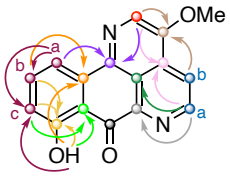


**12**
monomarginine

| | | | | | | | | | | | |
|---|---|---|---|---|---|---|---|---|---|---|---|
| a | C2 | | C4 | | C5b | b | C9 | | C11 |
| b | C3 | | C5 | | C7 | c | C10 | | C11a |
| | C3a | | C5a | a | C8 | | C10a | | C11b |

**Figure S8**. All the HMBC correlations observed for monomarginine **12**.[34]

34 General note for HMBC: correlations shown from H to C. The color of each arrow corresponds to the color of the carbon atom receiving the interaction. Full arrows are for correlations observed.

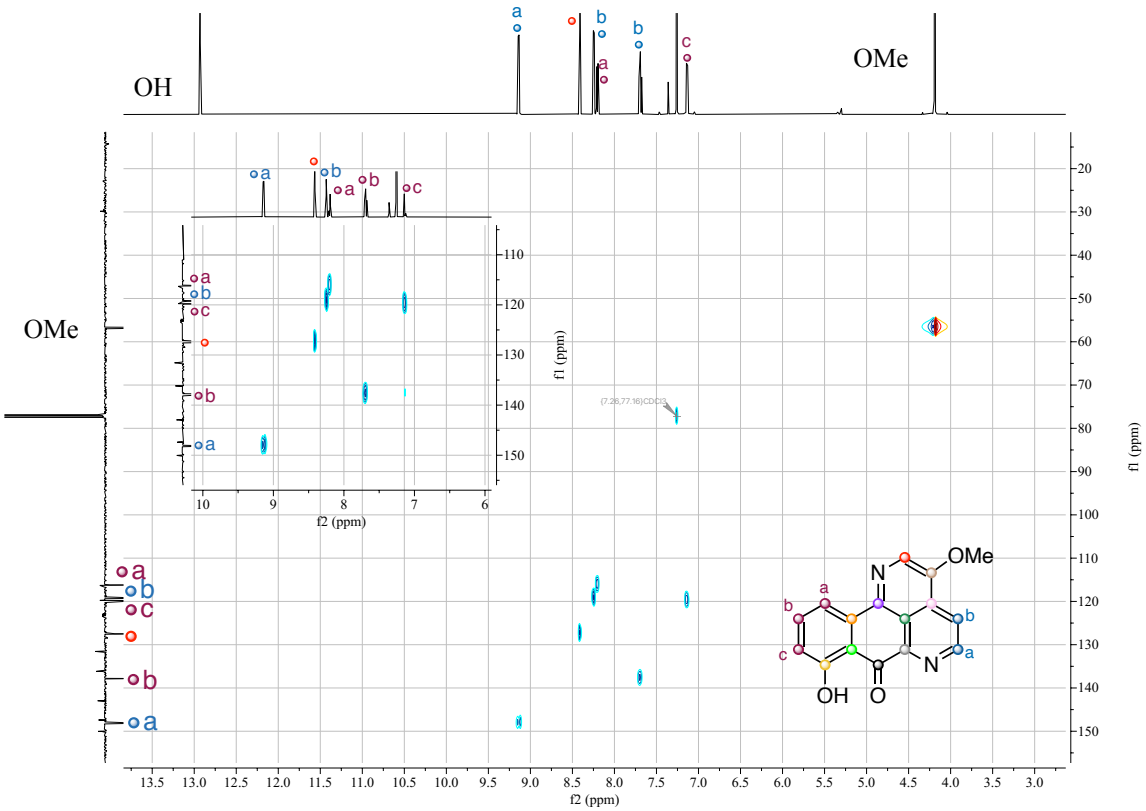


**Figure S9**. HSQC correlations of monomarginine **12**.

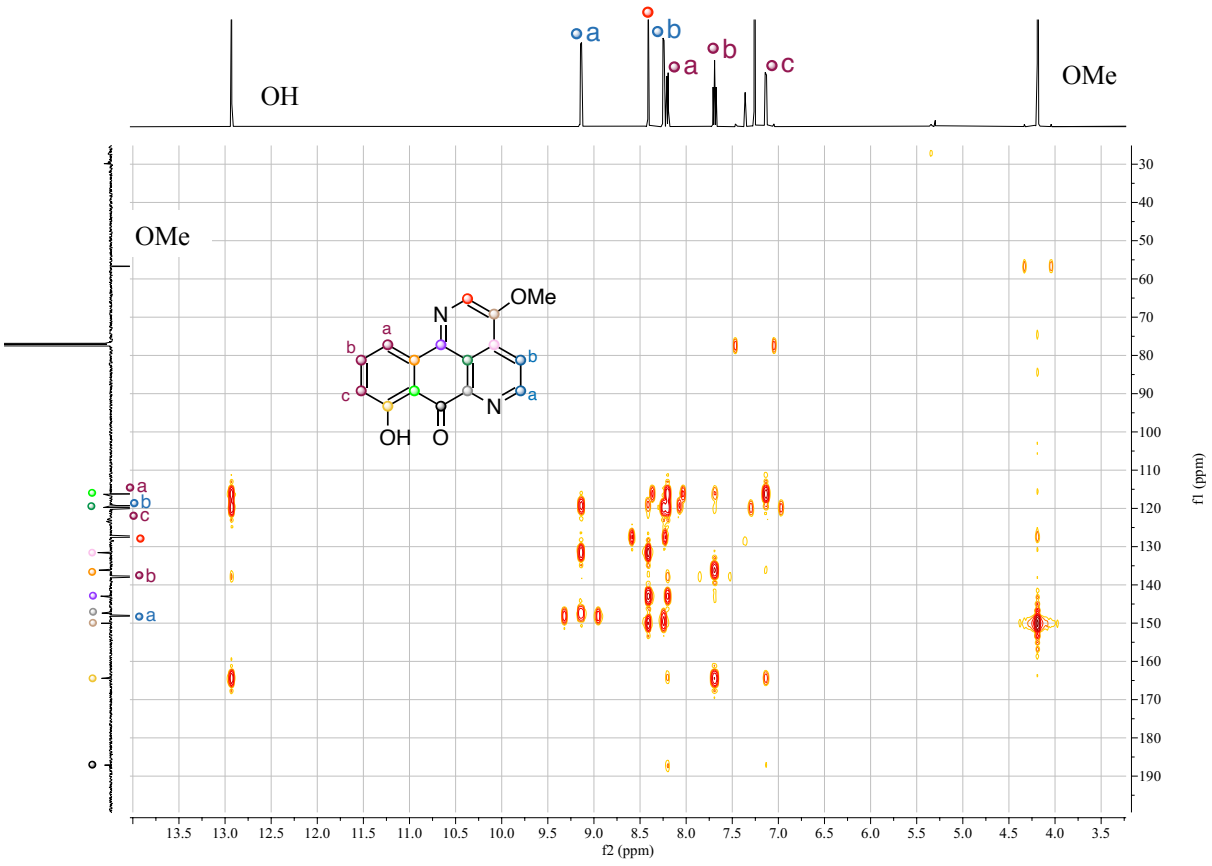


**Figure S10**. Full HMBC spectra for monomarginine **12**.

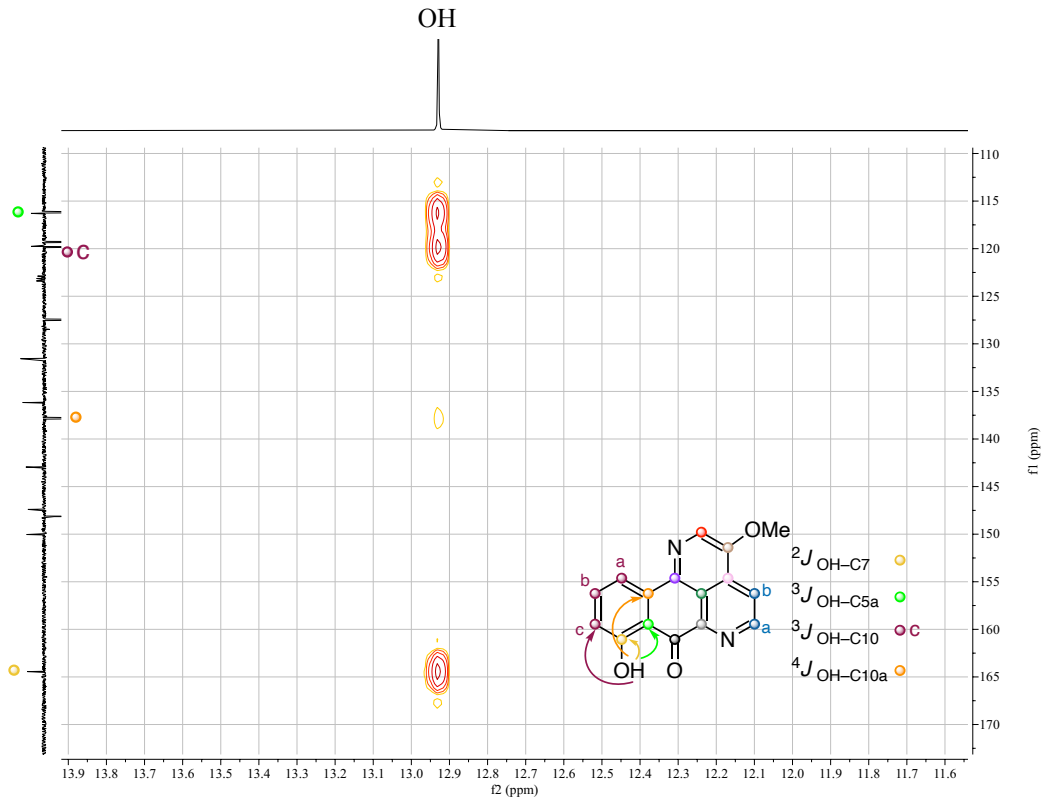


**Figure S11**. HMBC correlations zoomed for OH (12.93 ppm) in monomarginine **12**.

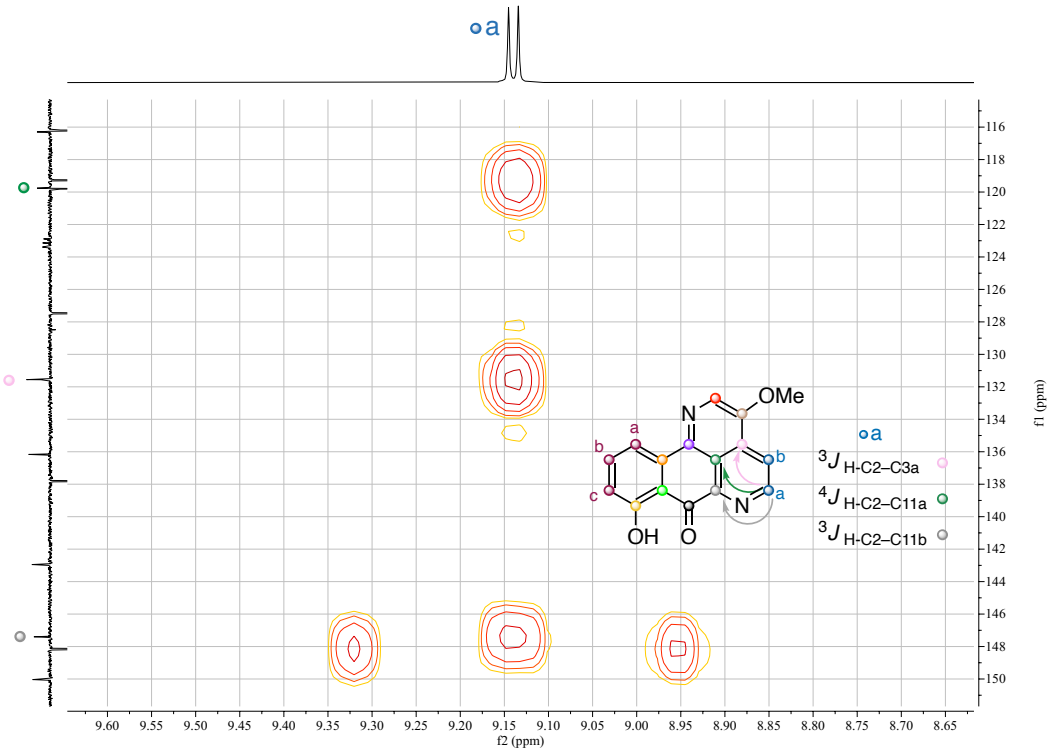


**Figure S12**. HMBC correlations zoomed for H-C2 (9.14 ppm) in monomarginine **12**.

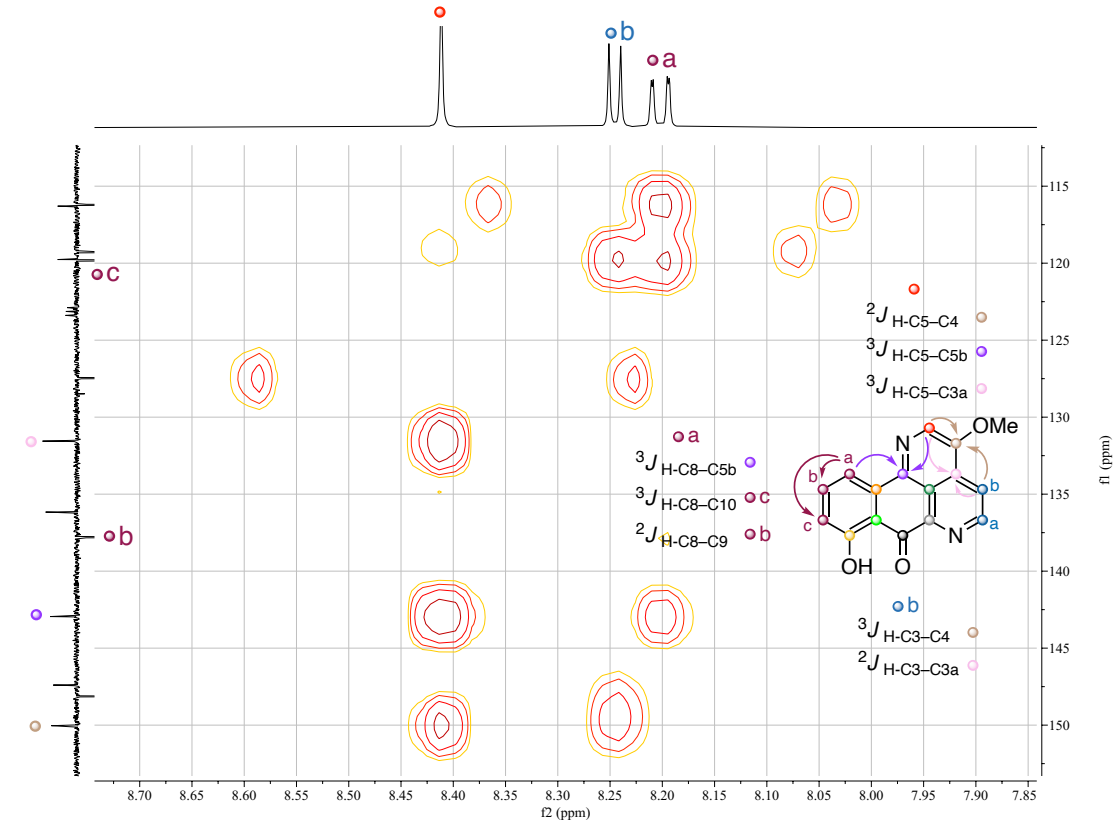


**Figure S13**. HMBC correlations zoomed for H-C5 (8.41 ppm) in monomarginine **12**.

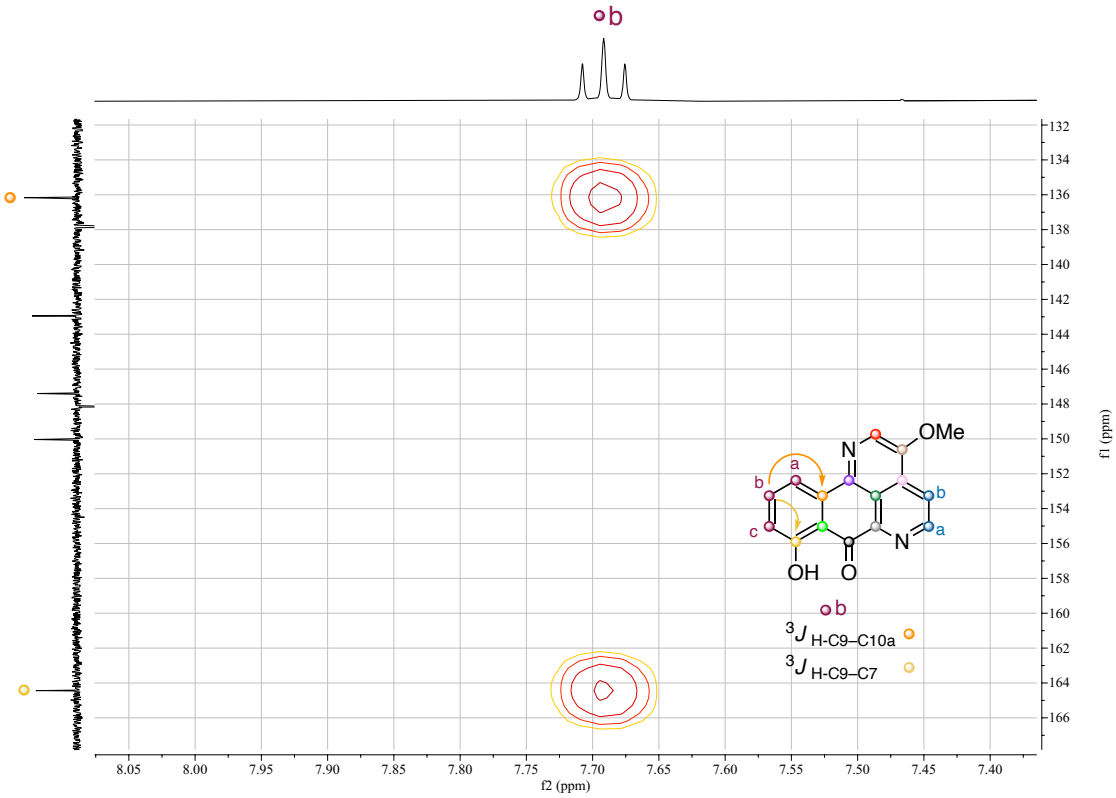


**Figure S14**. HMBC correlations zoomed for H-C9 (7.69 ppm) in monomarginine **12**.

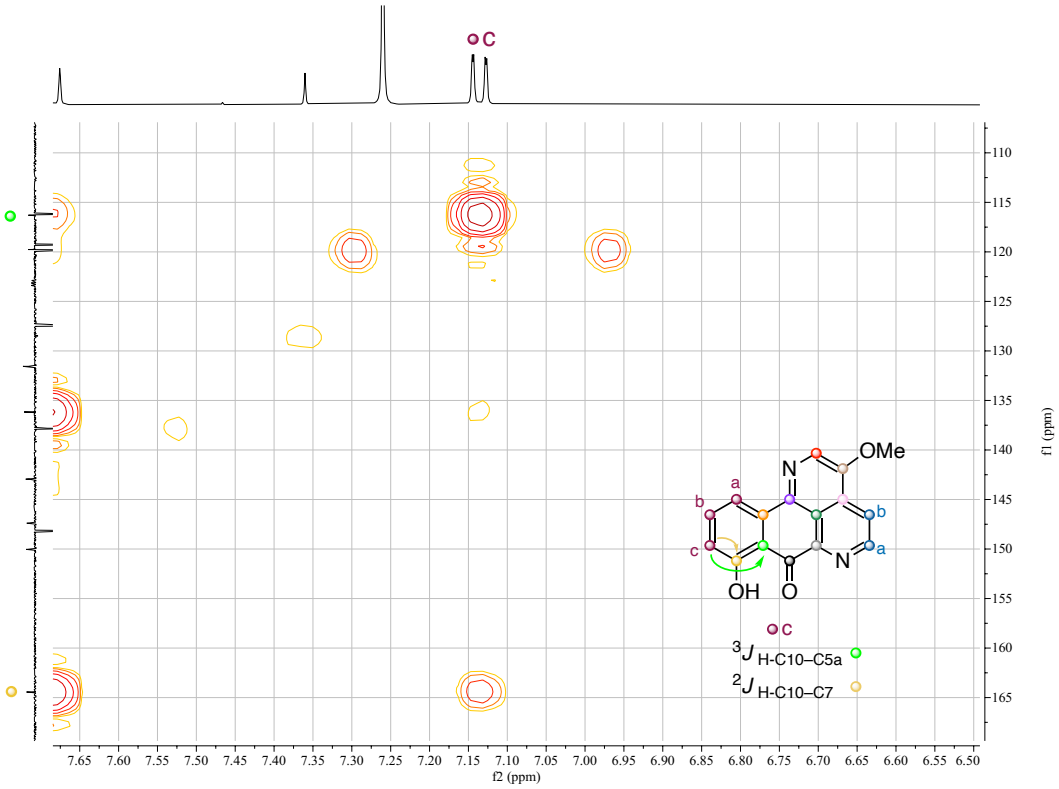


**Figure S15**. HMBC correlations zoomed for H-C10 (7.14 ppm) in monomarginine **12**.

**(*E*)-5-(Triisopropylsilyl)pent-2-en-4-ynal (15)**

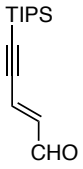


A reported procedure was adapted.[35] Under argon, to a solution of acrylaldehyde (429 mg, 7.65 mmol, 10.0 equiv) in DMF (1.53 mL, 0.5 M) is added $Pd(OAc)_2$ (8.6 mg, 0.04 mmol, 5 mol %), $K_2CO_3$ (264 mg, 1.91 mmol, 2.5 equiv). The mixture is left stirring for 25 min at 25 °C. Then, (bromoethynyl)triisopropylsilane (200 mg, 0.77 mmol, 1.0 equiv) is added dropwise to the solution. After 2 h stirring at 25 °C, the reaction is followed until consumption of the starting material by TLC (CyH/AcOEt 9:1). Reaction is quenched by addition of brine followed by extraction with AcOEt (x3). The combined organic layers are washed with brine (x2), dried over $MgSO_4$, filtered, and concentrated under reduced pressure. The crude was purified by flash column chromatography ($SiO_2$, CyH/AcOEt 90:10). Colorless oil (222 mg, 0.57 mmol, >7:1 *E*:*Z*, 61% yield).

35 Yanmei, W.; Huanfeng, J. Palladium-Catalyzed Coupling Reaction of 1-Bromoalkynes with Olefins to Synthesize Enynes, *Acta Chim. Sin.* **2012**, *70*, 1716.

**$^1$H NMR** ($CDCl_3$, 400 MHz) δ 9.58 (d, 1H, *J* = 7.8), 6.64 (d, 1H, *J* = 15.9), 6.49 (dd, 1H, *J* = 15.9, 7.8), 1.12-1.10 (m, 21H) ppm.

**$^{13}$C NMR** ($CDCl_3$, 100 MHz) δ 193.5, 140.4, 132.7, 108.9, 102.8, 18.7, 11.3 ppm.

The spectral data were fully consistent with those previously reported.[36]

**(*E*)-1,1-Dimethyl-2-((*E*)-5-(triisopropylsilyl)pent-2-en-4-yn-1-ylidene)hydrazine (16)**

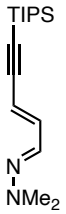


Compound **15** (67 mg, 0.28 mmol, 1.0 equiv) was dissolved in $CH_2Cl_2$ (2.8 mL, 0.1 M). *N*,*N*-Dimethylhydrazine (18.7 mg, 0.31 mmol, 1.1 eq.) and then AcOH (17.8 μL, 1.1 equiv) were added and the reaction was stirred at 25 °C until TLC indicated complete consumption of starting materials. The reaction mixture was poured into water and extracted AcOEt (x2). The combined organic layers were washed with brine and dried over $MgSO_4$. After filtration, the mixture was concentrated under reduced pressure. The crude was purified by flash column chromatography ($SiO_2$, CyH/AcOEt 98:2). Colorless oil (60 mg, 0.22 mmol, 4:1 *E*:*Z*, 76% yield).

**$^1$H NMR** (400 MHz, $CDCl_3$) δ 6.91 (d, *J* = 9.2 Hz, 1H), 6.77 (dd, *J* = 15.7, 9.2 Hz, 1H), 5.64 (d, *J* = 15.8 Hz, 1H), 2.93 (s, 6H), 1.10 (m, 3H), 1.08 (s, 18H) ppm.

**$^{13}$C NMR** (126 MHz, $CDCl_3$) δ 141.3, 132.6, 109.6, 106.8, 94.3, 42.7, 18.8, 11.4 ppm.

**General procedure GP1: amine and brominated building block coupling**

Amine **20** (1.5 equiv) is added to a solution of the corresponding brominated juglone derivative (1.0 equiv) in EtOH (0.03 M) in the presence of $Et_3N$ (2.2 equiv). The reaction was stirred at 25 °C for 2 h, with reaction completion determined by TLC monitoring based on the absence of starting material. Then, the reaction mixture was concentrated under reduced pressure. The crude was purified by flash column chromatography or recrystallization method.

36 Sohn, S. S.; Rosen, E. L.; Bode, J. W. *N*-Heterocyclic Carbene-Catalyzed Generation of Homoenolates: γ-Butyrolactones by Direct Annulations of Enals and Aldehydes, *J. Am. Chem. Soc.* **2004**, *126*, 14370–14371.

**_tert_-Butyl (5-(triisopropylsilyl)penta-2,4-diyn-1-yl)carbamate (19)**

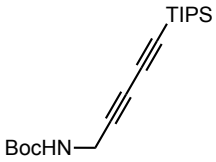


*N*-Boc-propargylamine **18** (86.2 mg, 0.56 mmol, 1.1 equiv) followed by (bromoethynyl)triisopropylsilane **12** (132 mg, 0.51 mmol, 1.0 equiv) were added to a stirred solution of CuCl (2.5 mg, 25 μmol, 5 mol %), $NH_2OH{\cdot}HCI$ (10.5 mg, 152 μmol, 0.3 equiv) and aqueous $EtNH_2$ (0.25 mL, 2M in $H_2O$) in MeOH (1.68 mL, 0.3 M) at 0 °C. After 10 min at 0 °C, $H_2O$ was added, and the mixture was extracted with $Et_2O$ (x3). The combined organic layers were washed with brine and dried over $MgSO_4$, filtered and concentrated under reduced pressure. The crude was purified by flash column chromatography ($SiO_2$, CyH/AcOEt 80:20). Off-white solid (77 mg, 0.23 mmol, 45% yield).

**M.p.** = 60 °C.

**$^1$H NMR** (500 MHz, $CDCl_3$) δ 4.71 (bs, 1H), 4.01 (d, *J* = 5.6 Hz, 2H), 1.44 (s, 9H), 1.07 (s, 21H) ppm.

**$^{13}$C NMR** (126 MHz, $CDCl_3$) δ 89.2, 83.6, 73.3, 68.6, 28.5, 18.6, 11.4 ppm.

**HRMS** (ESI+) calculated for m/z $[C_{19}H_{33}NNaO_2Si]^+$, $[M+Na]^+$: 358.2173; found: 358.2179.

**5-(Triisopropylsilyl)penta-2,4-diyn-1-amine (20)**

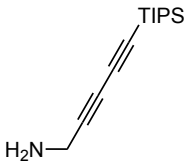


To a solution of **19** (1.0 equiv) in $CH_2Cl_2$ (0.2 M), was added TFA (10.0 equiv). After 1 h, concentration under reduced pressure provides the free amine which was used directly without further purification.

**$^1$H NMR** (500 MHz, $CDCl_3$) δ 3.94 (s, 2H), 1.08 (d, *J* = 3.1 Hz, 21H) ppm.

**3-Bromojuglone (21)**

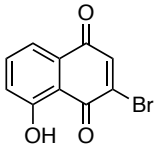


A reported procedure was followed.[37] A suspension of juglone (2.0 g, 9.19 mmol, 1 equiv) in AcOH (23 mL, 0.4 M) was treated in the dark at 25 °C with bromine (0.47 mL, 9.19 mmol, 1.0 equiv). After stirring for 60 min, the reaction mixture was poured onto ice. The resultant slurry was stirred for 10 min after which the dibrominated intermediate was filtered off under reduced pressure. The orange solid was washed with a little amount of ice-water and then immediately treated with EtOH (80 mL) and stirred for 10 min under reflux (80 ºC) using a pre-heated oil bath. The mixture was cooled down to room temperature and the red precipitate was filtered off under reduced pressure. The residue was washed with a small amount of cold EtOH and then subjected to flash chromatography ($SiO_2$, CyH/$CH_2Cl_2$ 60:40). Orange solid (901 mg, 5.56 mmol, 39%).

**$^1$H NMR** (300 MHz, $CDCl_3$) δ 11.73 (s, 1H), 7.68 (t, *J* = 7.4 Hz, 1H), 7.64 (dd, *J* = 7.4, 2.0 Hz, 1H), 7.50 (s, 1H), 7.31 (dd, *J* = 7.5, 2.0 Hz, 1H) ppm.

**$^{13}$C NMR** (500 MHz, $CDCl_3$) δ 182.8, 181.6, 162.0, 141.2, 139.3, 137.2, 131.6, 124.7, 119.9, 113.9 ppm.

The spectral data were fully consistent with those previously reported and its structure was confirmed by X-ray diffraction.

**5-Hydroxy-2-((5-(triisopropylsilyl)penta-2,4-diyn-1-yl)amino)naphthalene-1,4-dione (22)**

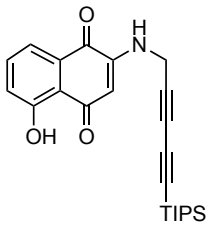


General procedure **GP1** was followed using freshly prepared amine **20** (70.0 mg, 0.3 mmol, 1.5 equiv) and 3-bromojuglone (50 mg, 0.2 mmol, 1.0 equiv). Purification by flash column chromatography ($SiO_2$, CyH/AcOEt 90:20 to 60:40) afforded **22** as an orange solid (20 mg, 0.5 mmol, 25% yield).

37 Tietze, L. F.; Singidi, R. R.; Gericke, K. M. Total Synthesis of the Proposed Structure of the Anthrapyran Metabolite δ-Indomycinone, *Chem. Eur. J.* **2007**, *13*, 9939–9947.

**$^{1}$H NMR** (500 MHz, $CDCl_3$) δ 12.85 (s, 1H), 7.59 (dd, *J* = 7.5, 1.2 Hz, 1H), 7.48 (t, *J* = 7.5 Hz, 1H), 7.25 (dd, *J* = 8.3, 1.1 Hz, 1H), 6.16 (t, *J* = 5.9 Hz, 1H), 5.74 (s, 1H), 4.09 (d, *J* = 5.8 Hz, 2H), 1.07 (bs, 21H) ppm.

**$^{13}$C NMR** (126 MHz, $CDCl_3$) δ 189.3, 180.8, 161.3, 147.8, 134.4, 130.5, 126.2, 119.4, 114.9, 101.9, 88.5, 85.2, 70.5, 69.8, 33.1, 27.1, 18.6, 11.3 ppm.

**HRMS** (ESI+) calculated for m/z $[C_{24}H_{29}NNaO_3Si]^+$, $[M+Na]^+$: 430.1809; found: 430.1822.

**Two-dimensional analysis for 22:**

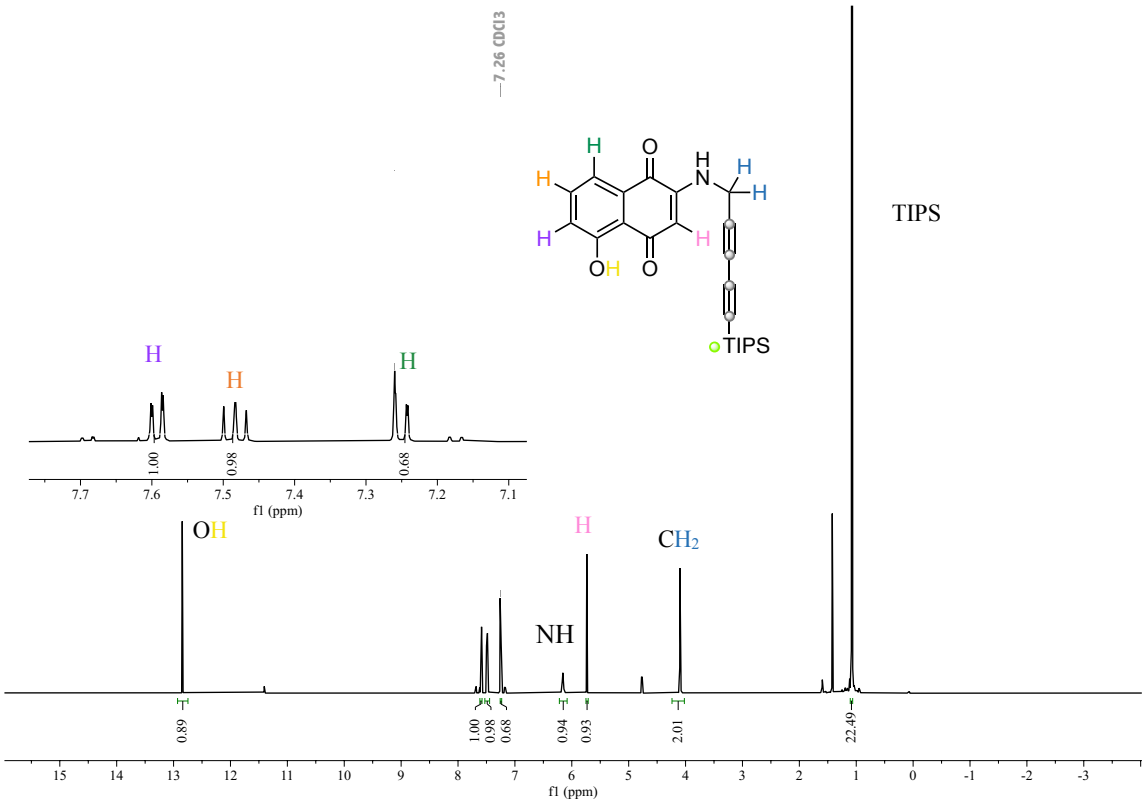


**Figure S16**. $^{1}$H NMR ($CDCl_3$) for **22**.

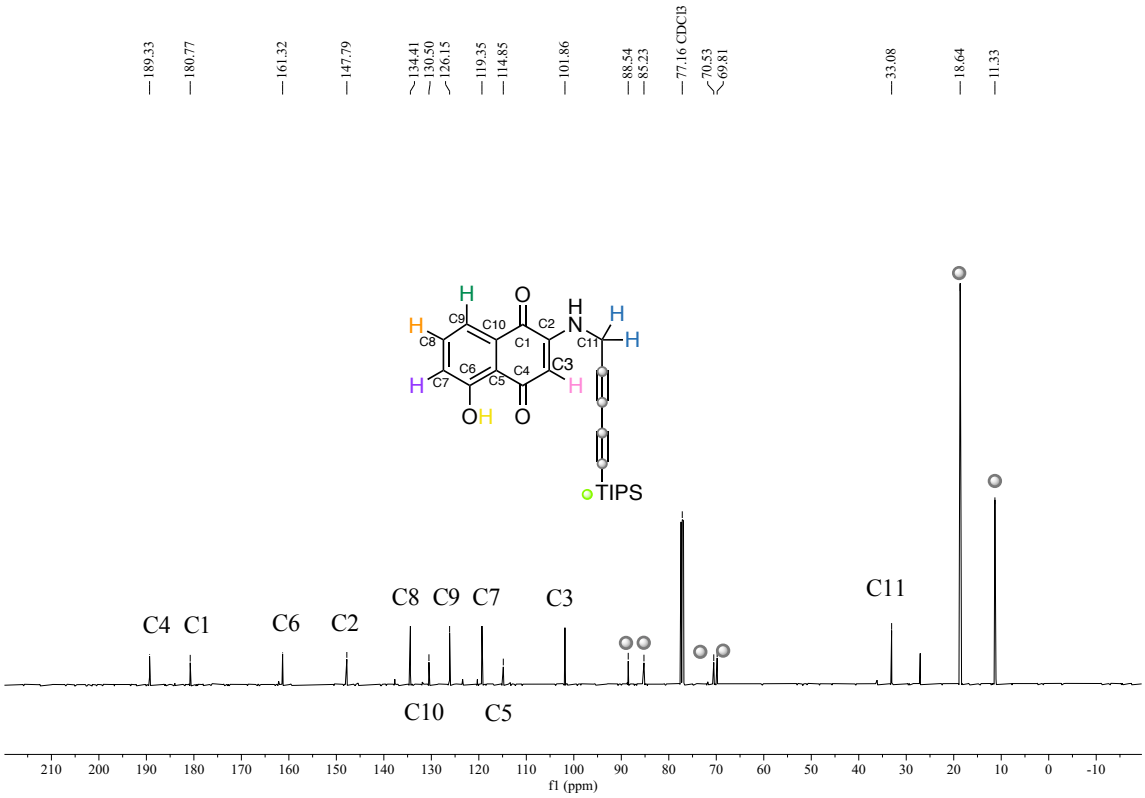


**Figure S17**. $^{13}$C {$^{1}$H} NMR ($CDCl_3$) for **22**.

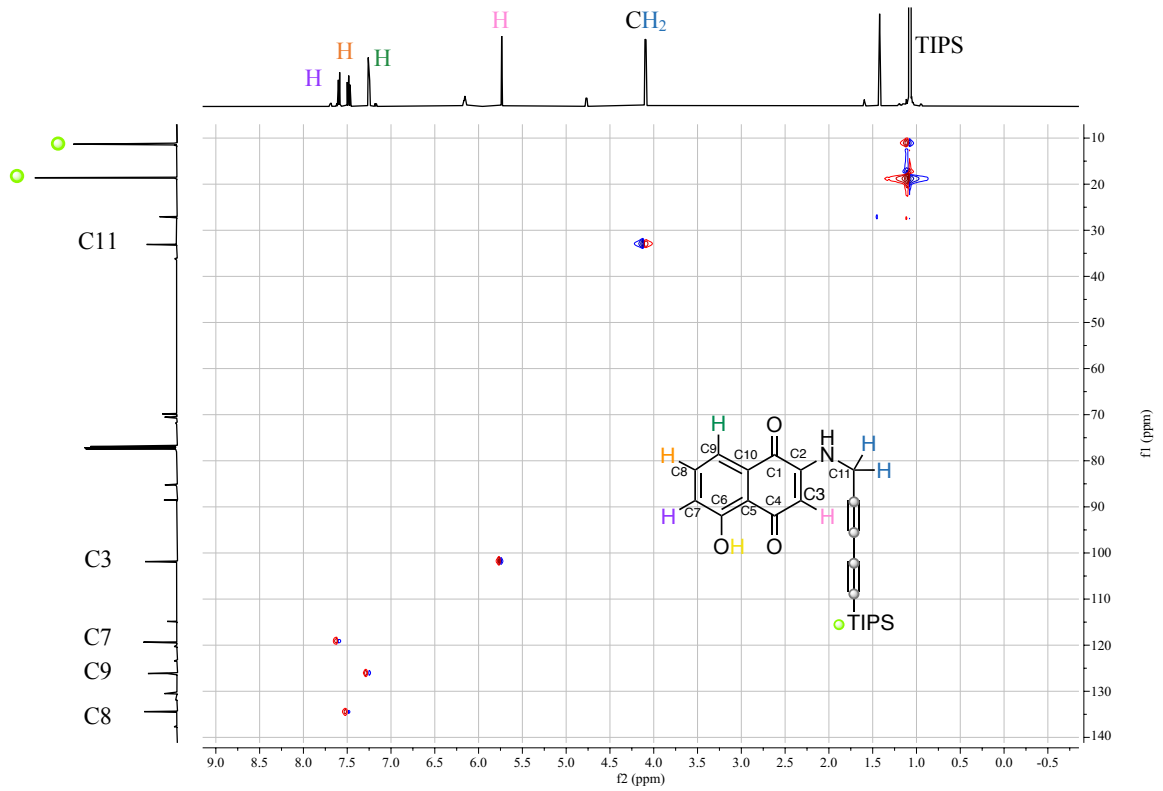


**Figure S18**. HSQC for **22**.

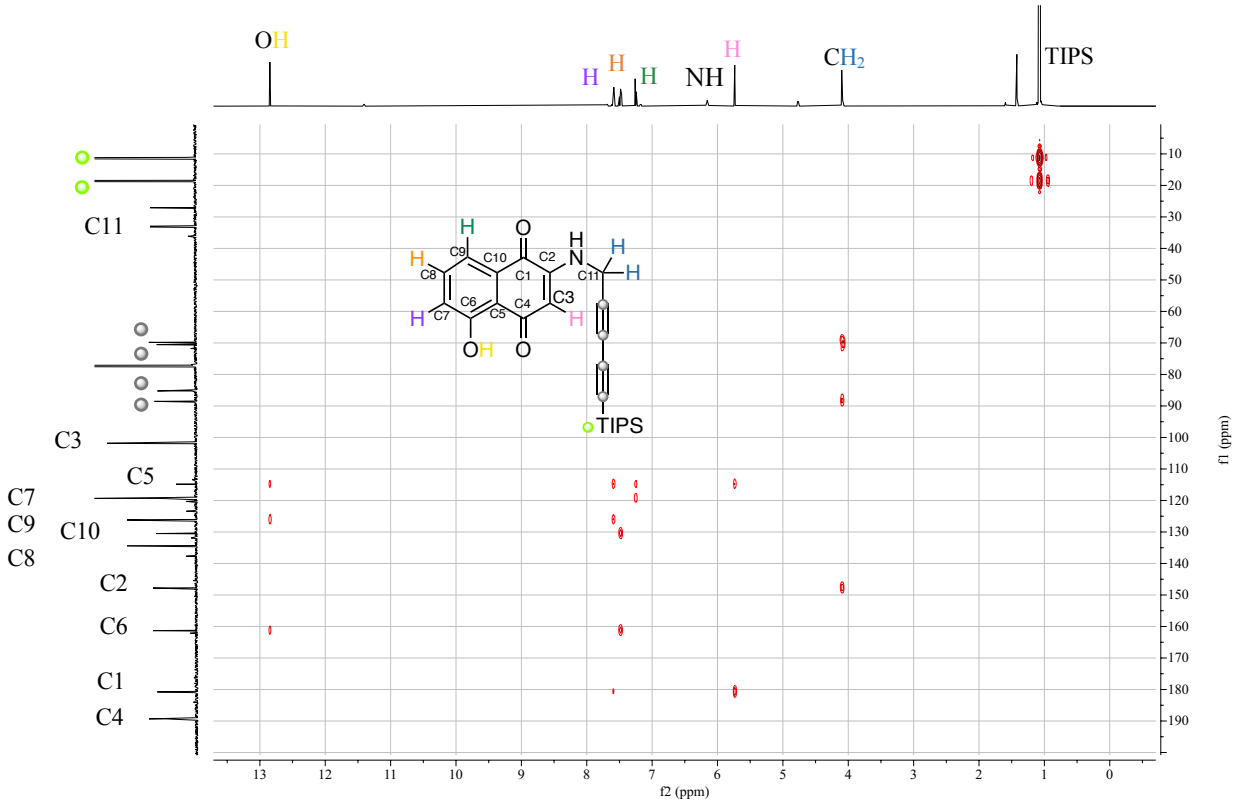


**Figure S19**. Fulls HMBC of **22**.

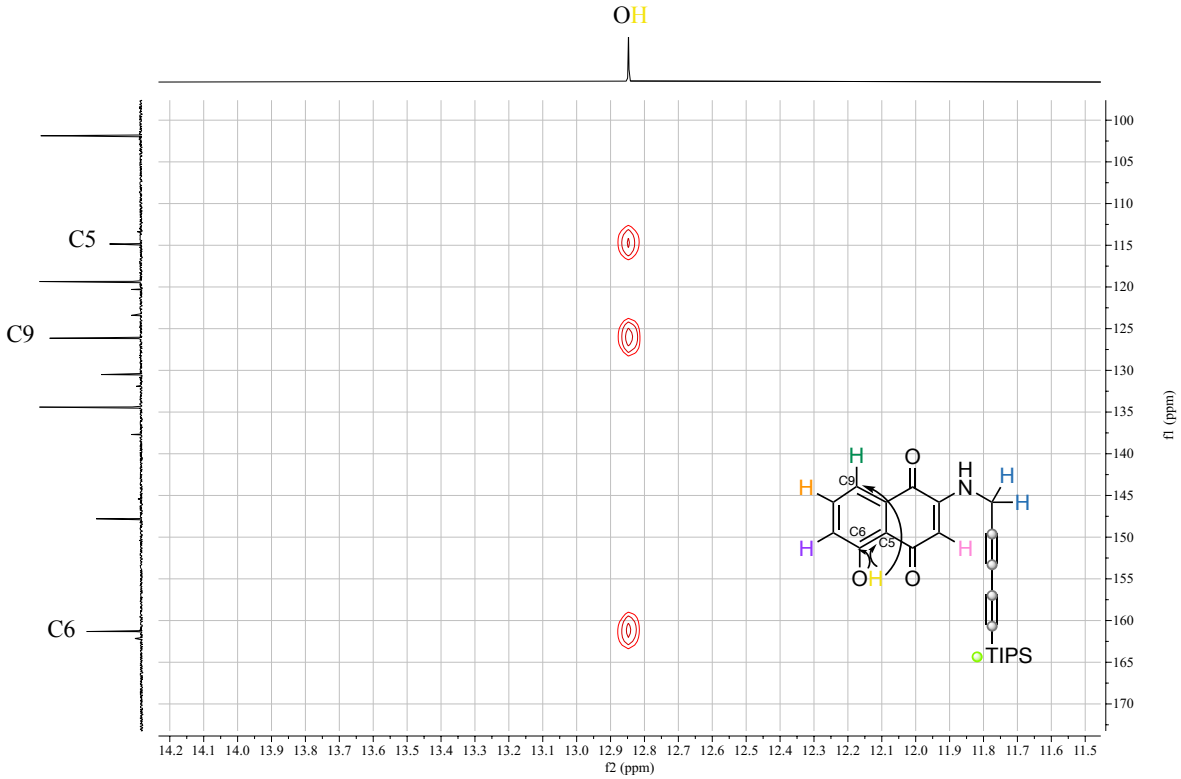


**Figure S20**. HMBC correlations for OH (12.85ppm) in **22**.

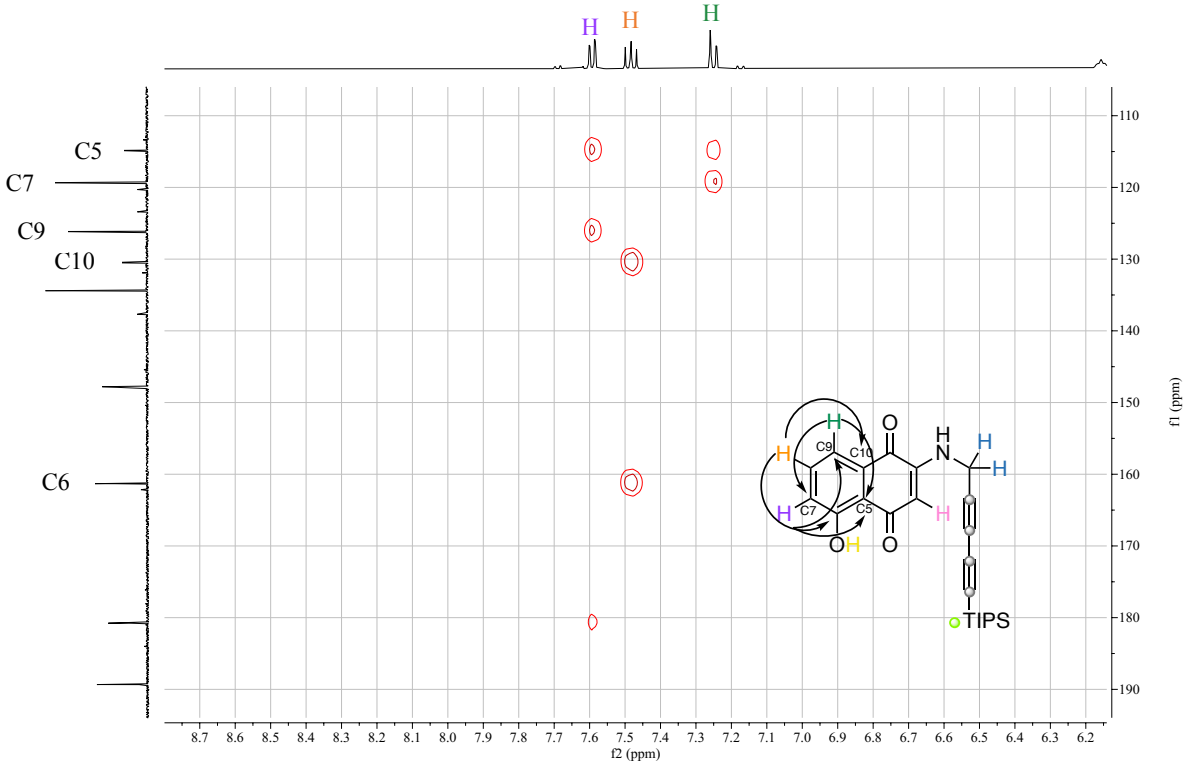


**Figure S21**. HMBC correlations for H (7.25ppm), H (7.48 ppm) and H (7.59 ppm) in **22**.

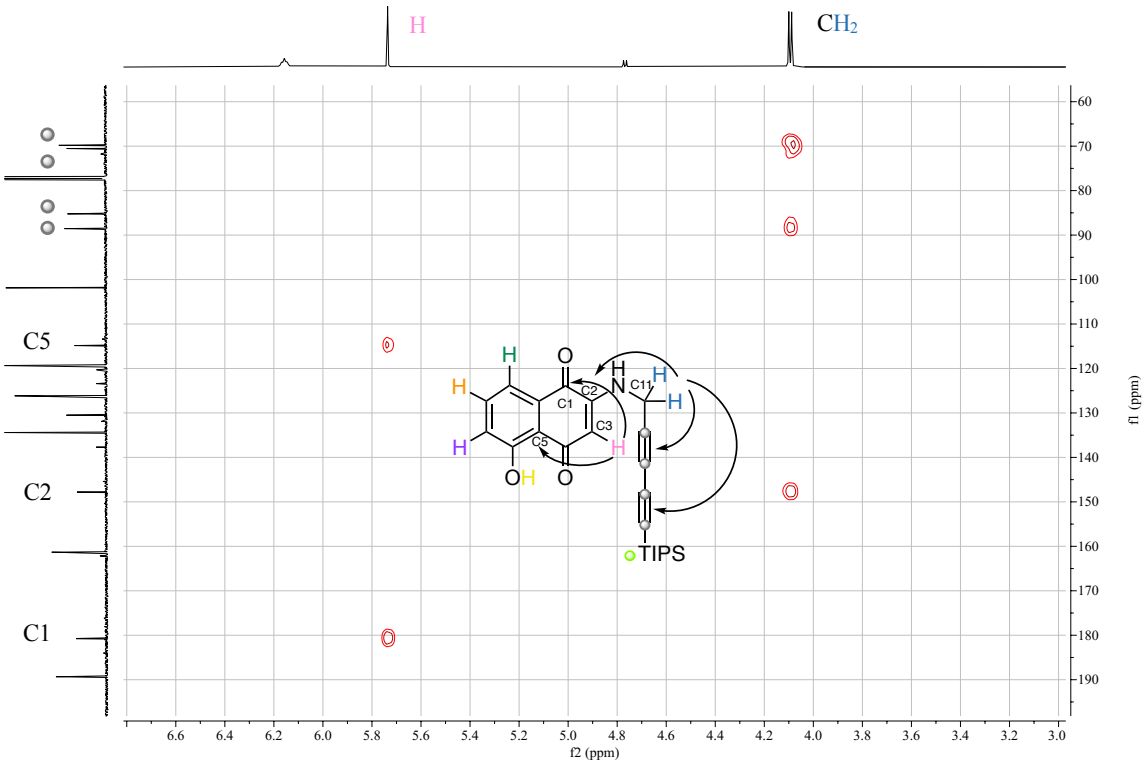


**Figure S22**. HMBC correlations for $CH_2$ (12.85ppm) and CH (5.74 ppm) in **22**.

**4-Ethynyl-6-hydroxybenzo[*g*]quinoline-5,10-dione (23)**

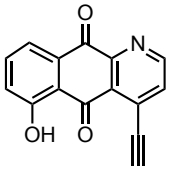

To a solution of **23** (27 mg, 0.07 mmol, 1.0 equiv) in acetic acid (1.3 mL, 0.05 M), was added chloro(triphenylphpsphine)gold(I) (3.3 mg, 6.62 µmol, 0.1 equiv) followed by AgOTf (1.7 mg, 6.62 µmol, 0.1 equiv) at 23 °C. Reaction was heated to 100 °C and was kept stirring for 1 h. Then, the solvent was removed under reduced pressure and the residue was redissolved in $CH_2Cl_2$, washed with $NaHCO_3$ sat. aq. solution (x2), water (x2), and brine (x2), successively. Then, the crude was filtered through a short $SiO_2$ pipette before directly using it in the next step without further purification. The crude was dissolved in THF (0.67 mL, 0.1 M) before adding TBAF (1 M in THF) (0.13 mL, 0.13 mmol, 2.0 equiv) at 23 °C. After 2h, solvent was removed under reduced pressure. Purification by flash column chromatography ($SiO_2$, CyH/AcOEt 100:0 to 60:40) afforded **23** as dark brown oil (5 mg, 0.02 mmol, 30% yield).

**$^1$H NMR** (500 MHz, $CDCl_3$) δ 12.37 (s, 1H), 9.07 (d, *J* = 4.9 Hz, 1H), 7.97 (dd, *J* = 7.5, 1.2 Hz, 1H), 7.85 (d, *J* = 4.9 Hz, 1H), 7.76 (dd, *J* = 8.4, 7.5 Hz, 1H), 7.41 (dd, *J* = 8.4, 1.2 Hz, 1H), 3.96 (s, 1H) ppm.

**$^{13}$C NMR** (126 MHz, $CDCl_3$) δ 187.2, 180.6, 162.9, 154.2, 150.1, 137.3, 133.7, 132.7, 131.4, 129.9, 125.4, 120.5, 115.9, 90.2, 80.5 ppm.

**HRMS** (ESI+) calculated for m/z $[C_{15}H_7NNaO_3]^+$, $[M+H]^+$: 272.0318; found: 272.0325.

The structure of this compound was also confirmed by X-ray diffraction.

**6-Hydroxy-4-(1-tosyl-1*H*-1,2,3-triazol-5-yl)benzo[*g*]quinoline-5,10-dione (24)**

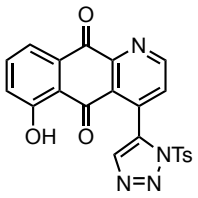


CuTC (1 mg, 5 μmol, 0.3 equiv) was added to a solution of **23** (4 mg, 16.1 μmol, 1.0 equiv) in toluene (80.3 μL, 0.2 M). Solution was cooled to 0 °C and *p*-toluenesulfonylazide (26.4 mg, 16.1 μmol, 1.0 equiv) was added. The reaction mixture was allowed to slowly warm to 23 °C. Reaction was quenched by addition of NH4Cl sat. aq. solution. Then, extraction with AcOEt (x2), filtration through celite and concentrated under reduced pressure. No further purification was performed. Dark red oil (3 mg, 7 μmol, 40% yield).

**$^1$H NMR** (500 MHz, $CDCl_3$) δ 12.15 (s, 1H), 9.13 (d, $J$ = 4.9 Hz, 1H), 8.88 (s, 1H), 8.20 (d, $J$ = 5.0 Hz, 1H), 8.14 – 8.08 (m, 2H), 7.95 (dd, $J$ = 7.5, 1.1 Hz, 1H), 7.75 (dd, $J$ = 8.4, 7.5 Hz, 1H), 7.49 – 7.44 (m, 2H), 7.38 (dd, $J$ = 8.4, 1.1 Hz, 1H), 2.49 (s, 3H) ppm.

**$^{13}$C NMR** (126 MHz, $CDCl_3$) δ 189.2, 180.7, 162.8, 154.8, 150.7, 148.0, 142.4, 139.4, 137.5, 132.9, 132.6, 130.8, 130.4, 129.1, 127.1, 126.3, 125.5, 120.5, 116.2, 22.1 ppm.

**HRMS** (ESI+) calculated for m/z $[C_{22}H_{14}N_4NaO_5S]^+$, $[M+Na]^+$: 469.0577; found: 469.0591.

**8-Hydroxy-2-((5-(triisopropylsilyl)penta-2,4-diyn-1-yl)amino)naphthalene-1,4-dione (27a)**

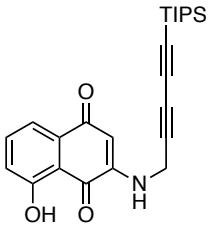


Compound **27a** was prepared following general procedure **GP1** was followed using freshly prepared amine **20** (60 mg, 0.25 mmol, 1.5 equiv) and **26a** (43 mg, 0.17 mmol, 1.0 equiv). Purification by flash column chromatography ($SiO_2$, CyH/AcOEt 100:0 to 95:5) afforded **27a** as an orange solid (11 mg, 0.03 mmol, 16% yield).

**$^{1}$H NMR** (500 MHz, $CDCl_3$) δ 11.49 (bs, 1H) 7.63 (q, *J* = 3.6 Hz, 2H), 7.19 – 7.12 (m, 1H), 5.98 (t, *J* = 5.9 Hz, 1H), 5.81 (bs, 1H), 4.09 (d, *J* = 5.8 Hz, 1H), 1.25 (bs, 3H), 1.07 (bs, 18H) ppm.

**$^{13}$C NMR** (126 MHz, $CDCl_3$) δ 185.7, 182.5, 161.9, 146.9, 137.9, 133.3, 122.7, 119.1, 114.1, 103.5, 88.58, 85.1, 70.4, 70.0, 33.0, 18.7, 11.3 ppm.

**HRMS** (ESI+) calculated for m/z $[C_{24}H_{30}NO_3Si]^+$, $[M+H]^+$: 408.1989; found: 408.1990.

**Two-dimensional analysis for 27a:**

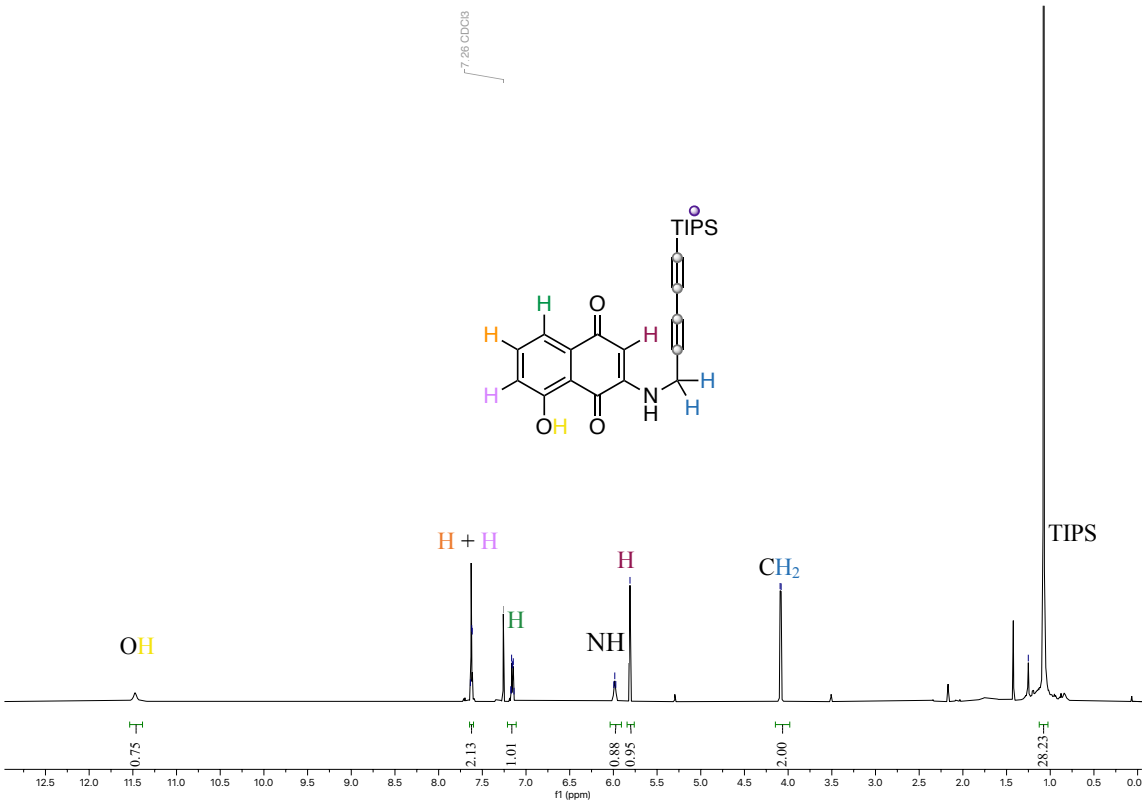


**Figure S23**. $^{1}$H NMR ($CDCl_3$) for **27a**.

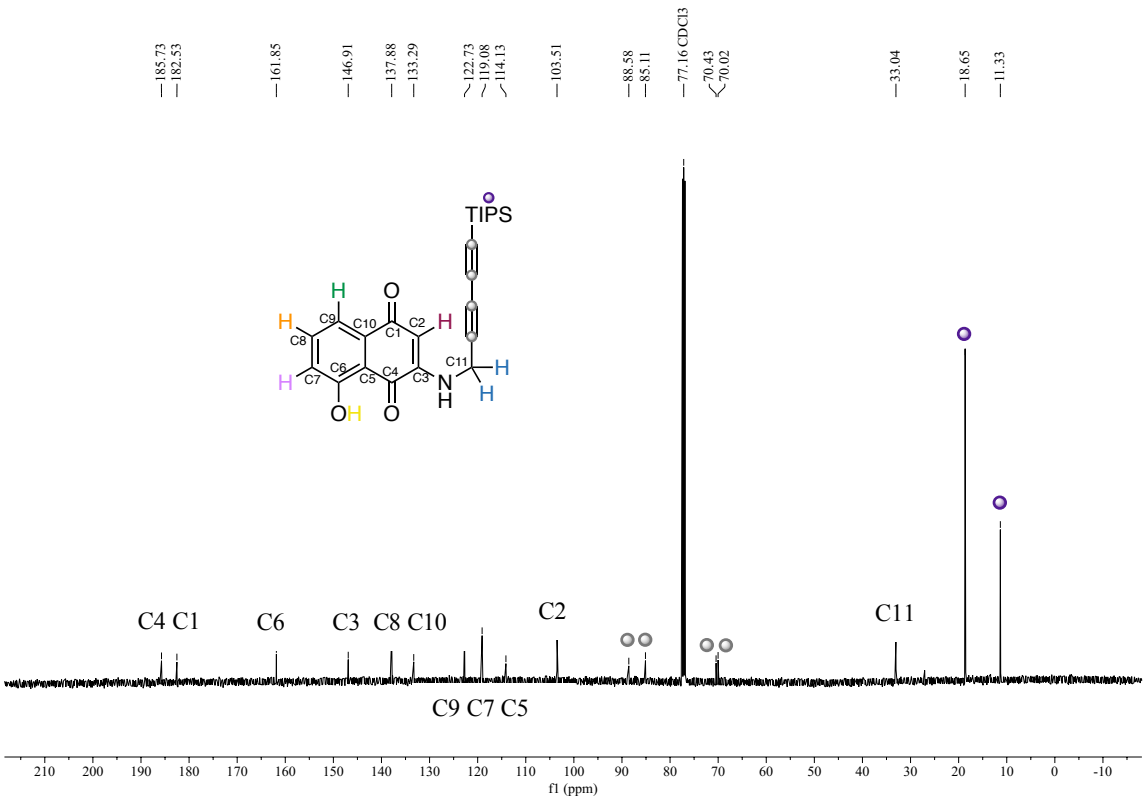


**Figure S24**. $^{13}C$ {$^{1}H$} NMR ($CDCl_3$) for **27a**.

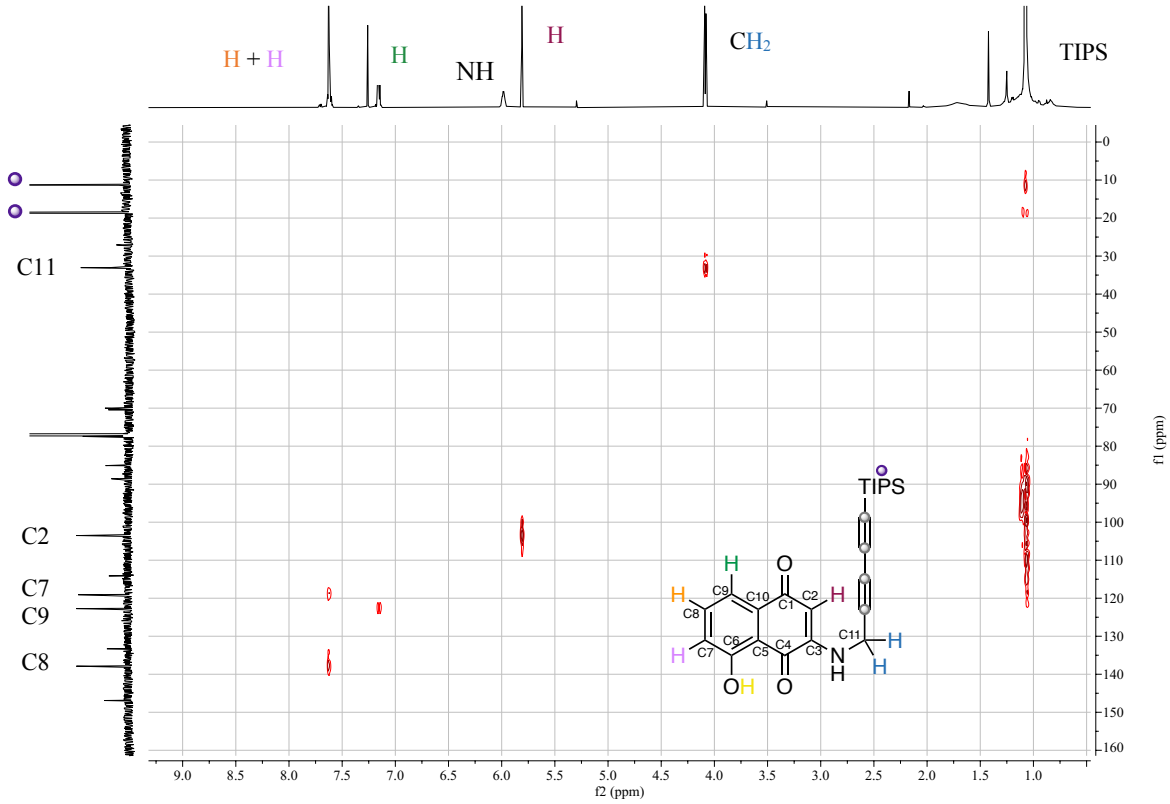


**Figure S25**. HSQC for **27a**.

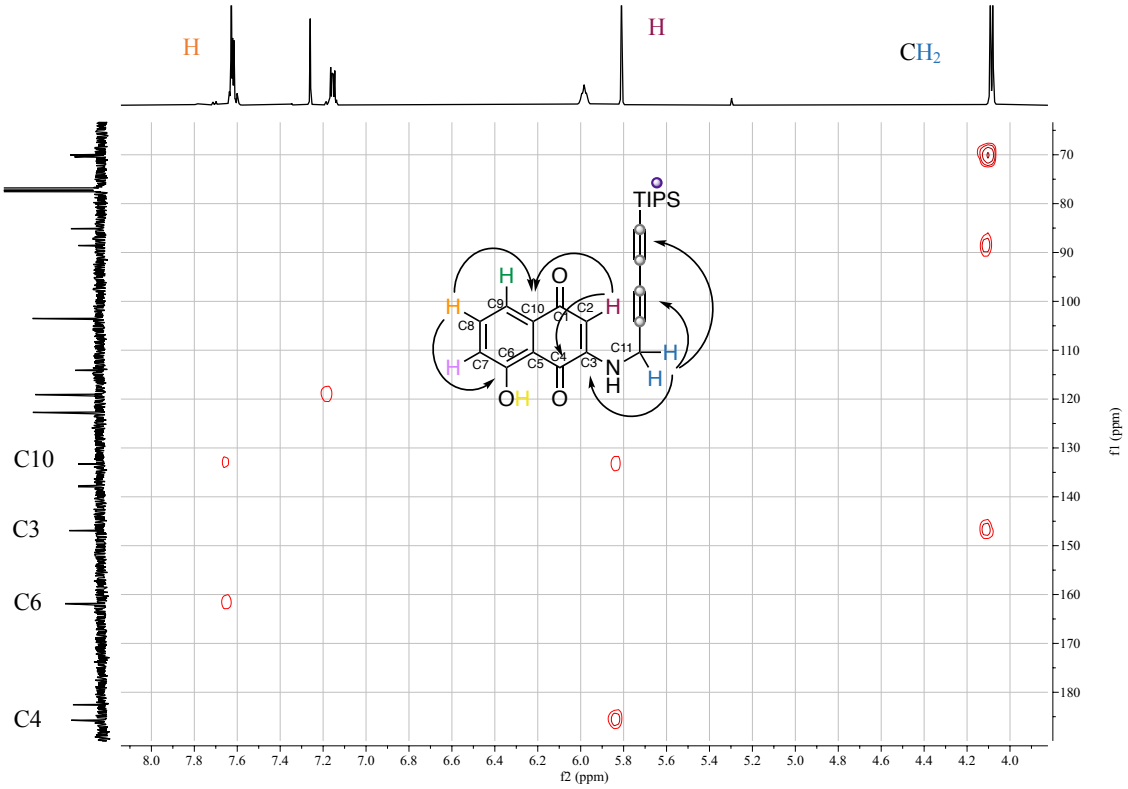


**Figure S26**. HMBC correlations for **27a**.

**8-methoxy-2-((5-(triisopropylsilyl)penta-2,4-diyn-1-yl)amino)naphthalene-1,4-dione (27b)**

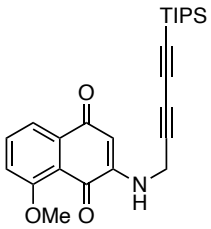


Compound **27b** was prepared following general procedure **GP1** was followed using freshly prepared amine **10** (44 mg, 0.19 mmol, 1.5 equiv) and **26b** (33 mg, 0.12 mmol, 1.0 equiv). Purification by flash column chromatography ($SiO_2$, CyH/AcOEt 90:20 to 70:30) afforded **27b** as an orange solid (11 mg, 0.03 mmol, 21% yield).

**$^1$H NMR** (500 MHz, $CDCl_3$) δ 7.79 (dd, *J* = 7.6, 1.1 Hz, 1H), 7.68 (dd, *J* = 8.5, 7.6 Hz, 1H), 7.20 (dd, *J* = 8.5, 1.1 Hz, 1H), 6.11 (t, *J* = 5.8 Hz, 1H), 5.78 (s, 1H), 4.07 (d, *J* = 5.8 Hz, 2H), 4.01 (s, 3H), 1.27 – 1.24 (m, 3H), 1.07 (s, 18H) ppm.

**$^{13}$C NMR** (126 MHz, $CDCl_3$) δ 182.9, 179.8, 160.3, 148.1, 136.2, 135.8, 119.3, 118.3, 116.3, 101.3, 88.7, 84.8, 70.5, 70.1, 56.6, 33.0, 29.9, 18.7, 11.3 ppm.

**HRMS** (ESI+) calculated for m/z $[C_{25}H_{32}NO_3Si]^+$, $[M+H]^+$: 422.2146; found: 422.2143.

**2-Bromo-5-hydroxy-3-((5-(triisopropylsilyl)penta-2,4-diyn-1-yl)amino)naphthalene-1,4-dione** (**28**) (orange solid; 28 mg, 0.06 mmol, 34% yield) was identified as the main byproduct and its structure was confirmed by X-ray diffraction.

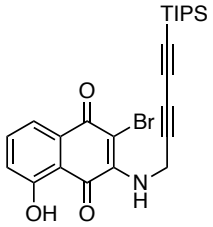


**M.p.** = decomposition at 170 °C.

**$^1$H NMR** (400 MHz, $CDCl_3$) δ 11.41 (s, 1H), 7.70 (dd, *J* = 7.5, 1.2 Hz, 1H), 7.61 (dd, *J* = 8.4, 7.5 Hz, 1H), 7.18 (dd, *J* = 8.4, 1.2 Hz, 1H), 6.04 (bs, 1H), 4.77 (d, *J* = 6.1 Hz, 2H), 1.11 (bs, 3H), 1.08 (bs, 18H) ppm.

**$^{13}$C NMR** (101 MHz, $CDCl_3$) δ 184.0, 176.2, 162.2, 145.4, 137.7, 131.9, 123.4, 120.3, 113.4, 88.7, 85.3, 71.8, 70.6, 36.2, 18.7, 11.4 ppm.

**HRMS** (ESI+) calculated for m/z $[C_{24}H_{29}BrNO_3Si]^+$, $[M+H]^+$: 486.1095; found: 486.1080.

The structure of this compound was also confirmed by X-ray diffraction.

**1-Ethynyl-6,10-dimethoxybenzo[f]quinoline (32)**

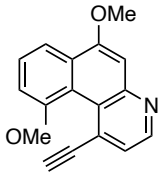


To a solution of **31** (50 mg, 0.11 mmol, 1.0 equiv) in $CH_2Cl_2$ (1.1 mL, 0.1 M) was added JohnPhosAuNCMeSbF$_6$ (8.6 mg, 11 μmol, 0.1 equiv) and the solution was stirred at 50 ºC for 1 h. Then, the reaction was quenched by addition of $Et_3N$ (*ca.* 3 drops), and solvent was removed under reduced pressure. The crude was directly dissolved in THF (1.1 mL, 0.1 M) before TBAF (0.22 mL from a 1 M solution in THF, 0.22 mmol, 2.0 equiv) was added and the reaction mixture was allowed to react at 25 ºC for 1 h. The reaction was quenched by addition of $NH_4Cl$, and the aqueous layer was extracted with $CH_2Cl_2$. The combined organic layers were dried over $MgSO_4$, filtered, and concentrated under reduced pressure. The crude was purified by flash column chromatography ($SiO_2$, *n*-pentane/AcOEt 60:40 + 1% $Et_3N$). Yellow solid (26 mg, 0.99 mmol, 88% yield over two steps).

**$^1$H NMR** (500 MHz, $CDCl_3$) δ 8.68 (d, *J* = 4.6 Hz, 1H), 7.92 (dd, *J* = 8.1, 1.1 Hz, 1H), 7.61 (t, *J* = 8.0 Hz, 1H), 7.47 (d, *J* = 4.7 Hz, 1H), 7.14 (dd, *J* = 8.1, 1.1 Hz, 1H), 7.13 (s, 1H), 4.09 (s, 3H), 4.00 (s, 3H), 3.68 (s, 1H) ppm.

**$^{13}$C NMR** (126 MHz, $CDCl_3$) δ 157.7, 156.7, 150.7, 147.7, 129.4, 129.0, 128.5, 123.9, 120.1, 120.0, 114.10, 108.8, 104.3, 85.7, 83.8, 56.0, 53.8 ppm.

The structure of this compound was also confirmed by X-ray diffraction.

**2-Amino-8-methoxynaphthalene-1,4-dione (36a)**

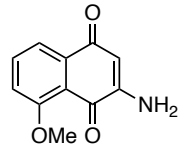


A reported procedure was followed.[21] *O*-benzylhydroxylamine hydrochloride (763.4 mg, 4.78 mmol, 1.2 equiv) was dissolved in EtOH (10 mL, 0.4 M). Temperature was lowered to 0 °C before $Et_3N$ (0.67 mL, 4.78 mmol, 1.2 equiv) was added followed by *o*-methyljuglone. Reaction was stirred at 25 °C for 18 h. Precipitate was filtered off and then, workup with $CH_2Cl_2$ and $H_2O$. The combined organic layers were dried over $MgSO_4$, filtered, and concentrated under reduced pressure. The crude was purified by flash column chromatography ($SiO_2$, CyH/AcOEt 90:20 to 50:50). Orange solid (0.69 g, 3.08 mmol, 87% yield).

**$^{1}$H NMR** (500 MHz, $CDCl_3$) δ 7.76 (dd, *J* = 7.6, 1.1 Hz, 1H), 7.67 (dd, *J* = 8.5, 7.6 Hz, 1H), 7.20 (dd, *J* = 8.4, 1.1 Hz, 1H), 5.94 (s, 1H), 5.22 (s, 2H), 4.01 (s, 3H) ppm.

**$^{13}$C NMR** (126 MHz, $CDCl_3$) δ 183.4, 180.4, 160.1, 149.4, 136.1, 135.9, 119.2, 118.4, 116.3, 103.5, 56.6 ppm.

**HRMS** (ESI+) calculated for m/z $[C_{11}H_{10}NO_3]^+$, $[M+H]^+$: 204.0655; found: 204.0652.

The spectral data were fully consistent with those previously reported.

***tert*-Butyl (8-methoxy-1,4-dioxo-1,4-dihydronaphthalen-2-yl)carbamate (36b)**

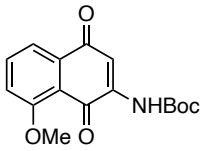


To a solution of **36a** (440.0 mg, 2.17 mmol, 1 equiv) in THF (21.7 mL, 0.1 M), was added $Boc_2O$ (477.3 mg, 2.19 mmol, 1.01 equiv) and reaction was heated to 70 °C. Then, DMAP (529.1 mg, 4.33 mmol, 2.0 equiv) is added resulting in a change of color from brown to black. After 1 h, consumption of starting material is determined by TLC (CyH/AcOEt 80:20). Concentration under reduced pressure was followed by purification of the crude mixture by flash column chromatography ($SiO_2$, CyH/AcOEt 100:0 to 70:30). Orange solid (502 mg, 1.66 mmol, 76% yield).

**M.p.** = 131–132 °C.

**$^1$H NMR** (400 MHz, $CDCl_3$) δ 7.71 (s, 1H), 7.63 – 7.54 (m, 2H), 7.14 (dd, *J* = 8.1, 1.5 Hz, 1H), 3.89 (s, 3H), 1.43 (s, 9H) ppm.

**$^{13}$C NMR** (101 MHz, $CDCl_3$) δ 184.5, 178.9, 160.2, 151.4, 141.9, 136.1, 134.5, 119.1, 117.0, 113.1, 82.4, 56.5, 28.1 ppm.

**HRMS** (ESI+) calculated for m/z $[C_{16}H_{17}NNaO_5]^+$, $[M+Na]^+$: 326.0999; found: 326.1005.

**2-Bromo-4-methoxy-6-nitrophenol (42)**

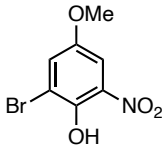


A reported procedure was adapted.[22b] To a suspension of commercially available 4-methoxy-2-nitrophenol **41** (4.0 g, 24 mmol, 1.0 equiv) and AcONa (3.9 g, 47 mmol, 2.0 equiv) in AcOH (25 mL, 0.96 M) was added a solution of dibromine (1.2 mL, 24 mmol, 1.0 equiv) in AcOH (4.9 mL) over 30 min. The mixture was stirred for 30 min at 25 °C and 2 h at 70 °C. After cooling to room temperature, the suspension was poured into cold $H_2O$ (800 mL) which was acidified by addition of concentrated HCl (10.5 mL) and the resulting solid was isolated by filtration. The solid was dissolved in AcOEt (*ca.* 300 mL) and the solution was washed with $H_2O$ and brine, dried over $Na_2SO_4$, filtered and volatiles were removed in vacuo. Product was used without further purification. Brown solid. (4.6 g, 19 mmol, 78% yield).

**$^1$H NMR** (400 MHz, $CDCl_3$) δ 10.80 (s, 1H), 7.53 (q, *J* = 3.1 Hz, 2H), 3.83 (s, 3H) ppm.

The spectral data were fully consistent with those previously reported.

**1-Bromo-2,5-dimethoxy-3-nitrobenzene (43)**

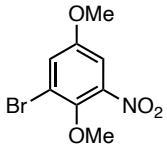


A reported procedure was adapted.[22b] A mixture of **42** (13.2 g, 53.219 mmol, 1.0 equiv), $Me_2SO_4$ (13.4 g, 10.1 mL, 106.4 mmol, 2.0 equiv) and $Cs_2CO_3$ (26.01 g, 79.8 mmol, 1.5 equiv) in acetone (106.4 mL, 0.5 M) was heated to 60 °C and stirred for 2h. The resulting suspension was filtered through a celite plug and filtrate was concentrated in vacuo. Purification by flash column chromatography ($SiO_2$, *n*-pentane/AcOEt 98:2). Yellow solid (4.9 g, 19 mmol, 35% yield).

**$^1$H NMR** (300 MHz, $CDCl_3$) δ 7.34 (d, *J* = 3.1 Hz, 1H), 7.29 – 7.26 (d, *J* = 3.1 Hz, 1H), 3.96 (s, 3H), 3.83 (s, 3H) ppm.

The spectral data were fully consistent with those previously reported.

**3-Bromo-2,5-dimethoxyaniline (44)**

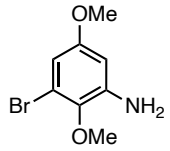


A reported procedure was adapted.[22b] To a solution of **43** (4.8 g, 18 mmol, 1.0 equiv) in EtOH/$H_2O$ (4:1 Ratio, 0.33 M) were added $NH_4Cl$ (4.9 g, 92 mmol, 5.0 equiv) and iron powder (7.2 g, 0.13 mol, 7.0 equiv) and the resulting suspension was heated to 70 °C for 4.5 h. The mixture was cooled to room temperature and filtered through a celite plug. The filtrate was concentrated, and the residue was dissolved in AcOEt and $H_2O$. The aqueous layer was extracted with AcOEt (x2). The combined organic extracts were washed with $H_2O$ (x2) and brine (x2), dried over $Na_2SO_4$, filtered and all volatiles were removed in vacuo. 3-bromo-2,5-dimethoxyaniline **44** was used without further purification. Brown oil (4 g, 0.02 mol, 90% yield).

**$^1$H NMR** (300 MHz, $CDCl_3$) δ 6.43 (d, *J* = 2.9 Hz, 1H), 6.21 (d, *J* = 2.8 Hz, 1H), 4.02 – 3.92 (m, 2H), 3.75 (s, 3H), 3.68 (s, 3H) ppm.

The spectral data were fully consistent with those previously reported.

**5-(Methoxymethylene)-2,2-dimethyl-1,3-dioxane-4,6-dione (45)**

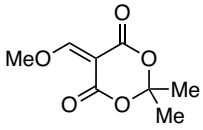


A reported procedure was adapted.[22d] Commercially available 2,2-dimethyl-1,3-dioxane-4,6-dione **45** (8.0 g, 55.5 mmol, 1.0 equiv) was dissolved in $CH(OMe)_3$ (27.8 mL, 2 M) and the solution was heated to 95 °C for 3 h. All volatiles were removed in vacuo and the resulting crude product triturated with 5% $CH_2Cl_2$ in hexane (33 mL) and the resulting solid was filtered, washed with pentane, and dried. Compound **46** was used without further purification. Light brown solid (8.8 g, 47.3 mmol, 85% yield).

**$^1$H NMR** (300 MHz, $CDCl_3$) δ 8.17 (s, 1H), 4.29 (s, 3H), 1.74 (s, 6H) ppm.

**$^{13}$C NMR** (101 MHz, $CDCl_3$) δ 175.0, 163.2, 158.6, 104.8, 96.8, 66.3, 27.3 ppm.

The spectral data were fully consistent with those previously reported.

**5-(((3-Bromo-2,5-dimethoxyphenyl)amino)methylene)-2,2-dimethyl-1,3-dioxane-4,6-dione (46)**

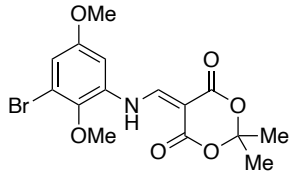


A reported procedure was adapted.[22d] To a suspension of **46** (4.19 g, 22.5 mmol, 1.0 equiv) in *i*PrOH (45 mL, 0.5 M) was added **44** (5.22 g, 22.5 mmol, 1.0 equiv) and the resulting mixture was heated to 85 °C and stirred for 3 h. The resulting brown solution was slowly cooled to room temperature and then to 0 °C and the precipitate formed was isolated by filtration, washed with cold *i*PrOH and pentane to give 5-(((3-bromo-2,5-dimethoxyphenyl)amino)methylene)-2,2-dimethyl-1,3-dioxane-4,6-dione (6.09 g, 15.8 mmol, 70%) as beige solid.

**M.p.** = 169–171 °C.

**$^1$H NMR** (400 MHz, $CDCl_3$) δ 8.63 (d, *J* = 14.4 Hz, 1H), 6.97 (d, *J* = 2.7 Hz, 1H), 6.83 (d, *J* = 2.8 Hz, 1H), 3.93 (s, 3H), 3.84 (s, 3H), 1.78 (s, 6H) ppm.

**$^{13}$C NMR** (101 MHz, $CDCl_3$) δ 165.4, 163.6, 157.2, 151.0, 141.6, 133.0, 118.4, 115.8, 105.5, 100.7, 88.6, 61.6, 56.3, 27.3 ppm.

**HRMS** (ESI+) calculated for m/z $[C_{15}H_{16}BrNNaO_6]^+$, $[M+Na]^+$: 408.0053; found: 408.0055.

The spectral data were fully consistent with those previously reported.

**7-bromo-5,8-dimethoxyquinolin-4(1*H*)-one (48)**

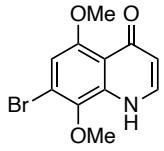


A reported procedure was adapted.[22b] Compound **47** (6.10 g, 15.8 mmol, 1.0 equiv) and $Ph_2O$ (24.3 mL, 0.7 M) were mixed and heated to 245 °C for 30 min. The deep brown solution was cooled to 25 °C and pentane was added. The resulting solid was isolated by filtration, thoroughly washed with pentane, and dried in vacuo to give **48** (3.95 g, 13.9 mmol, 88% yield) as a brown solid.

**M.p.** = 235–236 °C.

**$^1$H NMR** (500 MHz, DMSO) δ 7.62 (dd, *J* = 7.4, 5.9 Hz, 1H), 6.86 (s, 1H), 5.93 (dd, *J* = 7.4, 1.4 Hz, 1H), 3.80 (s, 3H), 3.78 (s, 3H) ppm.

**$^{13}$C NMR** (126 MHz, DMSO) δ 176.5, 155.9, 139.2, 137.4, 136.8, 130.0, 118.0, 112.2, 107.0, 61.1, 56.2 ppm.

**HRMS** (ESI+) calculated for m/z $[C_{11}H_{11}BrNO_3]^+$, $[M+H]^+$: 283.9917; found: 283.9919.

The spectral data were fully consistent with those previously reported.

**7-Bromo-5,8-dimethoxyquinolin-4-yl trifluoromethanesulfonate (49)**

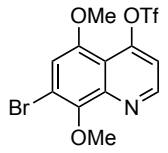


To an ice-cold suspension of **48** (3.19 g, 11.2 mmol, 1.0 equiv), DMAP (274 mg, 2.25 mmol, , 0.2 equiv) and 2,6-lutidine (1.68 g, 1.83 mL, 15.7 mmol, 1.4 equiv) in $CH_2Cl_2$ (112 mL, 0.1 M) was added trifluoromethanesulfonic anhydride (2.27 mL, 13.5 mmol, 1.2 equiv) and the resulting solution was stirred at 0 °C and slowly warmed to 25 °C for 18 h. The mixture was diluted with $CH_2Cl_2$ and the organic layer was washed with $H_2O$ (x2) and brine (x2), dried over $MgSO_4$, filtered and concentrated under reduced pressure. Purification by flash column chromatography ($SiO_2$, CyH/AcOEt 80:20). Off-white solid (3.05 g, 7.33 mmol, 65% yield).

**M.p.** = 200 °C.

**$^1$H NMR** (500 MHz, $CDCl_3$) δ 8.97 (d, *J* = 4.9 Hz, 1H), 7.25 (dd, *J* = 4.9, 0.7 Hz, 1H), 7.12 (s, 1H), 4.07 (s, 3H), 4.00 (s, 3H) ppm.

**$^{13}$C NMR** (126 MHz, $CDCl_3$) δ 153.3, 151.4, 150.4, 147.6, 118.8 (q, *J* = 318 Hz), 118.7, 117.6, 114.9, 114.1, 111.5, 62.2, 56.1 ppm.

**$^{19}$F NMR** (376 MHz, $CDCl_3$) δ -73.54 ppm.

**HRMS** (ESI+) calculated for m/z $[C_{12}H_{10}BrF_3NO_5S]^+$, $[M+H]^+$: 415.9415; found: 415.9420.

**General procedure GP2 for the oxidation of hydroquinones to benzoquinones**

To a solution of the corresponding hydroquinone (1.0 equiv) in $CH_3CN$ (0.05 M) was added a solution of CAN (2.5 equiv) in $H_2O$ (3.4 mL, 0.35 M) and the resulting solution was stirred for 30 min at 25 °C. The mixture was diluted with more $H_2O$ and the aqueous layer was extracted with $CH_2Cl_2$ (x3). The combined organic layers were washed with brine (x2), dried over $MgSO_4$, filtered, and concentrated under reduced pressure. The crude product was purified by flash column chromatography.

**7-Bromo-5,8-dioxo-5,8-dihydroquinolin-4-yl trifluoromethanesulfonate (54e)**

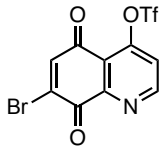


The title compound **54e** was obtained following general procedure **GP2** using **49** (300 mg, 0.72 mmol, 1.0 equiv) and CAN (0.99 g, 1.80 mmol, 2.5 equiv) after purification by flash column chromatography /$SiO_2$, CyH/AcOEt 90:10). Brown solid (130 mg, 0.37 mmol, 47% yield).

**M.p.** = 130 °C.

**$^1$H NMR** (400 MHz, $CDCl_3$) δ 9.15 (d, *J* = 5.4 Hz, 1H), 7.58 (m, 2H) ppm.

**$^{13}$C NMR** (101 MHz, $CDCl_3$) δ 179.5, 174.7, 156.6, 154.4, 149.0, 140.7, 139.7, 122.1, 118.6 (q, *J* = 321 Hz), 27.0 ppm.

**$^{19}$F NMR** (471 MHz, $CDCl_3$) δ -72.94 ppm.

**7-Bromo-5,8-dimethoxy-4-((trimethylsilyl)ethynyl)quinoline (50)**

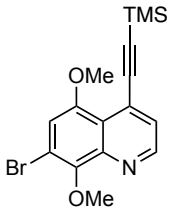


Compound **49** (3.56 g, 8.55 mmol, 1.0 equiv), copper(I) iodide (130 mg, 684 μmol, 0.08 equiv) and $(PPh_3)_2PdCl_2$ (240 mg, 342 μmol, 0.04 Eq) were put in flask and the flask was evacuated and back filled with argon three times. DMF and $Et_3N$ (57 mL, 1:1 ratio, 0.15 M) and ethynyltrimethylsilane (1.42 mL, 10.3 mmol, 1.20 equiv) were added and the resulting solution was stirred at 25 °C for 18 h. The solvent was removed in vacuo at 55 °C and the residue was dissolved in $Et_2O$ and poured into water (300 mL). The aqueous layer was extracted with $Et_2O$ (x4). The combined organic layers were washed with $H_2O$ (x2) and brine (x2), dried over $MgSO_4$, filtered, and concentrated under reduced pressure. Purification by flash column chromatography ($SiO_2$, CyH/AcOEt 85:15). Orange-brown oil (2.73 g, 7.49 mmol, 87% yield).

**$^1$H NMR** (500 MHz, $CDCl_3$) δ 8.80 (d, *J* = 4.5 Hz, 1H), 7.50 (d, *J* = 4.5 Hz, 1H), 6.96 (s, 1H), 4.03 (s, 3H), 3.91 (s, 3H), 0.29 (bs, 9H) ppm.

**$^{13}$C NMR** (126 MHz, $CDCl_3$) δ 152.3, 149.7, 147.7, 144.3, 127.9, 127.0, 120.3, 116.9, 110.1, 108.9, 104.2, 103.4, 62.0, 55.9, 27.0, -0.1 ppm.

**HRMS** (ESI+) calculated for m/z $[C_{16}H_{19}BrNO_2Si]^+$, $[M+H]^+$: 364.0363; found: 364.0365.

**7-Bromo-4-ethynyl-5,8-dimethoxyquinoline (51)**

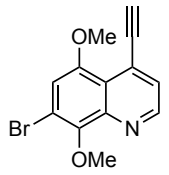


To an ice-cold solution of **50** (2.73 g, 7.49 mmol, 1.0 equiv) in THF (38 mL, 0.2 M) was added TBAF (1.0 M in THF) (8.99 mL, 8.99 mmol, 1.20 equiv) and the solution was warmed to 25 °C. The deep green-black reaction mixture was stirred for 30 min at 25 °C and was quenched with saturated aqueous $NH_4Cl$ solution. The aqueous layer was extracted with $CH_2Cl_2$ (x3), and the combined organic layers were dried over $MgSO_4$, filtered, and concentrated under reduced pressure. Purification by flash column chromatography ($SiO_2$, CyH/AcOEt 85:15). Pale-brown solid (1.72 g, 5.89 mmol, 79% yield).

**M.p.** = 157 °C.

**$^1$H NMR** (500 MHz, $CDCl_3$) δ 8.85 (d, *J* = 4.4 Hz, 1H), 7.56 (d, *J* = 4.4 Hz, 1H), 7.00 (s, 1H), 4.05 (s, 3H), 3.94 (s, 3H), 3.61 (s, 1H) ppm.

**$^{13}$C NMR** (126 MHz, $CDCl_3$) δ 152.2, 149.8, 147.8, 144.4, 127.5, 127.2, 120.5, 117.1, 110.4, 85.8, 82.3, 62.1, 56.1 ppm.

**HRMS** (ESI+) calculated for m/z $[C_{13}H_{11}BrNO_2]^+$, $[M+H]^+$: 291.9968; found: 291.9972.

**7-Bromo-5,8-dimethoxy-4-(1-tosyl-1*H*-1,2,3-triazol-4-yl)quinoline (52)**

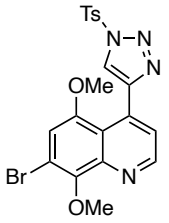


To a solution of **51** (200 mg, 685 µmol, 1.0 equiv) and CuTC (13.1 mg, 68.5 µmol, 10 mol %) in toluene (3.42 mL, 0.2 M) was added freshly prepared $TsN_3$ (149 mg, 753 µmol, 1.1 equiv) and the mixture was stirred at 25 °C. The reaction was quenched with saturated aqueous $NH_4Cl$ solution, and the aqueous layer was extracted with AcOEt (x3). The combined organic layers were washed with brine (x2), dried over $MgSO_4$, filtered, and concentrated under reduced pressure. The crude product was purified by flash column chromatography ($SiO_2$, CyH/AcOEt 50:50). Beige solid (243 mg, 497 µmol, 73% yield).

**M.p.** = 170–172°C.

**$^1$H NMR** (500 MHz, $CDCl_3$) δ 8.95 (d, *J* = 4.4 Hz, 1H), 8.19 (s, 1H), 8.13 – 8.04 (m, 2H), 7.49 (d, *J* = 4.4 Hz, 1H), 7.47 – 7.42 (m, 2H), 6.96 (s, 1H), 4.08 (s, 3H), 3.52 (s, 3H), 2.48 (s, 3H) ppm.

**$^{13}$C NMR** (126 MHz, $CDCl_3$) δ 151.9, 150.0, 148.1, 147.7, 146.2, 144.6, 134.7, 133.3, 130.7, 128.9, 124.3, 122.9, 118.7, 116.9, 110.7, 62.2, 55.8, 22.0 ppm.

**HRMS** (ESI+) calculated for m/z $[C_{20}H_{17}BrN_4NAO_4S]^+$, $[M+Na]^+$: 511.0046; found: 511.0035.

**7-Bromo-4-(1-tosyl-1*H*-1,2,3-triazol-4-yl)quinoline-5,8-dione (53)**

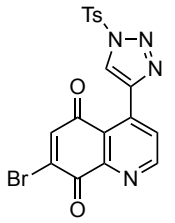


To a solution of **52** (217 mg, 0.48 mmol, 1.0 equiv) in $CH_3CN$ (10.1 mL, 0.05 M) was added a solution of CAN (655.4 mg, 1.2 mmol, 2.5 equiv) in $H_2O$ (3.4 mL, 0.35 M) and the resulting solution was stirred for 30 min at 25 °C. The mixture was diluted with more $H_2O$ and the aqueous layer was extracted with $CH_2Cl_2$ (x3). The combined organic layers were washed with brine (x2), dried over $MgSO_4$, filtered, and concentrated under reduced pressure. The crude product was purified by flash column chromatography ($SiO_2$, CyH/AcOEt 80:20). Off-yellow solid (100 mg, 0.22 mmol, 49% yield).

**M.p.** = 185 °C.

**$^1$H NMR** (500 MHz, $CDCl_3$) δ 9.08 (d, *J* = 5.1 Hz, 1H), 9.03 (s, 1H), 8.36 (d, *J* = 5.1 Hz, 1H), 8.09 (d, *J* = 8.5 Hz, 2H), 7.55 (s, 1H), 7.46 – 7.42 (m, 2H), 2.48 (s, 3H) ppm.

**$^{13}$C NMR** (126 MHz, $CDCl_3$) δ 183.0, 176.0, 154.2, 148.4, 148.0, 141.2, 141.1, 139.1, 138.7, 132.8, 130.8, 129.7, 129.1, 126.9, 125.2, 22.1 ppm.

**HRMS** (ESI+) calculated for m/z $[C_{18}H_{11}BrN_4NaO_4S]^+$, $[M+Na]^+$: 480.9577; found: 480.9556.

**7-Bromo-4-(bromoethynyl)-5,8-dimethoxyquinoline (55a)**

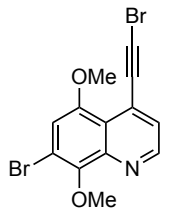


A reported procedure was followed.[23] To a solution of **51** (200 mg, 0.68 mmol, 1.0 equiv) in acetone (0.68 mL, 1M), was added NBS (146.2 mg, 0.82 mmol, 1.2 equiv) and $Ag_2O$ (9.3 mg, 0.55 mmol, 8 mol %). Reaction was left stirring for 2 h at 25 °C under exclusion of light. Then, reaction mixture was filtered through a celite plug followed by concentration under reduced pressure. The crude product was purified by flash column chromatography ($SiO_2$, CyH/AcOEt 90:10). Off-brown solid (166 mg, 0.45 mmol, 65% yield).

**M.p.** = 144–146 °C.

**$^1$H NMR** (500 MHz, $CDCl_3$) δ 8.83 (d, *J* = 4.5 Hz, 1H), 7.49 (d, *J* = 4.5 Hz, 1H), 6.98 (s, 1H), 4.04 (s, 3H), 3.96 (s, 3H) ppm.

**$^{13}$C NMR** (126 MHz, $CDCl_3$) δ 152.1, 149.8, 147.7, 144.4, 127.6, 127.0, 120.6, 117.1, 110.2, 79.1, 62.1, 59.2, 56.6 ppm.

**HRMS** (ESI+) calculated for $[C_{13}H_{10}Br_2NO_2]^+$, $[M+H]^+$: 369.9073 m/z; found: 369.9078 m/z.

**7-bromo-4-(iodoethynyl)-5,8-dimethoxyquinoline (55b)**

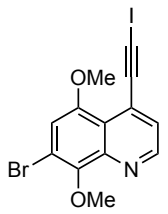


A reported procedure was followed.[24] A screw-cap vial equipped with a stirring bar was charged with [Au(SIPr)($Et_3N$)][$HF_2$] (17.8 mg, 0.021 mmol, 3 mol %), *N*-iodosuccinimide (308.1 mg, 1.4 mmol, 2 equiv), toluene (1.4 mL, 0.5 M) and compound **51** (200 mg, 0.68 mmol, 1.0 equiv). The vial was closed under an argon atmosphere, and the reaction mixture was stirred at 50 °C for 2 h. Then, reaction mixture was concentrated under reduced pressure. The crude product was purified by flash column chromatography ($SiO_2$, CyH/AcOEt 90:10). Off-yellow solid (218 mg, 0.52 mmol, 76% yield).

**M.p.** = 169–173 °C.

**$^1$H NMR** (500 MHz, $CDCl_3$) δ 8.84 (d, *J* = 4.5 Hz, 1H), 7.49 (d, *J* = 4.5 Hz, 1H), 6.99 (s, 1H), 4.05 (s, 3H), 3.97 (s, 3H) ppm.

**$^{13}$C NMR** (126 MHz, $CDCl_3$) δ 152.0, 149.7, 147.7, 144.2, 127.9, 127.4, 120.7, 117.0, 110.2, 93.0, 62.0, 56.6, 16.6 ppm.

**HRMS** (ESI+) calculated for $[C_{13}H_{10}BrINO_2]^+$, $[M+H]^+$: 417.8934 m/z; found: 417.8931 m/z.

**7-Bromo-4-(1-ethoxyvinyl)-5,8-dimethoxyquinoline (58)**

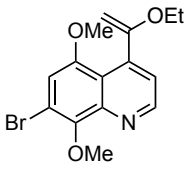


Under an argon atmosphere, to a stirred solution of **49** (489 mg, 1.18 mmol, 1.0 equiv) in NMP (11.9 mL, 0.099 M), was sequentially added LiCl (149.4 mg, 3.53 mmol, 3.0 equiv), $Ph_3As$ (72 mg, 0.24 mmol, 0.2 equiv), $Pd_2dba_3$ (107.6 mg, 0.12 mmol, 0.1 equiv) and tributylvinyltin (0.44 mL, 1.3 mmol,

1.1 equiv) at 25 °C. The reaction mixture was stirred at that temperature for 18 h before it was quenched with saturated aq. NaCl (~ 100 mL). The resultant mixture was extracted with $Et_2O$ (x3), dried over $MgSO_4$, filtered, and concentrated under reduced pressure. The crude product was purified by flash column chromatography ($SiO_2$, CyH/AcOEt 80:20). Yellow oil (360 mg, 1.06 mmol, 91% yield).

**$^1$H NMR** (400 MHz, $CDCl_3$) δ 8.88 (d, *J* = 4.3 Hz, 1H), 7.31 (d, *J* = 4.3 Hz, 1H), 6.99 (s, 1H), 4.29 (d, *J* = 2.4 Hz, 1H), 4.17 (d, *J* = 2.4 Hz, 1H), 4.03 (s, 3H), 3.94 (q, *J* = 7.1 Hz, 2H), 3.88 (s, 3H), 1.33 (t, *J* = 7.1 Hz, 3H) ppm.

**$^{13}$C NMR** (101 MHz, $CDCl_3$) δ 162.4, 152.3, 150.5, 147.6, 144.3, 143.2, 123.0, 119.3, 116.4, 110.4, 84.6, 63.4, 62.0, 56.5, 14.7 ppm.

**HRMS** (ESI+) calculated for $[C_{15}H_{17}BrNO_3]^+$, $[M+H]^+$: 338.0386 m/z; found: 338.0399 m/z.

**2-Bromo-1-(7-bromo-5,8-dimethoxyquinolin-4-yl)ethan-1-one (56a)**

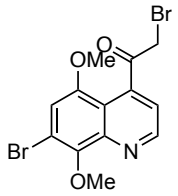


Compound **58** (729 mg, 0.22 mmol, 1.0 equiv) was exposed to in HBr/AcOH (33% HBr in AcOH solution) (3.7 mL, 0.59 M) at 0 °C. Reaction was left stirring at that temperature for 1 h. Then, $Br_2$ (0.12 mL, 1.1 equiv) was added dropwise, and reaction was heated to 70 °C and left stirring for 1 h. Reaction was quenched with $Na_2S_2O_3$ and then with $NaHCO_3$ followed by extraction with $CH_2Cl_2$ (x3). Organic phase was washed with brine (x2) before drying over $MgSO_4$, filtered, and concentrated under reduced pressure. The crude product was purified by flash column chromatography ($SiO_2$, CyH/AcOEt 90:10). Brown solid (323 mg, 0.83 mmol, 39% yield).

**M.p.** = 120–122 °C.

**$^1$H NMR** (500 MHz, $CDCl_3$) δ 9.00 (d, *J* = 4.3 Hz, 1H), 7.25 (s, 1H), 7.07 (s, 1H), 4.32 (s, 2H), 4.09 (s, 3H), 3.95 (s, 3H) ppm.

**$^{13}$C NMR** (126 MHz, $CDCl_3$) δ 196.1, 150.6, 150.0, 148.3, 143.7, 143.3, 118.7, 117.7, 116.8, 110.8, 62.3, 57.1, 35.5 ppm.

**HRMS** (ESI+) calculated for $[C_{13}H_{11}Br_2NO_3]^+$, $[M+H]^+$: 387.9178 m/z; found: 387.9188 m/z.

The structure of this compound was also confirmed by X-ray diffraction.

**7-Bromo-4-(2-bromoacetyl)quinoline-5,8-dione (54d)**

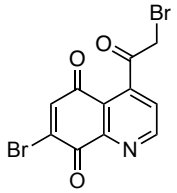


Following **GP2**, using **56a** (53 mg, 0.14 mmol, 1.0 equiv) and CAN (186.7 mg, 0.34 mmol, 2.5 equiv). The crude product was purified by flash column chromatography ($SiO_2$, CyH/AcOEt 70:30). Brown solid (26 mg, 0.07 mmol, 53% yield).

**M.p.** = decomposition at 230 °C.

**$^1$H NMR** (500 MHz, $CDCl_3$) δ 9.15 (d, *J* = 4.8 Hz, 1H), 7.62 (s, 1H), 7.59 (d, *J* = 4.8 Hz, 1H), 4.27 (s, 2H) ppm.

**$^{13}$C NMR** (126 MHz, $CDCl_3$) δ 195.5, 182.4, 175.2, 155.1, 147.1, 146.8, 141.8, 139.3, 126.7, 125.9, 33.1 ppm.

**HRMS** (MALDI+) calculated for $[C_{11}H_6Br_2NO_3]^+$, $[M+H]^+$: 357.8709 m/z; found: 357.8706 m/z.

**2-azido-1-(7-bromo-5,8-dimethoxyquinolin-4-yl)ethan-1-one (63)**

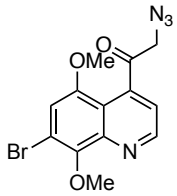


To a solution of **56a** (244 mg, 0.63 mmol, 1.0 equiv) in acetone/$H_2O$ (4:1 ratio, 0.06 M), $NaN_3$ (122.3 mg, 0.19 mmol, 3.0 equiv) was added and the reaction was stirred at 50 °C for 18 h. Then, the aqueous phase was extracted with $CH_2Cl_2$ (x3) and the combined organic layers were dried $MgSO_4$, filtered and concentrated under reduced pressure. The crude product was purified by flash column chromatography ($SiO_2$, CyH/AcOEt 90:10). Light-brown solid (125 mg, 0.36 mmol, 57% yield).

**M.p.** = 108–110 °C

**$^1$H NMR** (400 MHz, $CDCl_3$) δ 9.00 (d, *J* = 4.3 Hz, 1H), 7.19 (d, *J* = 4.3 Hz, 1H), 7.08 (s, 1H), 4.23 (s, 2H), 4.09 (s, 3H), 3.95 (s, 3H) ppm.

**$^{13}$C NMR** (101 MHz, $CDCl_3$) δ 199.1, 150.6, 150.1, 148.3, 143.7, 143.62, 117.8, 117.6, 116.9, 111.0, 62.3, 58.5, 56.9 ppm.

**HRMS** (ESI+) calculated for $[C_{13}H_{11}BrN_4NaO_3]^+$, $[M+Na]^+$: 372.9907 m/z; found: 372.9897 m/z.

**4-(2-Azidoacetyl)-7-bromoquinoline-5,8-dione (54c)**

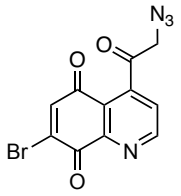

Compound **54c** was synthesized following **GP2** using **63** (75 mg, 0.21 mmol, 1.0 equiv) and CAN (292.7 mg, 0.53 mmol, 2.5 equiv). The crude product was purified by flash column chromatography ($SiO_2$, CyH/AcOEt 80:20). Off-yellow solid (46 mg, 0.14 mmol, 67% yield).

**M.p.** = decomposition at 145 °C.

**$^1$H NMR** (500 MHz, $CDCl_3$) δ 9.16 (d, *J* = 4.8 Hz, 1H), 7.63 (s, 1H), 7.50 (d, *J* = 4.7 Hz, 1H), 4.33 (s, 2H) ppm.

**$^{13}$C NMR** (126 MHz, $CDCl_3$) δ 198.4, 182.2, 175.2, 155.4, 147.8, 146.8, 141.7, 139.4, 126.2, 124.8, 57.8 ppm.

**HRMS** (APCI+) calculated for $[C_{11}H_6BrN_4O_3]^+$, $[M]^+$: 320.9618 m/z; found: 320.9614 m/z.

**1-(7-Bromo-5,8-dimethoxyquinolin-4-yl)ethan-1-one (60)**

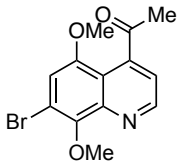

To a solution of **58** (100 mg, 0.3 mmol, 1.0 equiv) in THF (1.03 mL, 0.29 M) was added HCl (2.0 M in $H_2O$) (1.03 mL, 2.07 mmol, 7.0 equiv) and the resulting mixture was stirred at 25 °C for 15 min. The reaction was quenched by addition of $NaHCO_3$ aq. sat. solution and the resulting aqueous layer was extracted with $CH_2Cl_2$ (x3). The combined organic layers were dried over $MgSO_4$, filtered, and concentrated under reduced pressure. The crude product was purified by flash column chromatography ($SiO_2$, CyH/AcOEt 90:10). Brown solid (91.7 mg, 0.3 mmol, >99% yield).

**M.p.** = 112–114 °C.

**$^1$H NMR** (500 MHz, $CDCl_3$) δ 8.97 (d, *J* = 4.3 Hz, 1H), 7.15 (d, *J* = 4.3 Hz, 1H), 7.04 (s, 1H), 4.08 (s, 3H), 3.92 (s, 3H), 2.53 (s, 3H) ppm.

**$^{13}$C NMR** (126 MHz, $CDCl_3$) δ 203.2, 150.8, 150.6, 148.1, 147.6, 143.8, 117.4, 116.8, 116.6, 110.4, 62.2, 56.5, 31.5 ppm.

**HRMS** (ESI+) calculated for $[C_{13}H_{13}BrNO_3]^+$, $[M+H]^+$: 310.0073 m/z; found: 310.0082 m/z.

**4-Acetyl-7-bromoquinoline-5,8-dione (54f)**

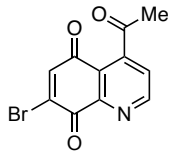


Compound **54f** was obtained folloing **GP2** using **50** (92 mg, 0.3 mmol, 1.0 equiv) and CAN (406.5 mg, 0.74 mmol, 2.5 equiv). The crude product was purified by flash column chromatography ($SiO_2$, CyH/AcOEt 70:30). Off-orange solid (43 mg, 0.15 mmol, 52% yield).

**M.p.** = decomposition at 230 °C.

**$^1$H NMR** (500 MHz, $CDCl_3$) δ 9.09 (d, *J* = 4.8 Hz, 1H), 7.59 (s, 1H), 7.44 (d, *J* = 4.8 Hz, 1H), 2.54 (s, 3H) ppm.

**$^{13}$C NMR** (126 MHz, $CDCl_3$) δ 201.3, 181.9, 175.5, 155.2, 151.0, 147.0, 141.0, 139.6, 125.3, 124.1, 30.41 ppm.

**HRMS** (ESI+) calculated for $[C_{11}H_6BrNNaO_3]^+$, $[M+Na]^+$: 301.9429 m/z; found: 301.9424 m/z.

**9a-Bromo-5,10-dioxo-9-((trimethylsilyl)oxy)-5,5a,6,9,9a,10-hexahydrobenzo[*g*]quinolin-4-yl trifluoromethanesulfonate (68b)**

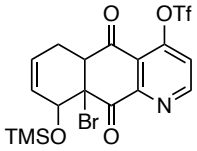


To a solution of **54e** (50 mg, 0.13 mmol, 1.0 equiv) in toluene (0.5 mL, 0.3 M) was added diene **67e** (33.2 mg, 0.23 mmol, 1.8 equiv) and the resulting solution was stirred for 1 h at 23 ºC. Then, an aliquote was taken to analyze the sample directly by $^1$H NMR.

**$^1$H NMR** (300 MHz, $CDCl_3$) δ 9.09 (d, *J* = 5.3 Hz, 1H), 7.48 (d, *J* = 5.3 Hz, 1H), 6.02 (ddd, *J* = 10.3, 5.0, 2.4 Hz, 1H), 5.81 – 5.70 (m, 1H), 4.57 (d, *J* = 4.9 Hz, 1H), 3.72 (d, *J* = 6.1 Hz, 1H), 3.30 – 3.11 (m, 2H), 2.57 – 2.43 (m, 1H), -0.26 (s, 9H) ppm.

**9a-Bromo-4-(2-bromoacetyl)-9-((trimethylsilyl)oxy)-5a,6,9,9a-tetrahydrobenzo[*g*]quinoline-5,10-dione (69a)**

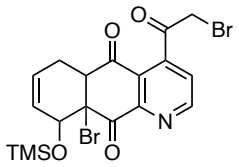


To a solution of **54d** (20 mg, 0.056 mmol, 1.0 equiv) in $d_8$-toluene (0.3 mL, 0.2 M) was added diene **67e** (14.3 mg, 0.1 mmol, 1.8 equiv) and the resulting solution was stirred for 1 h at 23 ºC. Then, an aliquote was taken to analyze the sample directly by $^1$H NMR.

**$^1$H NMR** (500 MHz, $d_8$-toluene) δ 9.14 (d, *J* = 4.7 Hz, 1H), 7.57 (d, *J* = 4.7 Hz, 1H), 6.02 (ddd, *J* = 10.3, 5.0, 2.5 Hz, 1H), 5.80 (ddd, *J* = 10.4, 5.0, 2.4 Hz, 1H), 4.58 (d, *J* = 4.8 Hz, 1H), 4.33 (d, *J* = 12.5 Hz, 1H), 4.27 (d, *J* = 12.4 Hz, 1H), 3.77 (d, *J* = 6.3 Hz, 1H), 3.27 – 3.21 (m, 1H), 2.62 – 2.55 (m, 1H), -0.24 (s, 8H) ppm.

**Crystallographic Data**
**Monomarginine (12)**

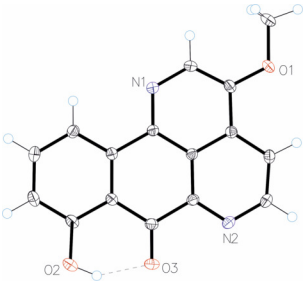


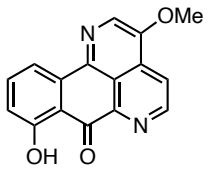


**Table S1**. Crystal data and structure refinement for monomarginine **12**.

| | |
|---|---|
| Identification code | GO1NPLT |
| Empirical formula | $C_{17.25}H_{10.95}Cl_{1.05}F_{0.3}N_2O_3$ |
| Formula weight | 337.15 |
| Temperature/K | 100.15 |
| Crystal system | triclinic |
| Space group | P-1 |
| a/Å | 8.2858(2) |
| b/Å | 8.4955(2) |
| c/Å | 11.8830(4) |
| α/° | 70.517(3) |
| β/° | 84.614(3) |
| γ/° | 64.441(3) |
| Volume/Å$^3$ | 710.17(4) |
| Z | 2 |
| $\rho_{calc}$g/cm$^3$ | 1.577 |
| μ/mm$^{-1}$ | 0.301 |
| F(000) | 346.0 |
| Crystal size/mm$^3$ | 0.15 × 0.04 × 0.02 |
| Radiation | Mo Kα (λ = 0.71073) |
| 2Θ range for data collection/° | 5.46 to 59.914 |
| Index ranges | -11 ≤ h ≤ 11, -11 ≤ k ≤ 11, -16 ≤ l ≤ 15 |
| Reflections collected | 15391 |
| Independent reflections | 3645 [$R_{int}$ = 0.0273, $R_{sigma}$ = 0.0218] |
| Data/restraints/parameters | 3645/223/325 |
| Goodness-of-fit on F$^2$ | 1.061 |
| Final R indexes [I>=2σ (I)] | $R_1$ = 0.0390, w$R_2$ = 0.1187 |
| Final R indexes [all data] | $R_1$ = 0.0444, w$R_2$ = 0.1225 |
| Largest diff. peak/hole / e Å$^{-3}$ | 0.39/-0.24 |

**3-Bromojuglone (21)**

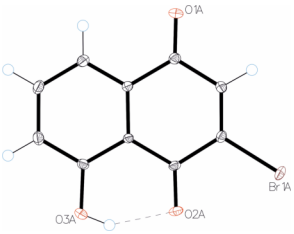


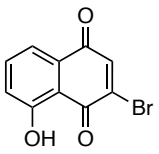


**Table S2**. Crystal data and structure refinement for **21**.

| | |
|---|---|
| Identification code | mo_GO-2-90_0m_a |
| Empirical formula | $C_{20}H_{10}Br_2O_6$ |
| Formula weight | 506.10 |
| Temperature/K | 99.68 |
| Crystal system | triclinic |
| Space group | P-1 |
| a/Å | a = 7.0939(6) |
| b/Å | 8.4013(7) |
| c/Å | 16.1645(13) |
| α/° | 90.027(2) |
| β/° | 100.300(2) |
| γ/° | 114.909(2) |
| Volume/Å$^3$ | 856.57(12) |
| Z | 2 |
| $\rho_{calc}$g/cm$^3$ | 1.962 |
| μ/mm$^{-1}$ | 4.770 |
| F(000) | 496.0 |
| Crystal size/mm$^3$ | 0.5 × 0.5 × 0.5 |
| Radiation | MoKα (λ = 0.71073) |
| 2Θ range for data collection/° | 2.57 to 66.83 |
| Index ranges | -10 ≤ h ≤ 7, -12 ≤ k ≤ 12, -25 ≤ l ≤ 24 |
| Reflections collected | 18650 |
| Independent reflections | 6302 [$R_{int}$ = 0.0342, $R_{sigma}$ = 0.0386] |
| Data/restraints/parameters | 6302/0/257 |
| Goodness-of-fit on F$^2$ | 1.040 |
| Final R indexes [I>=2σ (I)] | $R_1$ = 0.0290, w$R_2$ = 0.0696 |
| Final R indexes [all data] | $R_1$ = 0.0379, w$R_2$ = 0.0723 |
| Largest diff. peak/hole / e Å$^{-3}$ | 1.05/-0.91 |

**4-Ethynyl-6-hydroxybenzo[*g*]quinoline-5,10-dione (23)**

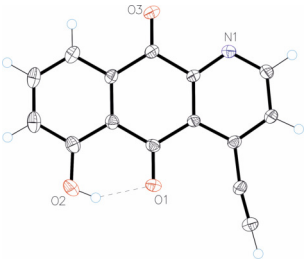


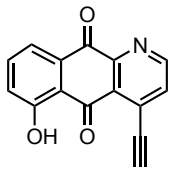


**Table S3**. Crystal data and structure refinement for **23**.

| | |
|---|---|
| Identification code | GO-2-78 |
| Empirical formula | $C_{15}H_7NO_3$ |
| Formula weight | 249.22 |
| Temperature/K | 100(2) |
| Crystal system | monoclinic |
| Space group | $P2_1/n$ |
| a/Å | 7.4686(2) |
| b/Å | 17.0322(4) |
| c/Å | 8.8419(2) |
| α/° | 90 |
| β/° | 101.198(3) |
| γ/° | 90 |
| Volume/Å$^3$ | 1103.33(5) |
| Z | 4 |
| $\rho_{calc}$g/cm$^3$ | 1.500 |
| μ/mm$^{-1}$ | 0.107 |
| F(000) | 512.0 |
| Crystal size/mm$^3$ | 0.6 × 0.2 × 0.1 |
| Radiation | Mo Kα (λ = 0.71073) |
| 2Θ range for data collection/° | 6.97 to 59.49 |
| Index ranges | $-9 \leq h \leq 10$, $-23 \leq k \leq 23$, $-12 \leq l \leq 11$ |
| Reflections collected | 15769 |
| Independent reflections | 2909 [$R_{int}$ = 0.0184, $R_{sigma}$ = 0.0151] |
| Data/restraints/parameters | 2909/0/174 |
| Goodness-of-fit on $F^2$ | 1.074 |
| Final R indexes [I>=2σ (I)] | $R_1$ = 0.0618, $wR_2$ = 0.1808 |
| Final R indexes [all data] | $R_1$ = 0.0692, $wR_2$ = 0.1870 |
| Largest diff. peak/hole / e Å$^{-3}$ | 0.99/-0.20 |

**2-Bromo-5-hydroxy-3-((5-(triisopropylsilyl)penta-2,4-diyn-1-yl)amino)naphthalene-1,4-dione (28)**

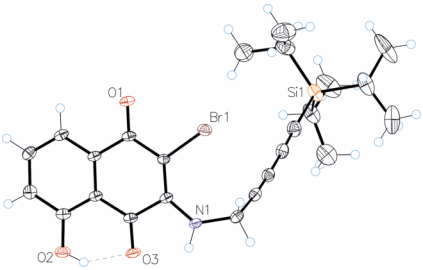


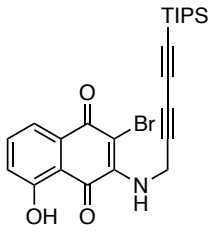


**Table S4**. Crystal data and structure refinement for **28**.

| | |
|---|---|
| Identification code | mo_GO296AF1 |
| Empirical formula | $C_{24}H_{28}BrNO_3Si$ |
| Formula weight | 486.47 |
| Temperature/K | 99.68 |
| Crystal system | monoclinic |
| Space group | $P2_1/c$ |
| a/Å | 21.548(3) |
| b/Å | 7.6809(10) |
| c/Å | 14.3135(18) |
| α/° | 90 |
| β/° | 92.212(3) |
| γ/° | 90 |
| Volume/Å$^3$ | 2367.2(5) |
| Z | 4 |
| $\rho_{calc}$g/cm$^3$ | 1.365 |
| μ/mm$^{-1}$ | 1.812 |
| F(000) | 1008.0 |
| Crystal size/mm$^3$ | 0.2 × 0.2 × 0.02 |
| Radiation | MoKα (λ = 0.71073) |
| 2Θ range for data collection/° | 3.784 to 61.05 |
| Index ranges | $-30 \leq h \leq 27$, $-9 \leq k \leq 10$, $-13 \leq l \leq 20$ |
| Reflections collected | 23618 |
| Independent reflections | 7042 [$R_{int}$ = 0.0446, $R_{sigma}$ = 0.0523] |
| Data/restraints/parameters | 7042/0/279 |
| Goodness-of-fit on F$^2$ | 1.042 |
| Final R indexes [I>=2σ (I)] | $R_1$ = 0.0424, $wR_2$ = 0.0901 |
| Final R indexes [all data] | $R_1$ = 0.0662, $wR_2$ = 0.0977 |
| Largest diff. peak/hole / e Å$^{-3}$ | 0.65/-0.69 |

**1-Ethynyl-6,10-dimethoxybenzo[f]quinoline (32)**

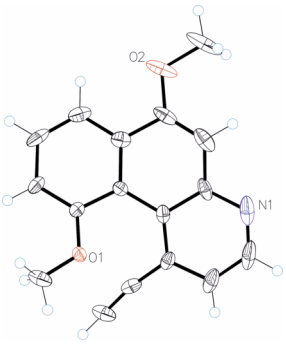


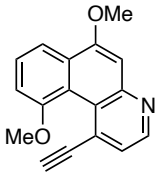


**Tabla S5**. Crystal data and structure refinement for **32**.

| | |
|---|---|
| Identification code | mo_PB51_0m |
| Empirical formula | $C_{8.5}H_{6.5}N_{0.5}O$ |
| Formula weight | 131.64 |
| Temperature/K | 99.21 |
| Crystal system | monoclinic |
| Space group | C2/c |
| a/Å | 14.935(3) |
| b/Å | 11.593(2) |
| c/Å | 7.5642(13) |
| α/° | 90 |
| β/° | 107.890(5) |
| γ/° | 90 |
| Volume/Å$^3$ | 1246.4(4) |
| Z | 8 |
| $\rho_{calc}$g/cm$^3$ | 1.403 |
| μ/mm$^{-1}$ | 0.092 |
| F(000) | 552.0 |
| Crystal size/mm$^3$ | 0.3 × 0.3 × 0.2 |
| Radiation | MoKα (λ = 0.71073) |
| 2Θ range for data collection/° | 4.534 to 60.366 |
| Index ranges | -21 ≤ h ≤ 21, -16 ≤ k ≤ 16, -10 ≤ l ≤ 10 |
| Reflections collected | 22114 |
| Independent reflections | 1853 [$R_{int}$ = 0.0288, $R_{sigma}$ = 0.0118] |
| Data/restraints/parameters | 1853/134/177 |
| Goodness-of-fit on F$^2$ | 1.164 |
| Final R indexes [I>=2σ (I)] | $R_1$ = 0.0597, w$R_2$ = 0.1337 |
| Final R indexes [all data] | $R_1$ = 0.0659, w$R_2$ = 0.1376 |
| Largest diff. peak/hole / e Å$^{-3}$ | 0.21/-0.25 |

**2-Bromo-1-(7-bromo-5,8-dimethoxyquinolin-4-yl)ethan-1-one (56a)**

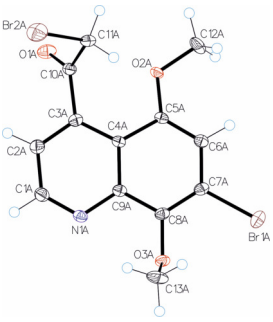


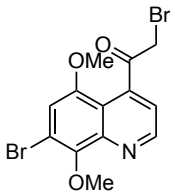


**Tabla S6**. Crystal data and structure refinement for **56a**.

| | |
|---|---|
| Identification code | mo_GO2154_0m |
| Empirical formula | $C_{13}H_{11}Br_2NO_3$ |
| Formula weight | 389.05 |
| Temperature/K | 99.82 |
| Crystal system | monoclinic |
| Space group | $P2_1/c$ |
| a/Å | 9.163(4) |
| b/Å | 7.498(3) |
| c/Å | 39.485(17) |
| α/° | 90 |
| β/° | 92.188(13) |
| γ/° | 90 |
| Volume/Å$^3$ | 2711(2) |
| Z | 8 |
| $\rho_{calc}$g/cm$^3$ | 1.907 |
| μ/mm$^{-1}$ | 5.983 |
| F(000) | 1520.0 |
| Crystal size/mm$^3$ | 0.2 × 0.1 × 0.1 |
| Radiation | MoKα (λ = 0.71073) |
| 2Θ range for data collection/° | 2.064 to 56.044 |
| Index ranges | $-11 \leq h \leq 12$, $-9 \leq k \leq 9$, $-51 \leq l \leq 36$ |
| Reflections collected | 21711 |
| Independent reflections | 6179 [$R_{int}$ = 0.0731, $R_{sigma}$ = 0.0919] |
| Data/restraints/parameters | 6179/300/351 |
| Goodness-of-fit on $F^2$ | 1.181 |
| Final R indexes [I>=2σ (I)] | $R_1$ = 0.0764, $wR_2$ = 0.1730 |
| Final R indexes [all data] | $R_1$ = 0.1006, $wR_2$ = 0.1823 |
| Largest diff. peak/hole / e Å$^{-3}$ | 2.36/-1.43 |

UNIVERSITAT ROVIRA I VIRGILI
Novel Supramolecular Gold(I)-Cavitand Catalysts and Approach to the Total Synthesis of Monomarginine
Gala Ogalla Estévez

# Appendix: *Truxene Gold(I) Complexes*

UNIVERSITAT ROVIRA I VIRGILI
Novel Supramolecular Gold(I)-Cavitand Catalysts and Approach to the Total Synthesis of Monomarginine
Gala Ogalla Estévez

## Introduction

Truxene 10,15-dihydro-5*H*-diindeno[1,2-*a*;1',2'-*c*]fluorene has been used for the construction of larger polyarenes.[1] Specially, the development of a practical synthesis of bowl-shaped fragments of fullerenes[2] to allow the construction of molecular cages with polycyclic aromatic walls that could encapsulate metal cations of small molecules,[3] has been of great interest. In this context, the synthesis of functionalized truxenes has been explored in our group (Scheme 1).[4] For instance, in 1999 our group reported the synthesis of a variety of *syn*-trialkylated truxenes *syn*-**2**, with $C_{3v}$ symmetry in gram scale from truxene **1** (scheme 1, top). The methodology was based on the alkylation of **1**, which gave an *anti*/*syn* mixture of inseparable isomers **2**. Then, a base-catalyzed isomerization of the crude mixture, formed *syn*-**2** in moderate to good yields with different aryl and alkyl substituents. Later, the regioselective functionalization of truxene **1** towards $C_{3h}$ truxenes derivatives **3** was achieved by using $Br_2$, followed by a Stille coupling reaction (Scheme 1, bottom).

---

1 For some examples see: (a) Plater, M. J. Synthesis of 1,3,5-Tri(benzo[c]phenanthrene-5-yl)benzene: A Potential Polycyclic Aromatic Hydrocarbon Precursor to $C_{60}$, *Synlett* **1993**, 405–406. (b) Rabideau, P. W.; Abdourazak, A. H.; Marcinow, Z.; Sygula, R.; Sygula, A. Towards the Total Synthesis of Buckminsterfullerene ($C_{60}$): Benz[5,6]-*as*-indaceno-[3,2,1,8,7-*mnopqr*]indeno[4,3,2,1-*cdef*]chrysene *J. Am. Chem. Soc.* **1995**, *117*, 6410–6411. (c) Diederich, F.; Rubin, Y. Synthetic Approaches toward Molecular and Polymeric Carbon Allotropes, *Angew. Chem. Int. Ed. Engl.* **1992**, *31*, 1101–1123.

2 (a) Scott, L. T. Fragments of Fullerenes: Novel Syntheses, Structures and Reactions, *Pure Appl. Chem.* **1996**, *68*, 291–300. (b) Rabideau, P. W.; Sygula, A. Buckybowls: Polynuclear Aromatic Hydrocarbons Related to the Buckminsterfullerene Surface, *Acc. Chem. Res.* **1996**, *29*, 235–242. (c) Rubin, Y. Organic Approaches to Endohedral Metallofullerenes: Cracking Open or Zipping Up Carbon Shells?, *Chem. Eur. J.* **1997**, *3*, 1009–1016.

3 (a) Rivera, J. M.; Martín, T.; Rebek, J. Chiral Spaces: Dissymmetric Capsules Through Self-Assembly, *Science* **1998**, *279*, 1021–1023. (b) Meyer, E. A.; Castellano, R. K.; Diederich, F. Interactions with Aromatic Rings in Chemical and Biological Recognition, *Angew. Chem. Int. Ed.* **2003**, *42*, 1210–1250. (c) Piatnitski, E. L.; Deshayes, K. D. Hemicarceplexes That Release Guests upon Irradiation, *Angew. Chem. Int. Ed.* **1998**, *37*, 970–972. (d) Stang, P. J. Molecular Architecture: Coordination as the Motif in the Rational Design and Assembly of Discrete Supramolecular Species—Self-Assembly of Metallacyclic Polygons and Polyhedra, *Chem. – Eur. J.* **1998**, *4*, 19–27.

4 (a) De Frutos, Ó.; Gómez-Lor, B.; Granier, T.; Monge, M. Á.; Gutiérrez-Puebla, E.; Echavarren, A. M. Syn-Trialkylated Truxenes: Building Blocks That Self-Associate by Arene Stacking, *Angew. Chem. Int. Ed.* **1999**, *38*, 204–207. (b) Gómez-Lor, B.; Frutos, Ó. de; Ceballos, P. A.; Granier, T.; Echavarren, A. M. Synthesis of New $C_{3h}$ and $C_{3v}$ Truxene Derivatives, *Eur. J. Org. Chem.* **2001**, *2001*, 2107–2114. (c) De Frutos, Ó.; Granier, T.; Gómez-Lor, B.; Jiménez-Barbero, J.; Monge, Á.; Gutiérrez-Puebla, E.; Echavarren, A. M. Synthesis and Self-Association of Syn-5,10,15-Trialkylated Truxenes, *Chem. Eur. J.* **2002**, *8*, 2879. (d) Ruiz, M.; Gómez-Lor, B.; Santos, A.; Echavarren, A. M. Overcrowded 5,10,15-Trisubstituted Derivatives: Synthesis of 5,10,15-Tri(fluorenylidene)truxene, *Eur. J. Org. Chem.* **2004**, *2004*, 858–866. (e) González-Cantalapiedra, E.; Ruiz, M.; Gómez-Lor, B.; Alonso, B.; García-Cuadrado, D.; Cárdenas, D. J.; Echavarren, A. M. New Building Blocks Based on Truxene Cores: Synthesis of Functionalized *Syn*-Tri- and -Hexasubstituted Derivatives, *Eur. J. Org. Chem.* **2005**, *2005*, 4127–4140.

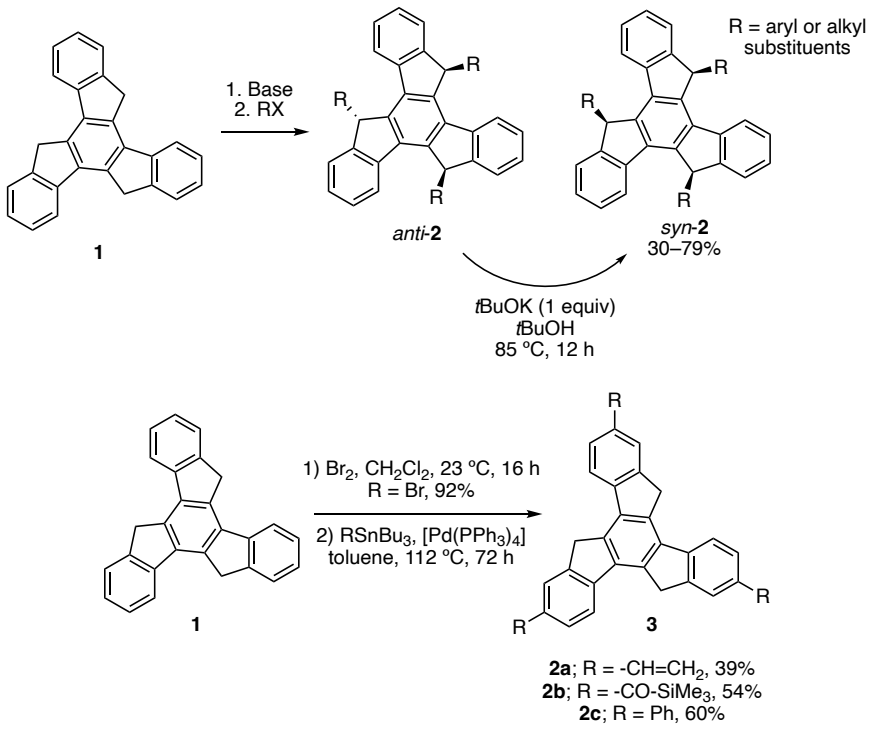


**Scheme 1**. Precedent work towards the synthesis of truxene derivatives.

In this context, we aimed to use this approach for synthesizing a new family of truxene derivatives that could act as precursors for the synthesis of gold(I) complexes with truxene-phosphine ligands (Scheme 2).

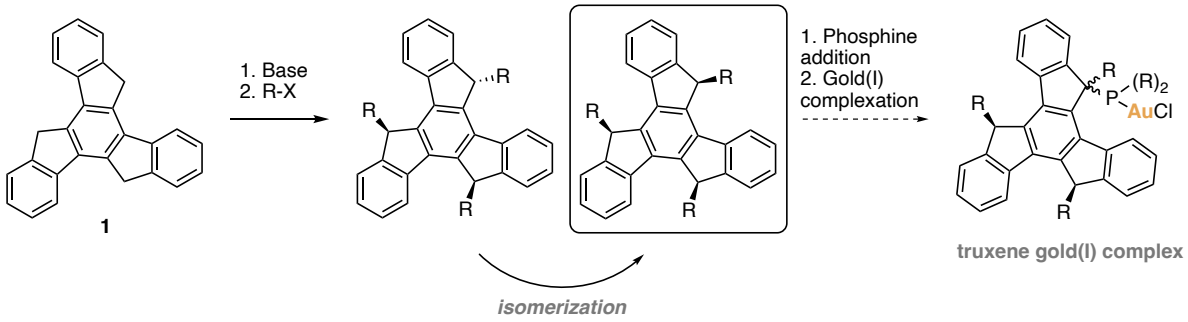


**Scheme 2**. Planned synthesis of truxene gold(I) complexes.

## Preliminary Results

We started the synthesis by adapting the reported conditions for the formation of truxene derivatives. From truxene **1**, using NaH as base and with different aryl bromide reagents, we were able to obtain the *anti*/*syn* mixture of derivated truxenes **2** in moderate to good yields (Scheme 3).

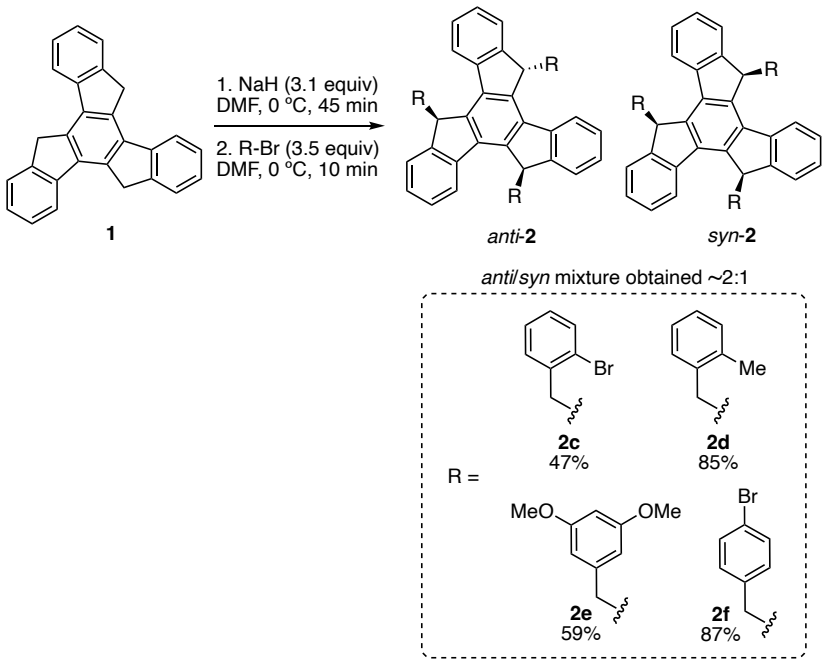


**Scheme 3**. Synthesis of functionalized truxenes **2**.

For the isomerization reaction, we encountered reproducibility issues when trying to use *t*BuOK as base. Therefore, after testing other possible base sources, we found that $Cs_2CO_3$ in DMSO under reflux was cleanly isomerizing the *anti*-truxenes **2** to their *syn*-**2** isomers in good to excellent yields (Scheme 4).

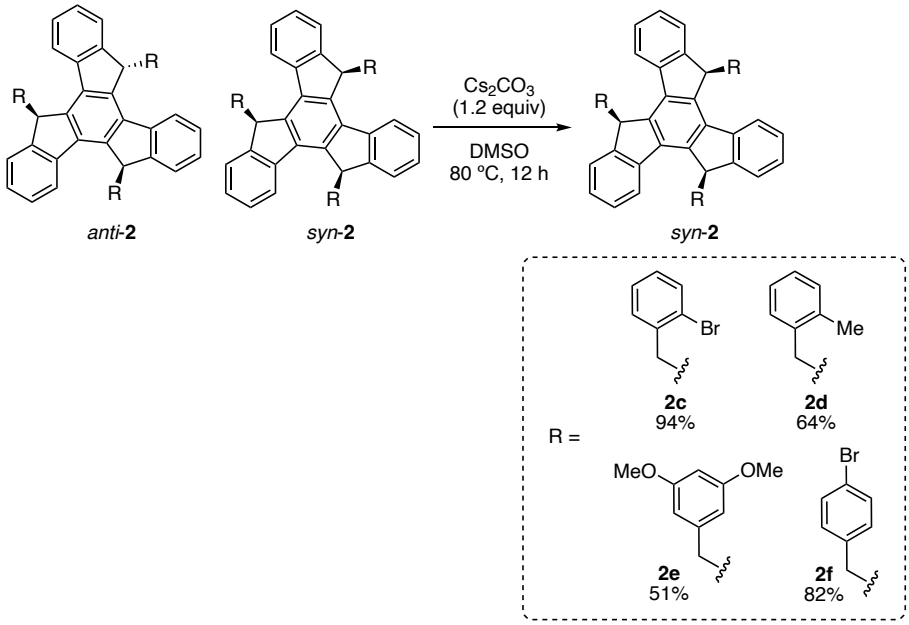


**Scheme 4**. Isomerization of *anti*-**2** truxenes to their corresponding isomers *syn*-**2**.

Interestingly, in the case of truxene **2c**, we were able to separate the *anti*/*syn* mixture by flash column chromatography. Taking advantage of this, we functionalized separately each isomer *via* a Stille coupling reaction to form the analogous compounds *anti*-**2g** and *syn*-**2g**, respectively. However, when

treating them with *n*BuLi followed by phosphine addition, no product was detected. Instead, only starting material was recovered. Presumably, steric hindrance was too high for the truxene derivatives **2g** to interact with the chlorophosphine reagent (Scheme 5).

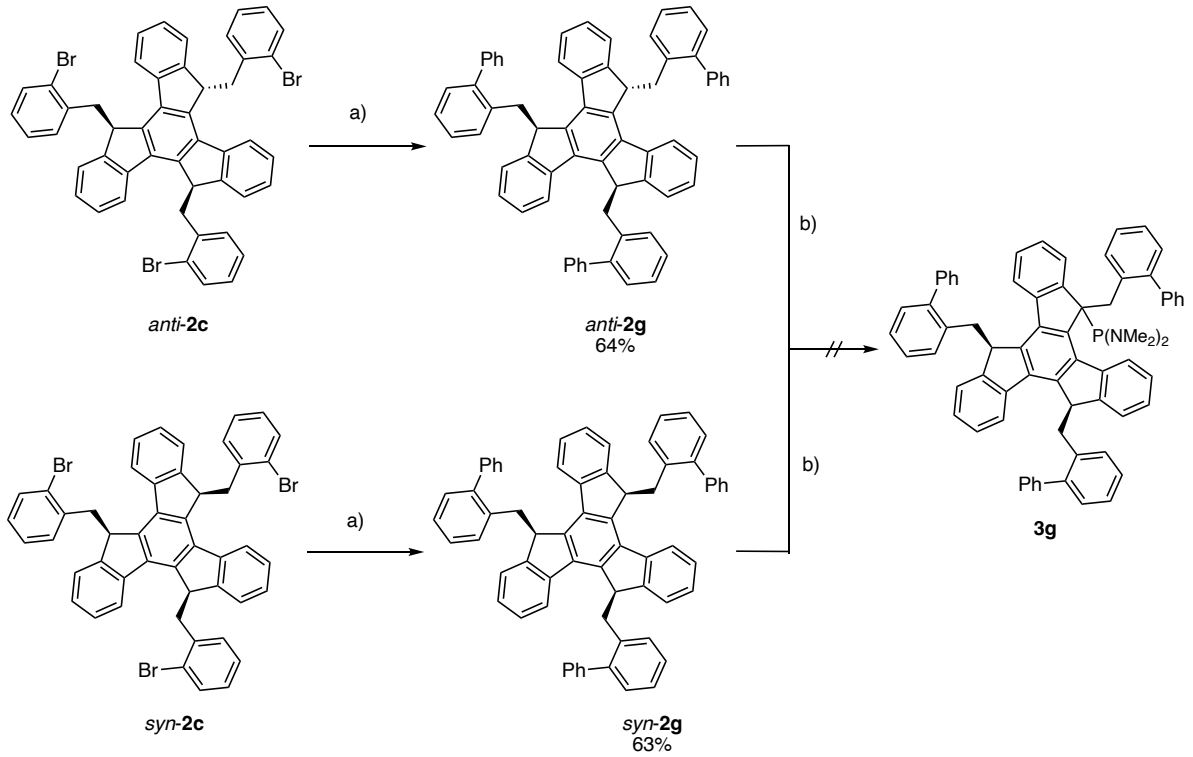


**Scheme 5**. Attempts for the functionalization of truxene derivatives *anti*- and *syn*-**2g**. a) $PhSnBu_3$ (3.6 equiv), $Pd(PPh_3)_4$ (10 mol %), 1,4-hydroquinone, toluene, 112 ºC, 16 h. b) *n*BuLi (1.0 equiv), -78 ºC to -10 ºC, 4 h. *Then*, $ClP(NMe_2)_2$ (1 equiv) -78 ºC to -10 ºC, 18 h.

Another attempt for the phosphine formation was performed with the truxene derivative *syn*-**2d** (Scheme 6). However, the same negative outcome was observed.

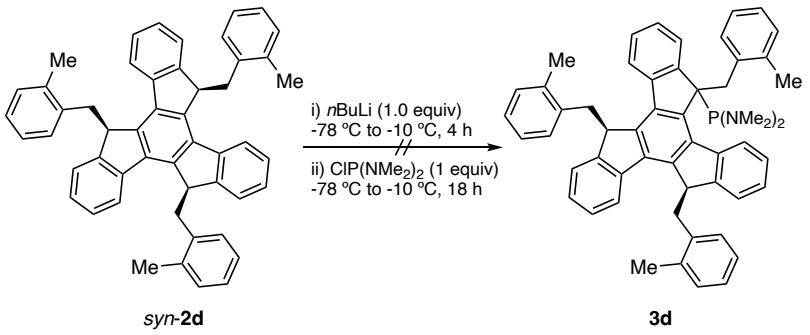


**Scheme 6**. Attempts for the functionalization of *syn*-**2d** to its phosphine derivative **3d**.

The treatment of fluorene, considered electronically comparable to truxene and so, its model substrate, was tested for the corresponding fluorene gold(I) complex **4** (Scheme 7, top). Under standard phosphine addition and gold(I) coordination conditions, we observed the formation of the desired complex **4**,

whose structure was confirmed by X-ray diffraction (Figure 1). Similarly, truxene **1** was treated under the same reaction conditions to afford gold(I) truxene complex **5** in 90% yield.

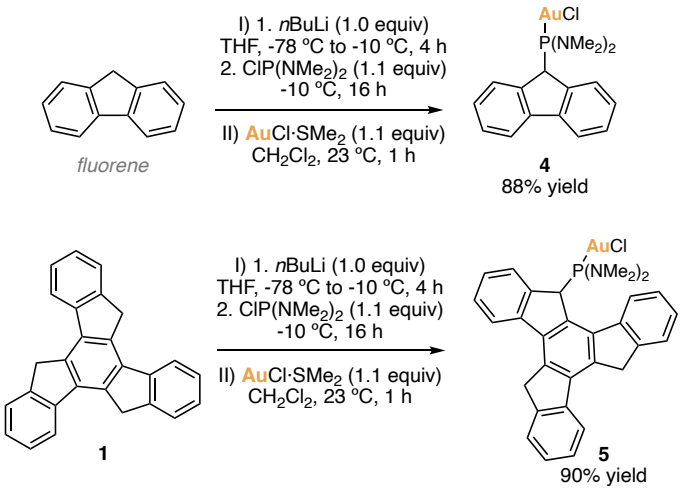


**Scheme 7**. Synthesis of fluorene and truxene gold(I) complexes **4** and **5**.

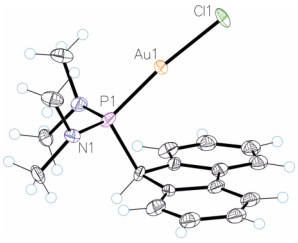


**Figure 1**. X-ray structure of fluorene gold(I) complex **4**.

Finally, the new gold(I) complexes were tested in cyclization reactions previously explored in the group.[5]. Enynes **6** and **8** with NTs as tether underwent exclusively the *endo*-skeletal rearrangement products **7** and **9** in excellent yields. On the other hand, reactions of *E*-1,6-enyne **10**, gave a mixture of the *exo*-skeletal rearrangement product **11a** and the tetracycle **11b**.[5a]

5 (a) Nieto-Oberhuber, C.; Muñoz, M. P.; Buñuel, E.; Nevado, C.; Cárdenas, D. J.; Echavarren, A. M. Cationic Gold(I) Complexes: Highly Alkynophilic Catalysts for the *exo* - and *endo* -Cyclization of Enynes, *Angew. Chem.* **2004**, *116*, 2456–2460. (b) Nieto-Oberhuber, C.; Muñoz, M. P.; López, S.; Jiménez-Núñez, E.; Nevado, C.; Herrero-Gómez, E.; Raducan, M.; Echavarren, A. M. Gold(I)-Catalyzed Cyclizations of 1,6-Enynes: Alkoxycyclizations and *exo*/*endo* Skeletal Rearrangements, *Chem. Eur. J.* **2006**, *12*, 1677–1693. (c) Nieto-Oberhuber, C.; López, S.; Muñoz, M. P.; Jiménez-Núñez, E.; Buñuel, E.; Cárdenas, D. J.; Echavarren, A. M. Gold(I)-Catalyzed Intramolecular Cyclopropanation of Dienynes, *Chem. Eur. J.* **2006**, *12*, 1694–1702.

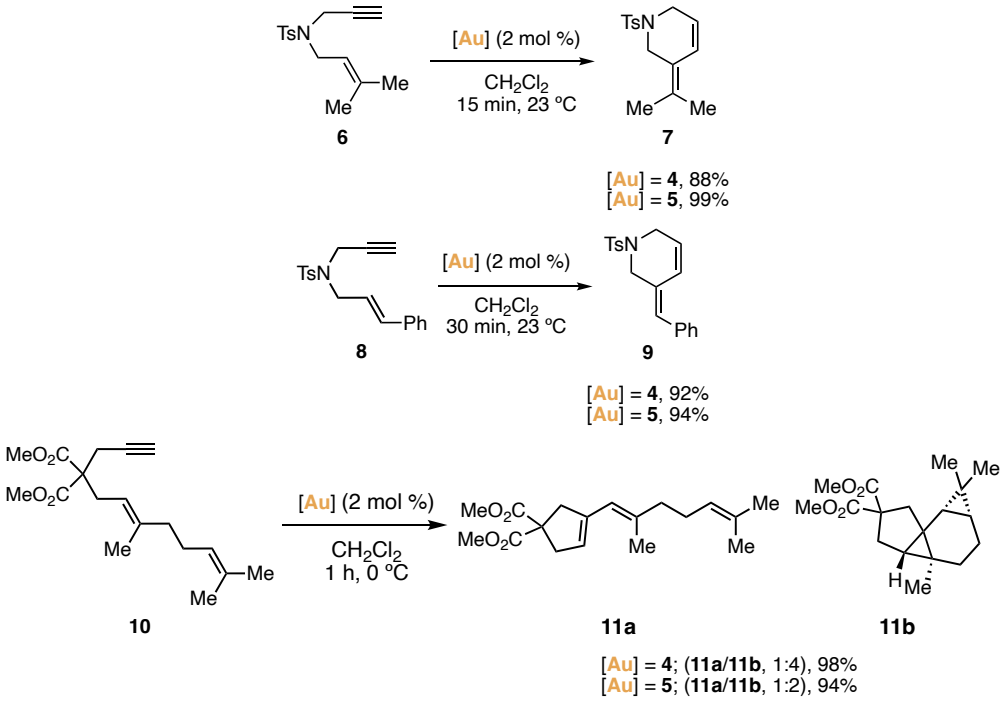


**Scheme 8**. Catalytic test of known intramolecular cyclization reactions with fluorene and truxene gold(I) complexes **4** and **5**, respectively.

Having proved the possibilities of catalyzing reactions of enynes with truxene based gold(I) complexes, further studies are ongoing in our group to expand the truxenes gold(I) complex family to form gold(I) complexes with very bulky ligands.

## Experimental Section

### General Methods

The general information has been provided in the experimental section of *Chapter I*.

The preparation of 10,15-Dihydro-5*H*-diindeno[1,2-*a*;1',2'-*c*]fluorene (truxene, **1**) has been described.[6]

Enynes 6,[7] 8[8] and 10,[9] have been described.

For the synthesis of *anti*- and *syn*-trialkylated truxenes, a reported procedure was adapted.[4c]

### Synthetic Procedures and Analytical Data

### General procedure GP1 for the synthesis of trialkylated truxenes:

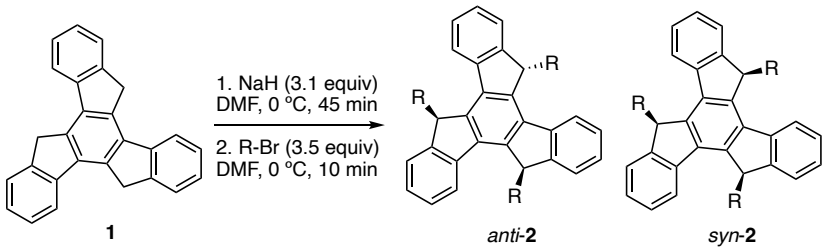


**Scheme S1**. General procedure GP1 for the trialkylated truxenes synthesis.

A mixture of truxene **1** (1.5 mmol, 1.0 equiv) and NaH (3.1 equiv, 60% in mineral oil) in DMF was sonicated for 45 min at 0 °C to give a bright-red mixture. On addition of a solution of the alkylating agent (3.5 equiv) in DMF (0.06 M final concentration), the red color faded almost immediately. After 10 min, the mixture was diluted with AcOEt, washed with 10% aqueous HCl and saturated aqueous NaCl solution, dried over $Na_2SO_4$, filtrated, and concentrated under reduced pressure. The residue was either treated with hexane or purified by flash column chromatography to give trialkylated truxenes **2** as an *anti*/*syn* mixture.

6 Dehmlow, E. V.; Kelle, T. Synthesis of New Truxene Derivatives: Possible Precursors of Fullerene Partial Structures?, Synth. Commun. **1997**, *27*, 2021–2031.

7 Kataoka, T.; Yoshimatsu, M.; Noda, Y.; Sato, T.; Shimizu, H.; Hori, M. Versatile Cyclisation Reactions Using Selenoboranes, *J. Chem. Soc. Perkin 1* **1993**, *1*, 121–129.

8 Nevado, C.; Charruault, L.; Michelet, V.; Nieto-Oberhuber, C.; Muñoz, M. P.; Méndez, M.; Rager, M.-N.; Genêt, J.-P.; Echavarren, A. M. On the Mechanism of Carbohydroxypalladation of Enynes. Additional Insights on the Cyclization of Enynes with Electrophilic Metal Complexes, *Eur. J. Org. Chem.* **2003**, *2003*, 706–713.

9 Trost, B.; Krische, M. J. Palladium-Catalyzed Enyne Cycloisomerization Reaction in an Asymmetric Approach to the Picrotoxane Sesquiterpenes. 2. Second-Generation Total Syntheses of Corianin, Picrotoxinin, Picrotin, and Methyl Picrotoxate, *J. Am. Chem. Soc.* **1999**, *121*, 6131–6141.

**General procedure GP2 for the synthesis of *syn*-trialkylated truxenes:**

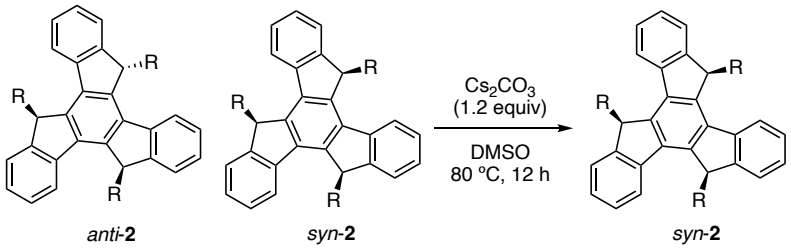


**Scheme S2**. General procedure GP2 for the isomerization process towards *syn*-trialkylated truxenes **2**.

An *anti*/*syn* mixture of the corresponding trialkylated truxenes **2** (1.0 equiv) was diluted in anhydrous DMSO (0.33 M) and $Cs_2CO_3$ (1.2 equiv) was added giving a deep-red solution. The mixture was heated to 80 °C and was left stirring for 12 h. Then, after cooling, the solvent was removed under reduced pressure. The residue was treated with hexane to give the corresponding *syn*-trialkylated truxene **2**. Further recrystallization from ethanol or toluene yielded pure compounds.

**(5*R*,10*R*,15*R*)-5,10,15-Tris(2-bromobenzyl)-10,15-dihydro-5*H*-diindeno[1,2-*a*:1',2'-*c*]fluorene (*anti*-2c)**

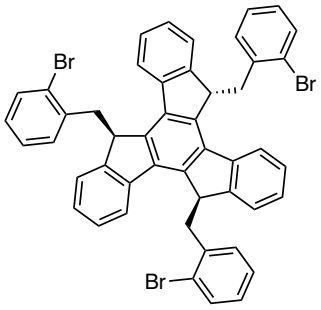


Following general procedure **GP1** using truxene **1** (600 mg, 1.75 mmol, 1.0 equiv), NaH (130.4 mg, 5.43 mmol, 3.1 equiv) and 1-bromo-2-(bromomethyl)benzene (1.53 g, 6.13 mmol, 3.5 equiv) in anhydrous DMF (29.2 mL, 0.06 M). The crude was obtained as a 2:1 *anti*/*syn* mixture of **2c**. After purification by flash column chromatography ($SiO_2$, CyH/AcOEt 99:1), *anti*-**2c** was isolated as a single isomer being an off-yellow solid (700 mg, 0.82 mmol, 47% yield).

**$^1$H NMR** (300 MHz, $CDCl_3$) δ 8.38 (t, *J* = 7.1 Hz, 2H), 8.23 (d, *J* = 7.7 Hz, 1H), 7.63 – 7.49 (m, 3H), 7.49 – 7.35 (m, 3H), 7.19 (tt, *J* = 7.4, 1.7 Hz, 1H), 7.08 – 7.01 m (9H), 6.92 (dd, *J* = 7.4, 2.0 Hz, 1H), 6.81 (d, *J* = 7.5 Hz, 1H), 6.71 (d, *J* = 7.5 Hz, 1H), 6.63 (d, *J* = 7.7 Hz, 1H), 5.16 (dt, *J* = 9.0, 4.5 Hz, 1H), 5.13 – 5.06 (m, 2H), 4.17 – 4.06 (m, 2H), 3.97 (dd, *J* = 14.3, 5.2 Hz, 1H), 2.89 (dd, *J* = 14.0, 9.6 Hz, 1H), 2.67 (dd, *J* = 14.2, 10.3 Hz, 1H), 2.48 (dd, *J* = 14.4, 10.6 Hz, 1H) ppm.

**$^{13}$C NMR** (101 MHz, $CDCl_3$) δ 146.9, 146.8, 146.7, 141.6, 140.7, 140.6, 140.4, 140.2, 139.9, 139.3, 138.8, 137.1, 137.0, 133.0, 132.9, 132.2, 132.1, 132.0, 128.3, 127.4, 127.3, 127.0, 126.2, 126.1, 126.0, 125.9, 125.7, 125.6, 125.5, 125.4, 123.1, 123.0, 122.8, 46.9, 46.5, 46.4, 39.1, 39.1, 39.0 ppm.

The spectral data were fully consistent with those previously reported.[4c]

**(5*R*,10*R*,15*R*)-5,10,15-Tris(2-bromobenzyl)-10,15-dihydro-5*H*-diindeno[1,2-*a*:1',2'-*c*]fluorene (*syn*-2c)**

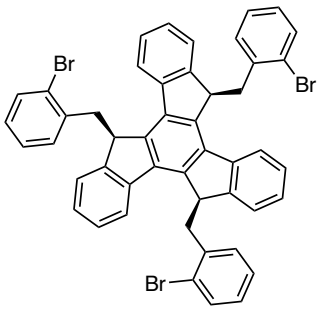


Following general procedure **GP2** using 2:1 *anti*/*syn* mixture of **2c** (50 mg, 59 μmol, 1.0 equiv) and $Cs_2CO_3$ (23 mg, 70.6 μmol, 1.2 equiv) in anhydrous DMSO (0.18mL, 0.33 M). After treatment with hexane, *syn*-**2c** was obtained as an off-white solid (47 mg, 55 μmol, 94% yield).

**$^{1}$H NMR** (300 MHz, $CDCl_3$) δ 7.93 (d, *J* = 7.7 Hz, 2H), 7.50 (dd, *J* = 7.8, 1.4 Hz, 3H), 7.39 (t, *J* = 7.5 Hz, 3H), 7.14 (qd, *J* = 7.4, 1.3 Hz, 6H), 7.04 (td, *J* = 7.6, 1.9 Hz, 4H), 6.86 (dd, *J* = 7.5, 1.9 Hz, 3H), 6.68 (d, *J* = 7.5 Hz, 3H), 4.37 (dd, *J* = 9.9, 5.0 Hz, 3H), 3.75 (dd, *J* = 14.2, 5.0 Hz, 3H), 2.73 (dd, *J* = 14.2, 9.9 Hz, 3H) ppm.

**$^{13}$C NMR** (126 MHz, $CDCl_3$) δ 147.0, 140.8, 140.2, 139.1, 136.0, 132.8, 131.8, 128.0, 127.2, 127.0, 125.9, 125.7, 125.5, 122.9, 46.1, 38.8 ppm.

**HRMS** (MALDI+) calculated for m/z $[C_{48}H_{32}Br_3]^+$, $[M-H]^+$: 845.0049; found: 845.0022.

The spectral data were fully consistent with those previously reported.[4c]

**5,10,15-Tris(4-bromobenzyl)-10,15-dihydro-5*H*-diindeno[1,2-*a*:1',2'-*c*]fluorene (*syn*-2f)**

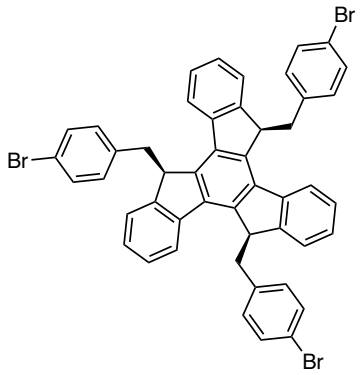


Following general procedure **GP1** using truxene **1** (100 mg, 0.29 mmol, 1.0 equiv), NaH (24.14 mg, 0.6 mmol, 3.1 equiv) and 1-bromo-4-(bromomethyl)benzene (170.3 mg, 0.68 mmol, 3.5 equiv) in anhydrous DMF (4.87 mL, 0.06 M). After treatment with hexane, **2f** was obtained as an inseparable *anti*/*syn* mixture. Yellow solid (143 mg, 0.17 mmol, 87% yield). The *anti*/*syn* **2f** mixture (50 mg, 58.9 µmol, 1.0 equiv) was exposed to conditions in general procedure **GP2** which afforded *syn*-**2f**. Purification was performed by recrystallization in toluene to give an off-white solid (41 mg, 48 µmol, 82% yield).

**$^1$H NMR** (500 MHz, $CDCl_3$) δ 7.55 (d, *J* = 7.6 Hz, 3H), 7.45 (td, *J* = 7.4, 1.2 Hz, 3H), 7.31 – 7.27 (m, 3H), 7.23 – 7.20 (m, 6H), 6.85 – 6.81 (m, 3H), 6.60 – 6.55 (m, 6H), 3.74 (dd, *J* = 9.6, 3.7 Hz, 3H), 3.35 (dd, *J* = 14.1, 3.7 Hz, 3H), 2.27 (dd, *J* = 14.1, 9.6 Hz, 3H) ppm.

**$^{13}$C NMR** (126 MHz, $CDCl_3$) δ 147.5, 140.4, 140.2, 137.8, 135.5, 131.09, 130.9, 127.3, 126.2, 125.5, 122.8, 120.1, 47.7, 47.4, 37.8 ppm.

**HRMS** (MALDI+) calculated for m/z $[C_{48}H_{32}Br_3]^+$, $[M\text{-}H]^+$: 845.0049; found: 845.0052.

The spectral data were fully consistent with those previously reported.[4c]

**(5*R*,10*R*,15*S*)-5,10,15-Tris([1,1'-biphenyl]-2-ylmethyl)-10,15-dihydro-5*H*-diindeno[1,2-*a*:1',2'-*c*]fluorene (*anti*-2g)**

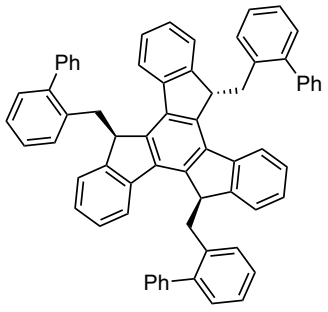


To a solution of *anti*-**2c** (200 mg, 0.24 mmol, 1.0 equiv) in anhydrous toluene (4.71 mL, 0.05 M) was added tri-*n*-butylphenylstannane (0.28 mL, 0.85 mmol, 3.6 equiv), $[Pd(PPh_3)_4]$ (27.2 mg, 23.5 µmol,

0.1 equiv) and hydroquinone (1.3 mg, 11.8 μmol, 0.05 equiv). The mixture was heated at 90 °C and was stirring for 16 h. After allowing to cool to room temperature, the mixture was filtered through a celite plug and solvent was evaporated under reduced pressure. The residue was treated with hexane to afford *anti*-**2g** as an off-yellow solid (127 mg, 0.15 mmol, 64% yield).

**M.p.** = 154 °C.

**$^1$H NMR** (400 MHz, $CDCl_3$) δ 7.62 (dd, *J* = 11.6, 7.6 Hz, 3H), 7.40 – 7.31 (m, 12H), 7.30 – 7.27 (m, 2H), 7.25 – 7.21 (m, 6H), 7.13 – 6.99 (m, 12H), 6.56 – 6.45 (m, 3H) 4.83 – 4.68 (m, 3H), 3.95 – 3.66 (m, 3H), 2.75 (dd, *J* = 13.9, 9.4 Hz, 1H), 2.20 – 2.05 (m, 2H) ppm.

**$^{13}$C NMR** (101 MHz, $CDCl_3$) δ 147.3, 147.2, 147.0, 143.2, 143.0, 141.8, 141.5, 140.9, 140.7, 140.4, 140.0, 139.8, 137.8, 137.6, 136.4, 136.2, 130.5, 130.4, 130.1, 129.5, 129.4, 128.1, 128.0, 127.7, 127.3, 126.56, 126.2, 126.1, 125.7, 125.7, 125.5, 122.6, 122.5, 122.4, 122.2, 121.9, 48.0, 47.5, 47.3, 35.6, 35.5, 35.4 ppm.

**HRMS** (MALDI+) calculated for m/z $[C_{66}H_{47}]^+$, $[M-H]^+$: 839.3672; found: 845.3679.

**(5*R*,10*R*,15*R*)-5,10,15-Tris([1,1'-biphenyl]-2-ylmethyl)-10,15-dihydro-5*H*-diindeno[1,2-*a*:1',2'-*c*]fluorene (*syn*-2g)**

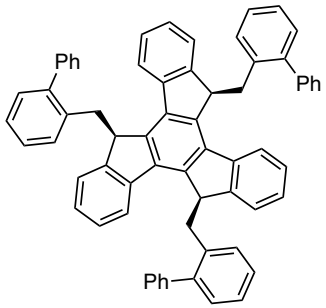


To a solution of *syn*-**2c** (50 mg, 58.9 μmol, 1.0 equiv) in anhydrous toluene (1.18 mL, 0.05 M) was added tri-*n*-butylphenylstannane (69 μL, 0.21 mmol, 3.6 equiv), $[Pd(PPh_3)_4]$ (6.8 mg, 5.9 μmol, 0.1 equiv) and hydroquinone (1 mg, 9 μmol, 0.15 equiv). The mixture was heated at 90 °C and was stirring for 16 h. After allowing to cool to room temperature, the mixture was filtered through a celite plug and solvent was evaporated under reduced pressure. The residue was treated with hexane to afford *syn*-**2g** as an off-yellow solid.(31 mg, 36.9 μmol, 63% yield).

**M.p.** = 148–150 °C.

**$^1$H NMR** (500 MHz, $CDCl_3$) δ 7.50 – 7.46 (m, 2H), 7.39 (d, *J* = 7.4 Hz, 4H), 7.36 – 7.31 (m, 6H), 7.23 (ddd, *J* = 11.1, 7.3, 1.7 Hz, 5H), 7.20 – 7.17 (m, 9H), 7.16 – 7.12 (m, 5H), 7.08 (td, *J* = 7.4, 1.1 Hz, 3H), 6.87 – 6.83 (m, 2H), 6.42 (d, *J* = 7.4 Hz, 2H), 4.07 (dd, *J* = 10.8, 4.6 Hz, 3H), 3.65 (dd, *J* = 14.3, 4.7 Hz, 3H), 2.23 (dd, *J* = 14.5, 11.1 Hz, 3H) ppm.

**HRMS** (MALDI+) calculated for m/z $[C_{66}H_{47}]^+$, $[M-H]^+$: 839.3672; found: 845.3662.

**(5*R*,10*R*,15*R*)-5,10,15-Tris(2-methylbenzyl)-10,15-dihydro-5*H*-diindeno[1,2-*a*:1',2'-*c*]fluorene (*syn*-2d)**

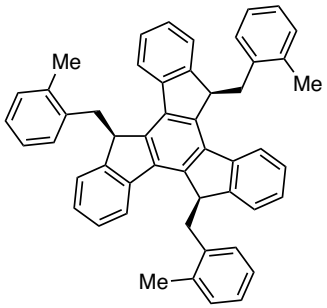


Following general procedure **GP1** using truxene **1** (400 mg, 1.17 mmol, 1.0 equiv), NaH (144.8 mg, 3.62 mmol, 3.1 equiv) and 1-(bromomethyl)-2-methylbenzene (756.6 mg, 4.09 mmol, 3.5 equiv) in anhydrous DMF (19.5 mL, 0.06 M). After treatment with hexane, **2d** was obtained as an inseparable *anti*/*syn* mixture. Yellow solid (653 mg, 1.17 mmol, 85% yield). The *anti*/*syn*-**2d** mixture (251 mg, 0.38 mmol, 1.0 equiv) was exposed to conditions in general procedure **GP2** which afforded *syn*-**2d.** Beige solid (160 mg, 0.24 mmol, 64% yield).

**M.p.** = 187 °C.

**$^1$H NMR** (500 MHz, $CDCl_3$) δ 7.62 (d, *J* = 7.6 Hz, 3H), 7.45 (td, *J* = 7.4, 1.1 Hz, 3H), 7.25 – 7.18 (m, 6H), 7.18 (m, 3H), 7.12 (d, *J* = 7.5 Hz, 3H), 7.09 – 7.05 (m, 3H), 6.50 (d, *J* = 7.4 Hz, 3H), 3.62 (d, *J* = 10.7 Hz, 3H), 3.49 (dd, *J* = 14.8, 4.1 Hz, 3H), 2.22 (dd, *J* = 14.7, 11.4 Hz, 3H), 1.81 (s, 9H) ppm.

**$^{13}$C NMR** (126 MHz, $CDCl_3$) δ 148.0, 141.4, 139.9, 138.3, 137.3, 135.2, 130.2, 129.3, 127.0, 126.2, 125.9, 125.8, 125.5, 123.1, 46.8, 35.1, 20.1 ppm.

**HRMS** (MALDI+) calculated for m/z $[C_{51}H_{41}]^+$, $[M-H]^+$: 653.3203; found: 653.3175.

**(5*R*,10*R*,15*R*)-5,10,15-Tris(3,5-dimethoxybenzyl)-10,15-dihydro-5*H*-diindeno[1,2-a:1',2'-c]fluorene (*syn*-2e)**

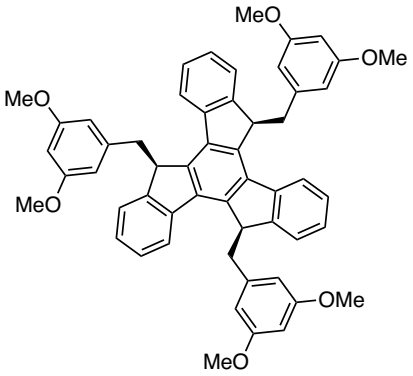


Following general procedure **GP1** using truxene **1** (400 mg, 1.17 mmol, 1.0 equiv), NaH (144.8 mg, 3.62 mmol, 3.1 equiv) and 1-(bromomethyl)-3,5-dimethoxybenzene (944.8 mg, 4.09 mmol, 3.5 equiv) in anhydrous DMF (19.5 mL, 0.06 M). After treatment with hexane, **2e** was obtained as an inseparable *anti*/*syn* mixture. Yellow solid (545 mg, 0.69 mmol, 59% yield). The *anti*/*syn*-**2e** mixture (250 mg, 0.32 mmol, 1.0 equiv) was exposed to conditions in general procedure **GP2** which afforded *syn*-**2e**. Beige solid (128 mg, 0.16 mmol, 51% yield).

**M.p.** = 198 ºC.

**$^1$H NMR** (500 MHz, $CDCl_3$) δ 8.13 (dd, *J* = 10.6, 7.6 Hz, 2H), 8.05 (d, *J* = 7.6 Hz, 1H), 7.50 – 7.42 (m, 3H), 7.26 – 7.20 (m, 3H), 7.13 (dd, *J* = 10.0, 7.5 Hz, 3H), 6.31 – 6.26 (m, 3H), 6.23 – 6.17 (m, 6H), 4.97 – 4.81 (m, 3H), 3.88 – 3.77 (m, 2H), 3.71 (dd, *J* = 14.2, 3.6 Hz, 1H), 3.68 (s, 6H), 3.64 (s, 6H), 3.64 (s, 6H), 2.65 (dd, *J* = 13.8, 9.4 Hz, 1H), 2.50 (dt, *J* = 14.2, 9.8 Hz, 2H) ppm.

**$^{13}$C NMR** (126 MHz, $CDCl_3$) δ 160.5, 160.5, 160.4, 147.9, 147.8, 147.7, 141.7, 141.5, 141.4, 141.3, 140.5, 140.4, 140.3, 140.2, 140.1, 136.8, 136.7, 136.5, 127.5, 127.5, 127.4, 126.3, 126.2, 126.2, 125.7, 125.6, 107.8, 107.7, 107.7, 98.7, 98.7, 98.3, 55.4, 55.3, 55.3, 48.2, 47.9, 47.7, 39.4, 38.8, 38.5, 27.1 ppm.

**HRMS** (ESI+) calculated for m/z $[C_{54}H_{48}NaO_6]^+$, $[M+Na]^+$: 815.3343; found: 815.3320.

**Fluorene complex 4**

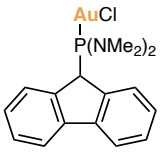


Under and argon atmosphere, *n*BuLi (2.08 M solution in hexane) (0.43 mL, 0.9 mmol, 1.0 equiv) was added to a solution of 9H-fluorene (150 mg, 0.9 mmol, 1.0 equiv) in anhydrous THF (9.0 mL, 0.1 M) at -78 °C observing an instant change of the colorless solution to a deep-red. The mixture was slowly

warmed to -10 °C over a period of 4 h. At that temperature, to the still dark-red solution, $ClP(NMe_2)_2$ (0.15 mL, 0.99 mmol, 1.1 equiv) was added and the solution turned pale-yellow immediately. The reaction was left stirring for 16 h at -10 ºC. Then, the solvent was removed under reduced pressure, and the crude was used without further purification (256.6 mg, 0.9 mmol, *ca*. quantitative yield). The crude material (257 mg, 0.9 mmol, 1.0 equiv) was dissolved in anhydrous $CH_2Cl_2$ (20 mL, 0.05 M) before $(Me_2S)AuCl$ (293 mg, 0.99 mmol, 1.1 equiv) was added. The reaction was left stirring at 23 ºC for 1 h. The crude was purified by flash column chromatography ($SiO_2$, CyH/AcOEt 90:10). White solid (410 mg, 0.79 mmol, 88% yield).

**M.p.** = decomposition at 220 °C.

**$^1$H NMR** (500 MHz, $CDCl_3$) δ 7.82 (ddt, *J* = 8.9, 6.9, 0.8 Hz, 4H), 7.46 (tq, *J* = 7.3, 0.8 Hz, 2H), 7.35 (td, *J* = 7.5, 1.3 Hz, 2H), 4.81 (d, *J* = 9.2 Hz, 1H), 2.51 (d, *J* = 11.8 Hz, 12H) ppm.

**$^{13}$C NMR** (126 MHz, $CDCl_3$) δ 142.0 (d, *J* = 3.8 Hz), 138.9 (d, *J* = 2.7 Hz), 128.5 (d, *J* = 2.4 Hz), 127.4 (d, *J* = 2.4 Hz), 126.8, 126.7, 120.5, 50.1, 49.8, 39.9, 39.8 ppm.

**$^{31}$P NMR** (202 MHz, $CDCl_3$) δ 115.7 ppm.

**HRMS** (ESI+) calculated for m/z $[C_{17}H_{22}AuClN_2P]^+$, $[M+H]^+$: 517,0875; found: 517.0846.

The structure of this compound was also confirmed by X-ray diffraction.

**Truxene complex 5**

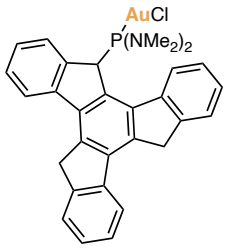


Under and argon atmosphere, *n*BuLi (2.08 M solution in hexane) (0.21 mL, 0.44 mmol, 1.0 equiv) was added to a solution of truxene **1** (150 mg, 0.44 mmol, 1.0 equiv) in anhydrous THF (14.6 mL, 0.03 M) at -78 ºC observing an instant change of the colorless solution to a deep-red. The mixture was slowly warmed to -10 ºC over a period of 4 h. At that temperature, to the still dark-red solution, $ClP(NMe_2)_2$ (0.07 mL, 0.48 mmol, 1.1 equiv) was added and the solution turned pale-yellow immediately. The reaction was left stirring for 16 h at -10 ºC. Then, the solvent was removed under reduced pressure, and the crude was used without further purification (201.7 mg, 0.44 mmol, *ca*. quantitative yield). The crude material (202 mg, 0.9 mmol, 1.0 equiv) was dissolved in anhydrous $CH_2Cl_2$ (20 mL, 0.05 M) before $(Me_2S)AuCl$ (142 mg, 0.48 mmol, 1.1 equiv) was added. The reaction was left stirring at 23 ºC for 1 h. The crude was purified by flash column chromatography ($SiO_2$, CyH/AcOEt 90:10). White solid (42.73 mg, 0.39 mmol, 90% yield).

**M.p.** = decomposition at 210 °C.

**$^{1}$H NMR** (500 MHz, $CDCl_3$) δ 8.05 (d, *J* = 7.0 Hz, 1H), 7.96 (d, *J* = 7.5 Hz, 1H), 7.92 (d, *J* = 7.6 Hz, 1H), 7.88 (d, *J* = 7.6 Hz, 1H), 7.73 – 7.67 (m, 2H), 7.65 (d, *J* = 7.5 Hz, 1H), 7.55 (d, *J* = 7.8 Hz, 1H), 7.51 (ddt, *J* = 6.4, 4.1, 1.9 Hz, 1H), 7.48 – 7.46 (m, 1H), 7.45 – 7.39 (m, 2H), 5.27 (d, *J* = 5.8 Hz, 1H), 4.36 – 4.17 (m, 2H), 3.98 (dd, *J* = 27.8, 21.6 Hz, 2H), 2.60 (d, *J* = 13.2 Hz, 6H), 1.97 (d, *J* = 10.1 Hz, 6H) ppm.

**$^{13}$C NMR** (126 MHz, $CDCl_3$) δ 143.9, 141.3, 140.9, 136.3, 131.5, 128.7, 127.5, 127.3, 127.0, 126.8, 126.4, 125.8, 125.3, 123.4, 122.5, 52.3, 39.4, 39.4, 39.2, 39.1, 36.7, 36.4 ppm.

**$^{31}$P NMR** (202 MHz, $CDCl_3$) δ 118.2 ppm.

**HRMS** (ESI+) calculated for m/z $[C_{31}H_{29}AuClN_2NaP]^+$, $[M+Na]^+$: 715.1315; found: 715.1302.

**Crystallographic Data**
**Complex 4**

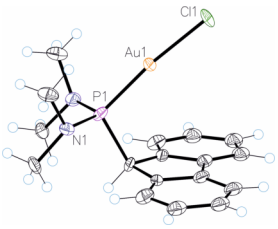


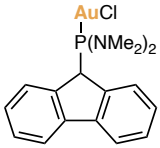


**Table S1**. Crystal data and structure refinement for complex **4**.

| | |
|---|---|
| Identification code | mo_GO422_0m |
| Empirical formula | $C_{17}H_{21}AuClN_2P$ |
| Formula weight | 516.74 |
| Temperature/K | 99.68 |
| Crystal system | monoclinic |
| Space group | $P2_1/m$ |
| a/Å | 7.492(4) |
| b/Å | 14.281(8) |
| c/Å | 8.534(4) |
| α/° | 90 |
| β/° | 110.124(14) |
| γ/° | 90 |
| Volume/Å$^3$ | 857.3(7) |
| Z | 2 |
| $\rho_{calc}$g/cm$^3$ | 2.002 |
| μ/mm$^{-1}$ | 8.827 |
| F(000) | 496.0 |
| Crystal size/mm$^3$ | 0.1 × 0.1 × 0.05 |
| Radiation | MoKα (λ = 0.71073) |
| 2Θ range for data collection/° | 5.084 to 50.866 |
| Index ranges | $-9 \le h \le 6$, $-17 \le k \le 16$, $-8 \le l \le 10$ |
| Reflections collected | 5502 |
| Independent reflections | 1611 [$R_{int}$ = 0.0633, $R_{sigma}$ = 0.0712] |
| Data/restraints/parameters | 1611/42/108 |
| Goodness-of-fit on $F^2$ | 1.141 |
| Final R indexes [I>=2σ (I)] | $R_1$ = 0.0574, $wR_2$ = 0.1432 |
| Final R indexes [all data] | $R_1$ = 0.0759, $wR_2$ = 0.1503 |
| Largest diff. peak/hole / e Å$^{-3}$ | 3.38/-3.13 |

UNIVERSITAT ROVIRA I VIRGILI
Novel Supramolecular Gold(I)-Cavitand Catalysts and Approach to the Total Synthesis of Monomarginine
Gala Ogalla Estévez

UNIVERSITAT ROVIRA I VIRGILI
Novel Supramolecular Gold(I)-Cavitand Catalysts and Approach to the Total Synthesis of Monomarginine
Gala Ogalla Estévez

# *General Conclusions*

UNIVERSITAT ROVIRA I VIRGILI
Novel Supramolecular Gold(I)-Cavitand Catalysts and Approach to the Total Synthesis of Monomarginine
Gala Ogalla Estévez

The research developed in this Doctoral Thesis has led to the following conclusions:

The synthesis of new gold(I)-cavitand complexes has been achieved based on resorcin[4]arene and quinoxaline walls as the main core. Modifications in the structure have allowed to study a novel family of gold(I)-cavitand complexes in different catalytic systems.

- For the incorporation of chirality on the cavitand core, two approaches have been followed. On one side, the integration of an aminoacid moiety as part of a cavitand wall was achieved. However, it could not be incorporated on the cavitand core. On the other hand, a chiral phthalimide wall was designed, synthesized and incorporated into the cavitand core, before the gold(I) complexation, to form a new chiral gold(I)-cavitand complex. Despite its demonstrated catalytic activity, its enantiomeric ratios were poor due to the distant position of the chiral information relative to the gold(I) center.
- A novel family of achiral gold(I)-cavitand complexes was synthesized with the inclusion of a urea moiety that allowed the H-bonding interactions with a chiral counteranions, upon complex activation. The system was studied for the enantioselective reaction of 1,6-enynes with different nuclophile additions.

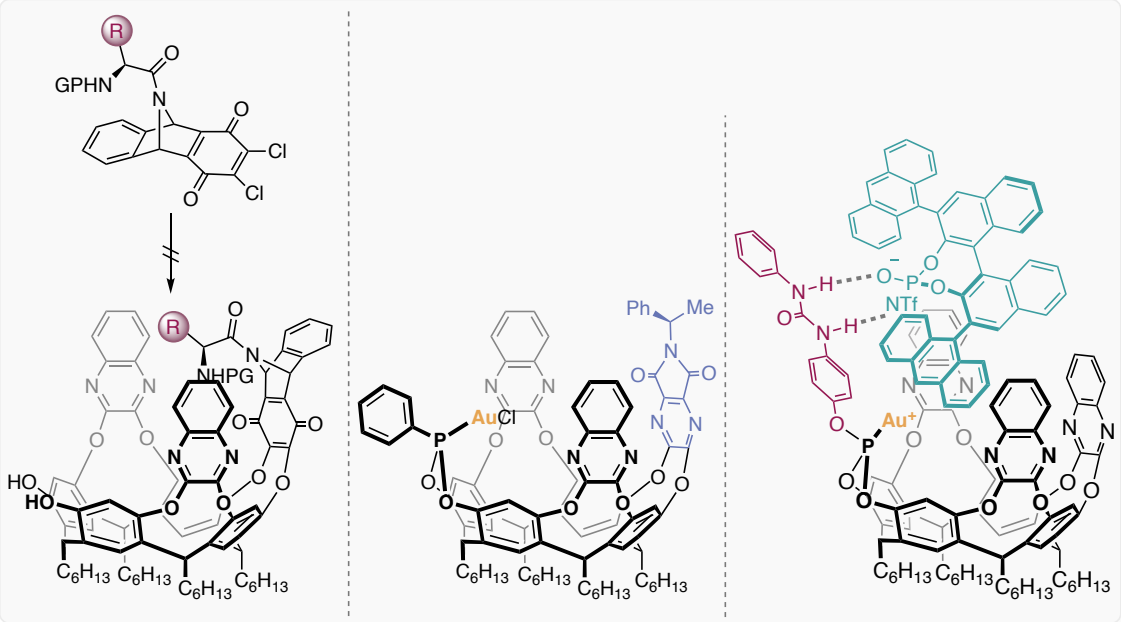


Finally, the application of gold(I)-cavitand complexes has been studied for the key-step alkoxycyclization reaction to form a possible precursor for to the synthesis of the renifolin family of natural products.

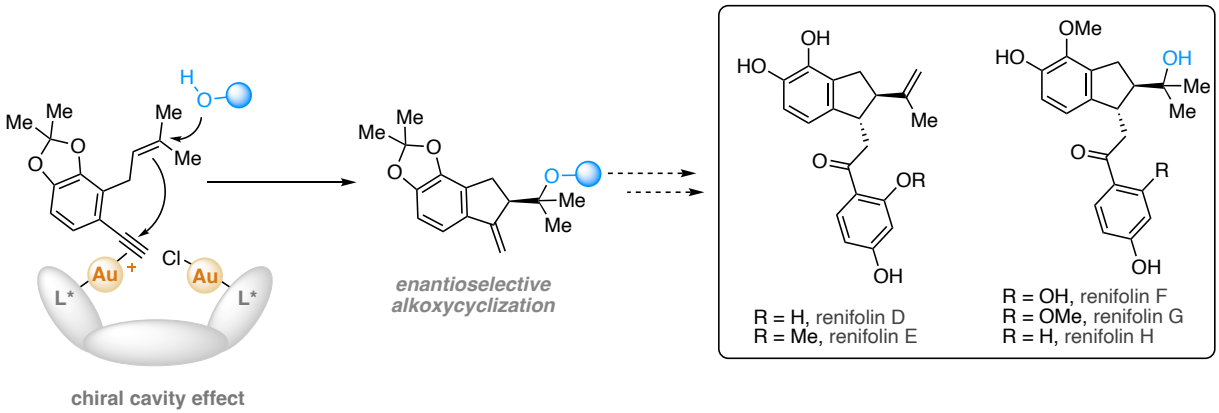


We have also performed the structure elucidation of monomarginine natural product throughout X-ray diffraction and NMR of a sample of the natural product. Then, efforts towards its synthesis have been explored. First, routes were focused on synthesizing the azaanthraquinone core *via* a gold(I)-catalyzed cyclization. On the other hand, the synthesis of the naphtyridine core was attempted as an alternative route. Efforts in our laboratory are currently ongoing to complete the total synthesis.

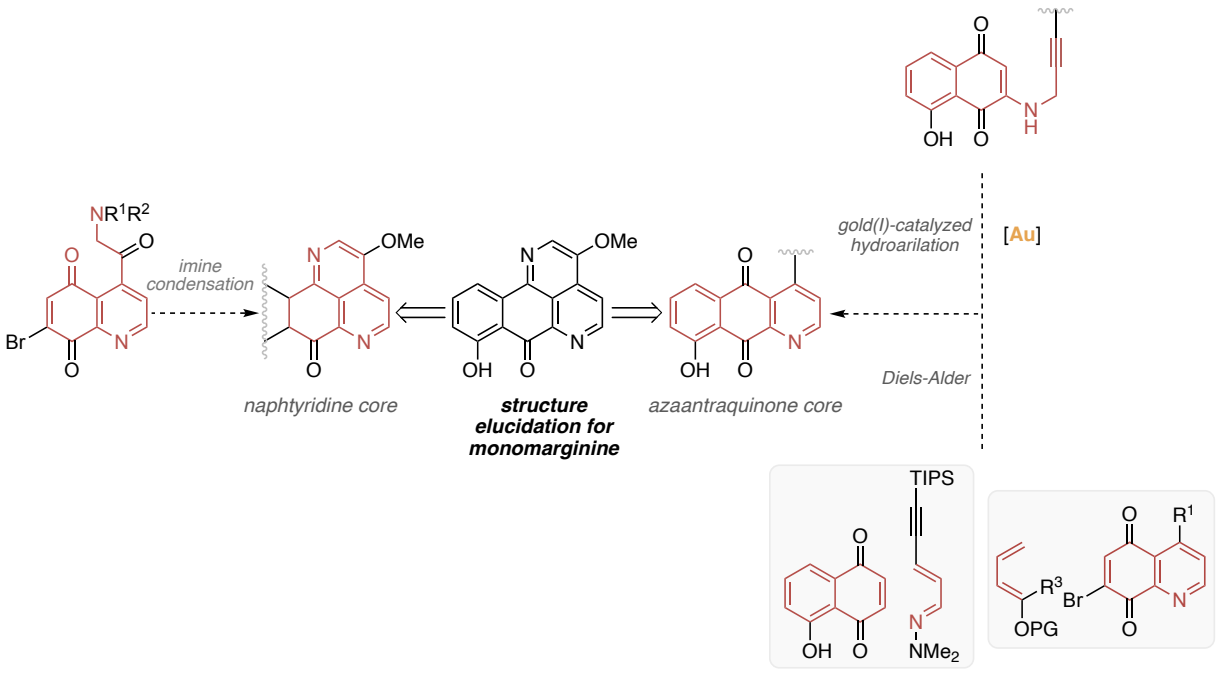

UNIVERSITAT ROVIRA I VIRGILI
Novel Supramolecular Gold(I)-Cavitand Catalysts and Approach to the Total Synthesis of Monomarginine
Gala Ogalla Estévez

UNIVERSITAT ROVIRA I VIRGILI
Novel Supramolecular Gold(I)-Cavitand Catalysts and Approach to the Total Synthesis of Monomarginine
Gala Ogalla Estévez

UNIVERSITAT ROVIRA I VIRGILI
Novel Supramolecular Gold(I)-Cavitand Catalysts and Approach to the Total Synthesis of Monomarginine
Gala Ogalla Estévez